Feasibility and Performance of a LoRa 2.4 GHz Network

Gwendoline Hochet Derévianckine

N°d'ordre NNT : 2024ISAL0127

THESE de DOCTORAT DE L'INSA LYON, membre de l'Université de Lyon

Ecole Doctorale N° 512
Informatique et Mathématiques

Spécialité/ discipline de doctorat :
Informatique

Soutenue publiquement le 17/12/2024, par :
Gwendoline Hochet Derévianckine

Feasibility and Performance of a LoRa 2.4 GHz Network

Faisabilité et performances d'un réseau LoRa 2.4 GHz

Devant le jury composé de :

PALATTELLA	Maria Rita	Directrice de Recherche	LIST	Rapporteure
PHAM	Congduc	Professeur des Universités	UPPA	Rapporteur
CAILLOUET	Christelle	Maître de Conférences HDR	Université Côte d'Azur	Examinatrice
DONSEZ	Didier	Professeur des Universités	UGA	Examinateur
NOËL	Thomas	Professeur des Universités	Université de Strasbourg	Examinateur
ORIFIAMMA	Davide	Director R&D	Semtech	Invité
GUITTON	Alexandre	Professeur des Universités	UCA	Co-encadrant de thèse
IOVA	Oana	Maître de Conférences	INSA-LYON	Co-encadrante de thèse
VALOIS	Fabrice	Professeur des Universités	INSA-LYON	Directeur de thèse

INSTITUT NATIONAL DES SCIENCES APPLIQUÉES LYON

Département de la Formation par la Recherche et des Études Doctorales (**FEDORA**)

Bâtiment Charlotte Perriand 3e étage
17, av. des Arts
69621 Villeurbanne Cédex
fedora@insa-lyon.fr

Référence : TH1168_HOCHET DEREVIANCKINE Gwendoline

L'INSA Lyon a mis en place une procédure de contrôle systématique via un outil de détection de similitudes (logiciel Compilatio). Après le dépôt du manuscrit de thèse, celui-ci est analysé par l'outil. Pour tout taux de similarité supérieur à 10%, le manuscrit est vérifié par l'équipe de FEDORA. Il s'agit notamment d'exclure les auto-citations, à condition qu'elles soient correctement référencées avec citation expresse dans le manuscrit.

Par ce document, il est attesté que ce manuscrit, dans la forme communiquée par la personne doctorante à l'INSA Lyon, satisfait aux exigences de l'Etablissement concernant le taux maximal de similitude admissible.

Département FEDORA – INSA Lyon - Ecoles Doctorales

SIGLE	ECOLE DOCTORALE	NOM ET COORDONNEES DU RESPONSABLE
ED 206 CHIMIE	**CHIMIE DE LYON** https://www.edchimie-lyon.fr Sec. : Renée EL MELHEM Bât. Blaise PASCAL, 3e étage secretariat@edchimie-lyon.fr	**M. Stéphane DANIELE** C2P2-CPE LYON-UMR 5265 Bâtiment F308, BP 2077 43 Boulevard du 11 novembre 1918 69616 Villeurbanne directeur@edchimie-lyon.fr
ED 341 E2M2	**ÉVOLUTION, ÉCOSYSTÈME, MICROBIOLOGIE, MODÉLISATION** http://e2m2.universite-lyon.fr Sec. : Bénédicte LANZA Bât. Atrium, UCB Lyon 1 Tél : 04.72.44.83.62 secretariat.e2m2@univ-lyon1.fr	**Mme Sandrine CHARLES** Université Claude Bernard Lyon 1 UFR Biosciences Bâtiment Mendel 43, boulevard du 11 Novembre 1918 69622 Villeurbanne CEDEX e2m2.codir@listes.univ-lyon1.fr
ED 205 EDISS	**INTERDISCIPLINAIRE SCIENCES-SANTÉ** http://ediss.universite-lyon.fr Sec. : Bénédicte LANZA Bât. Atrium, UCB Lyon 1 Tél : 04.72.44.83.62 secretariat.ediss@univ-lyon1.fr	**Mme Sylvie RICARD-BLUM** Laboratoire ICBMS - UMR 5246 CNRS - Université Lyon 1 Bâtiment Raulin - 2ème étage Nord 43 Boulevard du 11 novembre 1918 69622 Villeurbanne Cedex Tél : +33(0)4 72 44 82 32 sylvie.ricard-blum@univ-lyon1.fr
ED 34 EDML	**MATÉRIAUX DE LYON** http://ed34.universite-lyon.fr Sec. : Yann DE ORDENANA Tél : 04.72.18.62.44 yann.de-ordenana@ec-lyon.fr	**M. Stéphane BENAYOUN** Ecole Centrale de Lyon Laboratoire LTDS 36 avenue Guy de Collongue 69134 Ecully CEDEX Tél : 04.72.18.64.37 stephane.benayoun@ec-lyon.fr
ED 160 EEA	**ÉLECTRONIQUE, ÉLECTROTECHNIQUE, AUTOMATIQUE** https://edeea.universite-lyon.fr Sec. : Philomène TRECOURT Bâtiment Direction INSA Lyon Tél : 04.72.43.71.70 secretariat.edeea@insa-lyon.fr	**M. Philippe DELACHARTRE** INSA LYON Laboratoire CREATIS Bâtiment Blaise Pascal, 7 avenue Jean Capelle 69621 Villeurbanne CEDEX Tél : 04.72.43.88.63 philippe.delachartre@insa-lyon.fr
ED 512 INFOMATHS	**INFORMATIQUE ET MATHÉMATIQUES** http://edinfomaths.universite-lyon.fr Sec. : Renée EL MELHEM Bât. Blaise PASCAL, 3e étage Tél : 04.72.43.80.46 infomaths@univ-lyon1.fr	**M. Hamamache KHEDDOUCI** Université Claude Bernard Lyon 1 Bât. Nautibus 43, Boulevard du 11 novembre 1918 69 622 Villeurbanne Cedex France Tél : 04.72.44.83.69 direction.infomaths@listes.univ-lyon1.fr
ED 162 MEGA	**MÉCANIQUE, ÉNERGÉTIQUE, GÉNIE CIVIL, ACOUSTIQUE** http://edmega.universite-lyon.fr Sec. : Philomène TRECOURT Tél : 04.72.43.71.70 Bâtiment Direction INSA Lyon mega@insa-lyon.fr	**M. Etienne PARIZET** INSA Lyon Laboratoire LVA Bâtiment St. Exupéry 25 bis av. Jean Capelle 69621 Villeurbanne CEDEX etienne.parizet@insa-lyon.fr
ED 483 ScSo	**ScSo**[1] https://edsciencessociales.universite-lyon.fr Sec. : Mélina FAVETON Tél : 04.78.69.77.79 melina.faveton@univ-lyon2.fr	**M. Bruno MILLY** (INSA : J.Y. TOUSSAINT) Univ. Lyon 2 Campus Berges du Rhône 18, quai Claude Bernard 69365 LYON CEDEX 07 Bureau BEL 319 bruno.milly@univ-lyon2.fr

[1] ScSo : Histoire, Géographie, Aménagement, Urbanisme, Archéologie, Science politique, Sociologie, Anthropologie

Abstract

The long-range (LoRa) technology and the LoRaWAN protocol, which mainly uses the sub-GHz frequency bands, subject to regional laws, have become widely used as a result of the rise of the Internet of Things (IoT). To overcome these limitations, Semtech has released a version of LoRa dedicated to the 2.4 GHz industrial, scientific, and medical (ISM) band, which, among others, is worldwide available and has no duty-cycle limitations. However, this frequency band is already used by many wireless technologies, such as Wi-Fi and Bluetooth (BT), as well as by common devices like microwaves and surveillance cameras. It is essential to evaluate the feasibility and the possible performance of this frequency band shift before deploying LoRa on a large scale in the 2.4 GHz ISM band.

This thesis proposes a comprehensive experimental evaluation of LoRa technology in the 2.4 GHz ISM band, including a comparison of its communication range and reliability with the European sub-GHz band (868 MHz). We also study the coexistence of LoRa and Wi-Fi when they are overlapping transmissions. To improve the coexistence, we propose and compare several frequency hopping (FH) strategies for LoRa. Although the latter proposal is based on simulation, we also propose an original methodology for evaluating a frequency band and selecting the less noisy channels, which could facilitate the implementation of FH strategies in future LoRa 2.4 GHz gateways. Our work provides important recommendations for the deployment and expansion of LoRa in the 2.4 GHz ISM band.

Résumé

L'essor de l'Internet des Objets (IoT) ces dernières années a favorisé l'adoption de la technologie long-range (LoRa) et du protocole LoRaWAN, qui utilisent principalement les bandes de fréquences sub-GHz, soumises à des réglementations régionales. Pour surmonter ces limitations, Semtech a développé une version de LoRa pour la bande 2.4 GHz, qui est, notamment, accessible mondialement et n'impose pas de cycle d'activité. Cependant, cette bande de fréquence est déjà utilisée par de nombreuses technologies sans fil, telles que le Wi-Fi et le Bluetooth (BT), ainsi que par des appareils courants, comme le micro-ondes et les caméras de surveillance. Avant de déployer LoRa à grande échelle dans la bande industrielle, médicale et scientifique (ISM) 2.4 GHz, il est crucial d'évaluer la faisabilité et les performances potentielles de cette transition.

Cette thèse propose une évaluation expérimentale complète de la technologie LoRa dans la bande ISM 2.4 GHz, notamment en comparant sa portée et sa fiabilité avec celles de la bande sub-GHz européenne (868 MHz). Nous examinons également la coexistence entre LoRa et le Wi-Fi lorsque leurs transmissions se chevauchent. Pour améliorer cette coexistence nous proposons et comparons différentes stratégies de saut de fréquences (FH) pour LoRa. Bien que cette dernière proposition soit réalisée par simulation, nous proposons également une méthodologie originale pour évaluer une bande de fréquence et choisir les canaux les moins utilisés, ce qui pourrait faciliter l'implémentation des stratégies de FH dans les futures passerelles LoRa 2.4 GHz. L'ensemble de nos travaux fournissent des recommandations importantes pour le déploiement et l'expansion de LoRa dans la bande ISM 2.4 GHz.

Résumé long

Au cours de la dernière décennie, l'Internet des Objets (IoT) a pris de l'ampleur à l'échelle mondiale avec pour objectif principal d'améliorer notre vie quotidienne. Les applications typiques comprennent la surveillance du changement climatique, les compteurs intelligents, le suivi de matériel et d'équipements, les bâtiments intelligents et les villes intelligentes. Long-range® (LoRa), NB-IoT et Ingenu sont des exemples de technologies sans fil dédiées à l'IoT et regroupées sous le nom de réseaux longues distances à faible consommation d'énergie (LPWANs). Les industriels et les opérateurs de télécommunications du monde entier déploient ces nouvelles technologies pour plusieurs raisons : (i) elles répondent aux besoins d'une grande variété d'applications pour l'IoT, (ii) elles peuvent transmettre des paquets de données sur plusieurs kilomètres à de faibles débits (quelques centaines de bits par seconde), ce qui contribue à réduire le coût de déploiement d'un LPWAN, (iii) la faible consommation d'énergie, le faible coût des puces radio et la faible complexité globale des architectures LPWAN facilitent leur déploiement et leur maintenance.

LoRa, associé au protocole LoRaWAN®, est l'un des LPWAN les plus représentatifs qui ont inondé le marché. Ils sont largement utilisés pour la collecte de données IoT à faible consommation sur de grandes étendues. LoRa fonctionne généralement sur des bandes sub-GHz sans licence dans le monde entier, ce qui rend son déploiement spécifique à chaque région. Selon le pays, les réglementations relatives à ces bandes sub-GHz (par exemple 868 MHz en Europe, 915 MHz en Amérique du Nord) spécifient différents canaux de fréquence, un temps de transmission maximal, une puissance de transmission maximale et différents mécanismes d'accès au canal tels que le cycle de d'activité ou l'écoute du canal avant transmission (LBT). Ces paramètres doivent être pris en compte dans la conception des composants matériels et des protocoles de communication. Ces spécificités peuvent entraver le déploiement de la technologie LoRa si les applications ne sont pas conformes aux réglementations en vigueur.

En 2017, dans un effort pour outrepasser ces spécificités, Semtech a publié une version de LoRa pour la bande industrielle, scientifique et médicale (ISM) 2.4 GHz. Cette version a suscité l'intérêt de la communauté scientifique, car elle permet de construire un LPWAN qui bénéficie d'une interopérabilité mondiale et d'une absence de limitation du cycle de d'activité. Un autre avantage de la bande ISM 2.4 GHz est qu'une puce LoRa peut être déployée partout dans le monde, car ce spectre fréquentiel dispose d'un grand nombre de canaux partagés par tous les pays, ainsi que de plusieurs paramètres communs de la couche physique tels que la puissance de transmission maximale.

Cependant, LoRa 2.4 GHz présente également des inconvénients et doit relever plusieurs défis. En effet, LoRa 2.4 GHz fonctionne dans une bande de fréquences largement utilisée, notamment par le Wi-Fi et le Bluetooth (BT). Il en résulte un risque élevé d'interférences entre les technologies. Par conséquent, le principal défi de LoRa 2.4 GHz est la coexistence avec d'autres technologies radio occupant déjà la bande ISM 2.4 GHz. Un autre défi important est lié au développement d'un nouveau matériel pour permettre le déploiement

à grande échelle des réseaux LoRa dans la bande ISM 2.4 GHz, ainsi que le logiciel qui l'accompagne. Dans cette thèse, nous nous concentrons sur les défis technologiques que sont l'attribution des canaux LoRa dans la bande ISM 2.4 GHz ainsi que les défis liés à la gestion des interférences entre LoRa et les autres technologies fonctionnant dans la même bande de fréquence.

Motivations de la thèse

L'objectif principal de cette thèse est d'étudier la faisabilité d'un réseau LoRa dans la bande ISM 2.4 GHz. Nous nous concentrons sur les performances de cette nouvelle version de LoRa plus précisément en termes de connectivité et de portée de communication dans deux types d'environnements : intérieur et extérieur. Nous nous intéressons également à la coexistence de LoRa et Wi-Fi dans la bande ISM 2.4 GHz.

La LoRa Alliance® a manifesté son intérêt pour le déploiement de réseaux LoRa dans des réseaux privés au lieu des habituels réseaux publics visés jusqu'à présent. Cela implique que l'environnement de déploiement passe de l'industrie au particulier. Cela constitue également l'occasion de transférer la technologie LoRa des bandes de fréquences sub-GHz à la bande ISM 2.4 GHz.

Nous exposons les questions de recherche qui nous avons soulevées pour répondre à notre objectif de recherche.

Objectif de la recherche : Étudier la faisabilité d'un réseau LoRa dans la bande ISM de 2.4 GHz.

Questions de recherche : Les questions de recherche suivantes sont générales et ont guidé cette thèse. Nous avons détaillé dans chaque chapitre de contributions des questions de recherche plus spécifiques pour répondre à notre objectif de recherche.

RQ-1 : LoRa est-elle capable de communiquer (transmettre et recevoir) des données dans la bande ISM 2.4 GHz ?

RQ-2 : Quelles sont les performances, en termes de connectivité et de portée de communication, de LoRa 2.4 GHz par rapport à LoRa sub-GHz ?

RQ-3 : Comment LoRa coexiste-t-elle avec les autres technologies sans fil de la bande ISM 2.4 GHz ?

RQ-4 : Est-il possible d'améliorer la coexistence de LoRa dans la bande ISM 2.4 GHz en mettant en œuvre des mécanismes de gestion des interférences au niveau de la couche physique ?

Contributions de la thèse

Nos contributions présentées dans ce manuscrit de thèse sont les suivantes :

- Nous réalisons la première évaluation expérimentale des performances, dans des environnements extérieurs et intérieurs, comparant la portée et la fiabilité des communications LoRa 2.4 GHz et LoRa sub-GHz. Nous fournissons la conception et une évaluation en conditions réelles.
- Nous réalisons la première étude expérimentale sur l'impact mutuel des transmissions LoRa 2.4 GHz et Wi-Fi qui se chevauchent. En outre, nous fournissons une méthodologie pour étudier la coexistence de deux technologies sans fil utilisant la même bande de fréquence. Nous présentons la conception et une évaluation en conditions réelles, ainsi qu'en simulation.
- Nous concevons un algorithme de saut de fréquence (FH) pour améliorer la coexistence de LoRa 2.4 GHz et de Wi-Fi. Nous fournissons la conception, l'implémentation dans notre propre simulateur développé en Python, et une évaluation par simulation.
- Nous concevons une nouvelle méthodologie pour caractériser un environnement radio. Nous présentons la conception et une évaluation préliminaire en conditions réelles.

Dans cette thèse nous commençons par présenter les principales technologies sans fil susceptibles d'interférer avec LoRa et de dégrader ses performances dans la bande ISM 2.4 GHz : BT, Bluetooth Low Energy (BLE), la norme IEEE 802.15.4 et l'ensemble des normes IEEE 802.11. Nous présentons également les caractéristiques générales de la technologie LoRa et d'un réseau LoRaWAN, avant d'introduire la nouvelle version de LoRa dédiée à la bande ISM 2.4 GHz.

Les contributions de cette thèse sont organisées en trois chapitres.

Dans un premier chapitre, nous avons proposé plusieurs expériences pour étudier les performances de LoRa dans la bande ISM 2.4 GHz. Nous nous sommes concentrés sur la connectivité et la portée de communication obtenues par LoRa dans des environnements intérieurs et extérieurs. Nous avons évalué de manière exhaustive l'impact de chaque configuration LoRa possible en faisant varier trois paramètres : le facteur d'étalement (SF), la largeur de bande (BW) et le taux de codage (CR). Nous avons proposé une comparaison du taux de livraison de trames (FDR) LoRa en fonction de la bande de fréquence utilisée pour transmettre (868 MHz et 2.4 GHz dans notre cas). Enfin, nous avons analysé l'impact de l'environnement et des activités de la vie quotidienne, telles que la présence de personnes dans le bâtiment ou l'utilisation de technologies sans fil, sur le FDR LoRa 2.4 GHz. Nous avons démontré que malgré une portée de communication réduite dans la bande ISM 2.4 GHz, LoRa est capable de couvrir un bâtiment de deux étages avec une passerelle et d'atteindre une distance allant jusqu'à 2 km, en utilisant la configuration ayant la plus grande portée de communication, dans un environnement extérieur et dans des conditions de visibilité directe (LoS). En outre, nos résultats montrent que les activités à l'intérieur d'un bâtiment (mobilité des personnes et communications sans fil) dégradent la connectivité LoRa et doivent donc être prises en compte dans les futurs déploiements LoRa.

Dans le second chapitre de contribution, nous nous sommes concentrés sur la coexistence de LoRa dans la bande ISM 2.4 GHz. Pour cela nous avons proposé une méthodologie pour étudier expérimentalement l'impact mutuel de deux technologies sans fil, dans un scénario en intérieur, utilisant la même bande de fréquences. Nous l'avons ensuite appliqué à des appareils disponibles dans le commerce (COTS) LoRa et Wi-Fi pour la bande ISM 2.4 GHz. Nous avons examiné plusieurs paramètres (paramètres de la couche physique, topologie, version de la norme IEEE 802.11) afin de fournir les résultats pour les deux technologies. Cela nous a permis de fournir quelques recommandations pour le déploiement futur de LoRa 2.4 GHz en intérieur sans mettre en œuvre des mécanismes de gestion des interférences. Nous soulignons notamment que (1) la configuration LoRa doit être choisie en fonction des applications ciblées (débit de données versus fiabilité), (2) le FDR Wi-Fi peut subir d'énormes pertes en fonction de la modulation de la norme IEEE 802.11 utilisée, et (3) le déploiement des noeuds LoRa doit tenir compte de l'emplacement des points d'accès (APs) Wi-Fi afin de réduire au maximum les interférences entre les transmissions LoRa et Wi-Fi qui se chevauchent.

Enfin, dans le dernier chapitre de contribution, nous avons présenté une approche visant à améliorer la coexistence entre LoRa et Wi-Fi. Sur la base de nos résultats expérimentaux, nous avons extrait un modèle théorique des performances de LoRa et de Wi-Fi lorsqu'il y a des transmissions qui se chevauchent. Nous avons implémenté ce modèle dans notre propre simulateur développé en Python afin d'évaluer trois stratégies de saut de fréquence (FH) : deux stratégies de base utilisant les trois canaux LoRa proposés par Semtech, et une nouvelle proposition visant à sélectionner les trois meilleurs canaux de la bande ISM de 2.4 GHz, ce qui correspond aux canaux les moins bruyants. Nous avons également proposé une nouvelle méthodologie pour caractériser un environnement radio. Notre méthodologie consiste à balayer une bande de fréquence sur une largeur de bande représentative et ensuite associer un signal à une technologie sans fil connue. Nous avons validé notre approche en l'appliquant à deux signaux enregistrés : Wi-Fi et BT. Notre méthodologie pourrait être utilisée pour la caractérisation des canaux afin de sélectionner les canaux de notre stratégie FH des meilleurs canaux. Nous avons également conçu le protocole correspondant à l'écoute et la sélection des canaux qui serait exécuté par la passerelle LoRa. Nos résultats soulignent que la stratégie FH à mettre en œuvre dépend de l'application ciblée et du nombre d'APs Wi-Fi chevauchant les canaux LoRa.

L'ensemble des contributions de cette thèse repose sur le principe de reproductibilité. Nous avons également appliqué ce principe à l'état de l'art de cette thèse. Nous avons donné une description générale de notre méthodologie dans l'introduction du manuscrit de cette thèse et nous avons détaillé l'ensemble du processus d'analyse systématique de la littérature (SLR) que nous avons appliqué en annexe. Notre travail étant principalement basé sur des expériences, nous avons rencontré plusieurs difficultés, qui sont également énumérées en annexe. Les résultats de nos expériences sont extrêmement dépendants de l'endroit où nous les réalisons. Par conséquent, le fait de fournir le code mis à disposition du public, de la passerelle et des nœuds LoRa, ainsi qu'une méthodologie détaillée (références des

équipements, modus operandi, etc.) et les données de nos expériences, permet à la communauté industrielle et scientifique de réutiliser notre travail pour évaluer d'autres types d'environnements, de métriques ou de paramètres. De ce fait, une comparaison équitable entre les résultats est possible formant ainsi une base commune d'observations pour le déploiement futur de LoRa dans la bande ISM 2.4 GHz.

Contents

List of publications

Journals:

[1] Gwendoline Hochet Derévianckine, Alexandre Guitton, Oana Iova, Baozhu Ning, and Fabrice Valois. "Opportunities and Challenges of LoRa 2.4 GHz". In: *IEEE Communications Magazine* 61.10 (Oct. 2023), pp. 164–170.

International conferences:

[2] Carlos Fernández Hernández, Gwendoline Hochet Derévianckine, Alexandre Guitton, Oana Iova, and Fabrice Valois. "Indoor Performance Evaluation of LoRa® 2.4 GHz". In: *IEEE WCNC.* United Kingdom, 2023.

National conferences:

[3] Gwendoline Hochet Derévianckine, Alexandre Guitton, Oana Iova, Baozhu Ning, and Fabrice Valois. "Mais qui se cache ici?" In: *CoRes 2024 - 9èmes Rencontres Francophones sur la Conception de Protocoles, l'Évaluation de Performance et l'Expérimentation des Réseaux de Communication.* In French. France, 2024.

[4] Carlos Fernández Hernández, Gwendoline Hochet Derévianckine, Alexandre Guitton, Oana Iova, and Fabrice Valois. "On a testé pour vous : LoRa 2.4 GHz à l'intérieur". In: *CoRes 2023 - 8èmes Rencontres Francophones sur la Conception de protocoles, l'évaluation de performances et l'expérimentation de Réseaux de communication.* In French. France, 2023.

Submissions:

[5] Gwendoline Hochet Derévianckine, Alexandre Guitton, Oana Iova, Baozhu Ning, and Fabrice Valois. "Hate or Love in the 2.4 GHz ISM band: The Story of LoRa and IEEE 802.11g". under review. Nov. 2023. Major Revision submitted on Sept. 2024.

Presentations

[1] **LPWAN Days 2024**, presentation about "Experimental results on the coexistence of LoRa and Wi-Fi." – Pau, July 2024

[2] **Journées non Thématiques du GDR-RSD 2023**, presentation about "From the coexistence of LoRa 2.4 GHz" – Lyon, January 2023

[3] **LPWAN Days 2022**, presentation about "LoRa 2.4 GHz: a methodology to study coexistence in the 2.4 GHz ISM band" – Toulouse, July 2022

[4] **Journées non Thématiques du GDR-RSD 2022**, presentation about "LoRa 2.4 GHz: characteristics and performance evaluation" – Rennes, April 2022

List of Figures

List of Tables

Glossary

ACK Acknowledgement

ADR Adaptive data rate

AP Access point

AWGN Additive white Gaussian noise

BER Bit error rate

BLE Bluetooth Low Energy

BR Basic rate

BT Bluetooth

BW Bandwidth

CAP Contention access period

CBR Constant bit rate

CFP Contention-free period

CNN Convolutional neural network

COTS Commercial off the shelf

CR Coding rate

CSMA/CA Carrier sense multiple access with collision avoidance

CSS Chirp spread spectrum

D2D Device-to-device

DFNN Deep feedforward neural network

DSSS Direct-sequence spread spectrum

EDR Enhanced data rate

ETSI European Telecommunications Standards Institute

FCC Federal Communications Commission

FDMA Frequency division multiple access

FDR Frame delivery ratio

FFD Full-function device

FFT Fast Fourier Transform

FH Frequency hopping

FHSS Frequency hopping spread spectrum

GTS Guaranteed timeslot

IoT Internet of Things

ISM Industrial, scientific, and medical

ITU International Telecommunication Union

LBT Listen-before-talk

LE Low Energy

LoRa Long range

LoS Line-of-sight

LPWAN Low-Power Wide-Area Network

LR-FHSS Long-range frequency hopping spread spectrum

LTE Long term evolution

MCS Modulation coding scheme

MIMO Multi-input multi-output

MTU Maximum transmission unit

NLoS Non line-of-sight

OFDM Orthogonal frequency-division multiplexing

PAN Personal area network

PDR Packet delivery ratio

PER Packet error rate

PLR Packet loss ratio

PRR Packet reception rate

QoS Quality of service

RFD Reduced-function device

RSSI Received signal strength indication

SER Symbol error rate

SF Spreading factor

SFD Start of frame delimiter

SG-HAN Smart grid home area network

SINR Signal-to-interference-plus-noise ratio

SIR Signal-to-interference ratio

SLR Systematic literature review

SNR Signal-to-noise ratio

SoA State of the art

SUN Smart utility networks

TDD Time-division duplex

TDMA Time-division multiple access

ToA Time on air

USRP Universal software radio peripheral

WBAN Wireless body area network

WLAN Wireless local area network

WPAN Wireless personal area network

Chapter 1

Introduction

This manuscript aims to answer research questions around the feasibility and performance of a LoRa 2.4 GHz network. In the next sections, we present the context of this thesis along with the motivations behind our contributions. We also provide the methodology and the code used to produce the contributions presented in this manuscript. Finally, we highlight the outline of this manuscript.

1.1 Context

In the last decade, the Internet of Things (IoT) has gained global momentum. One of the aims of IoT is to improve our daily lives. Typical applications include climate change monitoring, smart metering, asset tracking, intelligent building, and smart cities [1]. Long range (LoRa)® [2], NB-IoT [3], and Ingenu [4] are examples of wireless technologies dedicated to the IoT and are grouped under the name Low-Power Wide-Area Networks (LPWANs). Industries and telecommunication operators around the world are deploying these new technologies for several reasons: (i) they answer the needs of a large variety of IoT applications, (ii) they can transmit data packets over several kilometers at low data rates (a few hundred bits per second), which helps reduce the cost of deployment of an LPWAN, (iii) the low-power consumption, the low cost of radio chips, and the overall low complexity of LPWAN architectures make their deployment and maintenance easier.

LoRa, combined with the LoRaWAN ® [5] protocol, are one of the most representative LPWANs that have flooded the market. They are widely used for low power IoT data collection in wide areas. LoRa typically operates on license-free sub-GHz bands around the globe, which makes it region-specific [6]. Depending on the country, regulations for these sub-GHz bands (e.g., 868 MHz in Europe, 915 MHz in North America) specify different frequency channels, maximum transmission time, maximum transmission power, and different medium access mechanisms such as duty-cycle or listen-before-talk (LBT). These parameters must be considered in hardware components and communication protocol design. These specificities can hinder the deployment of LoRa technology if the applications do not comply with regulations.

In 2017, in an effort to overcome these problems, Semtech[1] released a version of LoRa for the 2.4 GHz industrial, scientific, and medical (ISM) band. This version has spurred interest in the scientific community, as it enables the construction of a LPWAN that benefits from global interoperability and no duty-cycle limitation. The advantage of the 2.4 GHz ISM band is that a LoRa chip can be deployed everywhere in the world as this spectrum has a large set of channels shared by all countries, and also several common physical layer parameters such as the maximum transmission power.

1.1.1 Hardware characteristics and interests of LoRa 2.4 GHz

The extension of LoRa to the 2.4 GHz ISM band stems from hardware characteristics.

Single hardware and software: LoRa 2.4 GHz enables and simplifies the use of the same hardware everywhere in the world. While LoRa sub-GHz chips can now deal with all sub-GHz ISM bands, i.e., one chip irrespective of the region of the LoRa sub-GHz network deployment, the whole system still needs to have different RF configurations and different firmwares, because of differences in the LoRaWAN standard depending on the region of deployment. LoRa 2.4 GHz constructors can design, manufacture, test, stock, and sell a single system, which ultimately reduces the cost of the devices. Similarly, the software implementation of the network protocol becomes simpler and unique. Hardware and software certifications become easier to obtain for manufacturers, which reduces their capital expenditures. Also, the users can buy any LoRa 2.4 GHz chip and deploy it anywhere without having to take into consideration the deployment region beforehand.

Smaller sensor size: The wavelength of the 2.4 GHz ISM band is about a third of the wavelength of the sub-GHz band, which means the antenna size of LoRa 2.4 GHz devices is significantly smaller than with LoRa sub-GHz. This reduces the overall size of the end-device and allows a smaller and better integration of IoT devices, where miniaturization is a compelling requirement.

The use of LoRa in the 2.4 GHz ISM band also raises technical and scientific interests.

Better channel usage: LoRa 2.4 GHz does not have duty-cycle limitations, contrarily to some regional regulations for the sub-GHz band (e.g., 1% of the duty-cycle in Europe): a LoRa 2.4 GHz device can send data at any time, or ideally when the medium is free. In a LoRa 2.4 GHz network a device can use a channel to its full extent, regardless of whether the channel is used or not.

Lower impact of the overhead: The increase in the data rate of LoRa 2.4 GHz, compared to LoRa sub-GHz, enables the increase of the maximum payload size of packets, thus reducing the relative cost of the overhead caused by preambles and header.

Robustness to interference: Given the high robustness of the LoRa modulation, it is likely that LoRa 2.4 GHz communications will be able to be demodulated even in the presence of interference from other technologies, under specific conditions [7].

[1] Semtech and LoRa are registered trademarks or service marks of Semtech Corporation or its affiliates.

1.1.2 New applications for LoRa 2.4 GHz

While LoRa 2.4 GHz and LoRa sub-GHz are very similar, the version of LoRa dedicated to the 2.4 GHz ISM band allows the support of new applications.

Global roaming and tracking applications: The availability of a worldwide, single radio frequency band with shared configuration parameters eases the emergence of worldwide applications for LoRa 2.4 GHz. These applications can run anywhere, anytime, with a single hardware and software, without the adaptations due to regulations on regional radio frequency use. Examples include applications where the devices can operate in multiple regions where a maximum range of a few hundred meters is enough, in opposition to several kilometers as offered by LoRa sub-GHz. Such applications are global roaming and global tracking applications (e.g., maritime or air transport), where the location of the monitored objects (including goods, animals, and persons) is followed regularly. The monitored objects can now seamlessly cross the boundaries of countries or regions, thus opening the path for worldwide interoperability for IoT devices and applications.

Lower latency: LoRa 2.4 GHz can achieve low latency in packet transmission, as there is no duty-cycle limitation. The large latency of LoRa sub-GHz is one of its main drawbacks for some applications. With LoRa 2.4 GHz, it is possible to consider applications with a typical latency of up to tens of milliseconds.

Higher data rate: There is no duty-cycle limitation in the 2.4 GHz ISM band and a larger data rate can be obtained by LoRa 2.4 GHz compared to LoRa sub-GHz. When combining these two characteristics, it is possible to transmit multimedia content (such as sound or images) or to implement IoT applications with data rates of a few hundred kilobits per second.

High precision ranging: The use of higher bandwidths (BWs) in LoRa 2.4 GHz enables a highly accurate ranging mechanism up to 2 m. This enables in turn high accuracy localization, as well as new localization-based applications, including accurate object tracking [8]. Note that the accurate ranging feature is native in Semtech's SX1280 chip [9].

1.1.3 Challenges of LoRa 2.4 GHz

However, LoRa 2.4 GHz also has some disadvantages and has to face several challenges.

LoRa 2.4 GHz works in a widely used frequency band, alongside Wi-Fi and Bluetooth (BT). This leads to a huge possibility of interference between technologies. Hence, the main challenge of LoRa 2.4 GHz is the coexistence with other radio technologies already occupying the 2.4 GHz ISM band. This brings up a series of considerations that can make the success or break of LoRa 2.4 GHz.

Channel allocation. Semtech has proposed the use of LoRa 2.4 GHz in conjunction with a protocol emulating LoRaWAN with three mandatory channels. We explain in Section 2.3 that these channels are located in a part of the spectrum outside of Wi-Fi's most common channels and between two consecutive Bluetooth Low Energy (BLE) channels. However,

this choice has not been validated yet and needs to be studied. Moreover, it is still possible for Wi-Fi channels to completely overlap LoRa 2.4 GHz channels.

Interference mitigation. Cross-technology interference can limit the performance of technologies working in the same frequency band and having overlapping channels. It is of uttermost importance to evaluate and characterize the type of interference of other technologies on LoRa 2.4 GHz and vice-versa, so that we can design appropriate interference avoidance mechanisms. For example, we can imagine that LoRa transmissions happen during a small Wi-Fi silent time.

Demodulation. Because the LoRa modulation is robust and largely different from the other modulations in the 2.4 GHz ISM band, it might be possible for a LoRa 2.4 GHz frame to be demodulated with a low signal-to-noise ratio (SNR), even if a frame with a higher SNR is transmitted by another technology. To increase the connectivity (compute as the frame delivery ratio (FDR)) it will be very useful to design strategies that help recover LoRa signals in the presence of simultaneous cross-technology transmissions.

Cross-technology transmission. The coexistence of multiple technologies can also have some benefits. It is possible to modify the physical layer of a given technology to allow a transmitter to send frames that can be detected or decoded by the receiver of another technology. For instance, Li et al. propose to exploit the frequency hopping of BLE to emulate LoRa 2.4 GHz chirps [10]. Hence, BLE devices can notify LoRa 2.4 GHz devices of their presence. This type of exchange can help devices from different technologies make informed decisions and thus improve their coexistence.

Cognitive radio. To leverage the complexity of the competition in the 2.4 GHz ISM band, cognitive radios [11] can be used to adapt the physical layer configuration of LoRa 2.4 GHz to the environment. For instance, the channels could be dynamically shifted to increase the SNR, and LoRa parameters (spreading factor (SF), BW, coding rate (CR)) could be adapted based on the information from previous packet transmissions. Dynamically adapting the length of the data frames also achieves a trade-off between survivability and detectability as short data frames tend to collide less than long data frames which in turn are typically easier to detect by other technologies.

Another important challenge is related to the development of new hardware to support the efficient deployment of LoRa networks in the 2.4 GHz ISM band, as well as the software that goes with it.

Complex radio front-ends. Designing the radio front-ends for LoRa 2.4 GHz is difficult for several reasons. First, LoRa 2.4 GHz uses much larger bandwidths (typically, 812 kHz or 1625 kHz) than LoRa sub-GHz (typically, 125 kHz). Second, the available bandwidth in the 2.4 GHz ISM band is 80 MHz, which is very large and is not likely to be covered by a single low-cost front-end. A possible design of the LoRa 2.4 GHz gateway is to have several front-ends, each on a relatively small bandwidth (say 1 MHz), and followed by a base-band concentrator chip which can detect and demodulate multiple packets of different SFs and channels in parallel.

Parallel reception. Current LoRa 2.4 GHz gateways are based on the SX1280 chip [9], and can only listen to three configurations (SF/BW/channel) at the same time. It is likely that in the future, gateways will have to be able to receive more transmissions in parallel, as it is already the case in LoRa sub-GHz with 8, 16, or 64 (United States only with the SX1302 chip [12]) parallel reception paths. Moreover, since downlink communications often limit the network capacity and can also have a negative impact on uplink communications (LoRa gateways cannot receive and transmit packets at the same time) [13], full-duplex solutions should be imagined.

Multi-mode radios. We believe that LoRa 2.4 GHz networks will not replace LoRa sub-GHz networks, but could complement the actual standard with additional flexibility: on the one hand, LoRa sub-GHz provides large coverage but uses regional parameters, and on the other hand, LoRa 2.4 GHz has higher throughput and a single world-wide setting. These two technologies address different use cases. Semtech recently launched a new LoRa radio chip (LR1120) [14] that supports both LoRa sub-GHz and LoRa 2.4 GHz (and furthermore the long-range frequency hopping spread spectrum (LR-FHSS) modulation that targets satellite communications). The collaborative scenarios between the two bands are still to be assessed according to applications and use cases. It will require the development of appropriate software. Studies will have to define how to share and take advantage of the information learned from using different settings, and also if dual-band devices will need to run two MAC protocols in parallel.

Relay nodes. While relays are already used in some LoRa sub-GHz networks, these are isolated scenarios (e.g., for underground communication). Relays may become common in LoRa 2.4 GHz as they will help reach devices far away from the gateways. This will add an extra degree of complexity to the topology. Note, that the use of relays can be extended to support device-to-device (D2D) communications. Lumet et al. have already investigated the gain of using relays in a LoRa sub-GHz network, while keeping a low energy consumption, thus providing useful insights for LoRa 2.4 GHz on possible data aggregation techniques, lightweight relaying or even design of new routing protocol [15].

Finally, LoRa 2.4 GHz has a lower communication range compared to LoRa sub-GHz, especially in indoor scenarios. This comes from the fact that the 2.4 GHz ISM band has a higher attenuation when penetrating buildings or passing through walls and floors. Still, its communication range remains larger than other low-power technologies that operate in the 2.4 GHz ISM band. Presently, there is no amendment to LoRaWAN for the specific use of LoRa 2.4 GHz, which can be seen as a disadvantage and as an opportunity at the same time. Indeed, to the best of our knowledge, the LoRaWAN protocol is currently emulated above the physical layer of LoRa in the 2.4 GHz ISM band through an additional set of parameters [16].

We summarize all the challenges we presented in Table 1.1. In the rest of this manuscript, we focus on the channel allocation and the interference mitigation challenges.

Challenge	Category of challenge	
	Technology coexistence	Hardware related
Channel allocation	X	
Interference mitigation	X	
Cross-technology transmission	X	
Cognitive radio	X	
Complex radio front-ends		X
Parallel reception		X
Multi-mode radios		X
Relay nodes		X

TABLE 1.1: Challenges of LoRa 2.4 GHz and focus of the manuscript.

1.2 Motivation

The main goal of this manuscript is to study the feasibility of a LoRa network in the 2.4 GHz ISM band. We focus on the performance of this new version of LoRa more precisely in terms of connectivity and communication range in two types of environments: indoor and outdoor. We also focus on the coexistence of LoRa with Wi-Fi in the 2.4 GHz ISM band.

The LoRa Alliance® has shown interest in deploying LoRa networks in private networks instead of the usual public networks targeted until now. This implies that the environment of deployment is moved from industry to home. This is also an opportunity to transfer the LoRa technology from the sub-GHz frequency bands to the 2.4 GHz ISM band.

We outline the research questions that we raise to address our research goal.

Research Goal: To study the feasibility of a LoRa network in the 2.4 GHz ISM band.

Research Questions: The following research questions are general and guide our manuscript. We detailed in each chapter of contributions more specific research questions to answer our research goal.

RQ-1: Is LoRa able to communicate (transmitting and receiving) data in the 2.4 GHz ISM band?

RQ-2: What is the performance, in terms of connectivity and communication range, of LoRa 2.4 GHz compared to LoRa sub-GHz?

RQ-3: How does LoRa coexists with the other wireless technologies of the 2.4 GHz ISM band?

RQ-4: Is it possible to improve the coexistence of LoRa in the 2.4 GHz ISM band by implementing interference mitigation mechanisms at the physical layer?

1.3 Methodology of the thesis

For several years, the scientific community has shown interest in reproducible science. The definition of reproducibility is highly dependent on the domain of application [17] [18]. When defining reproducibility, there are four words that are not synonyms:

- **Repeatability:** research team 1 can re-run the same experiments with their algorithms and obtain the same results as before,
- **Replicability:** research team 2 can run the same experiments using the tools and equipment, described in a paper, and obtain the same results as the authors of the paper,
- **Reproducibility:** research team 2 can collect similar data and obtain the same results using their own tools that are different from the paper,
- **Reusability:** research team 2 improves the tools of the paper or reuses them to solve a different problem.

The difficulty of reproducibility increases from repeatability to reusability. In this manuscript, we define reproducibility as "the ability of a third party to reproduce the results of a scientific work published, for example, in a journal" [17].

1.3.1 Reproducibility in experiments

All the results presented in the next parts of this manuscript are obtained through real-world experiments and simulations. Our simulations are based on our experiment results. The available studies on LoRa in the 2.4 GHz ISM band are either theoretical or do not provide sufficient information to be reproducible. Thus, we focus on producing repeatable and replicable experiments. This rigorous approach to our work implies the use of commercially available hardware, and the provision of all code and experimental data when not submitted to a proprietary license.

1.3.2 Reproducibility applied to the state of the art

In this manuscript, we focus on the novelty and the coexistence challenges raised by LoRa for the 2.4 GHz ISM band. As the state of the art (SoA) is very different and sometimes very limited, we decided to include the corresponding SoA in each chapter. In that way, the reader will have a reminder of the available literature regarding the topic of each of our contributions. It also helps keep our message clear throughout this manuscript.

We extend to the SoA our will to produce contributions that are repeatable and replicable. We searched for a method to select the articles of our SoA that would produce the same set of articles if someone else applied the same method as we did. Thus, we decided to apply a systematic literature review (SLR) process [19] to choose the articles that are relevant depending on the focus of our work.

The different steps of a SLR process are the same irrespective of the literature domain we apply it on (see Figure 1.1).

First, we search keywords in databases that usually belong to the publishers of our scientific community, e.g., ACM and IEEE. We search articles corresponding to the combination of the words that summarize best our focus of interest, e.g., "LoRa" and "interference". We can also

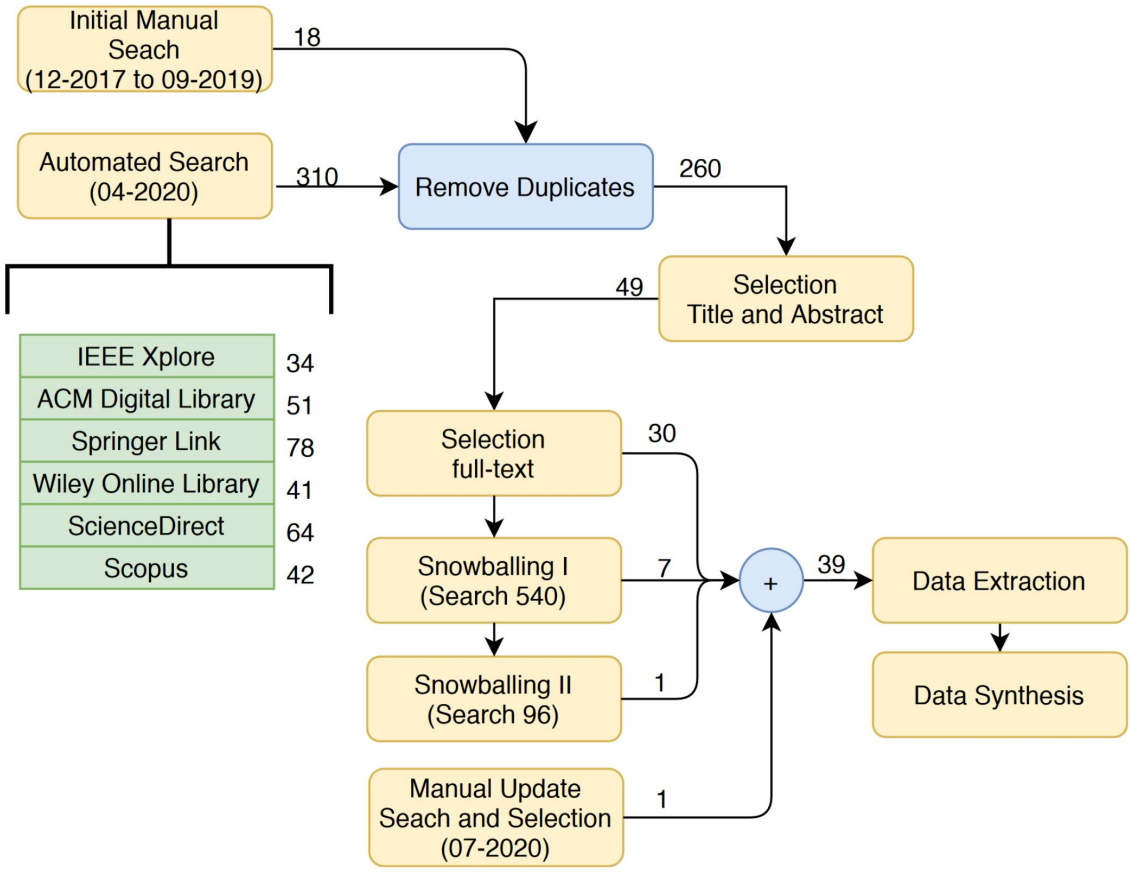

FIGURE 1.1: Example of a SLR process steps [19].

add papers manually that correspond to alerts or RSS feeds. Usually, these alerts are defined to keep abreast of recent papers published on our focus of interest. We then define inclusion criteria to select the potential papers of our SoA. In our case, we have different SoA along the manuscript. Thus, we first define mandatory inclusion criteria for all the papers of our SoAs, and then add specific criteria depending on the focus of our contribution.

This gives us a certain number of papers but with a possibility of having duplicated papers. Indeed, the different databases that we interrogate to retrieve papers can reference the same papers depending on the journals or the conferences where articles are published. We evaluate only one occurrence of each paper by removing the duplicates.

Second, we manually evaluate each article based on the title and the abstract using exclusion criteria. The exclusion criteria are defined in the same way as the inclusion criteria.

An optional step is to classify the articles depending on the rank of the conference or the journal where the study was published, e.g., A* conferences, and Q1 journals.

However, whether we apply the optional step or not, after applying the exclusion criteria there are two options. If the number of articles is sufficient to highlight the key results of the literature, we end our SLR process at this point. If we consider that the selected articles leave uncertainty on some parts of our contribution, e.g., methodology, we also keep the

non-ranked conferences/journals, or the articles with a high number of citations, and manually evaluate the relevance of the studies. Note that the criteria for the number of citations is set arbitrarily. In the latter case, we perform a full-text evaluation on all papers. We keep the studies according to the gap we wanted to fill by defining additional inclusion criteria and adding these articles in our SoA.

In this manuscript, we considered that 30 articles are sufficient to provide the key results of the literature. Note that, for each of our SoA, we never had a lower number of articles after the exclusion step. Thus, we do not need to go through the additional full-text evaluation step.

To summarize, a SLR process follows five steps, the first three are mandatory: (1) searching in databases, (2) defining inclusion criteria, (3) defining exclusion criteria, (4) classifying the papers, and (5) defining new inclusion criteria to fill a gap in the already selected papers.

We describe the general steps of our SLR process in Appendix A. We also highlight the additional parameters we use to pick the articles we included, or excluded, in our SoA for each chapter. We decided not to include the different criteria directly in the chapter to keep the readability of this manuscript.

1.4 Contributions

We summarize our contributions in this manuscript as follows:

1. We make the first experimental performance evaluation, in both outdoor and indoor environments, comparing LoRa 2.4 GHz and LoRa sub-GHz communication range and reliability. We provide the design and a real-world implementation of our performance evaluation.
2. We make the first experimental study on the mutual impact of LoRa 2.4 GHz and Wi-Fi overlapping transmissions. Moreover, we provide a methodology to study the coexistence of two wireless technologies. We provide the design and a real-world, and simulation, evaluation.
3. We design a frequency hopping (FH) algorithm for improving the coexistence of LoRa 2.4 GHz and Wi-Fi. We provide the design, a homemade simulator implementation, and an evaluation by simulation.
4. We design an original methodology to characterize a radio environment. We provide the design and a preliminary real-world evaluation.

1.5 Outline of the manuscript

The remainder of this manuscript is organized into a technical background, three chapters of contributions, and a conclusive and future work chapter.

In Chapter 2, we provide the technical background of this manuscript. We start by presenting the general features of the 2.4 GHz ISM band. We highlight that this frequency band is used by many wireless technologies. We present the main wireless technologies that could interfere with and degrade the performance of LoRa in the 2.4 GHz ISM band: BT®, BLE®, the IEEE 802.15.4 standard, and the IEEE 802.11 set of standards. Finally, we overview the LoRa technology, and the LoRaWAN protocol, and introduce the novelty of LoRa 2.4 GHz.

In Chapter 3, we investigate the performance of LoRa, in terms of connectivity and communication range, and we evaluate the feasibility of a network in the 2.4 GHz ISM band. At first, we exhaustively study the impact of the LoRa parameters on performance in an indoor environment. Secondly, as LoRa has been widely studied in the sub-GHz bands, we perform experiments in outdoor and indoor environments and compare the results of LoRa in both frequency bands (sub-GHz and 2.4 GHz). Finally, we assess the impact of the environment and daily life activities, such as the presence of people in the building or the wireless technologies usage, on the LoRa communications in the 2.4 GHz ISM band.

In Chapter 4, we investigate the coexistence of LoRa and Wi-Fi in the 2.4 GHz ISM band. We conceive a methodology to study the coexistence of two wireless technologies. We implement it on commercial off the shelf (COTS) devices and we investigate several parameters (PHY layer parameters, topology, version of the IEEE 802.11 standard) to provide the results for both technologies. We end the chapter by giving recommendations and highlighting good practices for future LoRa deployments in the 2.4 GHz ISM band.

In Chapter 5, we propose to improve the coexistence of LoRa and Wi-Fi in the 2.4 GHz ISM band by implementing FH mechanisms for LoRa transmissions. We design a homemade simulator to evaluate the benefits of our proposal. Based on our experimental results, we extract a theoretical model of the behavior of LoRa and Wi-Fi when there are overlapping transmissions. After validating our simulator, we analyze the performance gain of three FH approaches: a random FH and a round-robin FH using the three LoRa channels proposed by Semtech for the 2.4 GHz ISM band, and a random FH using the three best channels available in the frequency band, i.e., the less noisy channels. We also propose an original methodology to characterize a radio environment that can be used to select the channels of our random FH best channels strategy. It consists of scanning a frequency band and analyzing the sample energy to evaluate if there is a signal or not. Then, we manually associate the signal, using the BW, to a wireless technology of the 2.4 GHz ISM band. We also propose the protocol that could be implemented on LoRa devices to have a hardware implementation of our coexistence improvement proposal.

Finally, in Chapter 6, we provide our final conclusions and we highlight future work and improvements regarding the topic of this manuscript.

Chapter 2

Technical background

2.1 Introduction

In this chapter, we present the main technical concepts on which our contributions are based. First, we introduce the general characteristics of the 2.4 GHz ISM band. Then, we emphasize on the already existing wireless technologies using the 2.4 GHz ISM band, highlighting Wi-Fi as it is the main wireless technology deployed in this frequency band. We also present the LoRa technology insisting on the evolution brought by LoRa 2.4 GHz.

2.2 The 2.4 GHz ISM band and its technologies

Contrary to the sub-GHz ISM frequency bands that differ from one region to another, e.g., 863 to 870 MHz in Europe, and 902 to 928 MHz in North America, the 2.4 GHz ISM band is publicly available in most countries. The 2.4 GHz ISM band is typically the favorite choice for deploying wireless technologies without a license.

2.2.1 The 2.4 GHz ISM band

The ISM frequency bands are defined by the International Telecommunication Union (ITU) Radio Regulations (see article 5 from [20]) for non-communication purposes. Each country adapts the radio regulations article depending on national, or continental, limitations. For instance, in the United States, the Federal Communications Commission (FCC) describes the rules of the ISM bands, and in particular the allowed frequencies and maximum transmission power. In Europe, the European Telecommunications Standards Institute (ETSI) has the same role as the FCC.

Nowadays, one of the most popular devices using the 2.4 GHz ISM band is the microwave oven. Other devices are cordless phones, garage door openers, or baby monitors. More recently, the IoT community has shown interest in using ISM bands with technologies such as Z-Wave [21] and LoRa. Even if the initial purpose of the ISM bands was not for communication usage, their unlicensed properties make them appealing for telecommunications applications.

The counterpart of using the ISM bands is that the technologies must tolerate interference from (1) other users of the same technology, and (2) users of other technologies in the same frequency band. This raises coexistence challenges that need to be addressed, especially as the 2.4 GHz ISM band is known to be an overcrowded frequency band (see Figure 2.1) mainly used by short-range wireless communications systems.

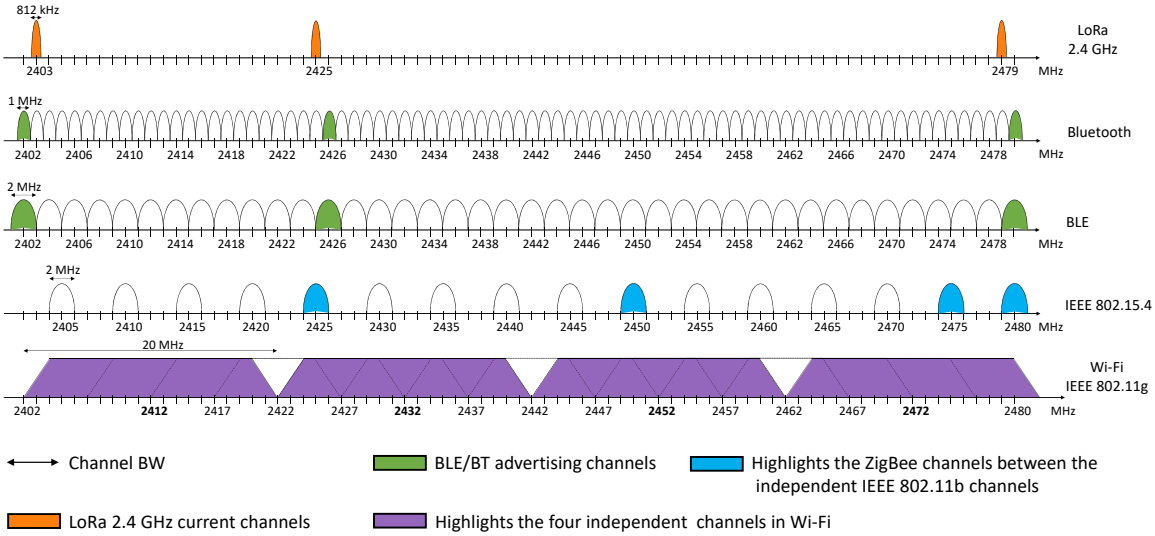

FIGURE 2.1: Spectrum occupancy of LoRa and the main wireless technologies using the 2.4 GHz ISM band.

The 2.4 GHz ISM band range from 2400 MHz to 2483.5 MHz thus offering a total bandwidth of 83.5 MHz. Figure 2.1 illustrates the characteristics (channels and bandwidth) and the co-existence challenges of the main wireless technologies using the 2.4 GHz ISM band: BT, BLE, IEEE 802.15.4, and IEEE 802.11g (the latest IEEE 802.11 standard designed for the 2.4 GHz ISM band only). We also represent the Semtech proposal for LoRa channels in the 2.4 GHz ISM band. These five technologies are different in terms of frequency channels, bandwidth, maximum transmission power, modulation, and MAC layer, as described in Table 2.1. We notice that these five wireless technologies overlap and thus are exposed to cross-technology interference. Note that depending on the IEEE 802.11 standard used, e.g., IEEE 802.11b and IEEE 802.11g, the bandwidth varies.

Technology	Number of channels	Overlapping channels?	Bandwidth (in kHz)	Maximum transmission power (in dBm)	PHY layer	MAC layer
LoRa	3	No	203, 406, 812, or 1625	13	CSS	Aloha
Bluetooth	79	No	1000	20	FHSS with GFSK	TDD
BLE	40	No	2000	10	FHSS with GFSK	FDMA or TDMA
IEEE 802.15.4	16	No	2000	18	DSSS with O-QPSK	IEEE 802.15.4 standard
IEEE 802.11b	13	Yes	22000	20	DSSS with CCK	CSMA/CA
IEEE 802.11g	13	Yes	20000	20	OFDM	CSMA/CA

TABLE 2.1: General characteristics of the main wireless technologies using the 2.4 GHz ISM band.

Regarding the propagation properties of the 2.4 GHz ISM band, due to the higher frequencies used the signal propagation is more subject to attenuation due to obstacles such as walls and trees. This is explained by the wavelength of the 2.4 GHz ISM band (see Equation 2.1). The 868 MHz frequency band has a wavelength of approximately 34.5 cm while the 2.4 GHz ISM band has a wavelength of approximately 12.5 cm, which is almost 3 times shorter and results in a shorter communication range.

$$\lambda = \frac{c}{f} \tag{2.1}$$

where:

c = the speed of light in m/s $\approx 3 \times 10^8$
f = the wave frequency in Hz

The regulation of the 2.4 GHz ISM band aims to avoid excessive interference. This is possible by limiting the transmission power or using modulation that minimizes interference. For example, Wi-Fi and BT devices have a maximum transmission power of 20 dBm (100 mW). The first generation of Wi-Fi (IEEE 802.11b) uses a spread spectrum modulation called direct-sequence spread spectrum (DSSS), while BT uses frequency hopping modulation called frequency hopping spread spectrum (FHSS).

In Table 2.1 we highlight two IEEE 802.11 standards: IEEE 802.11b [22] and IEEE 802.11g [23]. One of the main differences between the two standards is the physical layer (DSSS for IEEE 802.11b and orthogonal frequency-division multiplexing (OFDM) for IEEE 802.11g) but also the bandwidth they use. The IEEE 802.11b standard defines channels that are 22 MHz wide, while the IEEE 802.11g standard defines channels that are 20 MHz wide. However, according to the American channel plan, both standards have the same three independent channels: channels 1, 6, and 11 centered at 2412 MHz, 2437 MHz, and 2462 MHz respectively. More details on the IEEE 802.11 set of standards are provided in Subsection 2.2.2.

In this manuscript, we are interested in LoRa transmissions in the 2.4 GHz ISM band, which also have their own properties from existing technologies that use this frequency band. For example, Wi-Fi uses the 80 MHz band of the 2.4 GHz spectrum with 20 MHz bandwidth channels, while the largest available bandwidth for LoRa is 1625 kHz. In this context, Semtech proposed three channels for LoRa [16], located 1 MHz away from the Bluetooth advertising channels, and at the edge of the IEEE 802.11b independent channels.

Analyzing the 2.4 GHz ISM band occupancy is of uttermost importance to validate this choice of channels for LoRa, as well as to allow a fair deployment for the original users of this frequency band.

2.2.2 Technologies of the 2.4 GHz ISM band

We have seen that the 2.4 GHz ISM band is largely used by radio technologies. However, they are not all equally documented. Except for the main standards for wireless communications, there are a lot of other proprietary technologies using the 2.4 GHz ISM band, which are little or not at all documented. This is generally the case for applications such as garage door remote controls, babyphones, or microwave ovens. Consequently, it is difficult to know if the 2.4 GHz ISM band is used and by what technology at a given time.

We propose a quick overview of BT, BLE, IEEE 802.15.4, and Wi-Fi (based on the IEEE 802.11 set of standards) as they are the most popular wireless technologies of the 2.4 GHz ISM band.

Bluetooth

Bluetooth [24] is a short-range (less than 10 meters) wireless technology released in 1999. It was designed to replace the cables connecting fixed electronic devices. Nowadays, BT is a common technology to connect cellphones with portable stereo speakers. Devices need to establish a connection to exchange data. The energy consumption of BT is approximately 1 W.

The original version of BT is known as basic rate (BR) and offers a data rate of 721.2 kbps. It includes an optional extension, named enhanced data rate (EDR), providing a data rate of 2.1 Mbps. Data packets are sent using a frequency hopping pattern, which can be adapted to exclude a portion of the frequency spectrum that is used by interfering devices. BT sub-divides the physical channel into time units called slots. Data is transmitted in slots after accessing the medium following a time-division duplex (TDD) scheme.

Bluetooth Low Energy

In 2010, a low-energy version of Bluetooth, named Bluetooth Low Energy, was released. BLE is designed for Internet of Things applications and is based on the original version of BT called basic rate. The energy consumption of BLE is comprised between 0.1 and 0.5 W.

BLE uses the same frequency hopping approach as BT. Both sub-divide the physical channel into time units called events in BLE. Data is transmitted in events after accessing the medium following either a frequency division multiple access (FDMA) or a time-division multiple access (TDMA) scheme.

There are four possibilities for the physical layer of BLE, called Low Energy (LE):

- LE 1M, which is mandatory and offers a data rate of 1 Mbps,
- LE 2M, which doubles the data rate of LE 1M thus offering a data rate of 2 Mbps,
- LE Coded, which uses a coding scheme:
  - S = 2 symbols/bit which allows doubling the range of LE 1M at the expense of a decrease of the data rate to 500 kbps,

- S = 8 symbols/bit which allows quadrupling the range of LE 1M at the expense of a decrease of the data rate to 125 kbps.

In Table 2.1 we presented the only difference between BT and BLE regarding the number of channels and bandwidth: 79 channels of 1 MHz wide for BT and 40 channels of 2 MHz wide for BLE. Both versions proposed three channels for advertising, which can be compared to the Wi-Fi beacon, and the remaining channels are for data.

Additional information can be found in the specification of the BT technology [24] which also contains the BLE specification.

IEEE 802.15.4

The first IEEE 802.15.4 standard was ratified in 2003 [25] and targeted low power consumption, short range, and low throughput devices. The standard defines the PHY layer and the MAC layer specifications.

The initial version of the standard provided two optional PHY layers dedicated to two different frequency bands and a MAC layer. The last version, ratified in 2020, proposes six PHY layers with different coding schemes depending on the targeted application. The data rate also depends on the PHY layer and is between 4.8 and 500 kbps. The features of the PHY layer are among others the activation and deactivation of the radio transceiver, the energy detection, and the link quality indication.

The features of the MAC layer are among others the channel access, the association and dissociation, and the acknowledged frame delivery. A device receiving a beacon frame, which is transmitted by the coordinator of the IEEE 802.15.4 network, can respond with a request to join the network. Once the device has joined the network, it transmits periodic beacons to allow neighbor devices to join the same network. Between two beacons there are two periods of time where devices can communicate: the contention access period (CAP) and the contention-free period (CFP). The CAP starts immediately after the beacon. During the CAP the devices can randomly access the medium following a slotted carrier sense multiple access with collision avoidance (CSMA/CA) mechanism. The slot that starts after the CAP corresponds to the beginning of the CFP which is composed of portions called the guaranteed timeslots (GTSs).

An IEEE 802.15.4 network is composed of two types of devices: full-function devices (FFDs) and reduced-function devices (RFDs). An FFD is a device capable of acting as a personal area network (PAN) coordinator and routing packets, while a RFD does not have these features. Thus, an RFD is designed for applications with resource and memory constraints such as a light switch or a passive infrared sensor.

Two topologies are allowed to deploy an IEEE 802.15.4 network depending on the application requirements: the star topology and the peer-to-peer topology. In the star topology, the communication is established between devices and the PAN coordinator. The peer-to-peer topology adds the possibility for devices to communicate with each other directly as long as

they are in the range of one another. Thus, the peer-to-peer topology allows more complex networks such as mesh network topology.

The IEEE 802.15.4 standard is the basis of several protocols, which define the upper layers that are not covered by the standard, such as ZigBee [26], WirelessHART [27], or 6LowPAN [28]. Additional information can be found in the IEEE 802.15.4 standard [25].

Wi-Fi

The IEEE 802.11 set of standards defines the PHY and the MAC layers for wireless local area network (WLAN). It is the basis for wireless network products using the Wi-Fi brand. The IEEE 802.11 set of standards is intended for indoor networks to allow devices, e.g., laptops and printers, to communicate and access the Internet without connecting wires. The modulation scheme, the channel bandwidth and the data rates change depending on the version of the standard used.

The IEEE 802.11b (1999) and the IEEE 802.11g (2003) standards are dedicated to the 2.4 GHz ISM band. The IEEE 802.11b standard uses a DSSS modulation, offers a data rate up to 11 Mbps, and sends data over at least 11 channels that are 22 MHz wide. The IEEE 802.11g standard uses an OFDM modulation scheme along with 20 MHz bandwidth channels, with data rates between 6 and 54 Mbps. In Europe, there are two additional channels available (number 12 and number 13), and in Japan, there is a third additional channel (number 14).

The most recent versions such as IEEE 802.11n (2009) [29] and IEEE 802.11ax (2021) [30] can communicate either in the 2.4 GHz ISM band or the 5 GHz ISM band. The latest IEEE 802.11 standard is IEEE 802.11be (2023) [31] and can communicate in an additional frequency band: the 6 GHz. Note that IEEE 802.11be is still at the early stage of consumer deployment. In our daily life, most of the Wi-Fi access points (APs) are based on the IEEE 802.11n standard except for the new ones which are based on the latest widely distributed IEEE 802.11 standard: the IEEE 802.11ax. The IEEE 802.11n standard improves the IEEE 802.11g standard: (1) an additional bandwidth of 40 MHz is available, (2) the maximum theoretical data rate goes up to 150 Mbps, and (3) a multi-input multi-output (MIMO) feature, allowing four simultaneous flows, is implemented.

The IEEE 802.11 set of standards describes mechanisms that ensure the fair sharing of the medium and guarantee the radio link connectivity. Wi-Fi implements the following mechanisms: (1) the CSMA/CA that is used to access the medium, including listening to the channel to detect if it is free to transmit data, (2) the modulation coding scheme (MCS) that ensures the connectivity by adapting the transmission data rate and the redundancy of the data frames; it can also change the modulation depending on the link budget, and (3) the acknowledgement (ACK) that provides reliability to Wi-Fi transmissions. The Wi-Fi beacon is always sent with the IEEE 802.11b standard at 1 Mbps as this is the most robust configuration. The beacon contains information on the network such as the beacon interval, the supported rates, and the SSID of the network, i.e., the name of the access point. The beacon makes a network visible for devices in the range of the AP which send it.

2.3 LoRa and LoRaWAN

2.3.1 The LoRa PHY layer

LoRa [2] is a proprietary modulation scheme based on chirp spread spectrum (CSS). LoRa usually uses the sub-GHz bands (i.e., 433 MHz or 868 MHz frequency band in Europe). We present next the basis of the LoRa technology as well as the LoRaWAN protocol. The novelties introduced by LoRa 2.4 GHz are detailed in Subsection 2.3.3.

A LoRa signal is encoded using a sequence of chirps (see Figure 2.2) which are frequency sweeps over a given bandwidth. A chirp is either an up-chirp or a down-chirp, depending on whether its frequency increases or decreases. The starting frequency of a chirp encodes the value of the chirp. A frame starts with a preamble to synchronize the receiver with the sender. The preamble ends with 2.25 down-chirps which serve as the start of frame delimiter (SFD). The data are encoded in the following chirps. In Figure 2.2, we highlighted with a dotted rectangle the first chirp of the header. We highlight that apart from the chirps of the preamble all starting at frequency 0, each chirp of a LoRa frame is different. To demodulate the frame, the receiver synchronizes with the transmitter, and then it uses the highest peak of energy, resulting from the Fast Fourier Transform (FFT) of each chirp, to decode the sent data. Remember that the LoRa modulation and demodulation is proprietary. However, the research community tried to analyze and describe the process through a mathematical description [32].

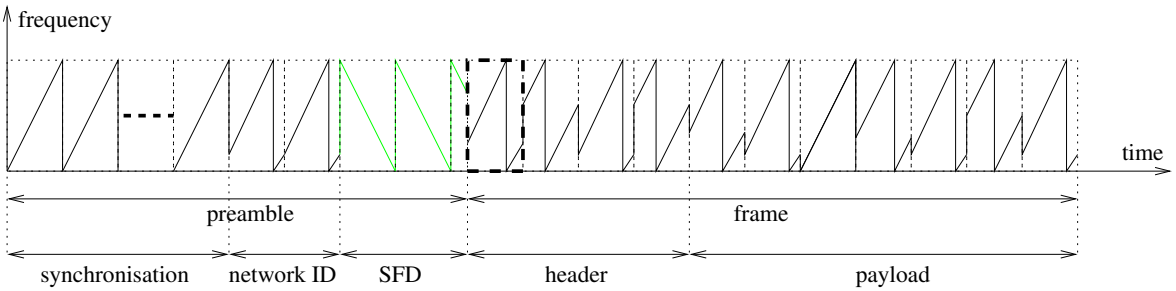

FIGURE 2.2: Example of an uplink LoRa frame. Up-chirps are represented in black, and down-chirps in green. The 2.25 down-chirps are used for time and frequency synchronization.

LoRa transmissions are either uplink or downlink and are detailed in Subsection 2.3.2. LoRa transmissions are a trade-off between energy efficiency, and reliability, and consequently data rate. This trade-off is controlled by the combination of three physical parameters: the SF, which contains the number of bits encoded into a chirp, the bandwidth, and the CR, which is used in LoRa to increase the redundancy of frames, and thus to add robustness. LoRa chips [33] [34] support different SFs. By increasing the value of the SF, the chirp duration increases, and so does the energy consumption, as it takes longer to transmit the same message. However, by increasing the SF, the reception sensitivity increases, which in turn increases the communication range. Considering the BW, an increased value decreases the chirp duration, thus being more energy efficient, but having the downside of reducing the reliability. Finally, the CR controls how many redundancy bits are added to the data in the

payload. SFs are quasi-orthogonal [35] allowing receiving different uplink transmissions using different SF values on the same channel without suffering a high level of interference. In brief, a large value for SF gives more robustness, and thus increases the communication range, while a small value allows a higher data rate.

2.3.2 LoRaWAN

The upper layers of a LPWAN using the LoRa technology are standardized in the LoRaWAN standard [5]. Note that currently LoRaWAN is only specified for sub-GHz bands. The low protocol overhead in a packet, limited to 13 bytes for any data frame, the sleep mode end-devices if there is nothing to transmit, and the small listening period after a transmission make LoRaWAN an energy-efficient protocol.

The simplicity of the network allows low-cost implementation of LoRaWAN. LoRaWAN networks have a star-of-stars topology (see Figure 2.3). The gateways forward the packets received from the end-devices and add information on the quality of the received signal. The gateways are connected to a network server that routes the packets received by the gateways to an application server. The communication is bi-directional but most of the traffic is uplink, i.e., from end-devices to the application server. An end-device can be in the range of several gateways. Thus, the network server receives all the packets and is responsible for the de-duplicating packets process. In case of a downlink transmission, the network server selects the gateway according to the quality information provided by the gateways. One of the special features of a LoRaWAN network is that once an end-device is connected to the network it remains connected unless it becomes out of range of the gateway.

The connection to a LoRaWAN network is made using join request and join respons frames. After an end-device is connected to the network, mostly data frames are exchanged.

The payload is the application data and is encrypted using AES-128 with a symmetric session key that only the end-device and application server know. It ensures end-to-end security as the network server cannot decrypt the application data.

End-devices belong to either Class A, Class B, or Class C. The mandatory class is Class A. Class B and Class C are optional and mutually exclusive, i.e., a Class B end-device cannot comply with Class C requirements and vice-versa. However, Class B and Class C comply with Class A. Each end-devices class defines the downlink opportunities.

Class A offers the lowest power consumption. All physical layer parameters are region-specific [6] [37] to comply with the regulations of the location where the LoRaWAN network is deployed. Apart from the rules on authorized channels and transmission power, there are two other constraints to be respected: the duty cycle and the dwell time. The duty cycle defines the amount of time a device can be busy over a given period. The duty cycle is set to ensure that devices using the same frequency band do not cause destructive interference to other devices. In some regions, like in Korea, instead of using a duty cycle, LoRaWAN end-devices have to implement the LBT mechanism. The dwell time is the time

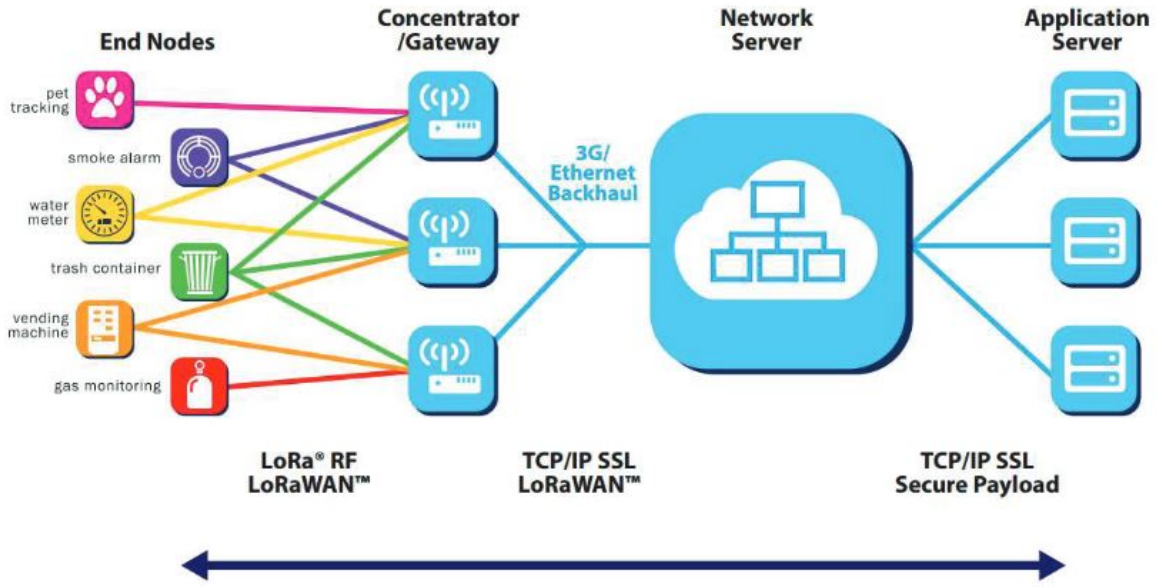

FIGURE 2.3: LoRaWAN network architecture [36].

needed to transmit a LoRaWAN message. The dwell time is used to limit the transmission time.

End-devices send data according to the ALOHA protocol. Each time an end-device has data to send, it selects a random channel in the list of the available channels, and transmits, leading to potential collisions as there is no mechanism verifying that the channel is idle. We summarize the main LoRaWAN channels plans in Table 2.2.

Geographic area (channel plan)	EU868	EU433	IN865	KR920	US915
Mandatory channels (in MHz)	868.10 868.30 868.50	433.175 433.375 433.575	865.0625 865.4025 865.985	922.10 922.30 922.50	**upstream:** 64 (902.3 to 914.9) + 8 (903.0 to 914.2) **downstream:** 8 (923.3 to 927.5)
Maximum number of channels	16	16	16	16	**upstream:** 64 (125 kHz) + 8 (500 kHz) **downstream:** 8 (500 kHz)
Duty cycle	<1%	<10%	No	LBT	No
Dwell time limitation	No	No	No	No	[0:63] 400 ms [64:71] No
Maximum transmit power (in dBm)	+16	+12.15	+30	+30	+30

TABLE 2.2: Main LoRaWAN channel plans characteristics (extracted from [37]).

After each uplink transmission, the end-device opens two short reception windows, called RX1 and RX2, for potential downlink transmissions (see Figure 2.4). For example, in Europe with frequencies between 863 MHz and 870 MHz, the RX1 window uses the same channel,

and the same SF, as the uplink. The RX2 window uses a different channel and a different SF (by default SF12 or SF9, BW 125).

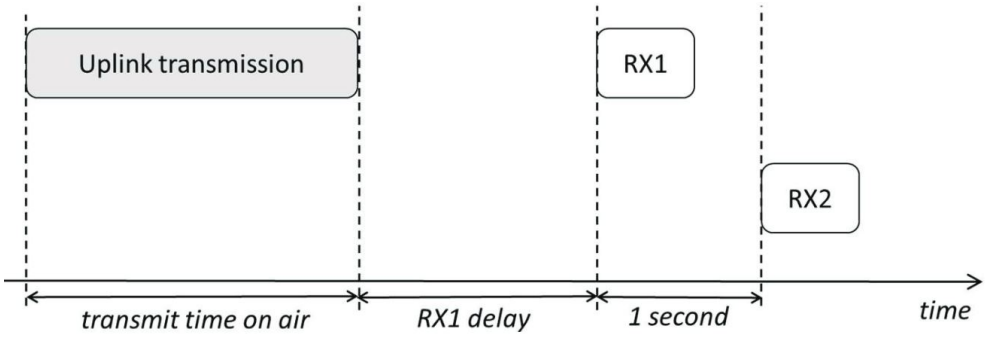

FIGURE 2.4: LoRaWAN Class A end-device operation [36].

Class B relies on a beaconing process. The network broadcasts a beacon via the gateways at periodic intervals of 128 s. The end-device must receive one of these beacons to be time-synchronized with the gateways and so with the network. Based on the beacon synchronization, class B end-devices can open an additional receive window called a ping slot. Any ping slot can be used by the network server to initiate a downlink communication.

Class C is the most energy-consuming mode but features the lowest latency for downlink communication. Indeed, the end-devices using this class listen almost continuously to potential downlinks. The reception window is stopped only during the transmission, i.e., uplink transmission, and the following RX1 and RX2 windows. Note that it is possible to temporarily enable Class C on end-devices for operations such as firmware upgrades over the air.

The LoRaWAN link layer specification defines a mechanism to dynamically adapt the physical layer parameters. The adaptive data rate (ADR) mechanism is similar to the MCS mechanism implemented in Wi-Fi. It adapts the radio configuration (SF and transmit power) based on the link budget to ensure the connectivity between an end-device and the gateway.

2.3.3 LoRa 2.4 GHz

LoRa 2.4 GHz uses essentially the same parameter values as LoRa sub-GHz to achieve a trade-off between reliability and energy consumption (and by consequence data rate) namely SF, BW, and CR. Table 2.3 summarizes the values of these parameters for both LoRa sub-GHz and LoRa 2.4 GHz. One of the most attractive features of the 2.4 GHz ISM band is the lack of duty-cycle allowing higher data rates than in sub-GHz bands. Also, the introduction of SF5 and higher bandwidths than in LoRa sub-GHz allows to increase significantly the data rate (up to 202 kbps) in LoRa 2.4 GHz. The preamble for SF5 and SF6 uses 12 up-chirps instead of 8. Due to the higher bandwidth in comparison with LoRa sub-GHz, the receiver needs more time for the synchronization when LoRa is used in the 2.4 GHz ISM band.

	LoRa sub-GHz	LoRa 2.4 GHz
SF	6 to 12	5 to 12
BW	125, 250, 500 kHz	203, 406, 812, 1625 kHz
CR	4/5, 4/6, 4/7, 4/8	
Data rates	183 bps - 62.5 kbps	297 bps - 202 kbps
Link budget	168 dB (SX1276 chip)	144.5 dB (SX1280 chip)
Energy consumption	Tx: 28 mA at 13 dBm Rx: 11.5 mA (SX1276 chip)	Tx: 24 mA at 12.5 dBm Rx: 7 mA for BW=812 (SX1280 chip)

TABLE 2.3: LoRa parameters and characteristics.

At the time of writing this manuscript, there is no MAC layer standardized yet for LoRa in the 2.4 GHz ISM band, which represents a key research challenge.

2.4 Conclusions

This chapter introduced the technical concepts to understand the rest of the thesis. We presented the frequency band of interest: the 2.4 GHz ISM band. We provided a quick overview of some of the main wireless technologies using the 2.4 GHz ISM band. We also presented the initial version of LoRa dedicated to sub-GHz frequency bands, as well as the LoRaWAN protocol, which defines the upper layers of the LoRa technology. Finally, we introduced the version of LoRa dedicated to the 2.4 GHz ISM band and compared its features with the sub-GHz version.

In the next chapter, we present our first contribution by making the first experimental performance evaluation of LoRa 2.4 GHz in both outdoor and indoor environments.

Chapter 3

Exploring LoRa connectivity in the 2.4 GHz ISM band

3.1 Introduction

The widely deployed LoRa technology uses the sub-GHz bands and thus devices are constrained, according to the regional regulations, in terms of channels and power transmission among others. The release of a new LoRa chip [9] dedicated to the 2.4 GHz ISM band brings the opportunity to have one hardware that could be used worldwide as the 2.4 GHz ISM band proposes a large common set of properties. However, the success of this new version of LoRa relies on its performance, in particular, connectivity and coverage as LoRa targets long-range communications. LoRa in the 2.4 GHz ISM band differs from LoRa in the sub-GHz band, as it uses new SFs and BWs. Thus, it is important to study the performance of LoRa in the 2.4 GHz ISM band.

In this chapter, we experimentally investigate the performance of LoRa in the 2.4 GHz ISM band under several scenarios. We analyze the connectivity and the coverage of LoRa to evaluate the feasibility of a network in the 2.4 GHz ISM band. To this end, we also compare our results with the sub-GHz version of LoRa to study the impact of changing the frequency band on the communication range.

Our experiments take place in outdoor and indoor environments. LoRa was first designed for long-range communication and thus has numerous outdoor applications such as smart cities or smart agriculture [38] [39]. For this reason, we decided to evaluate the version of LoRa for the 2.4 GHz ISM band in an outdoor context. LoRa built its success on several characteristics, especially its robustness and good building penetration resulting in various indoor applications such as smart metering [40]. For this reason, we decided to evaluate the version of LoRa for the 2.4 GHz ISM band in an indoor context. Another reason why we decided to evaluate the behavior of LoRa in an indoor context comes from the fact that the main wireless technologies in the 2.4 GHz ISM band are deployed indoors, e.g., Wi-Fi and BT. Finally, we wanted to study the impact of the environment on LoRa performance, thus we evaluate two types of indoor environments: (1) a faculty building where the mobility

happens at a periodic time, i.e., between two courses and at lunch break, and (2) a work building where the mobility is smooth over the entire day with activity peaks at lunch break.

Overall, we chose to carry out the following three experiments. The first experiment exhaustively investigates the impact of all LoRa parameters on the performance in an indoor environment (see Section 3.4). The second experiment proposes a performance comparison between LoRa sub-GHz and LoRa 2.4 GHz, using a representative subset of parameters (higher data rate, greatest communication range, and intermediate configurations), for both outdoor and indoor environments (see Section 3.5). Finally, in the third experiment, we perform an indoor week-long experiment taking into account the human activity within the building (see Section 3.6). It is derived from two factors we wanted to evaluate the impact on LoRa performance: (1) the human body absorbs part of the radio waves just as a wall does, and (2) the people influx inside a building varies depending on the days and the hours of the week.

We formalize the study of LoRa connectivity and communication range in the 2.4 GHz ISM band with the following research questions:

RQ3-1: What is the impact of physical layer parameters (SF, BW, CR) on the communication performance, i.e., communication range and frame delivery ratio (FDR) of LoRa 2.4 GHz?

RQ3-2: What is the difference, in terms of connectivity and communication range, between LoRa sub-GHz and LoRa 2.4 GHz?

RQ3-3: What communication range can we expect for LoRa in the 2.4 GHz ISM band in an outdoor environment?

RQ3-4: What communication range can we expect for LoRa in the 2.4 GHz ISM band in an indoor environment?

RQ3-5: How does LoRa connectivity vary as a function of the indoor environment (competing wireless technologies and people activity in the building)?

The experimental results described in this chapter help us to answer each research question through the subsequent contributions [1]:

- We make the first experimental indoor exhaustive evaluation of all the combinations of LoRa parameters (SF, BW, CR) in the 2.4 GHz ISM band to study the impact of each LoRa configuration on the performance in terms of FDR. From the results, we give recommendations on which configurations should be preferred depending on the targeted applications.
- We design and implement on real LoRa hardware a communication protocol between gateway and end-devices which automatizes our experiments. This communication protocol ensures the synchronization between LoRa uplink transmissions and gateways in the 2.4 GHz ISM band by guaranteeing that both equipment use the same configuration.

[1] This chapter extends the studies published in [41] [42] [43] and presented at [1].

- We compare LoRa performance in the sub-GHz and the 2.4 GHz ISM band in both indoor and outdoor environments. This allows us to assess whether, despite changing the frequency band of operation of LoRa, it still meets its design requirements especially robust and long-range communications. It also provides useful information on future LoRa network deployments regarding the number of gateways to ensure the coverage of a building for example.
- We evaluate the impact of people's mobility as well as their wireless technologies usage inside a building on LoRa connectivity. We run a week-long experiment and highlight peaks of activity thus allowing us to propose periods of time where LoRa transmissions will be less interfered. This finding highlights an opportunity for LoRa applications with sparse transmission requirements.

3.2 Performance evaluation of LoRa technologies: SLR process

IoT technologies use either unlicensed or licensed frequency bands. While LoRa and Sigfox preferred the use of the sub-GHz band, NB-IoT generally operates in the cellular frequency bands. As LoRa is one of the main technologies for LPWANs, its performance has been widely studied. However, the version of LoRa dedicated to the 2.4 GHz ISM band still needs to be evaluated. By changing the frequency band of deployment a set of parameters also change. For instance, the 2.4 GHz ISM band does not impose a duty-cycle giving the opportunity for LoRa to transmit at any time. Also, the wavelength of LoRa in the 2.4 GHz ISM band is about a third of the wavelength of LoRa in the sub-GHz band, thus LoRa 2.4 GHz will have a lower building penetration and a lower communication range compared to LoRa sub-GHz.

We propose to summarize the performance of LoRa in both sub-GHz bands and the 2.4 GHz ISM band, especially in terms of connectivity and communication range, as this is the focus of our work. To this end, we apply the SLR process detailed in Appendix A.2 to select the articles of our SoA. We synthesized the selected articles in Table 3.1, based on the methodology used to evaluate the coexistence (i.e., theoretical, network simulation, or real experiments) and the environment (i.e., indoor, outdoor, or both). The last line of the table highlights the novelty of our work compared to the existing literature.

The performance of LoRa has been widely studied using different methodologies [87] [88]. Depending on the focus of the paper, the approach is either theoretical, by simulations, by experiments, or a combination of them. For instance, a paper focusing on the scalability of a LoRaWAN network prefers simulations as it is complex to deploy a large-scale real-world LoRaWAN network. Meanwhile, theoretical approaches give an upper bound of the performance as they are based on mathematical models. Even if these models implement signal propagation formulas, including fading and shadowing effects, they cannot perfectly represent a real-world deployment, and thus provide optimistic results compared to the in-field results. Simulations allow to break free from deployment complexity or hardware limitations. This way, security mechanisms, or MAC protocols can be evaluated. Finally,

Ref	Environment	Theoretical	Simulations	Experiments	LoRa technology
[44]	Outdoor	X			LoRa sub-GHz
[38] [45][46] [47] [48] [49]	Outdoor		X		LoRa sub-GHz
[50] [51] [52] [53] [54] [55] [56] [57] [58] [59] [60] [61] [62]	Outdoor			X	LoRa sub-GHz
[63] [64] [65] [66]	Outdoor	X	X		LoRa sub-GHz and LoRa 2.4 GHz [66]
[67] [68]	Outdoor	X		X	LoRa sub-GHz
[69] [70] [71]	Outdoor		X	X	LoRa sub-GHz
[72]	Indoor		X		LoRa sub-GHz
[73] [74] [75]	Indoor			X	LoRa sub-GHz
[76]	Indoor	X	X	X	LoRa sub-GHz
[77]	Indoor and Outdoor	X			LoRa 2.4 GHz
[78]	Indoor and Outdoor		X		LoRa sub-GHz
[79] [80] [81] [82] [83]	Indoor and Outdoor			X	LoRa sub-GHz and Other [81]
[84]	Indoor and Outdoor	X		X	LoRa sub-GHz
[85] [86]	Indoor and Outdoor		X	X	LoRa sub-GHz
Our contribution	Indoor and Outdoor			X	LoRa sub-GHz and LoRa 2.4 GHz

TABLE 3.1: Performance state of the art classification in function of the methodology and the environment.

experiments provide results from real-world implementation and allow to understand the behavior of LoRa in a given environment. Note that it is unlikely that a paper focuses only on one metric. So, the papers we selected using our SLR process also provide insights into other metrics, than connectivity and communication range, such as throughput, scalability, or energy consumption.

One way to compare the different wireless technologies dedicated to LPWANs is to evaluate them depending on the applications targeted [44]. The authors propose to attribute a score index to each technology. The first step is to list the requirements of the targeted application to evaluate whether or not a LPWAN technology can comply with them. For instance, an application with high throughput or low latency cannot be supported by LPWAN technologies. Then depending on success factors such as the deployment cost and maintenance, the interoperability, or the data protection, each LPWAN technology is rated. The technology providing the highest score is the most suitable for the targeted applications.

LoRa performance is mostly evaluated for two types of environments: outdoor and indoor.

3.2.1 LoRa performance in outdoor environments

LoRa was first designed for long-range communications. This characteristic converts LoRa into the preferred choice for outdoor applications. Most of the studies propose experimental

evaluation of LoRa in outdoor environments. However, there are a few studies relying on theoretical, simulations, or a combination of both approaches.

The estimation of LoRa performance shows that the signal propagation depends on the fading channel and will not be the same for a Rayleigh, a Ricean, or a Nakagami channel [45] [63]. For instance, for a targeted bit error rate (BER) of 10^{-4} the minimum required SNR is 15 dB for a Rayleigh channel, -2 dB for a Ricean channel, and between 10 dB and 51 dB for a Nakagami channel depending on the fading parameters.

A lot of papers focus on the LoRa connectivity as a function of the distance to the gateway [51] [53] [54] [68] [69] [84] [85] [86]. The results depend on the propagation conditions: line-of-sight (LoS) or non line-of-sight (NLoS). In LoS conditions, LoRa achieves a packet delivery ratio (PDR) of 90% for a distance of 4 km using SF7, while it reaches only 0.1 km in NLoS. This type of performance evaluation significantly differs depending on the environment. For example, in an urban scenario LoRa achieves a PDR of 100% and 95% for a distance up to 1.5 km using SF12 and SF7 respectively. The PDR quickly decreases for distances exceeding 1.5 km: 68.1% with SF12 and 18.1% with SF7. Overall, the real-world characterization of the environment is necessary to deploy adequately a LoRaWAN network.

Apart from the distance between the gateway and the end-devices, several other factors can have an impact on the connectivity of LoRa.

First, the propagation conditions of the environment, such as the presence of vegetation, and the weather conditions, e.g., temperature, and humidity, have a significant impact on LoRa connectivity [50] [59] [67]. In LoS conditions, even for a low power transmission of 7 dBm, using SF6, BW 500, CR 4/5, for a distance of 450 m between the end-device and the gateway the PDR is 95%. The repetition of this same experiment in a forest environment results in a total loss of connectivity, i.e., PDR of 0%, for a distance of 90 m irrespective of the transmission power used. he results highlight that the presence of dense vegetation in the propagation environment decreases the LoRa communication range by a factor of almost 5.

Another factor that degrades LoRa performance is the mobility of end-devices [56] [71] [80]. Due to the long-range communication properties of LoRa, some works study the suitability of LoRa for mobile IoT applications including vehicular communications. Considering an end-device on the top of a vehicle whose speed varies between 8 km/h and 24 km/h, and a gateway located 160 m away from the end-device, the resulting PDR is approximately 98% and 91% respectively. The PDR decreases up to 62% and 55% approximately by increasing the distance between the gateway and the end-device to 800 m. The results indicate that even for a low speed, the packet delivery ratio is significantly impacted.

LoRa targets applications such as agriculture and environment monitoring. In these types of applications, the sensors can be located underground leading to an important signal attenuation due to the propagation through the soil [58] [60] [62]. The results show that the PDR is directly linked to the distance between the underground end-device and the aboveground gateway. For a LoRa end-device buried at 15 cm and a LoRa gateway located 2 m above

the ground and 100 m away from the end-device, the SF used has little impact and the PDR is at least 97%. Increasing the distance by 50 m, i.e., 150 m between the gateway and the end-device, which corresponds to as received signal strength indication (RSSI) of -130 dBm, only the SFs 10 to 12 achieves a PDR of 100%. Lower SFs provide a maximum PDR of 90% (SF9) and a minimum PDR of 9% (SF7). The smallest SFs lose entirely the connectivity for a distance of 200 m which corresponds to a RSSI of -135 dBm, and only the SF12 still provides a PDR of 100%.

Apart from the environment where the LoRa end-devices are deployed, the LoRa parameters themselves have an impact on performance.

LoRa transmits data following the ALOHA protocol. Thus, the traffic is not necessarily confirmed. However, some studies evaluate the benefits of implementing confirmed traffic [46] [65]. The results show that for a traffic load below 0.8 pkt/s, the confirmed traffic provides a better PDR than the unconfirmed traffic. For a traffic load of 0.8 pkt/s both confirmed and unconfirmed traffic provide a PDR of 94%. For higher traffic load the trend reverses and using unconfirmed traffic achieves higher PDR than with confirmed traffic. This behavior is explained by studying the reasons for packet losses for a traffic load of 0.8 pkt/s. The unconfirmed traffic suffers mainly from interference due to the multiple parallel LoRa transmissions. The confirmed traffic suffers from interference but also from gateway saturation and ACK collisions. Thus for higher traffic load, the addition of the multiple factors that affect the PDR of the confirmed traffic results in a lower PDR than for unconfirmed traffic.

The SF allocation impacts the communication range of LoRa [47] [64] [70]. A higher SF provides a lower data rate but also a higher link budget and consequently a higher communication range. The MAC layer of LoRa uses an ADR mechanism to dynamically adapt the end-devices physical layer configurations to ensure connectivity with the gateway. The results highlight that using ADR also permits to have a more stable LoRa PDR when the number of end-devices and the traffic load of the network increases. Without using ADR for a network of 170 end-devices, the PDR is 92.5% and 88% for a number of 12 pkt/day and 96 pkt/day respectively. For the same number of end-devices, and the same number of packets sent per day, with ADR implemented, the PDR is respectively 84.5% and 82%.

The last parameter on which literature focuses is how capacity, i.e., the number of end-devices served by a single gateway, impacts the connectivity [38] [79]. For a gateway covering a radius area of 1.5 km, simulations indicate a packet success rate above 95% when the gateway serves 15 000 end-devices.

While the impact of several parameters and environment conditions have been widely studied, only a few works comprehensively evaluate the performance of all physical parameters [55] [57] [83]. The results emphasize that some parameters have more impact on LoRa connectivity and communication range. The LoRa physical parameters should be adapted in the following order: SF, BW, and CR. Increasing the SF, the transmission power, the CR, the antenna height and gain, and using narrow BW result in a PDR increasing.

Finally, as LoRa targets IoT networks, it competes with other wireless technologies using the same unlicensed frequency band, such as Sigfox, but also with wireless technologies using licensed frequency bands such as NB-IoT. Consequently, several works propose to compare the performance of these IoT technologies [48] [49] [52] [61] [81] [89]. The results show that in an urban scenario, the difference between LoRaWAN and Sigfox networks performance increases with the distance. For a distance of 100 m between the gateway and the end-devices, the PDR is 98% and 86% for LoRaWAN and SigFox respectively. When the distance increases to 400 m the PDR is 76% for LoRaWAN and 40% for Sigfox. The comparison of LoRaWAN with NB-IoT demonstrates through simulations that depending on the application targeted the technology chosen will differ. LoRaWAN networks will be preferred for long-range communications while NB-IoT will target low-latency applications.

3.2.2 LoRa performance in indoor environments

The good building penetration properties of LoRa make the technology suitable for indoor applications. In the same way, as in outdoor scenarios, the distance between the end-devices and the gateway has an impact on LoRa connectivity [55] [73] [82] [85]. For an indoor scenario with the gateway and the end-device located at the same floor and 60 m away from each other, using SF7, BW 125 results in a PDR of 73% thus highlighting the good indoor propagation of LoRa signals. When the end-device is located several floors away from the gateway, the connectivity is almost lost using SF7, BW 500 which is the configuration providing the highest data rate. However, it has been shown that increasing the number of gateways allows to increase the PDR even for confirmed traffic and thus permits higher traffic load [72]. For a single gateway that serves end-devices using SF7, BW 125 the maximum traffic load is 0.6 pkt/s to ensure a PDR of 80%. Increasing the number to ten gateways increases the maximum traffic load to 4 pkt/s.

The results in indoor scenarios are consistent with the results obtained in outdoor scenarios regarding the impact of the physical parameters on LoRa performance [76]. Irrespective of the distance between the end-devices and the gateway, increasing the SF also increases the PDR. For a fix BW of 125 kHz, using SF7 provides a PDR of 8.7%. The PDR increases to 63% using SF9, and approaches 100% using SF12. The results demonstrate that the CR has less impact on the PDR. The PDR using a CR of 4/5 is 60% and increases to 76% for a CR of 4/6. For higher CRs (4/7 and 4/8) the PDR is 100%. The results thus validate that it is better to change the SF than the CR to increase the PDR.

Similarly to outdoor scenarios, several studies propose to compare LoRa performance with other wireless technologies having indoor applications [74] [75] [81]. In the same way, as for outdoor applications, depending on the targeted applications, one technology will be preferred among the others. For instance, if the application requires a low power consumption, LoRa is the better option compared to BLE and Wi-Fi. Likewise, LoRa will be preferred for indoor coverage applications as it provides a PDR of at least 94% when there are seven floors of difference between the gateway and the end-device. The indoor coverage difference with other wireless technologies is significant: BLE cannot cover a one-floor difference

between the transmitter and the receiver which results in a PDR of 0%, and Wi-Fi barely receives 8% of the packets. In contrast, if the application requires a good localization accuracy, Wi-Fi is more favorable by providing an accuracy up to 0.52 m while LoRa and BLE provide respectively an accuracy up to 0.76 m and 1.53 m.

3.2.3 LoRa 2.4 GHz performance

While the performance of LoRa has been widely studied in the sub-GHz bands, it is not at all the case for its counterpart in the 2.4 GHz ISM band. Only a few works have investigated the performance of LoRa 2.4 GHz in both indoor and outdoor environments [66] [77]. Theoretical results show that LoRa 2.4 GHz can achieve a maximum communication range of 133 km in a free space scenario, 443 m in an urban scenario, and 74 m in an indoor scenario. Simulations permit to evaluate the maximum outdoor communication range of all the LoRa parameters (SF, BW, and CR) in the 2.4 GHz ISM band. The results show that there are 24 configurations that achieve the maximum distance while keeping the energy consumption as low as possible. Consequently, the configuration providing the highest data rate (SF5, BW 1625) achieves a communication range of less than 100 m with an energy consumption of 0.025 mJ. The greatest communication range is 850 m using SF12, BW 203 with an energy consumption of almost 3 mJ.

We conclude that there is a lack of experimental evaluation on the performance of LoRa in the 2.4 GHz ISM band. In comparison with the previously cited studies, our work makes the first experimental study of all the physical parameters of LoRa in the 2.4 GHz ISM band in an indoor environment over an extended period of time. We also make the first comparison in terms of connectivity and communication range between LoRa sub-GHz and LoRa 2.4 GHz to validate theoretical and simulation results provided in the literature.

3.3 Applications, tools and metrics

In this chapter, we carry out various experiments to evaluate the potential of LoRa in the 2.4 GHz ISM band, for indoor and outdoor environments and several configurations (combination of SF, BW, and CR). We focus on the connectivity of LoRa, which allows us to estimate the communication range of this technology. This is the first milestone for future LoRa deployment in the 2.4 GHz ISM band as it permits to outline the possible applications specific to LoRa 2.4 GHz and also the hardware requirements (quantity and location).

In this section, we present all the material and the evaluation metrics used to setup our experiments. Each setup and scenario will be detailed later, in the corresponding sections. We design our experiments to be repeatable, as we need to run them many times. We also need the experiments to be reproducible, which is why we use COTS equipment.

We use a laser meter and `Google Maps` [90] to calculate the distance between the gateways and the end-devices in indoor and outdoor environments respectively. We use the Linux `screen` [91] utility to display the logs of the LoRa sub-GHz end-devices while saving data

into a file. Finally, we use the `netdownlink` utility, which is part of the gateway code owned by Semtech, to log useful information on the received LoRa frames, i.e., LoRa configuration, RSSI, SNR, and payload, to analyze the experiment results.

We provided the official gateway [92] and end-device [93] public code. We do not provide the code we modified for our experiments as we are working on the development branch of the Semtech code, which is not public. We also make available the experimental data we collected. We give the repository links in the corresponding sections. We designed our experiments using a minimal setup to make them easily movable to allow easy deployment and evaluation in different environments.

3.3.1 Performance evaluation metrics

We count the number of frames received to compute the FDR as a function of the distance and the LoRa configuration. We also analyze the RSSI and the SNR of each frame as these metrics give insights into the frame losses. We perform all our experiments using the LoRa physical layer for two reasons: (1) we want to study the LoRa communication performance without any mechanisms such as retransmissions or ADR, and (2) there is no standardized MAC layer for LoRa in the 2.4 GHz ISM band yet.

The **FDR** is a well-known metric to evaluate communication performance as it computes the ratio of frames received (and correctly decoded) over the number of frames sent (see Eq 3.1). The FDR allows to estimate the robustness of a wireless link between two devices. We compute the FDR by logging frames on both sides of the communication. We also verify that the received, and decoded, payload is equal to the sent payload. The FDR is taking value between 0 and 1 and is expressed as a percentage by multiplying the obtained value by 100.

$$\text{FDR} = \frac{\text{Number of received frames}}{\text{Number of sent frames}}. \tag{3.1}$$

The **RSSI** is a metric that gives the signal strength of the radio link for each received frame. If the signal strength is too low, frame losses are likely to occur with regard to sensitivity and reception antenna gain. However, according to the SX1280 datasheet [9] (LoRa chip for the 2.4 GHz ISM band), the RSSI (in dBm) is computed as the energy on the reception bandwidth and not the signal strength of frames received by the gateway. This chip tolerates a frequency offset, i.e., a crystal error, between the transmitter and the receiver, without sensitivity degradation of +/- 50 ppm when using a spreading factor 12. The allowed crystal error implies that the LoRa gateway listens on a wider bandwidth than the one used by the end-device to send frames. Note that the reception bandwidth is not linear. For example, for a transmission BW of 203 kHz, the corresponding reception BW is almost doubled, while for a transmission BW of 1625 kHz, the corresponding reception BW is around 2000 kHz.

The **SNR** is a metric that allows to quantify interference and noise. The SNR is computed as the average signal-to-noise ratio of frames received by the gateway. The SNR can be

expressed using a linear scale, or using a logarithmic scale, i.e., value in Watt or dB respectively (see Equation 3.2). The LoRa gateway stores the SNR according to the logarithmic scale. LoRa can receive frames under the noise floor. It means that the gateway can successfully decode a LoRa frame even with a negative SNR value. The SNR threshold for decoding depends on the LoRa configuration used to communicate, and especially the SF. An SF12 frame can be decoded if its SNR is -20 dB or higher. An SF5 frame can be decoded if its SNR is -2.5 dB or higher. We resume all the SNR thresholds for decoding depending on the SF in Table 3.2.

$$\begin{aligned} \text{SNR}_W &= \frac{P_{signal}}{P_{noise}}. \\ \text{SNR}_{dB} &= 10 \times \log_{10}(\frac{P_{signal}}{P_{noise}}). \\ \Leftrightarrow \text{SNR}_{dB} &= P_{signal_{db}} - P_{noise_{db}}. \end{aligned} \tag{3.2}$$

SF	SNR limit value (in dB)
12	-20
11	-17.5
10	-15
9	-12.5
8	-10
7	-7.5
6	-5
5	-2.5

TABLE 3.2: SNR limit value to correctly demodulate a LoRa signal depending on the SF. [33]

Both the RSSI and the SNR are required to understand the results of our experiments. In some cases, frames are lost whereas the RSSI is good enough. The SNR can explain such losses because it allows to characterize the quality of the radio environment along a transmission.

3.4 Impact of LoRa parameters on indoor performance

In Section 3.2, we established that the state of the art around the performance of LoRa in the 2.4 GHz ISM band does not provide sufficient real-world implementation, due to the rather recent release of LoRa 2.4 GHz in 2017. We fill the gap by performing experiments to exhaustively evaluate the impact of the LoRa parameters on its performance. These experiments focusing on the connectivity of LoRa in an indoor scenario aim to understand the trade-off brought by the LoRa parameters. [2]

[2]The results presented in this section and in Section 3.6 are derived from the supervision and the collaboration with an internship student in the Agora team, Carlos Fernández Hernández. Both the code and the data are available at `https://doi.org/10.5281/zenodo.7106073`. The code can be used according to the terms of the Revised BSD License. The results are published in [42] [43].

3.4.1 Exhaustive experiment setup

To answer the question "What is the impact of physical layer parameters (SF, BW, CR) on the communication performance, i.e., communication range and frame delivery ratio of LoRa 2.4 GHz?" (**RQ3-1**) we design an indoor experiment called the exhaustive experiment. We setup the exhaustive experiment to evaluate how all the physical layer parameters (SF, BW, and CR) impact the connectivity of LoRa in the 2.4 GHz ISM band. We study all the possible combinations of these three parameters (as presented in Table 3.3), which results in a total of $8 \times 4 \times 4 = 128$ combinations.

Parameter	Values
Spreading Factor	5, 6, 7, 8, 9, 10, 11, 12
Bandwidth (in kHz)	203, 406, 812, 1625
Coding Rate	4/5, 4/6, 4/7, 4/8

TABLE 3.3: Physical layer parameters for LoRa 2.4 GHz.

All the experiments were performed in the Inria building in La Doua Campus, Lyon (France). As we can see in the map from Figure 3.1, the building has a square shape of 20 m$\times$20 m with an elevator situated in the middle. We place the gateway on the 4^{th} floor in one of the corners, and the end-devices in the opposite corner of the building (one of each floor), to maximize the distance from the gateway.

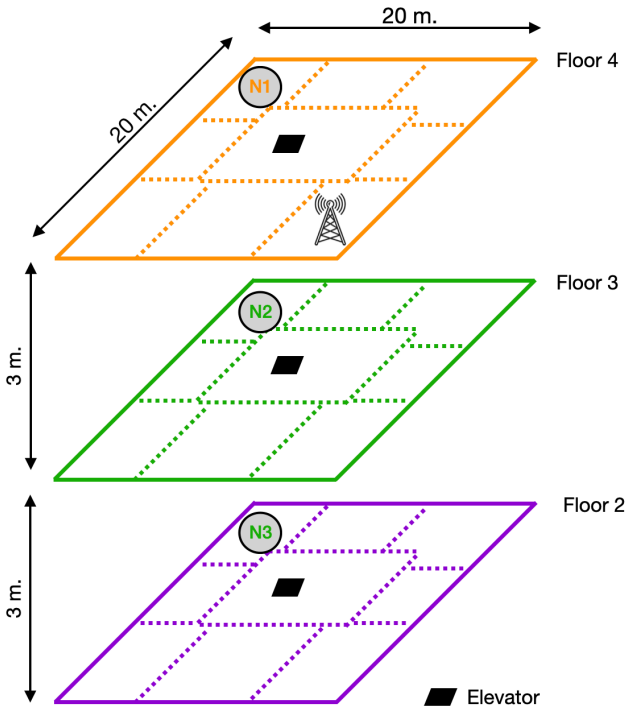

FIGURE 3.1: Architecture of the building that presents the placement of the gateway and the three end-devices in our exhaustive experiment.

The office building has several IEEE 802.11 access points as well as Bluetooth devices as any typical office building today. So, our transmissions are submitted to interference. However, in this study, we do not evaluate the impact of interference on LoRa transmissions. To reduce

as much external interference, these experiments were run during the weekend, when there was almost no one present in the building.

The equipment used for this experiment consists of three end-devices, one gateway, and a computer that collects and logs all the data received by the gateway. All LoRa devices use the SX1280 radio chip from Semtech. Each end-device is independently controlled using the STM32 NUCLEO-L476RG microcontroller, and powered by external batteries. The gateway is directly connected, and powered, to the computer via USB.

To be able to compare the performance obtained with the different parameter combinations (which are extracted from the physical layer parameters presented in Table 3.3) we used the same transmission power of 10 dBm for all end-devices. We also use the same channel for all LoRa transmissions which is centered at 2403 MHz. This channel is located at the extremity of the 2.4 GHz ISM band spectrum allowing less interference with, at least, Wi-Fi and BT. Indeed, the first Wi-Fi channel is centered at 2412 MHz and is, depending on the IEEE standard used to transmit, 20 or 22 MHz wide. There is also one BT advertising channel located 1 MHz away from the LoRa channel we use. For each configuration, we sent $N = 50$ frames, with a 20 bytes payload. This short payload is intended to model common LoRa applications.

3.4.2 Gateway to end-devices communication protocol

To put in place such an exhaustive performance evaluation, we needed to design an experimental protocol that would automatize the experimental runs and would be easily reproducible. Each end-device has to run a certain number of configurations (e.g., 128 in our exhaustive experiment scenario), which has to be repeated several times (to minimize the variations in the observed data). Moreover, to avoid interference between our end-devices, we decided that only one end-device would transmit at a given time. The focus of our study is the connectivity of LoRa and we do not evaluate the impact of concurrent transmissions on performance here. Our protocol ensures that the gateway and the transmitting end-device are using the same configuration, and so can communicate with each other.

The designed communication protocol is presented in Figure 3.2 and allows the initiation of the communication link between the end-device and the gateway. We implemented a round-robin scheduling to comply with our design requirement of having only one end-device transmitting at a time. The gateway activates the end-device by sending a downlink frame, denoted `SRT-Ed` (which stands for `START-End-device`). This downlink activates the end-device only if the configuration used to send it is the same as the one configured on the end-device. For example, in our experiment, the first downlink is sent with an SF12, BW203, CR4/5 as this is the first LoRa configuration we evaluate. Then, the end-device sends N uplink data frames with the corresponding parameters. In Figure 3.2, `Cnfg(i,j)` indicates that the end-device is sending the i-th frame of the j-th configuration. As LoRa 2.4 GHz gateway has three reception paths, we configure the end-devices in series of three configurations. Once the series of three configurations is finished for an end-device, it sends

an `END-Ed` message to the gateway. The gateway proceeds to the next end-device until the round-robin on the three end-devices is finished. Then, the gateway reconfigures itself on the next set of three configurations and restarts the process.

Note that a timeout is included in case either the `SRT-Ed` downlink or the `END-Ed` uplink is lost. This allows us to avoid dead times in the experiment, or de-synchronization between the gateway and the end-devices parameter configurations. Plus, the end-devices are always in reception mode meaning that they can receive a `SRT-Ed` message at any time.

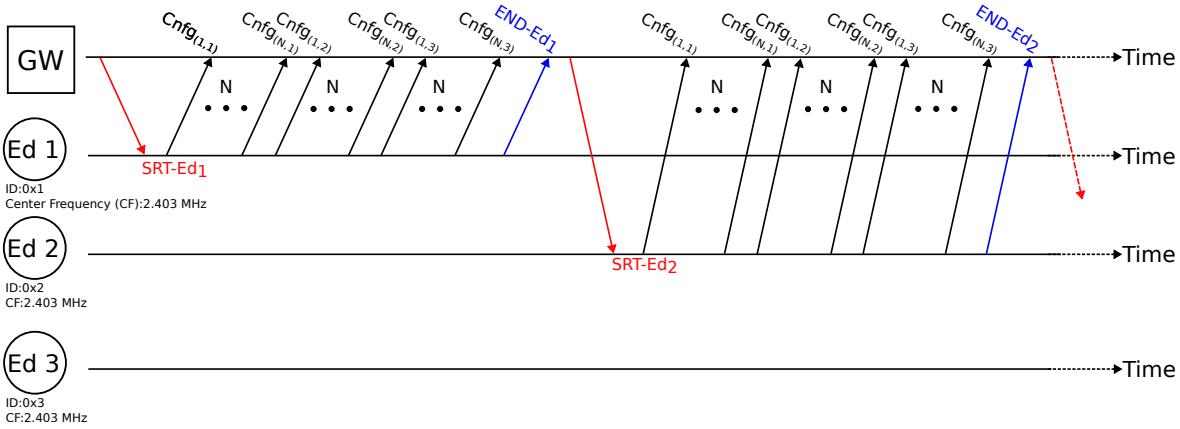

FIGURE 3.2: Gateway to end-devices communication protocol for one configuration cycle (three different parameter configurations). Red lines represent downlink end-device activation frames, blue lines represent uplink control frames and black lines represent uplink data frames for each configuration.

The proposed protocol is scalable as it can be modified to activate multiple end-devices either to have parallel LoRa transmissions on the same channel or evaluate different channels in the limit of three different configurations at a time, for now.

3.4.3 Exhaustive experiment results

The experiment ran for approximately 65 hours from Friday afternoon to Monday morning, with 3 repetitions for each configuration for a total of 19200 frames sent (50 frames per configuration per repetition). During this experiment, the building was mostly empty, and thus low interference from people occurred, and as a consequence, there was also a low Wi-Fi and BT activity.

The FDR results are summarized in Figure 3.3. The figure is composed of four blocks of three lines. Each block gathers the results depending on the CR evaluated. Each line represents the floor level evaluated. On the x-axis, we find the (SF, BW) combination used. It increases from the smallest SF (combined with the narrower BW) to the highest SF (combined with the wider BW). A color gradient illustrates the corresponding FDR ranging between 70% and 100%. The lowest FDR (70%) is obtained using the configuration providing the highest data rate, i.e., SF5, BW 1625 at floor 2 which is not surprising, as it corresponds to the further distance between the gateway and the end-devices.

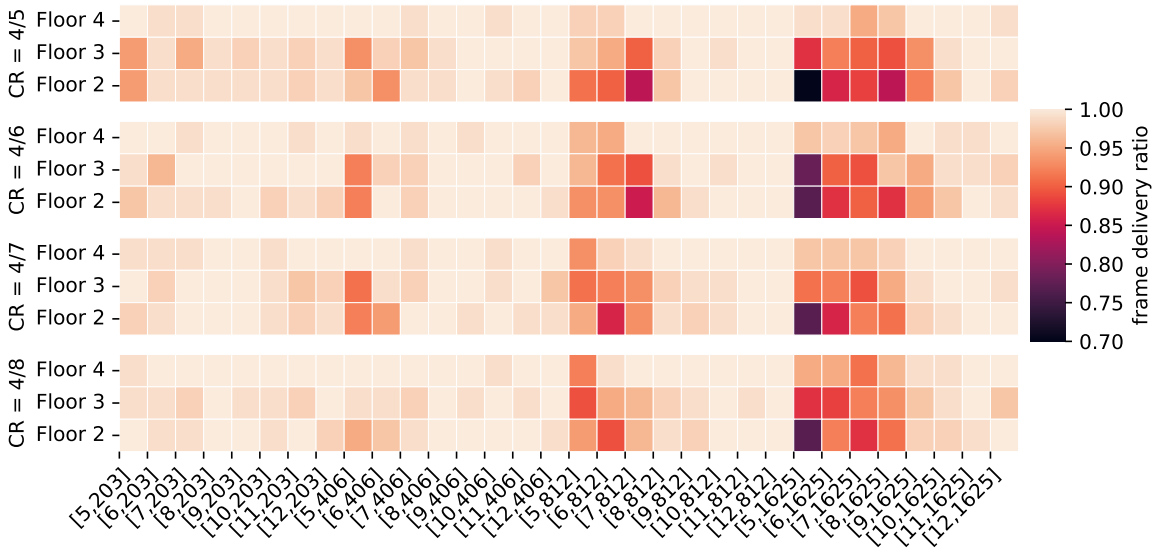

FIGURE 3.3: Heatmap of the LoRa FDR for the three end-devices and all possible combinations of SF, BW and CR.

The FDR starts degrading when we use a combination of low SF (5, 6, 7) and high BW (812 and 1625 kHz), as well as when we increase the distance from the gateway (2^{nd} and 3^{rd} floor). According to the SX1280 calculator [94], the data rate is 15.23 kb/s for configuration (SF6, BW 203, CR 4/5), while it is 6.98 kb/s for (SF11, BW 1625, CR 4/5). Although these two configurations yield a similar FDR, the use of a low SF and narrow BW yields a larger data rate (and hence lower energy consumption), which means it is better to decrease the SF and the BW, rather than to increase the SF and the BW for a given FDR.

From Figure 3.3 we observe that the CR has little impact on the FDR. For configurations having already a good FDR like SF8, BW 406, the FDR is always around 100% irrespective of the CR and the floor evaluated. The impact of the CR is more visible for less robust configurations. For example, the SF5 has a time on air (ToA) of approximately 1.6 ms. It allows a higher data rate, as well as a lower power consumption, but it has a lower communication range and it is more sensitive to interference. In this case, the CR increases the robustness of the communication. We thus go from a FDR of 95% using SF5, BW 203, to a FDR of 100% when the CR is 4/8 instead of 4/5. The improvement of using more redundancy, i.e., higher CR is less visible for the configurations using the wider BW value (1625 kHz). We make the assumption that in the presence of a wide interference, or burst of interference, the improvement brought by the higher CRs will be more visible on the resulting LoRa FDR. Still, our conclusions on the CR are consistent with what is observed in LoRa sub-GHz [83].

To see more clearly the impact of the physical layer variable parameters on the reliability of LoRa in the 2.4 GHz ISM band, we plot in Figure 3.4 the mean FDR for the configurations with the highest data rate. We analyze the FDR for the end-device located on floor 2, as this is the floor where the end-devices are the furthest away from the gateway. In each subplot, we set two parameters on fixed values and we vary the remaining parameter to evaluate all its possible values. In Figure 3.4a we set the SF and the BW to 5 and 1625 kHz respectively,

and we evaluate all the possible values of CR. In this case, changing the CR value does not have a significant impact on performance as the FDR remains between 70% and 80%.

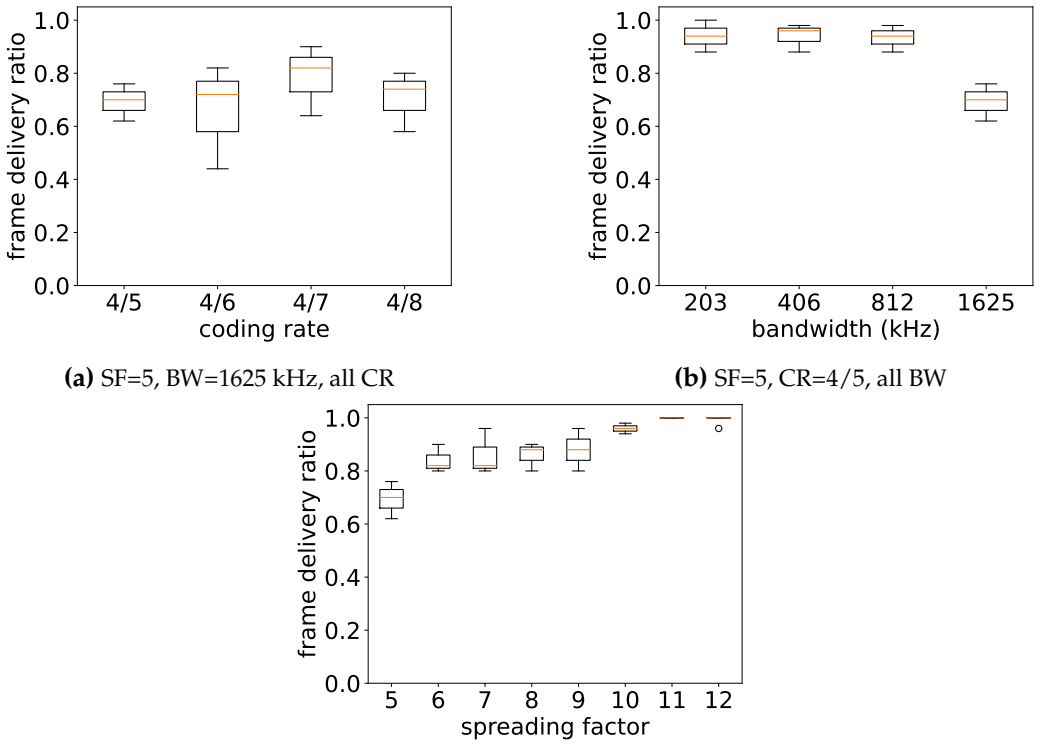

(a) SF=5, BW=1625 kHz, all CR

(b) SF=5, CR=4/5, all BW

(c) BW=1625 kHz, CR=4/5, all SF

FIGURE 3.4: LoRa parameters impact on FDR of the highest data rate configurations at floor 2.

In the same way, in Figure 3.4b we vary the BW for a SF5 and CR 4/5. Here, the relationship between the SF and the BW is clearly visible. Especially for the highest BW value (1625 kHz) where the FDR drops from nearly 95% to approximately 70%. This confirms that higher reliability is achieved using narrow BW even with the less robust SF. A wider BW allows a higher data rate at the expense of a higher interference level as the interference is spread on all the BW used to transmit the LoRa frames.

Finally, in Figure 3.4c we vary the SF for a BW 1625 and CR 4/5. The results highlight the same findings as Figure 3.4b. To counterbalance the large BW it is necessary to use higher values of SF as it increases the robustness. Thus, using a BW of 1625 kHz with SF5, the FDR is about 70%. It increases progressively by increasing the SF (approximately 80% with SF6) until reaching a FDR of 100% with SF11 and SF12.

To further analyze and explain the FDR results, we investigate the RSSI for each end-device and present it in Figure 3.5. We recall that according to Figure 3.3 the end-device with the best performance, i.e., with the higher FDR, is the one located on the same floor at the gateway (floor 4). The end-device with the worst performance is the one located further from the gateway (floor 2). The RSSI reflects this perfectly: the end-device located on the same floor as the gateway always provides a RSSI between -90 and -86 dBm, which demonstrates

a noisy environment. Still, the RSSI is about 10 dBm higher than the RSSI of the end-devices located on other floors than the gateway.

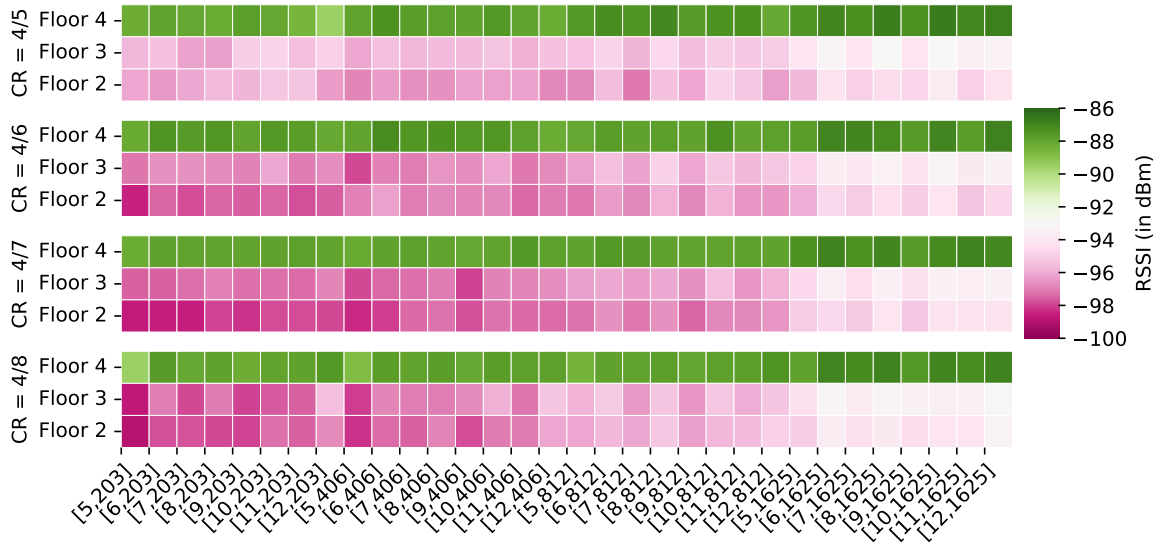

FIGURE 3.5: Heatmap of the RSSI for the three end-devices and all possible combinations of SF, BW and CR.

We also analyze the SNR, as the ambient noise in the building can impact the good reception of our LoRa transmissions, in Figure 3.6. As expected, the SNR decreases as the distance between the end-device and the gateway increases. For SF12, the SNR decreases compared to the other SF. This is especially noticeable for a BW of 203 kHz, as the SNR drops by almost 8 dB from the maximum recorded value for that BW. This lower SNR value for SF12 can come from its ToA. SF12 is the higher possible value for LoRa SF, which leads to the longer ToA when combined with the smallest BW value, i.e., 203 kHz. This way, a LoRa signal using the combination SF12, BW 203 to transmit data is exposed to interference for a longer time than other LoRa parameters combination. However, SF12 is the most robust SF against interference and can correctly receive frames with a SNR of -20 dB or higher.

For the configurations using a wider BW, we observe a negative SNR. Our results show that for all combinations of SF and CR with a small BW, and for all floors, the LoRa signal received by the gateway is stronger than the ambient noise in the building.

Note that the lowest SNR value recorded is around -4 dB. From Table 3.2, we extract that -4 dB is under the SNR limit value of SF5. Consequently, the configurations recording a value of SNR of about -4 dB but using a SF different of 5 will not suffer much in terms of FDR. Of course, the wider the bandwidth, the more a signal is submitted to interference, which can lead to frame losses when collisions occur. As a reminder, a LoRa signal interfered with another signal can be correctly demodulated if it is 3 dB stronger than the interferer.

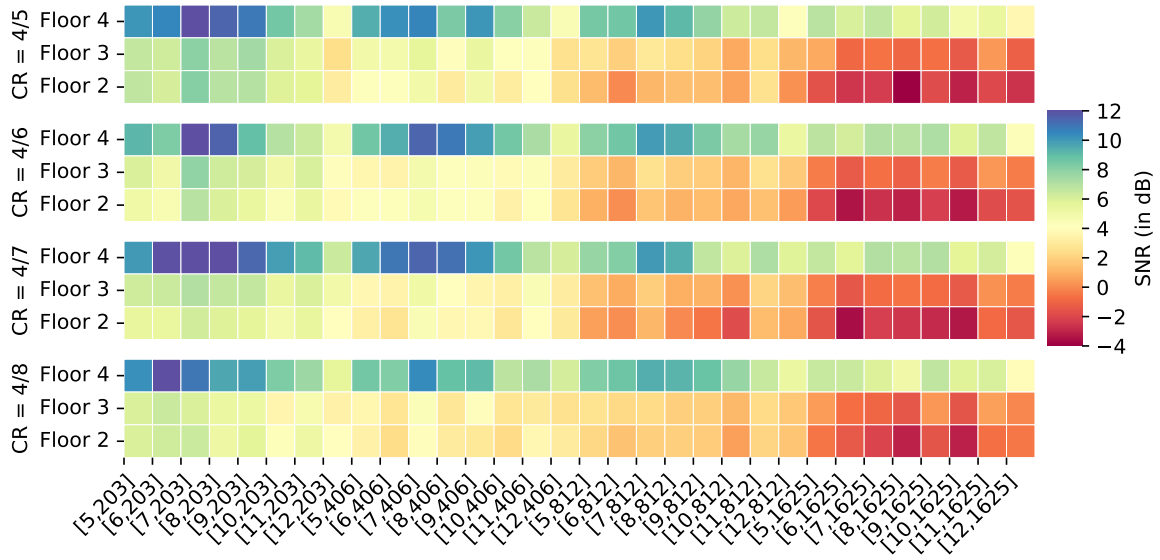

FIGURE 3.6: Heatmap of the SNR for the three end-devices and all possible combinations of SF, BW and CR.

This experiment provides an answer to the question "What is the impact of physical layer parameters (SF, BW, CR) on the communication performance, i.e., communication range and frame delivery ratio of LoRa 2.4 GHz?" (**RQ3-1**). The results highlight that LoRa 2.4 GHz connectivity remains very good in an indoor environment, as the lowest recorded FDR is about 70%. Additionally, using a SF12 combined with any BW and CR value, one gateway can be enough for a complete LoRa 2.4 GHz coverage. We also emphasize that there is a clear relationship between the BW and the SNR: the higher the BW, the lower the SNR. These results also give a first answer to the question "What communication range can we expect for LoRa in the 2.4 GHz ISM band in an indoor environment?" (**RQ3-4**).

3.5 Comparison with LoRa sub-GHz

LoRa was first designed for sub-GHz bands with both outdoor and indoor use cases. For this reason, in this section, we run a performance evaluation, using the same metrics as in Section 3.4, for a representative subset of LoRa configurations, i.e., greatest communication range, intermediate, and highest data rate. These experiments allow us to compare the connectivity as a function of the distance for both LoRa sub-GHz and LoRa 2.4 GHz in outdoor and indoor environments, and thus highlight the advantage of LoRa in the 2.4 GHz ISM band and its limitations [3].

In our case, the term LoRa sub-GHz refers to the version of LoRa using the 868 MHz frequency band, which is used in Europe.

[3]The results are published in [41] and have been presented at [1].

3.5.1 Communication range experiment design

We investigate the performance of LoRa sub-GHz and LoRa 2.4 GHz in outdoor and indoor scenarios, using equivalent configurations for both environments, as shown in Table 3.4. Recall that we design our experiments to be repeatable and replicable, and we use a minimal setup to easily move them to study different environments. Using the same setup ensures the consistency of our results as the devices and the configurations are identical for each version of LoRa (sub-GHz and 2.4 GHz) while evaluating different scenarios.

	LoRa sub-GHz	LoRa 2.4 GHz
Highest data rate, highest energy efficiency	SF7, BW=500, CR=4/5	SF5, BW=1625, CR=4/5
Intermediate configurations	SF8, BW=125, CR=4/5	SF7, BW=812, CR=4/5 SF11, BW=812, CR=4/5
Greatest communication range	SF12, BW=125, CR=4/8	SF12, BW=203, CR=4/8

TABLE 3.4: LoRa configurations for communication range experiments.

In Section 3.4, we evaluate all the possible combinations of the LoRa parameters through real-world experiments resulting in a high time-consuming. Thus, in this section, we evaluate the boundary LoRa configurations, that is: (1) the configuration providing the highest data rate, which is also the most energy-efficient configuration, (2) the configuration providing the greatest communication range, and (3) intermediate configurations for both the data rate and the communication range. The intermediate configurations are chosen so that there is the same difference in the receiver sensitivity between each configuration. In LoRa sub-GHz, changing the CR leads to a difference of less than 1 dB on the link budget. By dividing the BW by a factor of 2, the sensitivity is increased by 3 dB. By increasing the SF by one, the sensitivity is increased by 2.5 dB. Regarding these properties, we demonstrate that the sensitivity difference between the highest data rate configuration and the greatest communication range configuration is 18.5 dB and 26.5 dB for LoRa sub-GHz and LoRa 2.4 GHz respectively (see Equation 3.3).

$$\begin{aligned} \text{For LoRa sub-GHz: } 5 \times 2.5 + 2 \times 3 = 18.5 \text{ dB.} \\ \text{For LoRa 2.4 GHz: } 7 \times 2.5 + 3 \times 3 = 26.5 \text{ dB.} \end{aligned} \tag{3.3}$$

To ensure a difference of approximately 9 dB in the receiver sensitivity between each configuration, we need one intermediate configuration for LoRa sub-GHz, and two intermediate configurations for LoRa 2.4 GHz.

Note that for the highest data rate of LoRa sub-GHz, we decided to use SF7 rather than SF6, as SF7 is much more common than SF6 in LoRa sub-GHz. This comes from the fact that the LoRaWAN specification does not include SF6 even if it is available on LoRa devices. Although the CR does not significantly change the link budget of a LoRa configuration, we still decided to use the highest CR (4/8), i.e., the highest bits redundancy, for the greatest

communication range configuration, and the lowest CR (4/5) for the highest data rate configuration. In this way, we guarantee that the boundary LoRa configurations are indeed the two available extreme configurations.

The experiments were carried out between January and March 2022, using Arduino UNOs with SX1276 radio chip for LoRa sub-GHz, and Nucleo boards with SX1280 radio chip for LoRa 2.4 GHz (same equipment as in Section 3.4). We deployed all end-devices on wooden poles outdoor, or table stands indoor, at 1.5 m from the ground (see Figure 3.7). Each end-device is configured to send frames using one fixed configuration. Each LoRa sub-GHz gateway can receive and store the logs of a single configuration. On the LoRa 2.4 GHz side, each gateway can receive and store the logs of three different configurations simultaneously. We were not able to connect more than four gateways to the laptop to log the packets. Hence, we use three gateways and three end-devices for the LoRa sub-GHz evaluation (one Arduino per configuration per end-device/gateway), and one gateway and three end-devices for the LoRa 2.4 GHz evaluation. To evaluate the fourth LoRa 2.4 GHz configuration, we manually reconfigure one end-device and the gateway. Our communication range evaluation (see Figure 3.8) is composed of the following equipment:

- One laptop to store the logs of all LoRa gateways,
- Three LoRa sub-GHz gateways powered via USB by the laptop,
- Three LoRa sub-GHz end-devices powered by batteries,
- One LoRa 2.4 GHz gateway powered via USB by the laptop,
- Three LoRa 2.4 GHz end-devices powered by external batteries.

We use Varta AA battery to power the LoRa sub-GHz end-devices. To ensure the same level of battery for each experiment (one experiment corresponds to one measured distance which depends on the evaluated scenario), we replace the batteries with fully charged batteries regularly.

Because we are considering LoRa data frames and not LoRaWAN data packets, in addition to the no-duty cycle characteristics of the 2.4 GHz ISM band, we decided to free ourselves from the duty cycle limitation. Also, as we run our experiments at the physical layer, there is no MAC command, like retransmissions, used. We use the same channel for all end-devices. So, we rely on the almost orthogonal features of SF, and the ToA difference to achieve low intra-technology interference. Finally, for all settings, we used a MAC payload of 20 bytes and a transmission power of 13 dBm.

Each experiment consists of 10 series of 50 transmitted frames per configuration. Within a series, each end-device sends a frame every 2 seconds, and there are 30 seconds of idle mode between each series. One experiment lasts between 20 min and 40 min depending on the LoRa configuration used to transmit. It represents a total of 160 min for the outdoor performance evaluation and 560 min for the indoor performance evaluation. The indoor

FIGURE 3.7: LoRa devices deployment (outdoor and indoor) for communication range experiments.

FIGURE 3.8: Overall equipment for the LoRa communication range evaluation.

performance evaluation evaluates several floors of a building resulting in a longer experimental time compared to the outdoor performance evaluation.

3.5.2 Outdoor scenario

By using LoRa in the 2.4 GHz ISM band, we already know that the communication range will be lower than with LoRa sub-GHz (for the same antenna gains and transmission powers), as the frequency is higher. Through our outdoor scenario, we intend to verify if LoRa 2.4 GHz still reaches long-distance transmissions.

To choose the location of our outdoor experiments, we first compute the theoretical maximum distance reachable using the LoRa configuration providing the greatest communication range, i.e., SF12, BW 203, CR 4/8. We use the following definitions of signal propagation in free space:

> When the radio signal travels by a distance d, the signal power is P dB.
> When the radio signal travels by a distance $d * \sqrt{2}$, the signal power is $(P - 3)$ dB.
> When the radio signal travels by a distance $d * 2$, the signal power is $(P - 6)$ dB.

We apply these definitions to preliminary outdoor experiment results coming from tests we run to verify that our experiment setup works. For a distance of 700 m between the end-device and the gateway, the SNR of the greatest communication range configuration is above -5 dB. Consequently and according to Table 3.2:

- At $d = 2 * 700 = 1.4$ km, $SNR = -11$ dB.
- At $d = 2 * 2 * 700 = 2.8$ km, $SNR = -17$ dB which is higher than the SF12 SNR limit value for demodulating a signal.
- At $d = \sqrt{2} * 2 * 2 * 700 = 3.9$ km, $SNR = -20$ dB which is equal to the SF12 SNR limit value for demodulating a signal.

We obtained a theoretical distance of 3.9 km (more details and examples are provided in Appendix B). To perform our outdoor experiments, we had prerequisites concerning the location of the measurements: (1) at least 2 km in a straight line, (2) with LoS condition, (3) without buildings around, i.e., flat and open landscape, and (4) with a possibility to deploy sensors in a way that pedestrians do not block the LoS. For all these reasons, we chose the path along the Rhône river, near the city of Lyon (France) which is a flat rural area. The prerequisites allow us to evaluate several distances to study how the connectivity is distance-dependent, and also to comply with the computed theoretical distance by choosing a maximum distance inferior to the theoretical distance.

The gateways had fixed locations and end-devices were located between 0.5 km and 2 km from the gateways (see Figure 3.9). It was not possible to do experiments farther away without losing line-of-sight due to a bridge on the southwest side.

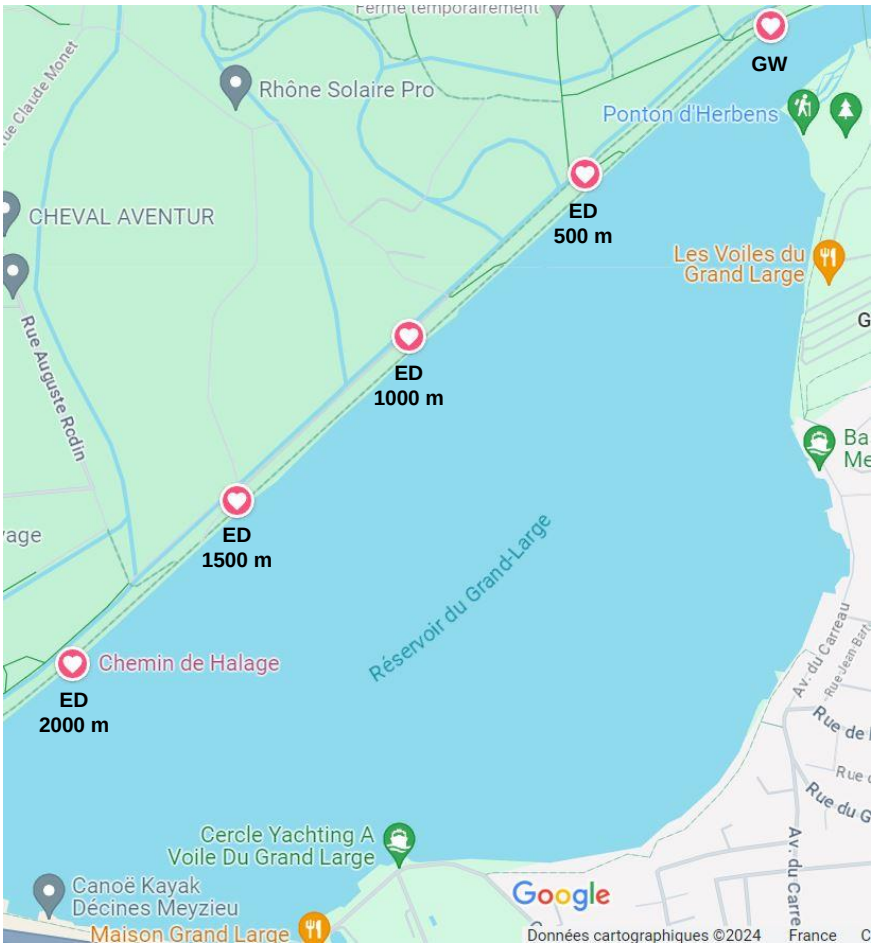

FIGURE 3.9: Location of communication range experiments along the Rhône river.

We planted the wooden poles, one per device, in the strip of land as far as possible from the water to avoid signal reflection. We checked that antennas were perpendicular to the ground (in the up position) to respect the antenna radiation pattern. To ensure the consistency of our experiments, i.e., the same setup at each evaluated distance, we aligned the end-devices in the same order from left to right, i.e., from the nearest from the river to the farthest from the river (see Figure 3.10):

- LoRa 2.4 GHz end-devices in SF ascending order,
- LoRa sub-GHz end-devices in SF ascending order.

On the gateways side, we follow the same order to have face-to-face communication, i.e., LoS, between transmitters and receivers using the same LoRa configuration.

We gathered the results in Figure 3.11. As we cannot evaluate the theoretical maximum distance reachable we compute, without losing the LoS, using LoRa 2.4 GHz configurations, we decided to plot and analyze only the boundary configurations for both frequency bands. We expect that the intermediate configurations will have a lower FDR than the greatest communication range configuration, and a higher FDR than the highest data rate configuration. We

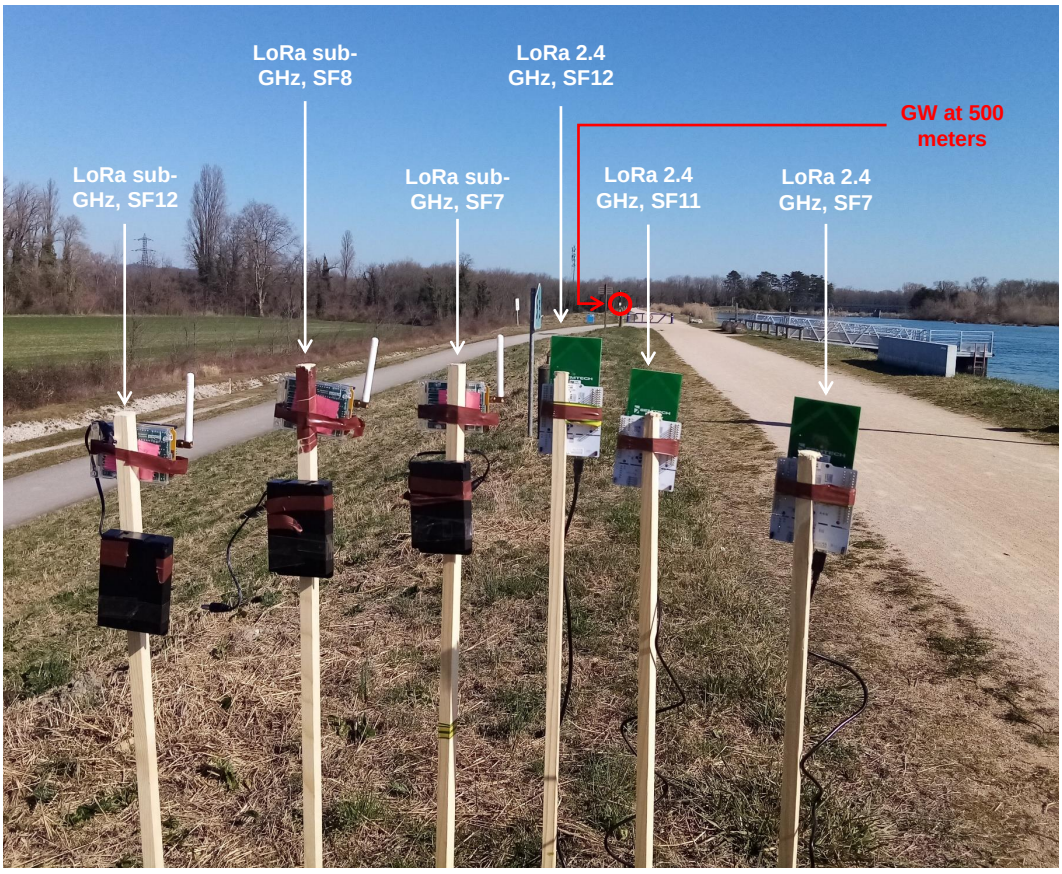

FIGURE 3.10: End-devices placement during communication range experiments.

differentiate the FDR obtained with LoRa sub-GHz and LoRa 2.4 GHz. In each plot, the orange bar represents the configuration providing the greatest communication range, and the yellow bar represents the configuration providing the highest data rate. For each distance, the median FDR is shown along with the first and the third quartile using whiskers.

Figure 3.11 shows that, as expected, LoRa can transmit further in the sub-GHz band than in the 2.4 GHz ISM band. However, at 2000 m we lose connectivity for both frequency bands using the configurations providing the highest data rate.

In Figure 3.11a, we can see that the LoRa greatest communication range configuration, i.e., SF12, BW 125, CR 4/8, provides a FDR of 100% for all distances. This shows that the maximum range is not reached which is not surprising as LoRa was designed for long-range communication. Indeed, several experiments have demonstrated a communication range bigger than 10 km [68] [84]. For the highest data rate configuration, i.e., SF7, BW 500, CR 4/5, we notice a FDR decrease at a distance of 1500 m. It is likely that the first losses using this configuration happened before 1500 m, but as we evaluate distance with a 500 m step, we do not know precisely the maximum communication range of this configuration. In Figure 3.11b, we observe the same trend: with the greatest communication range configuration, LoRa 2.4 GHz provides a FDR of 100% for all distances. However, at 1500 m, the connectivity is lost for LoRa 2.4 GHz, while LoRa sub-GHz maintains a FDR of about 50%.

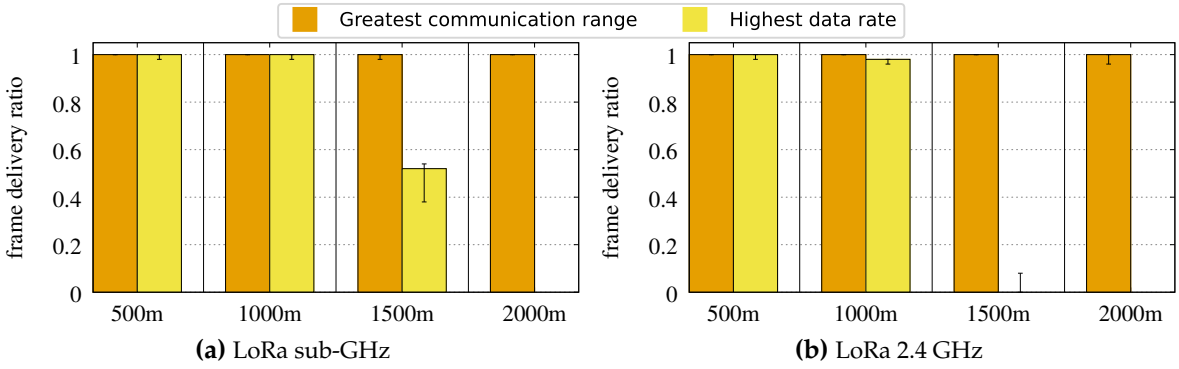

(a) LoRa sub-GHz **(b)** LoRa 2.4 GHz

FIGURE 3.11: FDR of LoRa sub-GHz and LoRa 2.4 GHz in the outdoor scenario. Orange bars represent the greatest communication range configuration, and yellow bars represent the highest data rate configuration.

The RSSI and SNR results are not provided here but are consistent with the trends observed in the FDR.

This experiment partially answers the question "What is the difference, in terms of connectivity and communication range, between LoRa sub-GHz and LoRa 2.4 GHz?" (**RQ3-2**) and responds to the question "What communication range can we expect for LoRa in the 2.4 GHz ISM band in an outdoor environment?" (**RQ3-3**). These results show that using LoRa in the 2.4 GHz ISM band in an outdoor environment leads to a reduced communication range, in comparison with the sub-GHz version of LoRa. From our experiments, we guarantee that in LoS condition and using the greatest communication range LoRa 2.4 GHz configuration a transmission over 2 km is possible without any losses. This result implies that using LoRa in the 2.4 GHz ISM band does not allow outdoor applications over distances of several kilometers. However, the worldwide availability of the 2.4 GHz ISM band makes applications such as international tracking possible using LoRa in this frequency band.

As we performed our experiments in LoS conditions, and the lower building penetration properties of the 2.4 GHz ISM band, we expect to see a performance decrease in the presence of constructions and obstacles.

3.5.3 Indoor scenario

From Section 3.4 we obtain a big picture of the performance of LoRa in an indoor environment in the 2.4 GHz ISM band. Now, we investigate another indoor environment. Moving our setup and running again our indoor experiments for LoRa 2.4 GHz give us two opportunities: (1) diversify the indoor environment evaluated (an office building and a university building respectively), and (2) have an accurate comparison of the indoor communication range of LoRa 2.4 GHz and LoRa sub-GHz.

We use the same setup as in the outdoor scenario to repeat our performance evaluation scenario in an indoor environment. Indeed, LoRa communications in the 2.4 GHz ISM band will probably face interference with other wireless technologies, such as Wi-Fi and BT, as this frequency band is widely used for short-range indoor transmissions (WLAN, wireless personal area network (WPAN)). Additionally, LoRa transmission in an indoor environment will probably face signal attenuation due to the propagation of a signal in an environment where there are walls, doors, and people.

The indoor evaluation took place in the building of the Telecommunications department at INSA Lyon, France, as it is a quite representative faculty building deployment with multiple IEEE 802.11 access points. The schematic map of the building is shown in Figure 3.12. The gateways were located in the spot A1 of floor 2, at one end of a corridor. End-devices were either located along this corridor (spots A1 to A4) or in a different corridor (spot B). The same spots were used on floor 1 and floor 0. We choose the different locations to study the connectivity by covering the entire building.

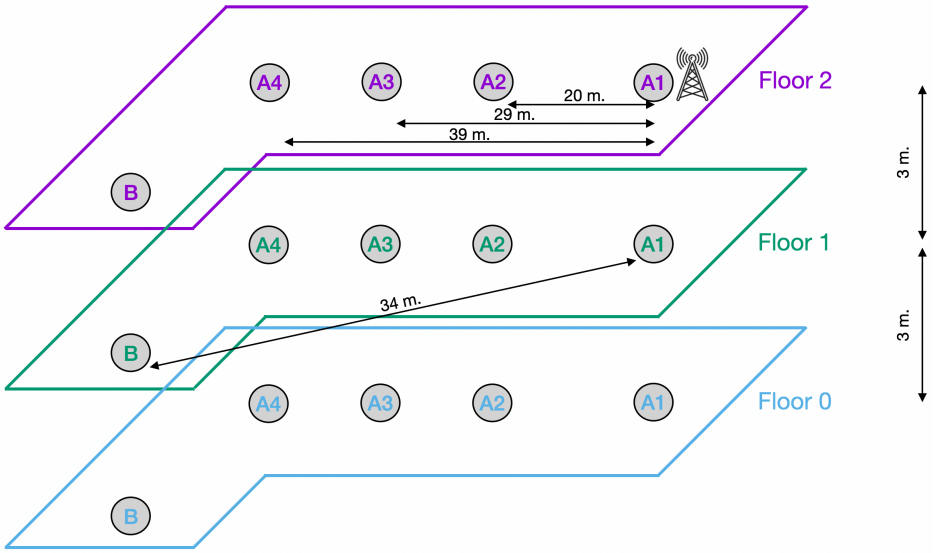

FIGURE 3.12: Building plan for indoor experiments.

On floor 2, spots A1 and A2 are in LoS of the gateway, while spots A3 and A4 are located behind a security door. Spot B is located in a part of the building hosting the CITI research laboratory. The CITI research laboratory focuses on computer science, networking, and digital communications. It implies that when we transmit with our LoRa end-devices at spot B, we are more susceptible to interfere with other technologies as this is one of the focus of the CITI laboratory. We did our experiments when the number of students and staff members in the corridors was low to cause low disturbance in the propagation, i.e., during class hours.

Figure 3.13 shows the average FDR for each location, for each floor, and for each selected configuration (see Table 3.4). For both evaluated frequency bands, we plot the LoRa configurations from left to right in the following order: (1) the greatest communication range, (2) the intermediate configurations in SF decreasing order, and (3) the highest data rate. In each plot, the purple bars represent the results of floor 2, the green bars represent the results of

floor 1, and the blue bars represent the results of floor 0. The height of the bars represents the median of the LoRa FDR computed over all the series. We also computed, and displayed, the first and the third quartile as confidence intervals (even if most are very small).

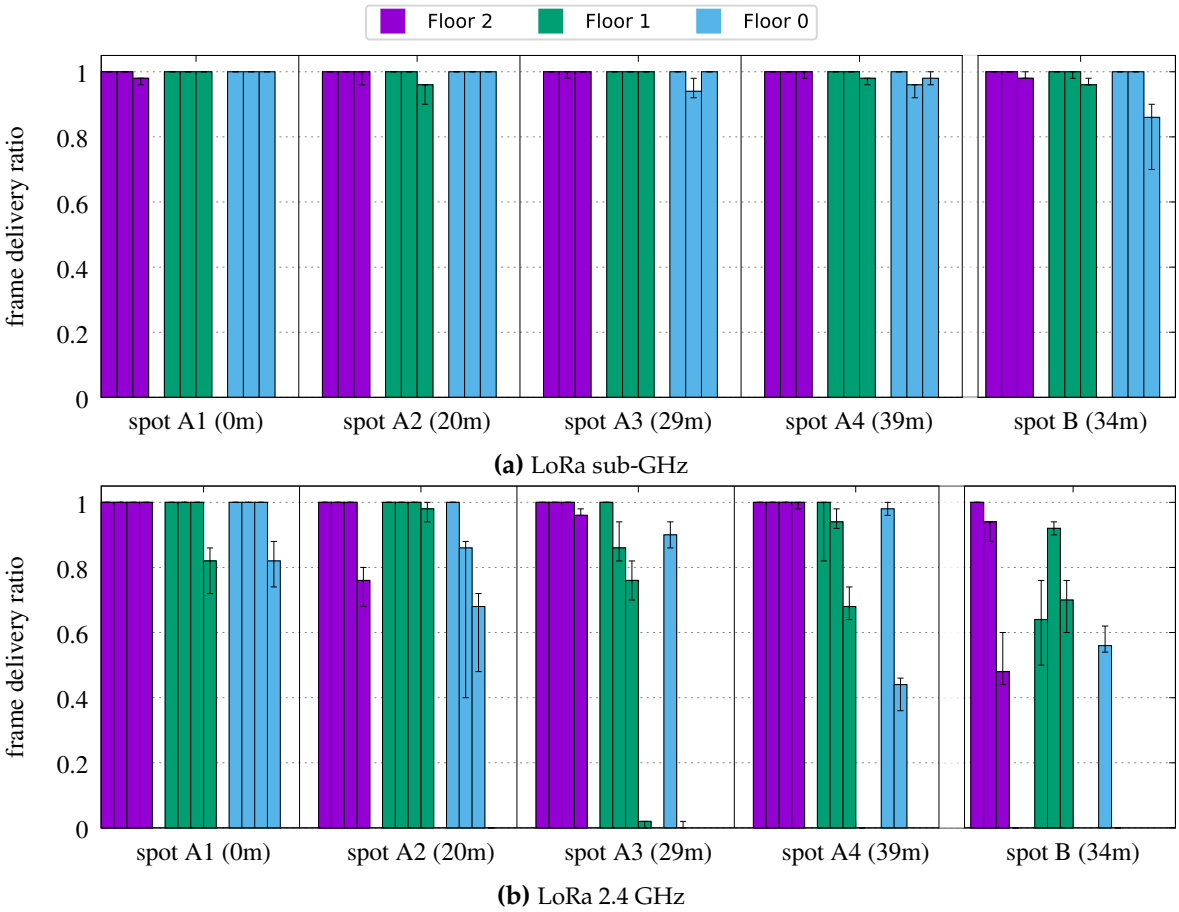

(a) LoRa sub-GHz

(b) LoRa 2.4 GHz

FIGURE 3.13: FDR of LoRa sub-GHz and LoRa 2.4 GHz in the indoor scenario. Purple bars represent floor 2, green bars represent floor 1, and blue bars represent floor 0. The LoRa configurations from left to right are the greatest communication range, the intermediate configurations in SF decreasing order, and the highest data rate.

The results show that the performance in an indoor scenario is directly impacted by the distance, obstacles, and number of floors between gateways and end-devices, whatever the frequency band is.

In Figure 3.13a, we see that with LoRa sub-GHz, all spots are covered with a high FDR, close to 100%. The performance drops slightly to 86% in the worst case (spot B, floor 0), with the highest data rate, which is also the less reliable configuration, i.e., SF7, BW 500, CR 4/5.

However, the results degrade quickly for LoRa 2.4 GHz (see Figure 3.13b). We expect this difference in performance between LoRa sub-GHz and LoRa 2.4 GHz. Indeed, due to the frequency band of operation, LoRa sub-GHz has better penetration into buildings and can reach further distances. When gateways and end-devices are on the same floor (floor 2, purple bars), the FDR of LoRa 2.4 GHz decreases with the distance, as expected. Still, the

SF12 configuration guarantees excellent performance with a FDR of 100% for all the spots on floor 2.

We note particular results in two distances: spot A3 at floor 0 (blue bars) and spot B. This particularity is more observable in LoRa 2.4 GHz. For example, at floor 0, using an intermediate configuration (i.e., SF11, BW 812, CR 4/5), and at spot A3 we already lose the connectivity. With the same LoRa 2.4 GHz configuration and the same floor, we reach a FDR of 44% at a further distance (spot A4). We explain the results by the architecture of the building. Unlike the other floors, at floor 0 end-devices are surrounded by concrete columns and the ceiling is lower. The LoRa signals have to penetrate all these architectural elements thus impacting the propagation. We can also note that the LoRa 2.4 GHz FDR for spot A3 is lower than for spot A4 looking at floors 1 and 0 respectively. This comes from the location of spot A3, which is slightly off from the line of sight.

If we look at spot B, regardless of the floor, the greatest communication range configuration for LoRa 2.4 GHz is the only one that manages to maintain connectivity with the gateway. The FDR degrades as we move further away: 64% at floor 1, and 56% at floor 0. Additionally, using the highest data rate configuration for LoRa 2.4 GHz, we immediately lose the connectivity at floor 0, unless we place the end-devices just under the gateway position, located at floor 2.

To explain the frame losses that we observed, we analyzed the RSSI and the SNR of LoRa 2.4 GHz (see Figure 3.14). The color chart and the order of the configurations are the same as for the FDR results: (1) purple for floor 2, green for floor 1, and blue for floor 0, and (2) from the greatest communication range to the highest data rate configuration from left to right on the figure. Each colored dot represents the average RSSI (and SNR respectively) value for the evaluated LoRa configuration.

Remember that the LoRa gateway does not log the RSSI of each correctly demodulated frame, but instead stores the RSSI of the channel. It implies that in case an interferer is located close to the gateway, the gateway stores the RSSI of the strongest signal. Still, in this experiment, the LoRa equipment are located far away from the potential interference (e.g., Wi-Fi APs are fixed to the ceiling). Thus, even if the RSSI stored is the RSSI of the channel, the signal of the interferer is likely to be weak, and so the logged RSSI corresponds to the LoRa frame received.

The first observation is that, in Figure 3.14a, as long as the end-devices are located on the same floor as the gateway, the RSSI is very good with values around -65 dBm. Spot B, irrespective of the floor where we place the end-devices, is an exception but it is explained by the building architecture and the multiple walls and doors the LoRa signal has to go through to reach the gateway. The RSSI quickly decreases through the floors until values below -90 dBm at spot A4, floor 0, corresponding to the maximum distance between gateways and end-devices. Usually, a signal with such RSSI value is considered unusable. If we combine our RSSI analysis with the SNR, we can estimate where losses are happening. Indeed, the SNR combines the RSSI value and the noise value. LoRa has the particularity to correctly

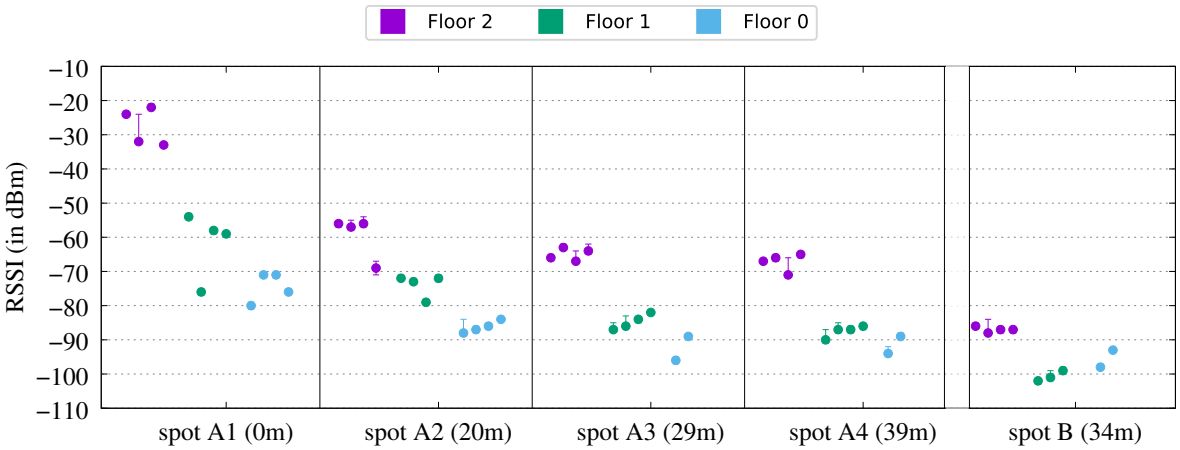

(a) LoRa 2.4 GHz RSSI

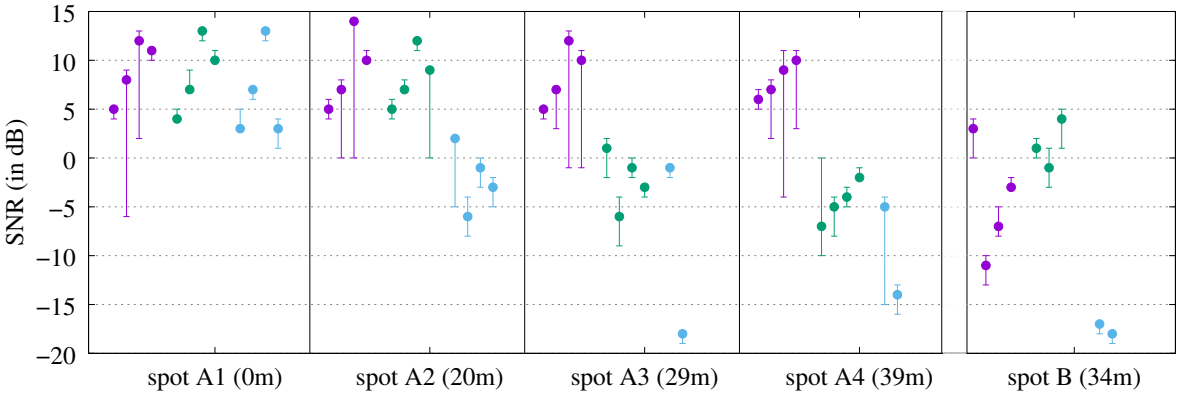

(b) LoRa 2.4 GHz SNR

FIGURE 3.14: RSSI and SNR of LoRa 2.4 GHz in the indoor scenario.

decode signal under the noise floor. Thus, even with a negative value of SNR, the LoRa gateway can detect and decode a frame. We take the example of spot A3 at floor 1, where the RSSI for the highest data rate configuration is about -80 dBm, which is already considered a bad signal quality. In Figure 3.14b we look at the corresponding SNR value: around -3 dB. This means that the noise is stronger than the signal. The SNR limit value for SF5 is -2.5 dB (see Table 3.2) so it is expected that LoRa signals cannot be correctly demodulated by the receiver. This analysis is consistent with the FDR results: at spot A3, floor 1, with an SF5 configuration for LoRa 2.4 GHz, we receive only 2% of the frames we sent. We reached the limit of connectivity of the highest data rate LoRa 2.4 GHz configuration in an indoor environment.

If we compare the results of this experiment with the one provided in Subsection 3.4.3, we observe the same trend. Both experiments are run over three-floor buildings, and in both cases, when the gateway and the end-device are located two floors from each other, the highest data rate configuration still achieves a FDR of 80%. This experiment complements the answer to the question "What is the difference, in terms of connectivity and communication range, between LoRa sub-GHz and LoRa 2.4 GHz?" (**RQ3-2**) provided in Subsection 3.5.2. It also gives an additional answer to the question "What communication range can we expect for LoRa in the 2.4 GHz ISM band in an indoor environment?" (**RQ3-4**). This result shows that using LoRa in the 2.4 GHz ISM band in an indoor environment we achieve a FDR of 98% for a distance of 39 meters over a three-floor university building. Consequently, to cover a building of several floors with LoRa 2.4 GHz, one gateway is enough using the greatest communication range configuration while multiple indoor gateways are required using the highest data rate configuration. The plurality of LoRa gateways in indoor environments is useful for localization applications. Moreover, using LoRa 2.4 GHz permits to cover the same space as ZigBee or BT which are short-range wireless technologies with IoT indoor applications, but with fewer anchors/access points, thus considerably lowers the cost and complexity of deployment.

3.6 Impact of the building use on performance of LoRa 2.4 GHz

In the previous sections, we evaluate the performance of LoRa in two different indoor environments: (1) a faculty building, and (2) a work building. For both buildings, the maximum distance between the gateways and the end-devices is 3 floors. The results show the same trends in terms of FDR: LoRa receives at least 70% of the frames over a three-floor building. The exhaustive experiment, carried out in the work building, was run during the weekend so the workers are not in the building either. The faculty building indoor experiment was run during office hours thus avoiding as much as possible people mobility in the corridors where we perform our experiments.

In this section, we perform a week-long experiment, called long-run experiment, to study the impact of people mobility and activity in an indoor environment on LoRa performance. We use the same setup, and the same indoor environment, as in the exhaustive experiment (see Section 3.4) as well as the same experimental protocol and evaluation metrics.

3.6.1 Long-run experiment results

The long-run experiment aims to answer the question "How does LoRa connectivity vary as a function of the indoor environment (competing wireless technologies and people activity

in the building)?" (**RQ3-5**). To this end, we design an experiment to evaluate how the environment and daily life activities, such as the presence of people in the building or the Wi-Fi and BT usage, impact the LoRa communications in the 2.4 GHz ISM band.

The main differences with the exhaustive experiment reside in the number of LoRa configurations we evaluate, as well as the overall duration of the experiments. As it would be too time-consuming to run all the 128 possible combinations of parameters, we decided to focus on a representative subset of six configurations extracted from Figure 3.4, corresponding to two BW (203 kHz and 1625 kHz), three SF (5, 8 and 12), and a fixed CR of 4/5. This way, we evaluate the narrowest and the widest BW as well as the smallest and the highest SF, and also an intermediate SF. These combinations of BWs and SF permit us to study the greatest communication range and the highest data configurations, along with several intermediate configurations. This small number of configurations runs in about 30 minutes, allowing us to log 153896 frames and thus have a good granularity for the long-run experiment. The experiment started on a Monday at 7:21 pm, and ended the next Monday at 4:48 pm, lasting one full week. This permits to study the day/night and weekday/weekend cycles.

In Figure 3.15 we present the FDR variations as a function of time for the entire duration of the experiment. We separate the results according to the BW used. The SF are differentiated by colors: blue for SF12, orange for SF8, and green for SF5. The x-axis is graduated with the hours for each day. Days are separated by gray dashed vertical lines. The results presented in Figure 3.15 are for the end-device located on the same floor as the gateway.

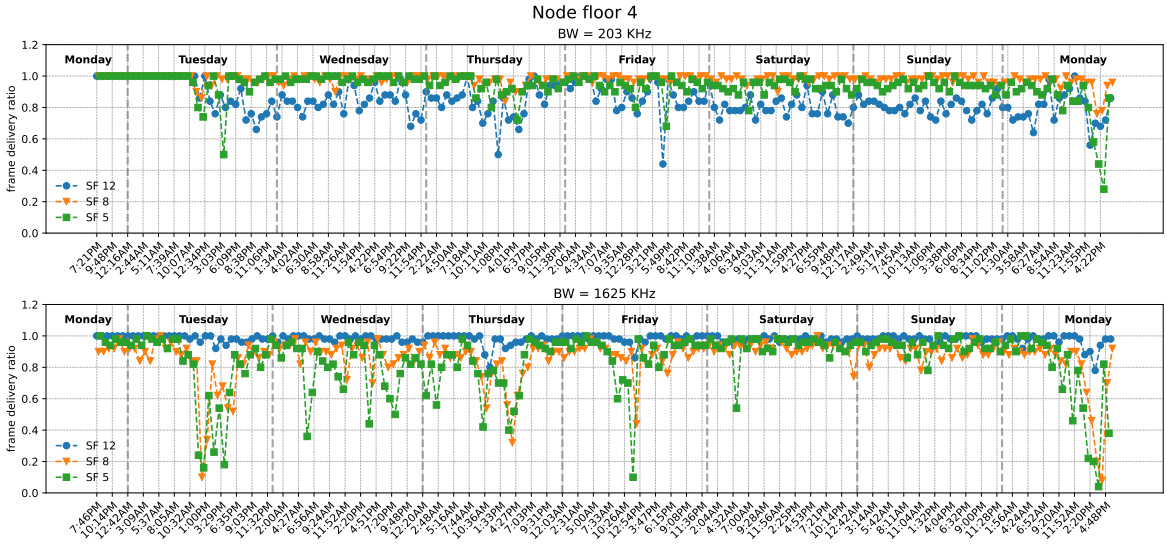

FIGURE 3.15: Evolution of the LoRa FDR as a function of time over a week.

We start by analyzing the results obtained using the narrower bandwidth: 203 kHz. SF5 and SF8 have similar results providing almost all the time a FDR above 80%. As the results overlap, we notice more variations of the green line, i.e., SF5 configuration. We observe that the greatest FDR is mostly obtained on the weekend. We noticed an exception on Wednesday where we have a very good FDR around 100%. This good performance is probably a consequence of remote work and the predilection of choosing Wednesdays to do it. The

performance drops, which are essentially observed on weekdays, are likely due to human activity in the building but because of the robustness provided by the narrow BW, it did not affect that much the LoRa performance. The SF12 configuration shows an unexpected behavior. Indeed, it is the configuration with the poorest performance. For example, on the fourth day of the experiment at 6 pm, we achieve a FDR down to 40% approximately while the SF8 and the SF5 configuration achieve a FDR of 100% and 65%. Recall that the SF12 configuration is supposed to be the more robust configuration resulting in the highest expected FDR. One possible explanation is related to the size of the frames for this configuration. SF12, BW 203 frames have a very long ToA of 892.94 ms. Because of this, we suspect that interference are occurring between LoRa 2.4 GHz frames and Wi-Fi frames. This is supported by the fact that we used a LoRa channel centered at 2403 MHz, which overlaps with the Wi-Fi channel 1 (centered at 2412 MHz). We investigated this channel overlapping by using the `NetSpot` tool [95] which shows the channel distributions of Wi-Fi APs around. We found out that channel 1 is indeed the channel used for the Wi-Fi networks in the building. Moreover, a Wi-Fi access point usually sends control traffic (beacon) each 100 ms, thus interfering several times an SF12, BW 203 frame. The distance between the LoRa gateway and the surrounding Wi-Fi access points, as well as the transmitting power of both technologies have probably also an impact on LoRa performance. As a reference, an SF8, BW 203 frame has a ToA of only 68.41 ms, which is almost 13 times lower than with a SF of 12. Hence, SF8 frames might be slightly impacted by Wi-Fi, while the SF12 frames are largely impacted by Wi-Fi when the BW is 203 kHz.

We now consider the wider bandwidth: 1625 kHz. Again the SF5 and SF8 configurations follow the same trends. The degradation is clearly seen for weekdays where the FDR sometimes drops below 20% and even falls near to 0%. These drops correspond to two periods of the day: (1) in the morning, probably when people start arriving at their offices, and (2) at noon when people leave their offices to go down to the cafeteria to have the lunch break. This contrasts with the behavior observed during the weekend: the average FDR is the same for all SF and is about 100%. It confirms the results obtained in the exhaustive experiment: during the weekend there is little activity registered in the building which leads to a higher FDR than during weekdays. The analysis of the FDR obtained using a SF12, demonstrates a clear difference with the results obtained using a BW of 203 kHz. Apart from some small drops, never below 80%, the FDR is always near 100% for all hours and all days of the experiment. The ToA of an SF12, BW 1625 is smaller than the ToA with a BW of 203 kHz. That could explain the performance difference. Still, the SF12, BW 203 is supposed to be the most robust configuration, the one which provides the greatest communication range. So, the drops observed in the FDR during the long-run experiment are unexpected. Further investigation including the repetition of the experiment is needed to understand completely what is happening in this context.

By running the long-run experiment we answer the question "How does LoRa connectivity vary as a function of the indoor environment (competing wireless technologies and people activity in the building)?" (**RQ3-5**). Overall, the best configuration in our indoor experiment is SF8, BW 203. This combination achieves a high robustness with a data rate of 5.08 Kb/s. Another candidate for high robustness is SF12, BW 1625, but the achievable data rate is only 3.81 Kb/s. The results also show a clear pattern of degradation in the times of the day in which there are activities in the building, that is during weekdays, between 8 am and 7 pm approximately. This means that before deploying a LoRa network in the 2.4 GHz ISM band, the influx of people and the work hours have to be taken into account.

3.7 Conclusions and engineering insights

In this chapter, we proposed several experiments to evaluate the performance of LoRa in outdoor and indoor environments in the 2.4 GHz ISM band. We also propose a qualitative comparison with LoRa sub-GHz, underlying the new SF5 and the new BW (812 kHz, 1625 kHz) available. The various experimental results permit to highlight some engineering insights on LoRa 2.4 GHz performance in both outdoor and indoor environments.

First, the results show that LoRa 2.4 GHz can reach a distance of communication of at least 1 km in an outdoor scenario while maintaining a FDR of 100% irrespective of the LoRa configurations used to transmit frames. Overall, when comparing LoRa sub-GHz and LoRa 2.4 GHz results, the achievable communication range follows the same trend: the highest data rate configurations have a smaller maximum communication range. Also, both versions of LoRa (sub-GHz and 2.4 GHz) ensure a FDR of 100% for a distance of 2 km (**RQ3-2** and **RQ3-3**).

Second, we showed that for a three-floor indoor deployment, with the highest data rate configuration, we achieve a FDR of about 70% when the end-device is placed in the same location as the gateway but on a different floor. With the most reliable configuration, the FDR is always around 100% for all floors and all distances evaluated. This clearly shows LoRa's robustness and coverage capabilities even in an indoor environment in the 2.4 GHz ISM band (**RQ3-4**).

Third, we showed that the FDR is considerably affected by people present in the building as well as their activities. Nevertheless, using the greatest communication range configuration enables to keep a FDR close to 100%, even under a peak of activity in the building (**RQ3-5**).

Overall, these results illustrate that the SF and the BW have a significant impact on the FDR (see Figure 3.4). Using a combination of parameters with an SF12 generally yields steady and reliable communication during the whole experiment. To achieve a high data rate with a robust link, it is better to use a low SF and a low BW, rather than to increase both the SF and the BW. For example, for a distance between the gateway and the end-device of two

floors, we recommend to use an SF5, BW 203, CR 4/8 LoRa configuration which delivers a FDR of 100%. By increasing the SF and the BW to use an SF8, BW 1625, CR 4/8 LoRa configuration, the FDR decreases to 90% (**RQ3-1**).

We believe that our results are useful to assess the real performance of LoRa 2.4 GHz technology, but also to guide the choices for future LoRa 2.4 GHz network deployments. The performance obtained with LoRa 2.4 GHz indicates that this technology is suitable for several indoor IoT applications. While its performance degrades when compared to LoRa sub-GHz, it still offers the highest range among all technologies operating in the 2.4 GHz ISM band (BT, Zigbee, Wi-Fi). We showed in Figure 3.13 that the greatest communication range configuration achieves a communication over 39 m, while the usual wireless technologies of the 2.4 GHz ISM band have a typical communication range of 10 m. Our results indicate that for complete coverage of a small multi-floor building, three or four gateways would be enough for the highest data rate LoRa 2.4 GHz configuration, which is compatible with an accurate localization. In the actual LoRa 2.4 GHz gateways, a ranging feature is implemented. With three distances we can identify the position of an end-device in an indoor environment. Adding more gateways increases the accuracy of the localization.

To use the 2.4 GHz ISM band, the first key technical challenge is the coexistence and interference management with other technologies. Indeed, during the day, we observed in our experiment that the signal was interfered by other wireless technologies used in the building thus decreasing the performance. However, we do not know how much the interference is destructive for the LoRa signal, and neither if the LoRa signal has an impact on the other wireless technologies using the 2.4 GHz ISM band.

The results obtained in Section 3.6 through the long-run experiment tend to indicate that the ToA of LoRa frames as well as the location of LoRa devices (gateways and end-devices) regarding the location of the Wi-Fi APs impact the LoRa performance in an indoor environment.

Hence, in the next chapter, we propose a methodology to study the coexistence between two wireless technologies using the same frequency band. We then apply our methodology to study the mutual impact of LoRa and Wi-Fi, in an indoor scenario, on the performance of each other.

RQ answered:

- **RQ3-1**: What is the impact of physical layer parameters (SF, BW, CR) on the communication performance, i.e., communication range and frame delivery ratio of LoRa 2.4 GHz? → Subsection 3.4.3
- **RQ3-2**: What is the difference, in terms of connectivity and communication range, between LoRa sub-GHz and LoRa 2.4 GHz? → Subsections 3.5.2 and 3.5.3
- **RQ3-3**: What communication range can we expect for LoRa in the 2.4 GHz ISM band in an outdoor environment? → Subsection 3.5.2
- **RQ3-4**: What communication range can we expect for LoRa in the 2.4 GHz ISM band in an indoor environment? → Subsections 3.4.3 and 3.5.3
- **RQ3-5**: How does LoRa connectivity vary as a function of the indoor environment (competing wireless technologies and people activity in the building)? → Subsection 3.6.1

RQ raised:

- **RQ4-***: How does LoRa coexist with other wireless technologies in the 2.4 GHz ISM band? → Chapter 4

Chapter 4

Addressing the coexistence of LoRa and Wi-Fi in the 2.4 GHz ISM band

4.1 Introduction

We showed in Subsection 1.1.3 that one of the main challenges of LoRa in the 2.4 GHz ISM band is the coexistence with other radio technologies such as Wi-Fi, BT, BLE, and ZigBee.

In the previous chapter, we investigated the potential of the LoRa technology in both indoor and outdoor environments, in the 2.4 GHz ISM band. The results demonstrated that LoRa is sensitive to its environment (mobility of people and external interference).

As a reminder, in Subsection 2.2.1 we provided an overview of the spectrum occupancy by the main wireless technologies of the 2.4 GHz ISM band. We focused on the channel allocation and commented on the choice of the three proposed LoRa 2.4 GHz channels by Semtech. The proposed LoRa 2.4 GHz channels are located 1 MHz away from the BLE advertising channels, and the three independent Wi-Fi channels completely overlap the LoRa channels. Cross-technology interference can limit the performance of the technologies using the same frequency band and having overlapping channels as overlapping transmissions frequently mainly lead to transmission losses and impact the performance of wireless technologies. Thus, it is of uttermost importance to evaluate the mutual impact of LoRa and the other users of the 2.4 GHz ISM band, as LoRa is one of the latest technologies in this crowded frequency band.

In this chapter, we study the coexistence of LoRa and Wi-Fi in the same frequency band. We focus on the Wi-Fi technology, among all technologies using the 2.4 GHz ISM band, for two reasons. First, Wi-Fi is the main and most known technology working in the 2.4 GHz ISM band. Second, Wi-Fi uses the entire channel bandwidth to transmit frames, which means a large period of interference with LoRa signals, as LoRa uses narrow bandwidths in comparison with Wi-Fi. We consider the coexistence between these two technologies as follows: we are interested in overlapping transmissions as it allows us to evaluate how they survive to interference from each other. To this end, we make a performance evaluation of LoRa and Wi-Fi interfering with each other transmissions in the 2.4 GHz ISM band. We thus investigate several parameters (e.g., bandwidth, center frequency, topology) on the coexistence of

LoRa and Wi-Fi to characterize various periods of overlapping transmissions between both technologies. We designed our experiments to be repeatable and replicable, and so that each technology is the main source of interference for the other technology being evaluated. Our experimental coexistence study focuses on the physical layer of LoRa and Wi-Fi especially because LoRa has no MAC layer standardized yet in the 2.4 GHz ISM band. This way, we compare the performance of LoRa and Wi-Fi considering the absence of any mechanisms (e.g., CSMA/CA, MCS, ACKs) that could improve the coexistence of both technologies in an overlapping transmission scenario.

We formalize the study of LoRa and Wi-Fi coexistence in the 2.4 GHz ISM band with the following research questions:

RQ4-1: How to study the coexistence of two wireless technologies using the same frequency band?

RQ4-2: How does Wi-Fi performance vary as a function of the LoRa occupancy channel rate?

RQ4-3: How does the communication reliability of both technologies vary as a function of the frequency offset between LoRa and Wi-Fi center frequency channels?

RQ4-4: How does the Wi-Fi communication reliability vary as a function of the used LoRa bandwidth and therefore of the ToA?

RQ4-5: Does the topology of the experiment, e.g., the distance between equipment using different wireless technologies, have an impact on the communication performance of both technologies?

RQ4-6: Does the Wi-Fi standard have an impact on the communication reliability of both technologies?

RQ4-1 to **RQ4-6** can be resumed into one general research question:

RQ4-7: What is the impact when there are LoRa and Wi-Fi overlapping transmissions on both technologies' communication reliability?

The results described in this chapter help us to answer each research question through the subsequent contributions [1]:

- We propose a methodology to evaluate the coexistence of LoRa and Wi-Fi in the 2.4 GHz ISM band. Our methodology can be applied to study the coexistence of LoRa with other wireless technologies.
- We make the first experimental evaluation of the coexistence between LoRa and Wi-Fi. We design and implement an experimental setup where we conceive a gateway to end-devices communication synchronization to automatize our experiments. We then compute the FDR as a metric of connectivity when the medium is shared for

[1] This chapter extends the study under review for publication [96]. Parts of the results have been presented at [3] and [4].

both evaluated technologies. We also log and analyze the RSSI and the SNR to characterize the radio environment of our experiments. The results permit to characterize the coexistence and can also serve as a basis for future works to improve the coexistence between LoRa and Wi-Fi.

- We extend the experimental results through simulations based on our performance evaluation setup by testing more configurations and parameters than is possible on real hardware.
- We establish a list of recommendations, especially on the best LoRa configurations, to improve both LoRa and Wi-Fi performances, and we propose how to choose the LoRa channel.

4.2 Studying the coexistence: SLR process

The 2.4 GHz ISM band refers to an ISM frequency band in the unlicensed spectrum. It is quite crowded already: mostly by Wi-Fi, but also by other wireless technologies such as Bluetooth or IEEE 802.15.4. Since several systems are communicating in the same environment, the question of coexistence is raised. We define coexistence as how much a technology is robust to overlapping transmissions, i.e., interfering signal, from another technology. This problem has already been widely studied as several technologies use the 2.4 GHz ISM band to communicate, either using network simulations or real testbeds. However, the emergence of LoRa in this frequency band imposes to study again eventual coexistence issues.

One of the most common devices using the 2.4 GHz ISM band is the microwave oven. At the end of the 1990s, Wi-Fi and Bluetooth started using the same frequency band leading to the first coexistence issues, as both technologies use the entire frequency spectrum of the 2.4 GHz ISM band. As these technologies have been widely studied in terms of performance, coexistence, interference, etc., we decided to apply the SLR process presented in Appendix A.3 to select the articles for our SoA. Our SLR process aims to collect papers in order to have an overview of the existing methodologies to study coexistence. Studying the coexistence of two technologies usually implies evaluating the impact of transmissions from one technology on the other technology. This kind of study analyzes the destructive impact of interference between wireless technologies on their performances, e.g., throughput, FDR. We synthesized the selected articles in Table 4.1, based on the methodology used to investigate the coexistence (i.e., theoretical, network simulation, or real experiments). The last line of the table highlights the novelty of our work compared to the existing literature.

4.2.1 Methodologies to study the coexistence

The methodologies to study coexistence can be divided into three approaches: (1) theoretical, (2) by simulations, and (3) by experiments. The simulations and experiments approaches can be divided into subcategories. The simulators either implement mathematical models, e.g., MATLAB simulation, or implement a protocol or are designed to simulate a

Ref	Theoretical	Simulations	Experiments	Technology
[97]	X			Wi-Fi
[98] [99] [100]		X		Wi-Fi [98] LoRa sub-GHz [99] [100]
[41] [42] [89] [101] [102] [103] [104] [105]			X	LoRa 2.4 GHz [41] [42] LoRa sub-GHz [89] [104] Wi-Fi [101] [105] Other [102] [103]
[106] [107] [108] [109] [110] [111] [112]	X	X		LoRa sub-GHz [106] [107] [109] [110] [111] Other [108] [112]
[113]	X		X	Wi-Fi
[7] [35] [114] [115] [116] [117]		X	X	LoRa 2.4 GHz [7] Wi-Fi [7] [115] LoRa sub-GHz [35] [114] [116] Other [117]
[118] [119]			X	Other [118] LoRa sub-GHz [119]
[120] [121]	X	X	X	Wi-Fi [120] Other [121]
[122]		X	X	LoRa sub-GHz
Our contribution		X	X	Wi-Fi and LoRa 2.4 GHz

TABLE 4.1: Coexistence state of the art classification.

specific technology such as the LoRa module in the NS3 simulator. In the same way, the experiments approaches are either real-world experiments based on commercial off the shelf equipment or run in a controlled environment, or generating a controlled signal, using universal software radio peripheral (USRP) for example. Note that these three approaches can be either used independently or combined. From these approaches, the coexistence is generally characterized in terms of percentage of occupation of a channel, BER or FDR.

Theoretical approaches rely on a mathematical model, which is an abstraction of the real world. Indeed, the environment and the behavior of the technologies are represented through mathematical equations. While it gives insights into coexistence, such theoretical approaches cannot evaluate nor represent unexplained phenomena present in a real deployment. For example, usually equations only take into account one propagation path whereas in the real world wireless communication is most of the time a multi-path signal. Theoretical approaches are also based on assumptions that model real-world signal propagation. For instance, a coexistence model in the time domain assuming that all the wireless technologies use the same center frequency and the spectrum is always occupied by at least one wireless technology [97].

Simulations-based approaches are facing the same issues: simulators do not implement a behavior that designers are not aware of. However, simulations permit to test configurations, or architecture that are very costly and time-consuming to implement through real-world experiments. Theoretical and simulation approaches have the advantage of giving boundary results on the coexistence.

Some studies use mathematics to generate a loss model [99]. Some works perform real-world measurements like noise measurements, and then use the collected data as the

entry to the simulation model. This allows the authors to estimate the probability of losses or the probability of interference [114] [115]. In several studies, the authors start the coexistence study using equations or simulations and then run experiments to validate their hypothesis [113]. Very often, when the coexistence study relies on simulations without real-world experiment validation, the interfering signal is not necessarily associated with a given technology. They rather evaluate an interferer signal such as a white Gaussian noise [106] [109]. Simulations can also focus on varying one parameter of the interfering signal, such as the distance between the interfered signal and the interferer [98].

The experiments are complementary to theoretical and simulation approaches. As experiments take place in the real world, they are subject to the variations of the environment but also to the potential constraints, limitations, and failures of the equipment.

One way to study the coexistence is to evaluate the occupancy of the frequency band. This means that irrespective of the technology, we focus on how much a frequency band is used, i.e., what percentage of the time the channel is occupied and on what frequency. This allows to identify the potential risks of interference when a technology is about to be deployed in a given environment [89]. We can also reverse the previous approach: we evaluate the performance of a technology in terms of communication range for example, and we assume that the observed losses can be a result of the other technologies present in the environment. We thus obtain preliminary results that evaluate the relevance of studying or not the coexistence. We adopted this approach in this thesis by evaluating the connectivity and the communication range of LoRa in the 2.4 GHz ISM band [41] [42] (details are provided in Chapter 3) and highlight the need to study the mutual impact of LoRa and other wireless technologies of the 2.4 GHz ISM band. Using experiments to study the coexistence can take many forms. We can be interested in the instant at which the interference occurs on the interfered signal (preamble, payload, etc.), as well as in the power difference between the two interfering signals. A common approach is to study the impact of the frequency channel offset on performance [117].

Depending on the studies, the impact on the performance of interference can be intra-technology [119], one technology over another, e.g., IEEE 802.11b/n on LoRa [7], or mutual [99]. All of these works, based on experiments, evaluate various types of environments: controlled, e.g., anechoic chamber [104], or real-world deployments, e.g., indoor [101].

4.2.2 Coexistence of wireless technologies

As mentioned in the previous subsection, the first step in the study of the coexistence of wireless technologies using the same frequency band is evaluating the channel occupancy. The results of a channel occupancy evaluation permit to indicate if the deployment of a new technology is possible and in which conditions (in terms of transmission time for example).

Regarding the study of the coexistence of wireless technologies, the frequency band of operation is not the focus of interest. We believe that the methods to study the coexistence are

independent of the frequency band of operation. Thus, we can apply the same methodology to study the coexistence of two wireless technologies in the sub-GHz bands as in the 2.4 GHz ISM band. Cognitive radios [123] propose to use the idle times of the spectrum to transmit on it.

Television white spaces are very attractive for cognitive radios. Not only WLAN could use it, but also cellular users [121]. It is possible to characterize the WLAN data traffic by considering the dependency between frequency sub-bands or time domain signals [120]. The authors evaluate the radio activity in an indoor environment through measurement campaigns. Then using the data collected, the authors derive a Gaussian model to determine whether or not a WLAN is an opportunity for low-power technologies such as BT and ZigBee as cognitive radios.

It is also possible to combine the channel occupancy study with the estimation of idle time of a channel [102]. The spectrum measurement analysis takes into account the bandwidth of the technologies already using the frequency band as well as the bandwidth of the technology that aims to be deployed in that frequency band. The authors define a threshold to determine whether or not a channel is occupied. The duty-cycle is computed over a time interval of one second. If the sample results in a value greater than 5% of the duty-cycle, the channel is considered occupied. The measurements last 24 hours per location and evaluate several bandwidths (5 MHz, 10 MHz, and 20 MHz). The results show that during office hours, the measurement point located in the library has a high occupancy channel between 10 am and 5 pm. On average, with a 10 MHz BW the channel occupancy is 14.73% with an average idle time of 28.88 s. In the suburban residential location, the occupancy channel is high between 8 pm and 11 pm. On average, with a 10 MHz BW the channel occupancy is 24.74% with an average idle time of 3.63 s. Thus, opportunistic transmissions must take into account both channel occupancy and idle channel time to choose where to deploy a new technology.

Another approach is to evaluate the quality of channels [103]. BT creates a channel map, based on the RSSI and the BER, after the connection between two BT devices. However, to simplify the channel map creation, *BluS* is proposed. In this proposition, the channel map is created without a connection between BT devices. The results show that this proposition is valid for detecting occupied channels and also the difference in channel usage in the case of several occupied channels.

In the context of IEEE 802.11 transmissions in the 2.4 GHz ISM band, it is possible to determine when a channel is idle and if it is occupied to differentiate the channel occupancy by IEEE 802.11 activity of non-IEEE 802.11 activity [113]. The results demonstrate that setting the sender and the receiver on different channels allows decreasing the total channel occupancy, i.e., computed as the sum of the channel occupancy caused by IEEE 802.11 transmissions and other wireless technologies or undecodable IEEE 802.11 transmission. For instance, an IEEE 802.11 frame using a DSSS modulation with a ToA of 3.2 ms and a frame rate of 10 frame/s, results in a channel occupancy of 5% when the sender and the receiver

use the same channel. With a difference of 3 channels between the sender and the receiver, the channel occupancy decreases to 0.8%.

The coexistence of the IEEE 802.11 standards is also studied in the 5 GHz ISM band. The channel utilization is used to measure the Wi-Fi spectrum occupancy [105]. The authors evaluate three standards: IEEE 802.11a, IEEE 802.11n, and IEEE 802.11ac. The maximum achieved throughputs are 29.20 Mbps, 66.28 Mbps, and 79.30 Mbps, respectively. When there is an overlapping transmission using the same standard, increasing the throughput of each pair (one transmitter and one receiver) results in a decrease in the achieved throughput for both pairs. Once the saturation is reached, the throughput of both pairs is constant and has a similar value. If the overlapping transmissions use different standards, i.e., IEEE 802.11a and IEEE 802.11n, at saturation, the IEEE 802.11n pair accesses the channel and transmits more often than the IEEE 802.11a pair. For example, at saturation, the throughput of the IEEE 802.11a pair is 3.3 Mbps while the IEEE 802.11n pair achieved a throughput of 53.3 Mbps.

The impact of interference on wireless technology performances is a focus of interest in the context of the coexistence study.

Usually, studies evaluate the impact of one or several wireless technologies on a given wireless technology. Each technology transmits data with different power and during different periods of time. The IEEE 802.15.4 standard defines a method to identify neighbors using the RSSI over the IEEE 802.15.4 channel (2 MHz). According to the RSSI values obtained, several thresholds are determined to classify the different sources of interference [118]. For example, if there is no RSSI value greater or equal to -85 dBm, the channel is considered unused and thus there is only noise in the channel. A WLAN interference is detected using the beacon periodicity. This classification algorithm returns the main source of interference (microwave ovens, BT, WLAN) that an IEEE 802.15.4 transmission can suffer from. This is a preliminary approach to investigate the impact of these sources of interference on IEEE 802.15.4 transmissions. It has been shown that in a ZigBee network, for a distance between the interferer and the receiver of 4 m, the packet error rate (PER) when a Bluetooth device or a microwave oven is interfering is constant around 2% [101]. For an IEEE 802.11g interferer, the distance between the ZigBee transmitter and receiver has an impact on performance. While for a distance less than 6 m the PER is constant around 2%, it increases up to 4% for a distance of 10 m.

However, IEEE 802.15.4-based networks are not always the best option for overlapping transmissions [117]. Depending on the width of the interference, one of the four PHY layers of BLE should be preferred. For a scenario where there a two pairs of overlapping transmissions with a maximum number of transmission attempts set to 4, the BLE 2M PHY provides a PER of about 15% while in the same conditions, the IEEE 802.15.4 PHY gives a PER of 75%.

From real-world measurements noise and interference power levels can be computed [115]. Wi-Fi is identified as the main source of interference in a city center. Through simulations,

the authors compute the PER of IEEE 802.15.4 under Wi-Fi interference. In a city center environment, the Wi-Fi interference prevents the use of IEEE 802.15.4 (PER near 100%). Moving to other locations such as a university campus or a suburban residential area highlights the availability of multiple channels with a PER under 40% and reach 0% when the transmission occurs around 2480 MHz which is the edge of the 2.4 GHz ISM band spectrum. We can conclude that Wi-Fi heavily impacts IEEE 802.15.4 transmissions when there is a lot of APs in the environment.

The coexistence is sometimes studied for a specific use case such as smart grid home area network (SG-HAN) [97] [98]. In case of interference from the same wireless technology, the throughput of the interfered technology decreases when the payload of the interferer increases. For an interfered technology payload size of 50 bytes, a signal-to-interference-plus-noise ratio (SINR) of -2 dB, the resulting throughput is almost 30 kbps and decreases to about 10 kbps for an interferer payload size of 50 bytes and 97 bytes respectively. In case of interference from other wireless technologies using the 2.4 GHz ISM band (IEEE 802.11b/g/n, BT, microwave oven), for an interferer payload size of 22 bytes, if the SINR is higher than -2 dB, increasing the interfered technology payload size also increases the throughput. In the industrial context, ISA100.11a is an open standard using the 2.4 GHz ISM band. The results in [98] show that increasing the distance between the IEEE 802.11b transmitter and the ISA100.11a node results in a decrease of the ISA100.11a PER. On the other hand, the ISA100.11a PER increases with either an increasing number of IEEE 802.11b APs or an increasing IEEE 802.11b transmitting power. However, the PER of ISA100.11a never reaches one because the technology transmits following a channel hopping scheme.

Finally, the coexistence of two wireless technologies can be evaluated as the gain of collaborating or competing for accessing the medium [108]. This can be modeled as a spectrum-sharing game. The results show that the cooperation is valid when networks have a small number of nodes. Otherwise, competing offers a higher gain to successfully access the medium to transmit.

Wi-Fi is the main wireless technology using the 2.4 GHz ISM band. We summarize in Table 4.2 the studies, extracted from our SLR process, on the impact of Wi-Fi on other technologies of the 2.4 GHz ISM band. The column "Robustness" highlights the impact of Wi-Fi on other wireless technologies. For example, the third line of the table indicates that ZigBee has a very good PER when transmissions overlap with IEEE 802.11b transmissions. Overall, we conclude that Wi-Fi has a significant impact on the performance of other wireless technologies. However, there is a lack of studies focusing on the impact of other wireless technologies on Wi-Fi performance. Our work aims to fill the gap regarding the robustness of Wi-Fi against LoRa interference.

4.2.3 LoRa coexistence

LoRa sub-GHz robustness to interference has also been widely studied. Before deploying a new technology in a frequency band, studies focus on the occupancy channel and

Ref	Technology	Metric	Robustness
[97]	IEEE 802.15.4 over IEEE 802.15.4 other wireless technologies over IEEE 802.15.4	Throughput	intra-technology + inter-technology - -
[98]	IEEE 802.11b over ISA100.11a	PER	ISA100.11a -
[101]	IEEE 802.11g over ZigBee BT over ZigBee Microwave oven over ZigBee	PER	under IEEE 802.11b +++ under BT +++ under microwave oven +++
[115]	Wi-Fi (IEEE 802.11a/b/g/n) over IEEE 802.15.4	PER	IEEE 802.15.4 - - -

TABLE 4.2: Wi-Fi coexistence studies.

the potential interference present in the frequency band. These approaches are very similar to the papers we presented in Subsection 4.2.2. For instance, in the city of Aalborg, in Denmark, measurements have been made to evaluate the probability of interference that LoRa or Sigfox deployment could suffer from [89]. The results indicate that there is a 22% to 33% probability of having a signal above -105 dBm in the range of frequency 868.0 MHz to 868.6 MHz. In this specific case, deploying LoRa and Sigfox networks in the shopping area or the business park of the city might be an issue especially since it is very likely that there will be other LoRa and Sigfox networks around, thus generating additional interference. Measurement results are then used in simulations to evaluate the capacity and the coverage, under interference, of LoRa and Sigfox [114]. For an indoor penetration loss of 20 db and without interference, LoRa and Sigfox provide more than 99% coverage. In case of external interference, LoRa and Sigfox provide 78% and less than 50% coverage respectively.

LoRa uses an unlicensed frequency band to transmit data and is thus exposed to interference. But LoRa is also exposed to intra-technology interference. Most of the studies focus on the impact of the distance between two LoRa networks interfering each other on performance [107] [122] or a signal-to-interference ratio (SIR) threshold to allow the demodulation of two LoRa signals using the same SF [35] [111]. For instance, to ensure a BER higher than 10^{-5} when the distance between two LoRa networks is 0 km, the network capacity is approximately 1450 end-devices. When the distance between the two LoRa networks increases to 1 km, the network capacity decreases to approximately 250 end-devices. Results also show that to ensure a BER of 1%, the SIR threshold for same-SF interference is 0 dB. If the interfering LoRa signals use different SFs, the minimum SIR threshold is -8 dB and is obtained for an SF7 signal interfering with an SF6 signal. Finally, studies demonstrate that if the LoRa packets are transmitted simultaneously, with perfect synchronization, increasing the SIR prevents the preamble detection and thus the decoding of packets [119].

Simulation works have demonstrated the good resilience of LoRa to additive white Gaussian noise (AWGN). Combining AWGN and same-SF interference decrease the symbol error rate (SER) [106]. To ensure a SER of 10^{-3} with an SF9, the SNR is -10 dB which is 3 dB higher than when only AWGN is interfering with the LoRa transmission. The impact on BER of multipath channels is also higher than the impact of an AWGN [109] [110]. Indeed, for a BER of 10^{-5} under AWGN interference, the SNR is -12 dB. In case of 6-path and 10-path

channels, the SNR is -10.5 db and -9 dB respectively to ensure the same BER of 10^{-5}.

LoRa and Sigfox are usually described as competitors in particular because the two French technologies were created in 2009 and target IoT applications. Thus, several studies focus on their performances [99] [109] [112]. Deep learning approach can be used to detect uplink LoRa transmissions under same-SF and Sigfox interference. The authors proposed two optimizations of a previous work [124] using a deep feedforward neural network (DFNN) and a convolutional neural network (CNN). The results show that the optimized LoRa receivers using deep learning approaches improve the previous work. For instance, for interfering LoRa and Sigfox users following a Poisson distribution with parameter λ 0.5, for a targeted SER of 10^{-3}, the SNR is -7 dB with the first version of the DFNN while the SNR is -4 dB with the optimized DFNN. In addition, studies show that the probability of interference between LoRa and Sigfox, for the same duty-cycle and in a worst case (-130 dBm of RSSI), is 30.3% and 21% for LoRa using an SF10 and an SF12, and 36% for Sigfox. The distance between the interfered technology and the interferer, as well as the power transmission, also plays a role in the performance degradation. For a RSSI of -120 dBm, simply setting a distance of 500 m between LoRa and Sigfox end-devices decreases the probability of interference from 14% to 7% for LoRa and from 12% to 6% for Sigfox. In this case, adding distance between LoRa and Sigfox end-devices provides a 50% reduction of the probability of interference.

LoRa also coexists with other technologies such as IEEE 802.15.4. Experiments showed that LoRa is more robust to IEEE 802.15.4 interference than the contrary. For the same center frequency, using SF9, BW 500, LoRa packet reception rate (PRR) is around 60% while the IEEE 802.15.4 PRR is almost 0% [104]. The variant of the IEEE 802.15.4 PHY such as IEEE 802.15.4 smart utility networks (SUN) suffers from LoRa overlapping transmission as well [116]. The density of LoRa end-devices per km^2 heavily impacts the packet loss ratio (PLR) of IEEE 802.15.4-SUN. For two LoRa end-devices per km^2 transmitting with SF7, BW 125 and a density of IEEE 802.15.4-SUN end-devices varying between 2 and 8 per km^2, the IEEE 802.15.4-SUN PLR is 5%. Increasing the LoRa density from 2 to 8 end-devices per km^2, increases the IEEE 802.15.4-SUN PLR to 18%.

The deployment of LoRa in the 2.4 GHz ISM band brings new coexistence challenges in particular with Wi-Fi which is one of the main wireless technologies in this frequency band. Studies showed that for an IEEE 802.11b co-channel interference i.e., same center frequency, and a power difference of -42 dB between LoRa 2.4 GHz and IEEE 802.11b signals, LoRa can achieve a BER of 10^{-2} using SF12, BW 125 [7].

We summarize in Table 4.3 the studies, extracted from our SLR process, on the impact of LoRa on other wireless technologies. We emphasize in the column "Robustness" the communication reliability of LoRa when there are overlapping transmissions with other wireless technologies. We conclude that the modulation and the communication parameters (SF, BW, CR) used by LoRa are key factors of its robustness to external interference. However, the existing studies focus on the impact of other wireless technologies on the performance of LoRa sub-GHz. We highlight the lack of study focusing on the coexistence of LoRa with other

wireless technologies in the 2.4 GHz ISM band. In comparison with the previous cited studies, our work makes the first study of the mutual effects of LoRa and Wi-Fi in the 2.4 GHz ISM band through real-life experiments, in an indoor environment, in terms of FDR. More specifically, we evaluate the robustness of LoRa against two IEEE 802.11 standards using two different modulations.

Ref	Technology	Metric	Robustness
[7]	IEEE 802.11b/n over LoRa	BER	under IEEE 802.11b + IEEE 802.11n ++
[99]	LoRa and Sigfox (mutual)	Probability of interference	LoRa + Sigfox ++
[104]	LoRa and IEEE 802.15.4 (mutual)	PRR	LoRa ++ IEEE 802.15.4 -
[116]	LoRa over IEEE 802.15.4-SUN	PLR	IEEE 802.15.4-SUN -

TABLE 4.3: LoRa coexistence studies.

4.3 A new methodology for coexistence experiments

In this section, we propose an original methodology to evaluate the coexistence of LoRa and Wi-Fi in the 2.4 GHz ISM band. We also present the metrics and the networking tools used to setup our performance evaluation. As in all our experiment designs, we have kept in mind the will to make our work reproducible. Similarly to Chapter 3, we provide the official gateway [92] and end-device [93] public code. We do not provide the code we modify for our experiments as we are working on the development branch of the Semtech code which is not public. We make available the experimental data we collected, and the post-processing scripts [2]. As the environment in which our experiments take place has an impact on the results, we design an experimental scenario using a minimal, easily transportable setup. This permits us to evaluate different environments at different times of the day. Similarly, our methodology can be applied to study the coexistence of LoRa with other wireless technologies. We already started a preliminary study on the coexistence of LoRa and BT that will be further developed in the future (see Subsection 6.2.3).

4.3.1 Coexistence experiment design

We have shown in Section 4.2 that the few available studies on the robustness of LoRa to interference only consider how the interfering technology affects LoRa performance. The only paper on LoRa 2.4 GHz in our state of the art on coexistence evaluates through simulations the impact of IEEE 802.11b and IEEE 802.11n on LoRa BER [7]. Nowadays, Wi-Fi APs are deployed in every building and used by everyone at universities, in working offices, and in residential areas. So, we need to experimentally evaluate the feasibility of deploying LoRa in the 2.4 GHz ISM band where the coexistence with Wi-Fi might be challenging. Indeed, if the impact of LoRa drastically degrades the reliability of Wi-Fi communication, it is likely

[2]Both the code and the data will be available upon acceptance of the paper [96]. The code can be used according to the terms of the Revised BSD License.

that LoRa 2.4 GHz will not be used. For this reason, we decided to study the reciprocal impact of LoRa and Wi-Fi overlapping transmissions on each other. This aims to answer the question "What is the impact when there are LoRa and Wi-Fi overlapping transmissions on both technologies' communication reliability?" (**RQ4-7**).

Before running our coexistence performance evaluation, we propose a methodology to answer the question "How to study the coexistence of two wireless technologies using the same frequency band?" (**RQ4-1**).

We design our experiments to have time periods where only one technology is transmitting without interference from the other technology and considering several LoRa configurations. The free-interference periods aim to setup a baseline for each technology that we evaluate. This way, we can compare the communication reliability in the presence and absence of controlled interference and thus analyze how much interference prevents transmissions. Figure 4.1 shows the timeline we designed for our experiments, which allows us to automatize the experiments through the LoRa gateway to end-devices communication protocol, and Python scripts for Wi-Fi, described in Subsection 4.3.2. We design the experiments with four phases: (1) only Wi-Fi is transmitting, to have a benchmark for Wi-Fi performance, (2) LoRa starts transmitting and thus interferes with the Wi-Fi traffic, (3) Wi-Fi stops transmitting letting LoRa transmitting alone, to have a benchmark for LoRa performance, and finally (4) Wi-Fi starts transmitting and interferes with the LoRa traffic. These phases allow us to compute the percentage of frame received, called the FDR, for Wi-Fi alone, the FDR for Wi-Fi when LoRa is transmitting, the FDR for LoRa alone, and finally the FDR for LoRa when Wi-Fi is transmitting, for a given LoRa configuration and at a given time. Although, phases (2) and (4) are similar, we designed our experiments in that way to assess whether the interfering technology, i.e., the one that starts while the other technology is transmitting, has a significant impact on the performance of the interfered technology. The duration of each phase is customizable. We conceived our experimental timeline to guarantee that: (1) a representative number of frames is sent per LoRa configuration to compute the FDR, and (2) each phase lasts the same period for each LoRa configuration. For example, if the duration of Phase 1 is two minutes, Phase 2 also lasts for two minutes per LoRa configuration. Each LoRa configuration has a different ToA depending on the combination of parameters used, in particular SF and BW values. Hence, to ensure the same duration for each LoRa configuration, we modify the number of frames, and the interval between two frames, during a period.

For a fair comparison of LoRa and Wi-Fi performances, we evaluate only the communications at the physical layer for both technologies. Indeed, as discussed in Subsection 2.3, no MAC layer is standardized for LoRa in the 2.4 GHz ISM band yet. On the Wi-Fi side, we do not consider the mechanisms ensuring the reliability of the communications mentioned in Subsection 2.2.2. This way, we focus on the transmissions of both technologies regarding only the impact of their configurations and modulations on their communication reliability. We consider our results as a lower bound since results represent the raw performance of

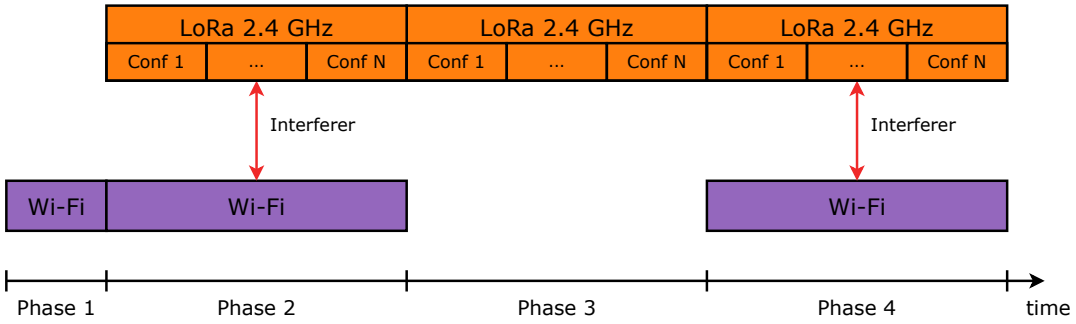

FIGURE 4.1: Timeline of an experiment divided into four phases: (1) Wi-Fi only, (2) Wi-Fi + LoRa, (3) LoRa only, and (4) LoRa + Wi-Fi.

LoRa and Wi-Fi in an overlapping transmission scenario considering the absence of interference mitigation mechanisms.

To evaluate the impact of the LoRa parameters on the performance of overlapping transmissions (**RQ4-2**), we studied typical LoRa configurations, i.e., the ones providing the greatest communication range (SF12, BW 203) and the highest data rate (SF6, BW 1625), as well as intermediary configurations (SF9, BW 812). We refer to a configuration as a triple that contains (1) the spreading factor, (2) the bandwidth, and (3) the coding rate that is used in LoRa to increase the redundancy of bits in the frames, and thus add robustness.

We mentioned in Subsection 2.2.1, the bandwidth difference between LoRa and Wi-Fi: between 203 kHz and 1625 kHz for LoRa, and 20 MHz or 22 MHz for the IEEE 802.11g and IEEE 802.11b standards respectively. Thus, we vary the center frequency of the LoRa channel to change the overlap between LoRa and Wi-Fi to observe the impact of the chosen LoRa channel (**RQ4-3** and **RQ4-4**). Our timeline experiment represents the evaluation of various LoRa configurations for one LoRa center frequency. In our case, one experiment is composed of various repetitions of the timeline where we vary the LoRa channel and evaluate the same LoRa and Wi-Fi configurations for each LoRa channel.

As the location of LoRa and Wi-Fi equipment has an impact on the results, we designed a worst case topology (**RQ4-5**) where the LoRa transmitter is next to the Wi-Fi receiver and conversely (see Figure 4.2). This is the worst case because each time the LoRa gateway receives a frame, there is a possibility that a Wi-Fi frame is transmitted simultaneously meaning that our transmissions will suffer from the highest possible interference. LoRa frames are sent at the maximum transmit power (13 dBm). So if the LoRa end-device sends a frame and a Wi-Fi frame arrives at the receiver at the same moment, the Wi-Fi frame could be lost because of a degraded RSSI due to signal propagation losses and interference coming from the LoRa transmission.

Most of the results presented in the next sections evaluate the IEEE 802.11g standard. We choose this version of IEEE 802.11 because of a hardware limitation coming from our experimental equipment. We also evaluate the IEEE 802.11b standard and provide the results in

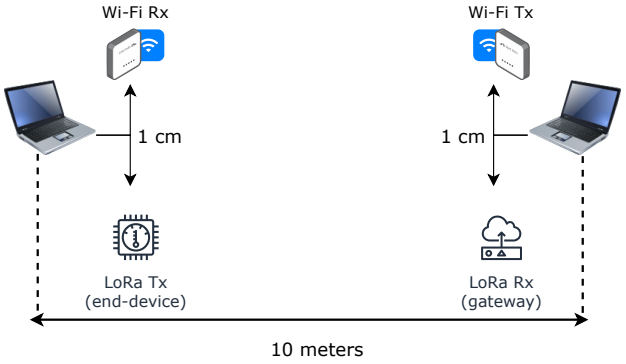

FIGURE 4.2: Experimental setup composed of two laptops with wireless interfaces in monitor mode, one LoRa gateway, and one LoRa end-device. Transmitters and receivers are approximately 10 meters away.

Subsection 4.5.6. However, the IEEE 802.11b and IEEE 802.11g standards provide different data rates and use different modulations. So, even if we are constrained by our experimental equipment in the IEEE 802.11 standard choice, we still are able to evaluate two standards with distinct characteristics. For simplicity, we use the term Wi-Fi to refer to the IEEE 802.11 physical layer (DSSS for IEEE 802.11b and OFDM for IEEE 802.11g) for the rest of this chapter.

The characteristics of LoRa and Wi-Fi are very different. Thus, we must carefully choose the payload size to use in our experiments. LoRa typical applications have low data rates, and send small amounts of data over long distances. We set the payload size to have a reasonable ToA and also to represent a common payload size that can be found in LoRa applications [125]. So, we use a 20 bytes payload resulting in a ToA between 3 ms and 1054 ms depending on the LoRa configurations. Meanwhile, Wi-Fi typical applications have high data rates, and send long data frames over short distances. The usual Wi-Fi payloads vary depending on the type of data sent. We scanned our environment with `Wireshark` for a few minutes during office hours and observed a payload size between 190 and 350 bytes for beacon frames, and a payload size between 1200 and 1460 bytes for data frames. So, we decided to use 1400 bytes for the Wi-Fi payload size to cover a wide range of Wi-Fi applications sending data.

Regarding the traffic model, we use a constant bit rate (CBR) for both LoRa and Wi-Fi. To be fair, and to compare the results of the different LoRa configurations used, we use the same occupancy channel rate (see Equation 4.2) for each evaluated LoRa configuration. The typical Wi-Fi control traffic (e.g., beacon) is periodic. In our experiments, we reproduce the Wi-Fi traffic periodicity by using 100 ms as it is the standard inter-beacon frame time. The Wi-Fi `Wireshark` logs confirm that the MAC layer is disabled. By default, a Wi-Fi transmitter retransmits up to 7 times a frame that is not being acknowledged by the receiver. As the ACK mechanism is not present at the physical layer, it explains why our receiver logs contain 8 frames for each transmitted frame. The first frame is the original one and the seven

following frames are tagged with a 1-bit value indicating that this is a retry transmission. So, a frame is transmitted every $\frac{100 \text{ ms}}{8} = 12.5$ ms. However, in our study, we consider only the original frames. This ensures a period of coexistence between LoRa and Wi-Fi even for the shortest LoRa frames. The minimal interference period between LoRa and Wi-Fi original frame is 1 ms. The shortest LoRa frames last approximately 3 ms while the IEEE 802.11g frames last 1 ms.

$$\text{occupancy channel rate} = \frac{\text{time on air} \times \text{number of frames to send for one LoRa configuration}}{\text{test duration of one LoRa configuration}}, \tag{4.1}$$

with time on air extracted from [9]

$$\text{time on air} = \frac{2^{SF}}{BW} \times N_{symbol}. \tag{4.2}$$

4.3.2 Coexistence gateway to end-devices communication protocol

In Subsection 3.4.2, we designed and motivated a gateway to end-devices communication protocol for the synchronization of LoRa equipment to automatize our experiments. In this chapter, we reuse the original protocol and adapt it to our coexistence experiments.

To automatize the LoRa experiments, we need a protocol between the gateway and the end-device to ensure that they are using the same configuration. The end-device has to run a certain number of configurations depending on the series of experiments, which must be repeated several times to average the possible variations in the results. The modified version of the original protocol is presented in Figure 4.3. The main difference with the original protocol is that in our coexistence study: (1) we use only one LoRa end-device, and (2) we reconfigure the gateway after the three LoRa configurations we chose to evaluate to change the center frequency of the LoRa channel. As a reminder, the gateway activates the end-device by sending a downlink frame. Then, the end-device sends N uplink data frames with the configured parameters. An end-device can run different configurations, one after the other. For example, end-device 1 in Figure 4.3 runs three different LoRa configurations. When the end-device finishes sending all the data frames for each configuration, it informs the gateway by sending a specific message. Then, the gateway can reconfigure itself and move to the next center frequency to be evaluated, or to the next set of configurations.

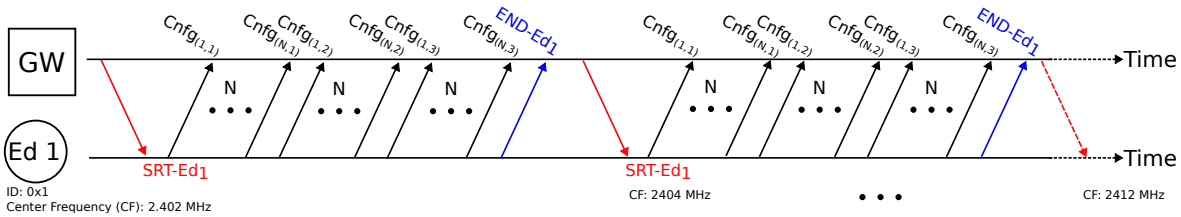

FIGURE 4.3: Protocol used between the LoRa gateway and end-devices. Red lines represent downlink end-device activation frames, blue lines represent uplink control frames and black lines represent uplink data frames for each configuration.

Note that, as the LoRa gateway has to send frames to allow the end-device to start transmitting, the downlink activation frames have to be sent with a configuration that is robust to interference and signal propagation losses. We ran some tests to evaluate which configuration to use to send the activation frames and we concluded that in order to always receive at least one downlink frame we have to send the activation frame using SF12, BW 203.

The automation of the Wi-Fi part consists of a timer in the Python scripts used to generate the frame transmissions because we considered a single Wi-Fi configuration. The timer is chosen to allow the synchronization of the four phases (see Figure 4.1).

For both technologies, the start of the experiment is manual and then the rest of the experiment (transmission periods, idle periods, and gateway reconfigurations) are automatized.

4.3.3 Coexistence evaluation metrics

Our performance evaluation aims to characterize the coexistence between LoRa and Wi-Fi at the physical level. We are interested in the communication reliability achieved by a technology under interference, i.e., with overlapping transmissions, from another technology. We thus look at the number of frames lost and compute the FDR as a metric of reliability when the medium is shared for both evaluated technologies. We also log and analyze the RSSI and the SNR to characterize the radio environment of our experiments.

The **FDR** indicates the proportion of received frames to sent frames and is a commonly used metric to assess network performance. This metric gives insights into the robustness of a wireless link between two devices. Based on the FDR it is possible to evaluate the reliability and the communication range of a transmission between devices depending on the environment, on the configuration setup, and other physical parameters such as the antenna reception gain. We compute the FDR by logging frames at the transmitter and the receiver sides for both technologies. As our experiments take place in an open indoor environment, we cannot control all the Wi-Fi APs. Thus, even if we scan our environment, we do not know the volume of data transferred by other interfering traffic. For the Wi-Fi, we filter the source and destination MAC addresses to count only the frames we are generating. Note that, we do not evaluate any retransmission mechanism for LoRa or Wi-Fi, as we only considered the physical layers of both technologies.

The **RSSI** is a metric that gives the signal strength of the radio link for each received frame. Frame losses are likely to happen if the signal strength of the radio transmission is too low. In our case, analyzing the RSSI variations can explain and complement the results obtained by computing the FDR. The RSSI is a measurement of the power of each received frame at the receiver side in dBm. Generally, RSSI values vary between -30 dBm and -90 dBm for Wi-Fi, and between -20 dBm and -140 dBm for LoRa (according to SX1280 Datasheet "Ranging RSSI section" [9]).

The **SNR** is a metric that allows to quantify interference and noise. We compute the SNR as the average signal-to-noise ratio of frames received by the gateway. Due to our topology where equipment of different technologies are collocated, we expect that analyzing the SNR

will not provide any added value. Indeed, equipment of different technologies will experience a similar noise; so the SNR does not give us additional information. However, we still measure the SNR during our experiments and then analyze it to confirm or deny our assumption.

4.3.4 Networking tools

To retrieve and compute these metrics, we use the following networking tools.

Scapy: This is a Python library, which permits to forge and send IEEE 802.11 frames through the wireless interface of a computer. We specify the source and destination MAC addresses of the frames, the wireless interface to send the frames, the payload size, and the data payload to send. As far as we know, this Python library cannot change directly the IEEE 802.11 standard, or the MCS, used for the transmissions [126]. For instance, the wireless interface traffic rate can be modified directly in the hardware parameters but not through `Scapy`. Usually, `Scapy` using the IEEE 802.11 layer is used to simulate network attacks, e.g., send a fake beacon making devices believe that an AP is available or injecting data and forcing the disconnection of an AP. However, in our coexistence scenario, we use `Scapy` to generate the Wi-Fi traffic. In our configuration, depending on the laptop used to forge the `Scapy` frames, `Scapy` selects either the IEEE 802.11b or the IEEE 802.11g standard although our wireless interface supports more recent standards such as IEEE 802.11n and IEEE 802.11ac. Remember that to use `Scapy` the wireless interfaces have to support the monitor mode.

Tcpdump: `Tcpdump`, when used in monitor mode, permits to observe the IEEE 802.11 headers of the Wi-Fi frames and the control frames (beacon, ACK). We use this command line utility program to monitor and log all the traffic sniffed through the wireless interface of the transmitter and the receiver. We are especially interested in the IEEE 802.11 traffic that permits us to analyze our own Wi-Fi traffic. `Tcpdump` stores, for each frame, information such as the source and destination MAC addresses, the IEEE 802.11 standard used to send the frame, the data rate, and the RSSI. By post-processing the file saved through `Tcpdump`, we can compute the FDR and observe the RSSI variations over our experiments [127].

Netdownlink utility: The `netdownlink` utility is part of the gateway code owned by Semtech. Through the LoRa gateway, the `netdownlink` utility allows to save each frame received by the LoRa gateway into a CSV file. It retrieves information such as the LoRa configuration used to send the frame (SF, BW, CR), the RSSI, the SNR, the payload size and the payload content. This log permits us to compute the FDR, as we count the number of frames received by the gateway, and observe the RSSI, and the SNR, variations that can explain the frame losses.

We use two additional networking tools: `Wireshark` [128] and `Netspot` [95]. `Wireshark` allows us to visualize the `Tcpdump` logs. We also confirm that the MCS used for the Wi-Fi traffic was fixed since the MCS field of the Wi-Fi frames was empty. `Netspot` allows us to visualize the Wi-Fi APs present in the environment of our coexistence as well as their RSSI (min, max, and average values).

4.4 Coexistence experimental description

Existing coexistence studies evaluate the impact of a few parameters, usually the transmission channel, and the distance between the source of interference and the interfered technology receiver, on the interfered technology performance [101]. In our experimental coexistence evaluation, we analyze a wide set of parameters that could impact LoRa and Wi-Fi communication reliability. The parameters to evaluate are chosen to answer the questions **RQ4-2** to **RQ4-7** on the performance in indoor environment of LoRa and Wi-Fi overlapping transmissions in the 2.4 GHz ISM band. To this end, we design and conduct two series of experiments:

1. **General experiment**. This experiment is designed to evaluate the impact of the LoRa traffic load and the choice of the LoRa channel on the performance of both technologies. In these series, we use three different combinations of SF, BW, and CR, for a LoRa occupancy channel rate of 10%.

2. **Bandwidth experiment**. This experiment is designed to evaluate the impact of a given BW on LoRa and Wi-Fi performances. We focus on the BW for two reasons. First, the interference is spread over the entire BW of the interfered signal. So, we evaluate the impact of interference as a function of the BW of the interfered technology. Second, changing one parameter in a LoRa configuration modifies the time on air of a frame, and we are studying BW impact, and thus the ToA impact, on the performance of LoRa and Wi-Fi respectively. For that, we use fixed spreading factor and coding rate values for a LoRa occupancy channel rate of 18%.

We evaluate a maximum occupancy channel rate of 18% because this is a hardware limit when the LoRa configuration is SF6, BW 1625. The maximum occupancy channel rate corresponds to a number of frames sent over a given period with no inter-frame time, meaning that the only delay between transmitted frames comes from the hardware operation. The theoretical number of frames is computed according to the ToA of one frame and the inter-frame time (see Equation 4.4). Then we experimentally evaluate the effective duration to send the number of frames computed and adjust it until fitting the targeted phase duration. In this numerical example, we compute the number of frames to ensure ten minutes of continuous LoRa transmission.

$$\text{theoretical number of frames} = \frac{\text{test duration} \times \text{targeted occupancy channel rate}}{\text{time on air}} \tag{4.3}$$

$$= \frac{600000 \text{ ms} \times 0.18}{3.1 \text{ ms}} = 34838 \text{ frames.} \tag{4.4}$$

Both series were run at least three times, to smooth out variations that might arise from a change in the environment. We do not observe a significant difference between working days and weekends results so we ran our experiments irrespective of the day of the week. We start our coexistence study with the General experiment that evaluates a subset of LoRa configurations with SF, BW, and CR varying. The General experiment was run only by

night. We use the General experiment to evaluate the impact of the LoRa channel, and the topology of experiments, on the performance of Wi-Fi and LoRa. From the results obtained with the General experiment, we design the Bandwidth experiment that only changes the ToA of the LoRa frames. We use the Bandwidth experiment to evaluate and compare the results obtained at different running times: by night and day. Changing the time of running our experiment allows us to evaluate how external wireless technologies usage in the environment of the experiments, Wi-Fi in our case, impacts the communications of the evaluated technologies. The duration of each experiment is about 6 hours.

We summarize the general parameters used for both series of experiments in Table 4.4. Table 4.5 focuses on the specificities of the LoRa parameters used in the Bandwidth experiments.

Technology	Configuration number	PHY Configuration	Center frequency (in MHz)	Payload size (in bytes)	Time on air (in ms)
Wi-Fi	/	802.11g, BW 20 MHz	2412 (channel 1)	1400	1
LoRa	1	SF12, BW 203, CR 4/8	2402, 2404,	20	1054
	2	SF9, BW 812, CR 4/8	2406, 2408,		38
	3	SF6, BW 1625, CR 4/5	2410, 2412		3

TABLE 4.4: Parameters of the General experiment.

Configuration number	Spreading Factor	Bandwidth (in kHz)	Coding Rate	Time on air (in ms)
2.a	9	203 812 1625	4/8	152
2.b				38
2.c				24
3.a	6			32
3.b				8
3.c				4

TABLE 4.5: Parameters of the Bandwidth experiment for LoRa.

4.4.1 Coexistence scenario

In Chapter 3, we studied the performance of LoRa in the 2.4 GHz ISM band in two indoor environments: a university building where classes are given, and an office building hosting the Inria Lyon Centre. These previous experiments give us insights into the impact of people's mobility and activity inside the building on LoRa connectivity. In this chapter, we study the coexistence challenge of LoRa and Wi-Fi in the 2.4 GHz ISM band, by evaluating a third type of indoor environment: a residential one. Using a residential building to perform our experiments allows us to represent a real interference case for LoRa, as one of the main applications of the IoT is smart home. We analyze how the presence of the residents in the building, and more precisely the likelihood of external interference caused by people using devices in the 2.4 GHz ISM band, as it would probably have an impact on LoRa transmissions(**RQ4-5** and **RQ4-6**).

All the experiments were performed in an apartment located on the fifth floor of a building in Lyon (France) in a dense area. As depicted in Figure 4.2, we collocate the LoRa gateway

with the Wi-Fi transmitter, and the LoRa end-device with the Wi-Fi receiver, to evaluate a worst case topology.

We use the same equipment as in our previous experiments that consist of one end-device sending uplinks and one gateway listening to uplink transmissions on the LoRa side. Although our LoRa gateway can listen to three configurations in parallel, our setup only uses one end-device, so the configurations are tested one after the other.

On the Wi-Fi side, we use two computers in monitor mode: one acts as the transmitter and the other as the receiver. The transmitter computer generates the Wi-Fi traffic through `Scapy`, and both computers monitor and log the traffic. Having logs on both sides of the Wi-Fi transmission allows us to compute the Wi-Fi FDR by counting the received frames over the sent frames. The Wi-Fi chipsets used by the computers are Intel Corporation Wireless 8265 / 8275 (rev 78) [129], or Broadcom Corporation BCM4313 802.11bgn Wireless Network Adapter (rev 01) [130]. Remember that the monitoring mode does not aim to generate traffic and thus does not permit to change the transmit power of the wireless interfaces of our laptop. Using `Netspot` we can estimate the RSSI of our Wi-Fi traffic by taking the average value of the AP present in the apartment. The average RSSI value is -41 dBm. We chose the payload size within the maximum transmission unit (MTU) of Wi-Fi and in accordance with the analysis of the wireless environment presented in Section 4.3.

In Table 4.4, we detailed the LoRa configurations we evaluate in our coexistence performance evaluation. The LoRa configurations are referred to as configuration numbers 1, 2, and 3, respectively. Note that while LoRa allows the use of a SF 5, our initial experiments highlight a hardware limitation: small inter-frame times led to gateway failure, causing it to shut down. Indeed, the gateway has no time to demodulate incoming frames before switching to listening for new ones and eventually becomes blocked in a deadlock. Thus, we decided to use the smallest SF value able to provide a stable operation which is SF6. The chosen LoRa configurations are set up (i.e., number of frames and inter-frame time) to ensure a transmission time of five minutes per configuration, corresponding to 29, 791, and 9900 LoRa frames respectively.

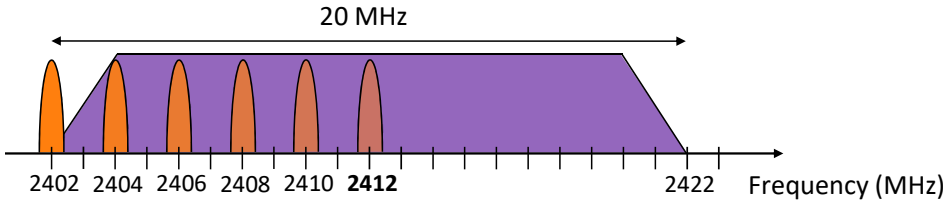

FIGURE 4.4: Evaluated LoRa and Wi-Fi channels.

In Figure 4.4 we visualize the narrow bandwidth properties of LoRa (203, 406, 812 or 1625 kHz) regarding the bandwidth of Wi-Fi (20 MHz). We evaluate different center frequencies for LoRa transmissions, from 2402 MHz to 2412 MHz with a 2 MHz step. Since the Wi-Fi spectrum is symmetrical around the center frequency, for a given channel, transmitting LoRa frames with a fixed frequency in the first part of the Wi-Fi spectrum will give the

same results as transmitting on the second part of the Wi-Fi spectrum. This assumption is true only if there is no wireless communication on the adjacent overlapped channels. Thus, we evaluate six LoRa channels to cover only the first lobe of Wi-Fi channel 1, which is centered at 2412 MHz with a bandwidth of 20 MHz. This choice allows us to avoid interference from Wi-Fi signals on channels 2 to 5, as Wi-Fi channels are separated by 5 MHz. With our setup, `Scapy` allows us to use the IEEE 802.11g standard with a 12 Mbps data rate. As the physical layer of the IEEE 802.11n standard is an improvement of the IEEE 802.11g standard (see Subsection 2.2.2), our performance evaluation allows us to evaluate a popular Wi-Fi standard when LoRa is transmitting.

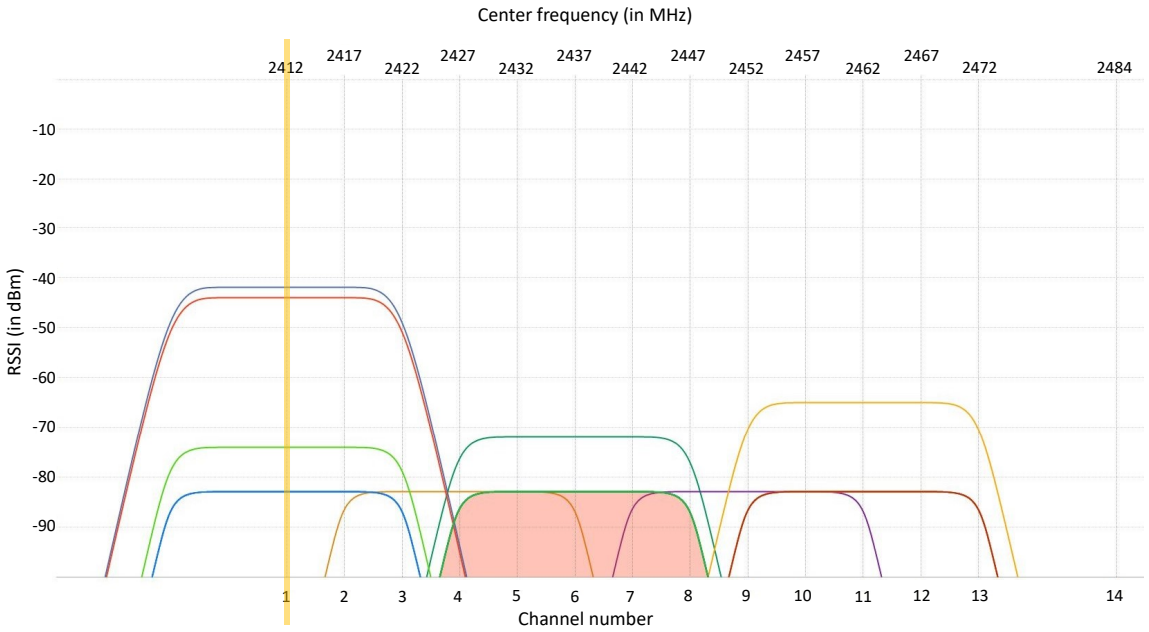

FIGURE 4.5: Capture of the `NetSpot` tool showing the distribution of the access points of the wireless environment where our experiments take place. The yellow vertical line highlights the Wi-Fi channel used in our experiments.

In Figure 4.5, we can see the distribution of the APs in the environment where the experiments take place. Out of the ten APs visible in the figure, four are on channel 1, two on channel 6, and two on channel 11, which confirms that the default Wi-Fi deployments are generally on one of the three independent channels. In our experiment, we also evaluate the Wi-Fi channel 1. Regarding the Wi-Fi APs distribution, we observe that our transmissions will coexist with four other Wi-Fi networks that we considered at external interference. Three out of the four Wi-Fi APs are located in other apartments and have an average RSSI value between -72 dBm and -83 dBm. Due to propagation losses, transmissions coming from these networks might have little impact on our results. The last Wi-Fi AP is located inside the apartment and has an average RSSI value of -41 dBm. Still, during our experiments, we did not use this Wi-Fi AP, i.e., we did not generate data traffic, so the only traffic interfering with our transmissions is the control traffic. We assume that if this control traffic has an impact on our results, it would be smoothed over the entire experiment and repetitions.

4.5 Coexistence performance evaluation

In this section, we provide an answer to each of the research questions raised in the introduction to this chapter.

4.5.1 Impact of the LoRa occupancy channel rate

To answer the question "How does Wi-Fi performance vary as a function of the LoRa occupancy channel rate?" (**RQ4-2**), we start with a first evaluation of the impact of LoRa transmissions on Wi-Fi performance. To estimate the effect of the LoRa occupancy channel rate on the Wi-Fi FDR, we send LoRa frames centered at 2402 MHz for ten minutes for three different values of occupancy channel rate: 75%, 50%, and 25%. We imagine that these occupancy channel rates correspond to a critical IoT application such as emergency advertisement in the industrial domain. In this use case, the occupancy channel rate is chosen according to the LoRa end-device resource application requirements and the number of end-devices in the network. Therefore, for high resource application requirements and a small number of end-devices, the occupancy channel rate is set to 75%. In the opposite case, i.e., low resource application requirements and an important number of end-devices, the occupancy channel rate is set to 25%. For the intermediate case where there is a trade-off between resource application requirements and the number of end-devices, the occupancy channel rate is set to 50%. Note that LoRa sub-GHz transmissions are constrained to 1% of duty-cycle in Europe. So, using LoRa in the 2.4 GHz ISM band leads to the possibility of transmitting more often than in LoRa sub-GHz.

We do not evaluate the SF6 configuration, because the maximum occupancy rate reachable with SF6 and BW 1625 is 18% according to Equation 4.2.

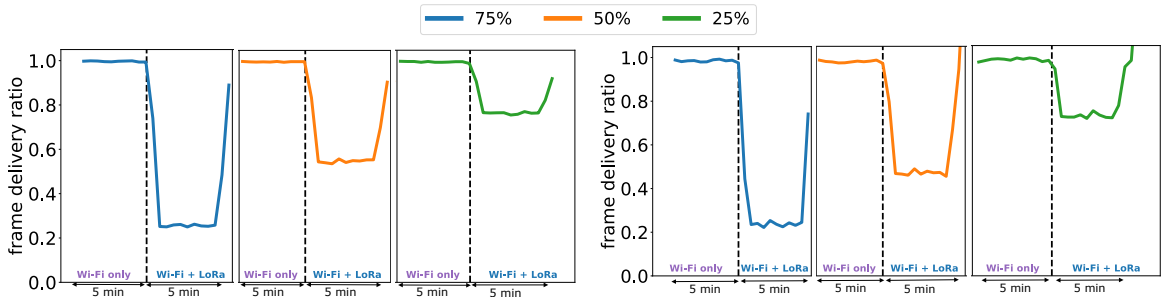

(a) Wi-Fi FDR for different configuration 1 occupancy rates

(b) Wi-Fi FDR for different configuration 2 occupancy rates

FIGURE 4.6: Wi-Fi FDR for several LoRa occupancy channel rates.

In Figure 4.6 the Wi-Fi FDR is displayed depending on the LoRa occupancy channel rate: blue lines represent an occupancy channel rate of 75%, orange lines represent an occupancy channel rate of 50%, and green lines represent an occupancy channel rate of 25%. For each occupancy channel rate tested the total duration of the experiment is 10 minutes and is divided into periods of 5 minutes. During the first period of 5 minutes there are only

Wi-Fi transmissions. During the second period of 5 minutes, there are overlapping Wi-Fi and LoRa transmissions.

In Figure 4.6a, we can see the Wi-Fi FDR as a function of the occupancy rate using LoRa configuration 1, i.e., SF12/BW203. From these results, we can see that the LoRa occupancy channel rate has a direct impact on the Wi-Fi FDR. With a LoRa occupancy channel rate of 75%, the Wi-Fi FDR is about 25%. The same applies to a LoRa occupancy channel rate of 50% leading to a Wi-Fi FDR about 50%, and to a LoRa occupancy channel rate of 25% leading to a Wi-Fi FDR about 75%. In Figure 4.6b, we observe that the results obtained by the intermediate configuration (SF9) are almost identical to those of the greatest communication range (SF12). The Wi-Fi FDR decreases between the two configurations is approximately 5%. So the LoRa configuration has less impact on the Wi-Fi FDR than the LoRa occupancy channel rate.

As a LoRa SF12 signal is more robust than a signal using an SF9, we thought we would see significant variations of the Wi-Fi FDR depending on the LoRa interfering signal configuration. In the next sections, we will further investigate these results.

This first evaluation provides an answer to the question "How does Wi-Fi performance vary as a function of the LoRa occupancy channel rate?" (**RQ4-2**). The results show that the higher the occupancy channel rate, the lower the Wi-Fi FDR. This trend is similar for both LoRa configurations tested. In addition, the Wi-Fi FDR decrease is directly linked to the intensity of the LoRa traffic rather than to the LoRa configuration.

4.5.2 Impact of the LoRa center frequency

In Figure 4.4 we hinted that the choice of the LoRa channel may have an impact on performance. Depending on the center frequency of the LoRa channel, the LoRa channel is disjoint, partially overlapping, or fully overlapping with the spectrum of the Wi-Fi AP. This raises the research question "How does the communication reliability of both technologies vary as a function of the frequency offset between LoRa and Wi-Fi center frequency channels?" (**RQ4-3**) we aim to answer in this subsection.

Figure 4.7 shows the LoRa FDR for a range of center frequencies and for the three configurations detailed in Table 4.4. The trends observed in the results are the same for all the repetitions of the experiment. Hence, to ease the understanding of the results, in Figure 4.7 we display the results of only one experiment.

We conclude from the results that the closer the center frequency of the LoRa channel is from the center frequency of the Wi-Fi channel (2412 MHz), i.e., the biggest channel overlap, the higher the impact on the LoRa FDR. For example, for the intermediate configuration (see Figure 4.7b) until 2404 MHz the FDR is 100%. Then the LoRa FDR decreases from 82% to 35% as we get closer to the Wi-Fi center frequency. When using a less robust LoRa configuration (e.g., small SF combined with high BW, such as configuration 3) the impact on LoRa

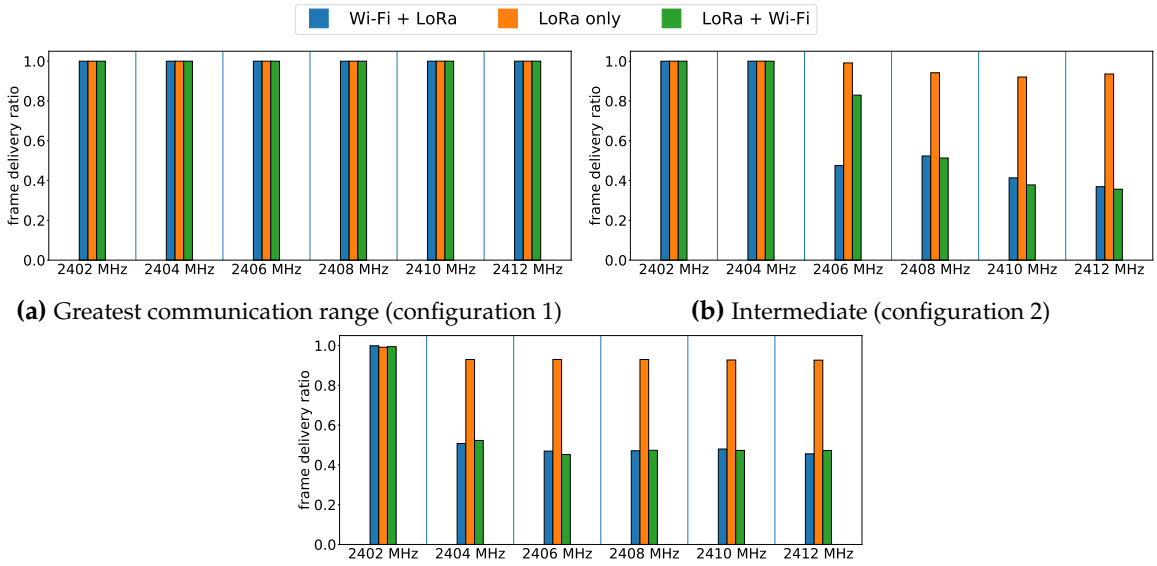

(a) Greatest communication range (configuration 1)

(b) Intermediate (configuration 2)

(c) Highest data rate (configuration 3)

FIGURE 4.7: LoRa FDR depending on the center frequency.

performance appears sooner (at 2404 MHz). For the configuration providing the highest data rate (see Figure 4.7c), the results show that for all the tested center frequencies, except 2402 MHz, the LoRa FDR without interference is above 92% whereas under interference it decreases to a minimum of 45%. Finally, for the greatest communication range LoRa configuration (see Figure 4.7a), and thus the most robust configuration, the results indicate that the Wi-Fi has negligible impact on LoRa performance as we always received 100% of the transmitted frames. Indeed, LoRa is known to be able to demodulate a signal below the noise floor: as a high SF and a small BW increase the robustness, the interference from the Wi-Fi frames is not sufficient to impact the received frames.

We also observe that the LoRa FDR is equivalent regardless of whether we look at the Wi-Fi + LoRa or LoRa + Wi-Fi bars. There is an exception in Figure 4.7b at 2406 MHz where the blue bar, representing Wi-Fi + LoRa overlapping transmissions, shows a FDR of 47% while the green bar, representing LoRa + Wi-Fi overlapping transmissions, show a FDR of almost 83%. Between these two phases of the experiment, there is a difference of 30 minutes according to the timeline of our experiments. There is a chance that during the Wi-Fi + LoRa phase we suffer from a burst of interference such as a firmware update of the Wi-Fi AP present in the apartment. Then when the LoRa + Wi-Fi phase starts, and according to the results, we assume that the interference peak has disappeared validating the assumption on a possible firmware update on the Wi-Fi AP.

To explain the results we obtained, we computed the RSSI of LoRa. Each LoRa frame received by the gateway has a RSSI and a SNR value. To ease the visualization of the results, we plot the mean RSSI value for each phase of the experiment in Figure 4.8.

As expected, in Figure 4.8a, with or without Wi-Fi interference, the RSSI is very good with a lowest value of -58 dBm and a maximal value of -50 dBm. These values correspond to the

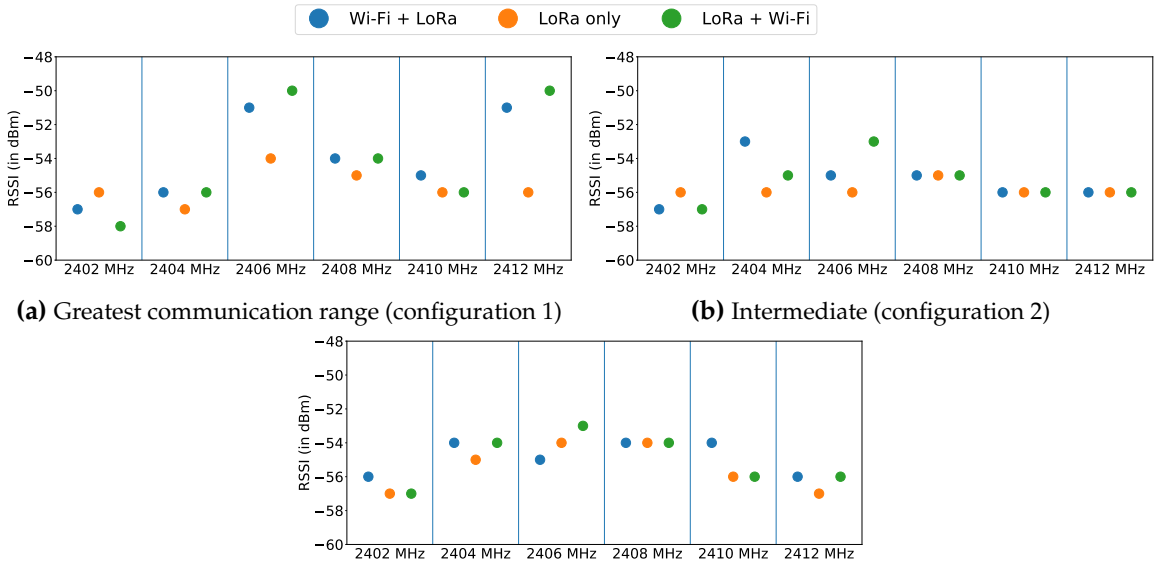

(a) Greatest communication range (configuration 1)

(b) Intermediate (configuration 2)

(c) Highest data rate (configuration 3)

FIGURE 4.8: LoRa RSSI variations depending on the center frequency.

LoRa performance using the greatest communication range where 100% of the transmitted frames are received. The RSSI obtained with the intermediate and the highest data rate configuration (Figures 4.8b and 4.8c respectively) cannot explain the decrease of the FDR we observe in Figure 4.7. Most of the RSSI values are around -56 dBm with the lowest RSSI of -57 dBm. It means that irrespective of the LoRa configuration used, the RSSI is very good, which is not consistent with the frame losses we observed. Indeed, with these RSSI values, and taking into account the robustness of LoRa to interference, we expected to receive many more frames than we monitored. To explain the frame losses we notice, we expected an RSSI around -80 dBm or less.

Remember that the RSSI stored by the LoRa gateway is the RSSI of the channel at a given time and not the RSSI of the received frame (see Subsection 3.3.1). In this chapter, we designed a worst case topology for our experiments. Due to the close location of the transmitter and the receiver of overlapping technologies, the stored RSSI will correspond to the strongest signal transmitting when the LoRa gateway receives a frame. Consequently, we have to analyze the LoRa SNR to explain the frame losses observed (see Figure 4.9).

We expected to see SNR variations where, for the less robust LoRa configurations, the SNR limit value is reached (see Table B.2). We observe a very different behavior. The less robust the LoRa configuration is, the higher the SNR value is. For example, if we compare the transmissions for a LoRa channel centered at 2406 MHz, under Wi-Fi interference (e.g., blue and green points), we note a SNR of -4 dB, 11 dB and 13 dB respectively for configurations 1 to 3. Once again, we assume that these values come from the topology of our experiments. Configuration 3 uses SF6, BW 1625, thus providing the highest data rate, but it is also less resistant to interference. So, the frames correctly received, and demodulated by the gateway, have to be much stronger than the Wi-Fi frames interfering. The SNR value observed for configuration 1, i.e., SF12, BW 203, and especially the negative ones, can be explained by

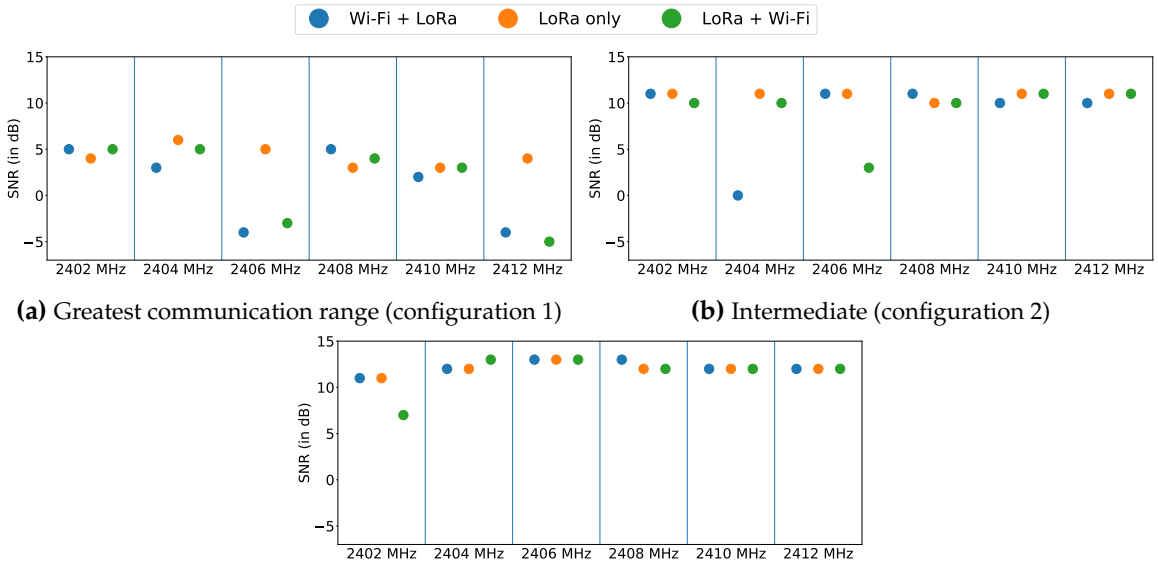

(a) Greatest communication range (configuration 1)

(b) Intermediate (configuration 2)

(c) Highest data rate (configuration 3)

FIGURE 4.9: LoRa SNR variations depending on the center frequency.

the ToA difference between LoRa frames and Wi-Fi frames. Indeed, a LoRa frame using the greatest communication range configuration is interfered by several Wi-Fi frames. In other words, a LoRa frame with a long ToA experiences more interference from Wi-Fi than a LoRa frame with a small ToA. The addition of the interfering Wi-Fi frames on the LoRa frame using configuration 1 can lead to a negative SNR when the LoRa gateway demodulates the frame. But, as the SNR limit value is not reached, we still receive all the LoRa frames. We conclude that the analysis of the RSSI and the SNR for LoRa transmissions is not sufficient to explain the frame losses experienced and focus only on the FDR in the rest of this chapter.

Going back to the objective of this section, we analyze next the Wi-Fi FDR depending on the LoRa channel in Figure 4.10. The purple bars represent the Wi-Fi FDR without LoRa interference. Then we distinguished the LoRa configurations for the two periods where we have LoRa and Wi-Fi overlapping transmissions: the first blue and green bars correspond to LoRa configuration 1, the second blue and green hatched bars correspond to LoRa configuration 2, and the third blue and green spotted bars correspond to LoRa configuration 3.

The results highlighted here show that the LoRa channel, used in overlapping transmission with Wi-Fi, has no significant impact on Wi-Fi performance. Indeed, the Wi-Fi FDR is on average 91%, 87%, and 55% for LoRa configuration 1, 2, and 3 respectively, and irrespective of the LoRa channel evaluated.

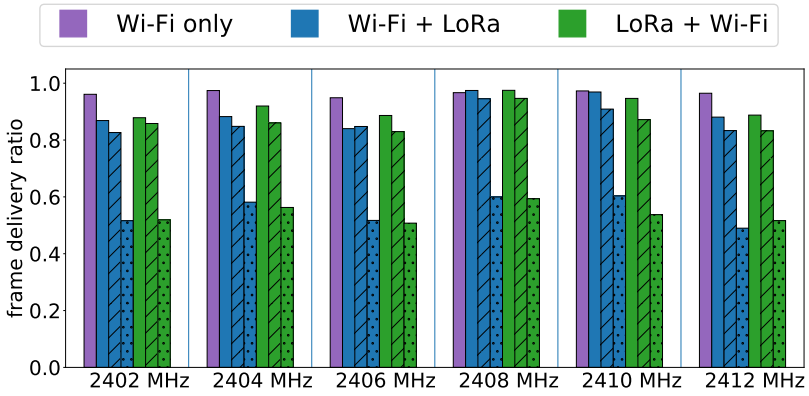

FIGURE 4.10: Wi-Fi FDR depending on LoRa center frequency. Blue and green bars correspond to the following LoRa configurations: empty bars for configuration 1, hatched bars for configuration 2, and spotted bars for configuration 3.

The evaluation of the impact of the LoRa channel center frequency on LoRa and Wi-Fi performances answers the question "How does the communication reliability of both technologies vary as a function of the frequency offset between LoRa and Wi-Fi center frequency channels?" (**RQ4-3**). We conclude that for Wi-Fi, the center frequency of the LoRa traffic has no significant impact on Wi-Fi performance as the FDR is similar for each LoRa configuration. For LoRa, the results show that the impact on the LoRa FDR increases with the decrease in frequency offset between LoRa and Wi-Fi center frequency channels.

This result shows that LoRa channels have to be taken into account for future LoRa networks deployment to ensure a good coexistence with Wi-Fi. As the LoRa FDR under Wi-Fi interference is 100% for both LoRa channels at 2402 and 2404 MHz, at least for the greatest communication range and the intermediate configurations, we can validate the choice of these channels. We can also validate the 2403 MHz LoRa channel as a good option, as proposed by Semtech, as we validated channels on either side of this frequency. As the other two channels proposed by Semtech are located at the edge of an independent Wi-Fi channel (channels 1, 6, and 11), and as the Wi-Fi spectrum is symmetrical around the center frequency, we assume that the results obtained in our coexistence study also apply for the other independent Wi-Fi channels. Thus we validate the 2425 MHz and 2479 MHz LoRa channels as a good option.

4.5.3 Impact of the LoRa bandwidth on the Wi-Fi performance

The results obtained by evaluating the impact of the LoRa center frequency channel, highlight that the ToA difference of LoRa and Wi-Fi frames is a lead to explain the losses we experienced. Thus, to answer the research question "How does the Wi-Fi communication reliability vary as a function of the used LoRa bandwidth and therefore of the ToA?" (**RQ4-4**), we designed the Bandwidth experiment presented in Section 4.4, and focus on the Wi-Fi performance we obtain through both experiments and simulations. Since the LoRa greatest communication range does not experience frame losses (see Subsection 4.5.1), in this subsection, we focus on the intermediate and the highest data rate configurations.

Experiment results

In this series of experiments, we fixed the LoRa occupancy channel rate to 18% to be able to evaluate the highest data rate configuration because, as demonstrated in Equation 4.4, 18% is (almost) the maximum occupancy channel rate for LoRa using SF6 and BW 1625.

Figure 4.11 shows the Wi-Fi FDR for the LoRa configurations 2.a, 2.c, 3.a and 3.c (see Table 4.5), i.e., SF9 and SF6 combined with the smallest and the highest available bandwidths. In each subfigure, the purple bar represents the Wi-Fi FDR without LoRa interference. It is still possible that external transmissions (from Wi-Fi APs in the environment) interfered with our Wi-Fi traffic. Then, for the two periods where we have overlapping LoRa and Wi-Fi transmissions, the Wi-Fi FDR is computed depending on the LoRa bandwidth used: the first blue and green solid bars correspond to BW 203 kHz, while the second blue and green hatched bars correspond to BW 1625 kHz.

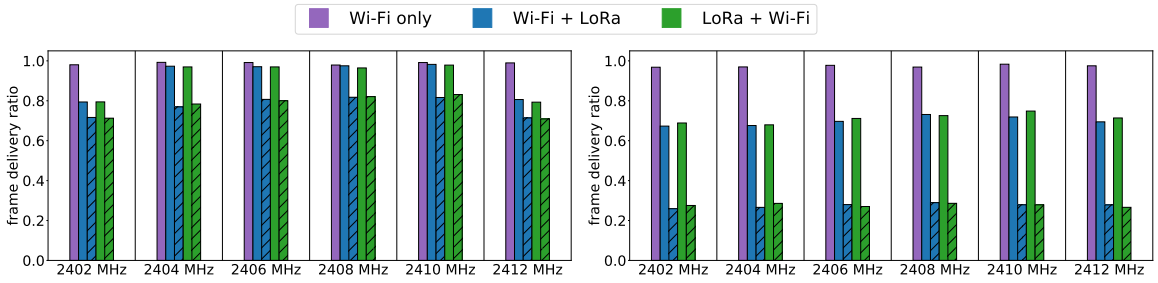

(a) Wi-Fi FDR for LoRa configurations 2.a and 2.c

(b) Wi-Fi FDR for LoRa configurations 3.a and 3.c

FIGURE 4.11: Wi-Fi FDR for several LoRa bandwidths. Blue and green bars correspond to the following LoRa bandwidth: empty bars for BW 203 kHz, and hatched bars for BW 1625 kHz.

Figure 4.11a shows that the LoRa bandwidth has an important impact on the Wi-Fi FDR. For example, for a LoRa traffic centered at 2410 MHz, using the configuration 2.a, i.e., SF9, BW 203, the Wi-Fi FDR under interference is 98% for both periods of overlapping transmissions. In the same way, for LoRa using the configuration 2.c, i.e., SF9, BW 1625, the Wi-Fi FDR is only 82%.

We also observe that for LoRa overlapping transmissions using a channel centered at 2402 MHz, the Wi-Fi FDR is lower than for the other center frequencies. For a LoRa channel

centered at 2402 MHz, we assume there is possible interference coming from other wireless technologies, in particular BT/BLE, which use the 2402 MHz frequency as center frequency for one of their advertisement channels. We use an USRP to analyze this specific channel frequency, and we observed that nearby cellphones are constantly beaconing on the BT/BLE advertisement channels, thus validating our hypothesis about possible interference. After validating our assumption on the behavior of BT equipment, we carried out the rest of the experiments with our BT devices switched off. The results in Figure 4.11a correspond to a series of experiments where BT devices were switched on. The Wi-Fi FDR for LoRa configurations 2.a and 2.c at 2402 MHz are 79% and 72% respectively, while the Wi-Fi FDR is on average 97% and 80% for the center frequencies from 2404 MHz to 2410 MHz. The results in Figure 4.11b, correspond to a series of experiments where BT devices were switched off. The results show that, regardless of the center frequency of the LoRa traffic, the Wi-Fi FDR under interference is on average 70% for LoRa configuration 3.a, and 28% for LoRa configuration 3.c, i.e., SF6, BW 203 and SF6, BW 1625 respectively. The Wi-Fi FDR difference between the two figures comes from the LoRa configurations. However, we see that when the BT devices are switched off, the Wi-Fi FDR for a LoRa channel centered at 2402 MHz is similar to the FDR obtained for the other center frequencies.

In addition, at 2412 MHz, the Wi-Fi FDR is 80% and 71% for LoRa configurations 2.a and 2.c respectively. We make the assumption that the Wi-Fi FDR decreases when the LoRa channel has the same center frequency as the Wi-Fi channel, 2412 MHz in our case, the LoRa transmissions have more impact on Wi-Fi. The Wi-Fi spectrum is not constant and has a lower power at the center frequency than on the rest of the BW. This could explain why we observe a FDR decreases at 2412 MHz when LoRa uses this frequency to transmit.

The result clearly shows that for the same LoRa occupancy channel, the LoRa bandwidth has a significant impact on the Wi-Fi FDR as we observe a FDR under 100% during LoRa transmissions. Moreover, a low SF combined with a high BW has a higher impact on the Wi-Fi FDR than a large SF with a low BW. This means that the Wi-Fi FDR decreases as a function of the LoRa time on air. Thus, to guarantee good Wi-Fi performance, it is better to use a small bandwidth with an SF value of at least 9. The difference between the Wi-Fi performance when using SF9 or SF6 can be explained by the time on air of the frames. A Wi-Fi frame lasts approximately 1 ms for the IEEE 802.11g 12 Mbps standard, and a frame is transmitted every 100 ms. On the LoRa side, an SF9, BW 1625 frame lasts 24 ms and is transmitted every 106 ms, whereas an SF6, BW 1625 frame lasts 4 ms and is transmitted every 24 ms. Approximately one over two Wi-Fi frames interfere with one LoRa SF9 frame, while a Wi-Fi frame interferes with a maximum of three LoRa SF6 frames. So Wi-Fi traffic is more likely interfered by LoRa SF6 frames than LoRa SF9 frames.

In addition to Figure 4.11, and to observe the FDR decrease using configuration 3, we also evaluate the LoRa 812 kHz bandwidth (see Figure 4.12).

The results show that, except for 2402 MHz and 2412 MHz, the Wi-Fi FDR under interference is on average 70%. For the two LoRa boundary channels tested, i.e., 2402 MHz and

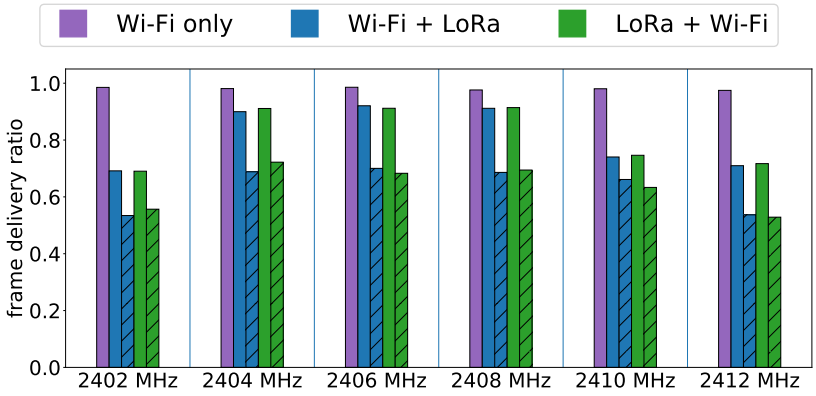

FIGURE 4.12: Wi-Fi FDR for LoRa 3.a and 3.b configurations.

2412 MHz, the Wi-Fi FDR decreases to approximately 55%. We conclude that the bandwidth, and thus the resulting ToA of LoRa frames has an impact on the Wi-Fi FDR. The Wi-Fi FDR decreases as the LoRa bandwidth increases.

Simulation results

We extend the experimental results through simulations based on our performance evaluation setup by testing more configurations and parameters than is possible in real world. To quantify the impact of the LoRa time on air, combined with the occupancy channel rate, on the Wi-Fi FDR, we used `MATLAB` simulations. It allows us to study various occupancy rates (1%, 10%, 18%, and 30%) for all the possible LoRa spreading factors (from 5 to 12). These simulations compute the theoretical Wi-Fi FDR when the medium is shared with LoRa transmissions.

To compute the theoretical Wi-Fi FDR, we make the assumption that if a Wi-Fi frame overlaps with a LoRa transmission, the Wi-Fi frame is lost irrespective of the arrival time of the LoRa frame. In other words, even if the Wi-Fi and the LoRa frames partially overlap, the Wi-Fi frame is lost. This way we give a lower bound FDR for Wi-Fi transmissions interfered by LoRa transmissions. We then compute the theoretical Wi-Fi FDR in Equation 4.9 (details are provided in Appendix C).

The time during which LoRa and Wi-Fi frames overlap is:

$$y = \frac{WiFi_p}{LoRa_p} \times (WiFi_{ToA} + LoRa_{ToA}) \tag{4.5}$$

The probability that a Wi-Fi frame is interfered by a LoRa frame during a Wi-Fi period is:

$$P_{inter} = \frac{WiFi_p}{LoRa_p} \times \frac{WiFi_{ToA} + LoRa_{ToA}}{WiFi_p} \tag{4.6}$$

$$= \frac{WiFi_{ToA} + LoRa_{ToA}}{\frac{LoRa_{ToA}}{LoRa_{OR}}} \tag{4.7}$$

$$= (\frac{WiFi_{ToA}}{LoRa_{ToA}} + 1) \times LoRa_{OR} \tag{4.8}$$

The FDR is then computed as:

$$\text{FDR} = 1 - (\frac{WiFi_{ToA}}{LoRa_{ToA}} + 1) \times LoRa_{OR} \tag{4.9}$$

where:

$$\begin{aligned}
WiFi_{ToA} &= \text{Wi-Fi time on air} \\
WiFi_{sleep} &= \text{Wi-Fi sleep time, i.e., inter-frame time} \\
WiFi_{p} &= \text{Wi-Fi period} = WiFi_{ToA} + WiFi_{sleep} \\
LoRa_{ToA} &= \text{LoRa time on air} \\
LoRa_{sleep} &= \text{LoRa sleep time, i.e., inter-frame time} \\
LoRa_{p} &= \text{LoRa period} = LoRa_{ToA} + LoRa_{sleep} \\
LoRa_{OR} &= \text{LoRa occupancy channel rate} \\
P_{inter} &= \text{probability of interference}
\end{aligned}$$

The theoretical Wi-Fi FDR we computed represents the probability that a Wi-Fi frame is not overlapping with any LoRa frame during the transmission. The results are shown in Figure 4.13. where each color corresponds to one LoRa occupancy channel rate, and each point of a given color corresponds to a LoRa configuration, from left to right, represented as a ToA in the simulations. We choose to evaluate a fix BW of 1625 kHz to have the maximum frequency overlap between LoRa and Wi-Fi transmissions.

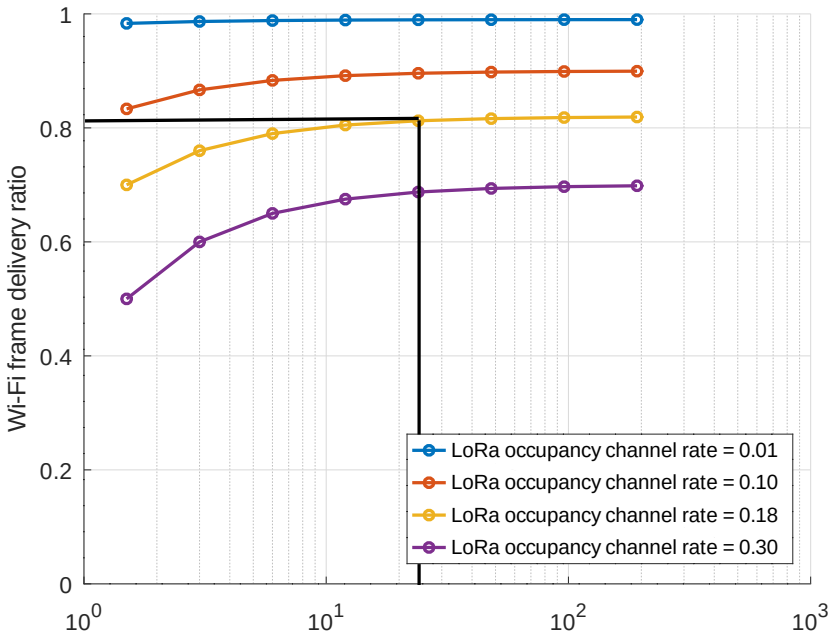

FIGURE 4.13: Simulated Wi-Fi FDR for several LoRa ToA of frames and channel occupancy rates. Black lines highlight the experimental Wi-Fi FDR for LoRa configuration 2.c.

We observe that increasing the SF and thus the ToA of the LoRa frames also increases the Wi-Fi FDR. Additionally, LoRa frames with a small ToA interfere more frequently Wi-Fi

frames which also decreases the Wi-Fi FDR. For a LoRa occupancy channel rate of 18% represented in yellow, as in our experiments, and for a LoRa ToA of 24 ms, which corresponds to the ToA of the configuration 2.c, i.e., SF9, BW 1625, the Wi-Fi FDR is 81%. In our experiments, we obtained a Wi-Fi FDR of 82%. We conclude that our experiment results are consistent with the theoretical results.

A way to increase the Wi-Fi FDR is to decrease the LoRa occupancy channel rate. In Figure 4.13, we see that for a LoRa SF9 configuration, the Wi-Fi FDR increases from 68% to 98%, by decreasing the occupancy channel rate from 30% to 1% respectively.

These results answer the question "How does the Wi-Fi communication reliability vary as a function of the used LoRa bandwidth and therefore of the ToA?" (**RQ4-4**). The time on air of the LoRa frames has a significant impact on the Wi-Fi performance. For a given LoRa occupancy channel rate, decreasing the SF and increasing the BW drastically decreases the Wi-Fi FDR until 28% using the highest data configuration. The theoretical results depicted in Figure 4.13 confirm these experimental results.

4.5.4 Impact of the environment

In the previous subsections, we evaluated the coexistence of LoRa and Wi-Fi in the 2.4 GHz ISM band by varying the physical parameters of LoRa (i.e., configurations, channels, traffic load). To fully validate the answers to the research questions **RQ4-3** and **RQ4-4**, we now explore the impact of the time of day when we run our experiments. We aim to study if there are periods of time where LoRa transmissions will less compete with Wi-Fi transmissions. Depending on our results, this could be an opportunity for a smooth coexistence between Wi-Fi and LoRa as each technology will have free from interference period of times. To evaluate this, we perform several repetitions of our experiments: by night and by day. We do not observe a significant difference between working days and weekends results so we regroup all daytime experiments. We expect that during the night, the Wi-Fi activity is less present than during the day because, as our experiments take place in a private environment, there are fewer wireless networking activities, since people are sleeping. With low Wi-Fi activity, there is less interference, so we conjecture an improvement of the LoRa performance. Some existing studies show that there are activity peaks in the early morning before people leave for work, at noon, and in the evening when people come back from work [131][132]. Since the pandemic, working remotely from home has become more popular, resulting in potential interference throughout the day.

We run the experiments and compute the results, for all the possible intermediate LoRa configurations detailed in Table 4.5. The concluding remarks on the results are the same, thus we present as an example the results for a bandwidth of 812 kHz, since this represents an intermediate LoRa configuration. Figures 4.14a and 4.14b show the LoRa FDR during night and day experiments respectively. Each point corresponds to a measurement from

one experiment, and the point's color indicates the type of transmission: blue and green represent overlapping transmissions, and orange represents LoRa interference-free transmissions. Note that when only point is displayed this indicates that the results of all the experiment repetitions provide the same FDR. Each experiment lasts approximately 6 hours, corresponding to 348, 9492, and 118800 frames depending on the LoRa configuration used. This allows us to evaluate a significant period of time where variations in the wireless environment might happen. We conclude that for both technologies, the performances are similar. Regardless of the time of the day when we run the experiments, we do not observe significant changes in the FDR. We assume this comes from the fact that we are not using the Wi-Fi AP present in the apartment, which constitutes the main external source of interference for our experiment. This way, our results are not dependent on the time of the day at which we run our experiments. The main source of interference of LoRa is our Wi-Fi traffic and reciprocally, and external interference have a negligible effect on LoRa FDR.

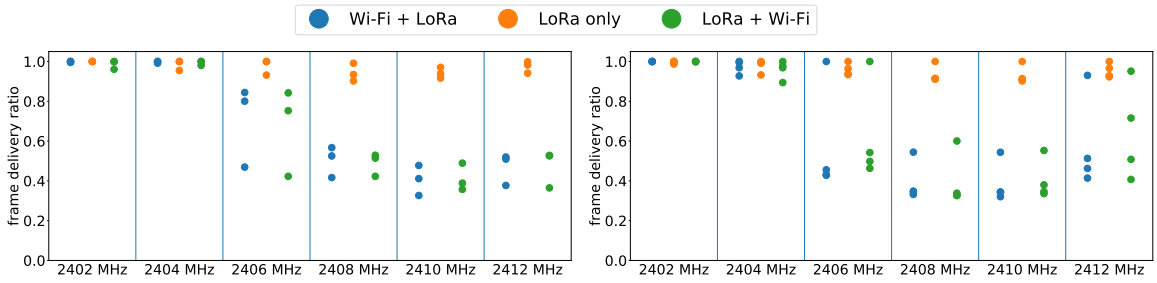

(a) LoRa FDR by night

(b) LoRa FDR by day

FIGURE 4.14: LoRa FDR for configuration 2.b, for several repetitions during night and day.

By comparing Figures 4.14a and 4.14b for LoRa channels centered at 2402 and 2404 MHz, we observe a slight amelioration of the FDR during the night. However, the lowest LoRa FDR on these channels by day, under interference, is 92% which is still very good. For the other center frequencies, we observe some variations between the different repetitions of the same experiment. We assume it comes from the environment of our experiment which can be different from one day to the next. Overall, by night the FDR varies from 32% to 56% with an average of 47%, whereas by day it varies from 32% to 54% with an average of 43%. The FDR variations follow the same trend.

In the same way, we analyze the Wi-Fi FDR by night and by day, when the LoRa transmissions use an SF9 combined with bandwidths of 203 and 812 kHz. It allows us to compare the low variation of the LoRa FDR with the Wi-Fi FDR. Figures 4.15a and 4.15b show the Wi-Fi FDR with colors coded as follows: blue and green represent overlapping transmissions, and purple represents Wi-Fi interference-free transmissions. Circles are for the first LoRa configuration evaluated, i.e., 2.a, and triangles correspond to the second LoRa configuration evaluated, i.e., 2.b.

The results show more variations of the Wi-Fi FDR by night (Figure 4.15a) than by day (Figure 4.15b). We show in Figure 4.5 that transmissions coming from the surrounding Wi-Fi

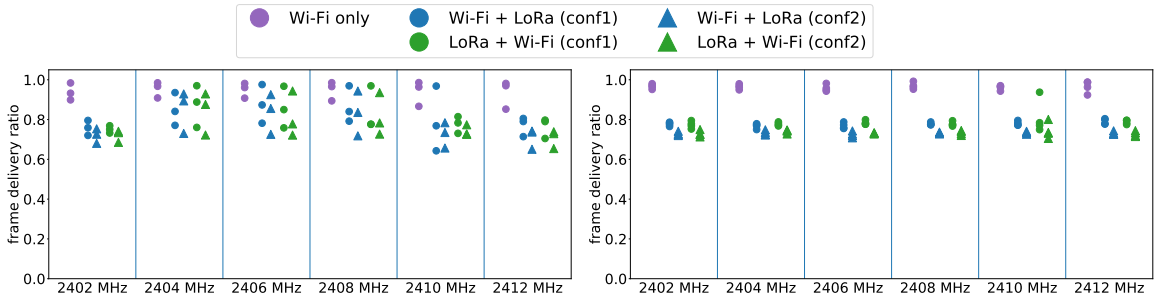

(a) Wi-Fi FDR by night

(b) Wi-Fi FDR by day

FIGURE 4.15: Wi-Fi FDR, for LoRa configurations 2.a and 2.b, for several repetitions during night and day.

APs that could interfere with our transmissions are sufficiently attenuated by signal propagation to not have a significant impact on our results. So, the only Wi-Fi AP with a potential impact on our transmissions is the one located inside the apartment where we run our experiments. Remember that we switch off this Wi-Fi AP during our experiments, so only control traffic interferes with our transmissions. However, during the night there is a possibility that the Wi-Fi AP in the apartment download updates which leads to an increase of the Wi-Fi traffic load and eventually causes additional interference with our experiments. Nevertheless, the average Wi-Fi FDR by night and by day for LoRa configuration 2.a, i.e., SF9, BW 203, is 78% whereas for the LoRa configuration 2.b, i.e., SF9, BW 812, the FDR is in average 73% by night and 72% by day. We conclude the same as for the results of Figure 4.14: we do not observe significant changes of the FDR between night and day experiments.

These results imply that in future deployments of LoRa, interference mitigation mechanisms have to be implemented to allow the coexistence of LoRa and Wi-Fi in the 2.4 GHz ISM band. The good coexistence of these two wireless technologies is not ensured even with LoRa applications sending frames only by night, as they would suffer from similar interference as during the day.

4.5.5 Impact of the topology

The way we designed our experiments can have an impact on the LoRa and Wi-Fi performances we obtained. This raises the research question "Does the topology of the experiment, e.g., the distance between equipment using different wireless technologies, have an impact on the communication performance of both technologies?" (**RQ4-5**). Hence, we study the impact of the topology. In addition to the worst case topology, where the transmitter of one technology is collocated with the receiver of the other technology evaluated, we consider another topology, called collocated transmitters topology, where both LoRa and Wi-Fi transmitters (and receivers) are collocated (see Figure 4.16) (i.e., one laptop with LoRa and Wi-Fi transmitters and another laptop for LoRa and Wi-Fi receivers).

Figures 4.17, 4.18, and 4.19 show the FDR of LoRa and Wi-Fi depending on the topology

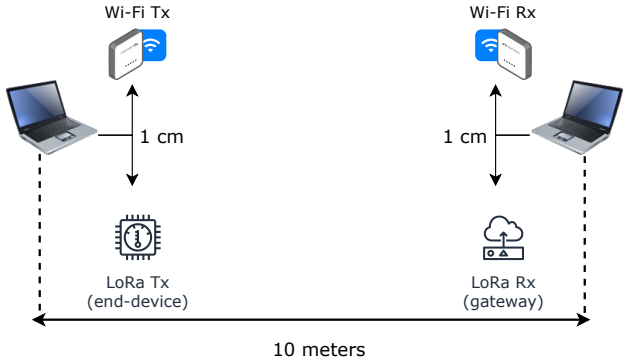

FIGURE 4.16: Experimental setup for the topology impact study. One laptop with LoRa and Wi-Fi transmitters and one laptop with LoRa and Wi-Fi receivers. Transmitters and receivers are approximately 10 meters away.

used. We compute the results for both technologies, for the three possible LoRa configurations: greatest communication range, intermediate, and highest data rate (see Table 4.4).

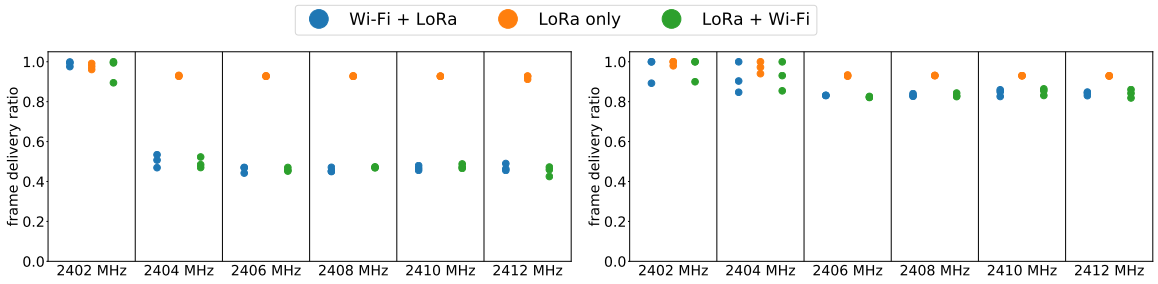

(a) LoRa FDR for the worst case topology

(b) LoRa FDR for the collocated transmitters topology

FIGURE 4.17: LoRa highest data rate configuration FDR for several repetitions and topologies.

On the LoRa side, the results show that collocating the transmitters of both technologies leads to significantly increased performance when there are overlapping transmissions between LoRa and Wi-Fi. This result makes sense as we initially designed our experiments to have the higher interference between the two technologies evaluated.

We note a significant LoRa FDR increase in Figure 4.17 when comparing the worst case and the collocated transmitters topologies, for the configuration that gives the highest data rate, and thus the smaller communication range. This configuration is also less robust to interference, so the gain obtained by changing the topology is outstanding. We observe that the FDR increases significantly, for all centered frequencies when using the collocated transmitters topology. For example, for a LoRa traffic under Wi-Fi interference centered between 2404 MHz and 2412 MHz, the FDR in the worst case topology is on average 47%, whereas in the collocated transmitters topology, the FDR increases to 84%. For a LoRa channel centered at 2402 MHz, the performance is already extremely good for the worst case topology (almost 100%) and is still equal when we collocate the transmitters. It means that by simply changing the topology, the LoRa performance can be significantly improved.

We observe the same improvement for the two other LoRa configurations we investigated, i.e., SF12, BW 203 and SF9, BW 812 respectively, although the improvement due to the change in topology is less impressive (see Figure 4.18).

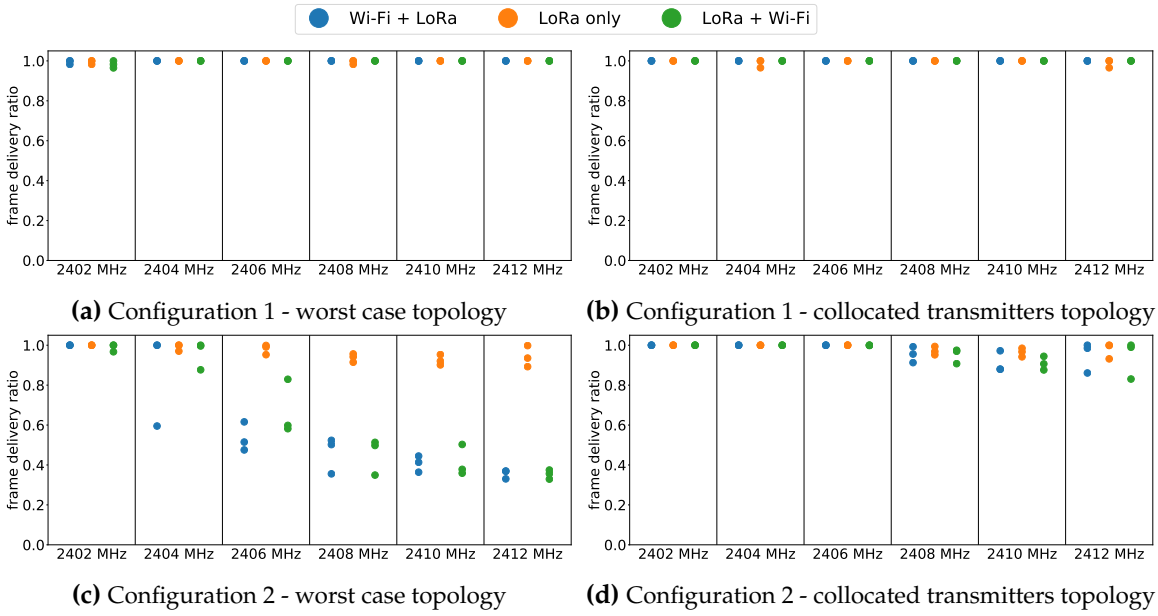

(a) Configuration 1 - worst case topology

(b) Configuration 1 - collocated transmitters topology

(c) Configuration 2 - worst case topology

(d) Configuration 2 - collocated transmitters topology

FIGURE 4.18: LoRa FDR for configurations 1 and 2, for several repetitions and topologies.

In both Figures 4.18a and 4.18b the FDR, irrespective of the LoRa channel used, is on average 100%. This result comes from the robustness of the configuration used: the higher SF (12) combined with the smallest BW (203 kHz). For the intermediate configuration, i.e., SF9, BW 812, the impact of the LoRa channel on FDR is visible for center frequencies from 2406 to 2412 MHz, for the worst case topology. Consistently with the results depicted in Figure 4.17, by changing the topology, the FDR increases from 36% to 90% on average. This result also highlights that the highest data rate configuration we evaluate provides better performance than the intermediate one. Once again, this is explained by the ToA of the intermediate configuration: the frame duration is 38 ms every 327 ms, while a Wi-Fi frame lasts approximately 1 ms and is transmitted every 100 ms. It means that a LoRa frame using this configuration is interfered by a maximum of three Wi-Fi frames. Contrary to configuration 1, the intermediate configuration is less resistant to interference and suffers from frame losses.

On the Wi-Fi side, the performance improvement is less noteworthy (see Figure 4.19). Indeed, the increase of the Wi-Fi FDR is only noticeable for a LoRa traffic centered at 2402 and 2404 MHz. We were expecting that the results of the worst case topology would show that moving away from the Wi-Fi center frequency channel, would increase the FDR. Our results demonstrate that this is not the case because the topology of the experiments has more impact on the performance than the center frequency of the LoRa channel. The results of the collocated transmitters topology confirm the intuition and expectations we had when first experimenting with the worst case topology. For example, the results of Wi-Fi FDR,

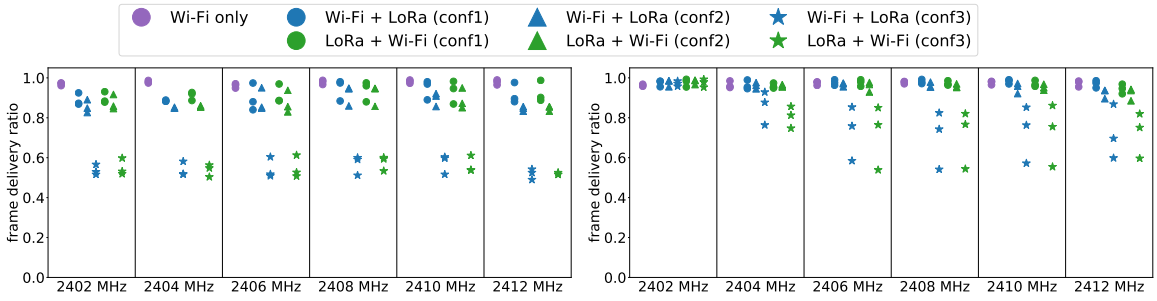

(a) Wi-Fi FDR for the worst case topology **(b)** Wi-Fi FDR for the collocated transmitters topology

FIGURE 4.19: Wi-Fi FDR for several repetitions and topologies.

when the medium is shared with LoRa, centered at 2402 MHz, transmitting with the highest data rate configuration, depicted with blue and green stars in Figure 4.19a, is on average 53%, and it increases up to 99% in the collocated transmitters topology.

The evaluation of the topology impact on LoRa and Wi-Fi performances responds to the question "Does the topology of the experiment, e.g., the distance between equipment using different wireless technologies, have an impact on the communication performance of both technologies?" (**RQ4-5**). The results show that depending on the distance between LoRa and Wi-Fi transmitters and receivers, the communication of both technologies is increased. We can conclude that one way to improve the LoRa performance under Wi-Fi interference is to focus on the deployment, especially considering collocated transmitters topology. This is achieved by deploying LoRa gateways far away from Wi-Fi APs to reduce the interference between the transmitted and the received frames of both technologies. In other words, the network deployment of LoRa in the 2.4 GHz ISM band should consider the location of Wi-Fi devices, especially access points, working in the same area. Overall, the impact of LoRa on Wi-Fi for a given LoRa occupancy channel rate depends, from the higher to the lower impact, on (1) the LoRa configuration, (2) the LoRa topology deployment, and (3) the LoRa center frequency channel.

4.5.6 Impact of the IEEE 802.11 interfering standard

To answer the research question "Does the Wi-Fi standard have an impact on the communication reliability of both technologies?" (**RQ4-6**), we propose a last evaluation to evaluate another IEEE 802.11 standard: IEEE 802.11b 1 Mbps which has a different modulation from IEEE 802.11g.

We use the three LoRa configurations detailed in Table 4.4. We repeated several times the experiment and we also ran one experiment using the collocated transmitters topology. As the tendencies are the same for all the repetitions of the experiment, we provide the results of one experiment at a time for ease of visualization.

The first observation is that the LoRa performances are very similar irrespective of the IEEE 802.11 standard used (see Figure 4.20). Indeed, with the greatest communication range configuration the FDR is near 100% for all the LoRa channels tested. We can make the same observation for the intermediate configuration for which the impact of the LoRa centered frequency appears at 2406 MHz thus decreasing the FDR to 58%. Finally, using the highest data rate configuration, the FDR starts decreasing for a LoRa channel centered at 2404 MHz down to 49%. Note that, changing the topology to collocate the transmitters results in a LoRa FDR of 100% on average for all LoRa configurations and all frequencies.

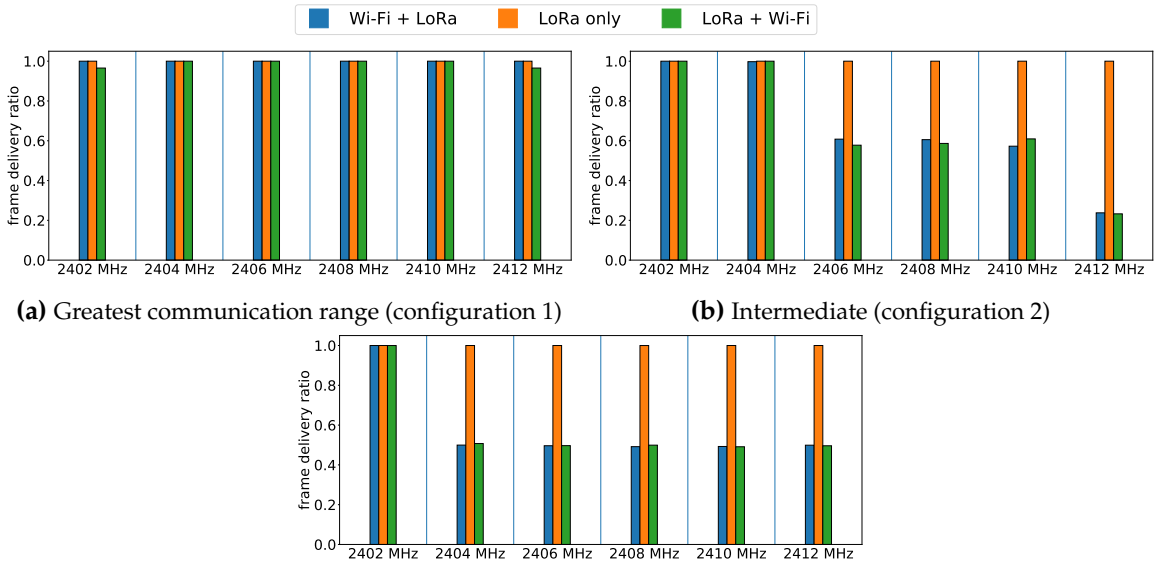

(a) Greatest communication range (configuration 1)

(b) Intermediate (configuration 2)

(c) Highest data rate (configuration 3)

FIGURE 4.20: LoRa FDR under IEEE 802.11b interference for a worst case topology.

By analyzing the Wi-Fi results, for a worst case and the collocated transmitter topologies, we detect an unexpected behavior (see Figure 4.21): at 2402 MHz and 2408 MHz, the Wi-Fi FDR using the collocated transmitter topology is lower, for most of the LoRa configurations, than using the worst case topology. We make two major observations on these results. First, in Figure 4.21a for the worst case topology, the Wi-Fi FDR suffers from a huge decrease for all the LoRa configurations interfering at 2412 MHz. The connectivity is almost lost when the LoRa intermediate configuration competes with Wi-Fi transmissions: only 1% of the frames are received. In Figure 4.21b, despite the more friendly topology, the Wi-Fi FDR at 2412 MHz is no better. Second, with the collocated transmitters topology, we notice a great improvement of the Wi-Fi FDR for a LoRa channel centered at 2404 or 2406 MHz. Even for the configuration 3, the FDR increases from 60% to 98%.

We make the assumption that the Wi-Fi FDR decrease is a result of the modulation used by the IEEE 802.11b standard. While the IEEE 802.11g standard uses an OFDM modulation, the IEEE 802.11b standard uses a DSSS modulation. The DSSS modulation is similar to the CSS modulation used by LoRa as they both spread the signal over the entire bandwidth. The biggest impact can be observed for a LoRa channel centered at 2412 MHz, which is also the

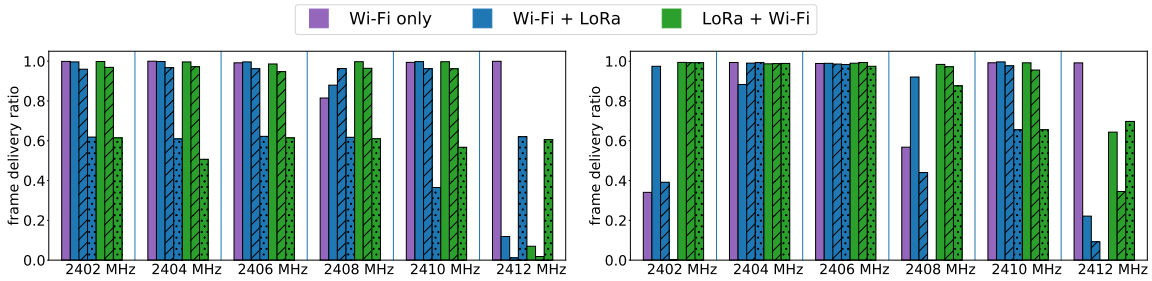

(a) Worst case topology

(b) Collocated transmitters topology

FIGURE 4.21: IEEE 802.11b FDR for different topologies. Blue and green bars correspond to the following LoRa configurations: empty bars for the greatest communication range configuration, hatched bars for the intermediate configuration, and spotted bars for the highest data rate configuration.

centered frequency of the Wi-Fi channel 1. The spread spectrum modulation used by both technologies can explain why we observe a higher impact of LoRa on Wi-Fi performance when both technologies are transmitting on the same channel.

To rule out the hypothesis of an interferer centered at 2412 MHz thus decreasing the Wi-Fi FDR we obtained, we change our experiments from a residential environment to a single-family home environment. The results show the same conclusions as previously.

We further investigate the phenomenon depicted in our results by repeating our experiment and by changing the LoRa center frequency channels: from 2400 to 2404 MHz with a 1 MHz step. We also reduce the Wi-Fi payload size to ensure the same ToA, below 1 ms, using the IEEE 802.11b standard as using the IEEE 802.11g standard. The results are shown in Figure 4.22.

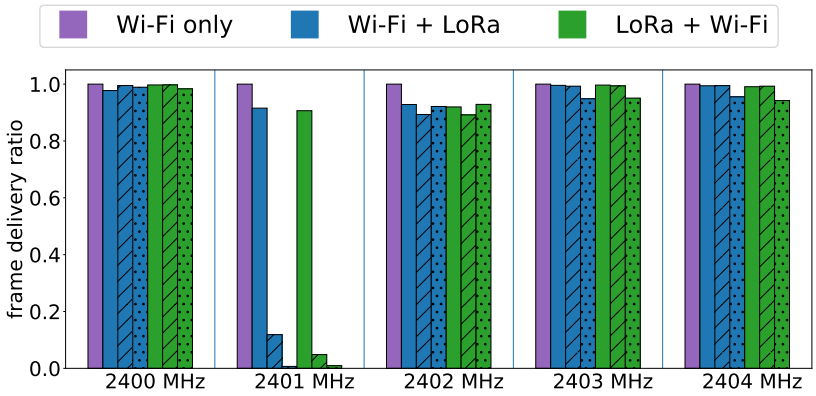

FIGURE 4.22: IEEE 802.11b FDR for LoRa channel from 2400 to 2404 MHz.

The LoRa channel centered at 2400 MHz is located outside of the IEEE 802.11b spectrum. Thus, we expected to see a FDR of 100% with or without interference from LoRa transmissions. Using a smaller payload size leads to an increase of the Wi-Fi FDR when LoRa transmits using the highest data rate configuration. From Figures 4.21a and 4.22, we see that the FDR increases from 60% to 95% at 2404 MHz. This enhancement is comparable to that obtained by changing the topology of the experiment. It is noteworthy to highlight

that simply by changing the payload size of the IEEE 802.11b frames, for a LoRa channel centered at 2402 MHz, the Wi-Fi FDR rises from 40% and 10% to 91% and 82% for LoRa configurations 2 and 3.

We did not anticipate the result obtained at 2401 MHz. The Wi-Fi FDR drops drastically from 90%, with a LoRa SF12, BW 203 interferer, to 11% with an SF9, BW 812 interferer, and to 0.6% with an SF6, BW 1625 interferer. To date, we still have no understanding of this result. We observed that a smart TV is beaconing on its BT advertising channel centered at 2402 MHz, which is not supposed to interfere at 2401 MHz. Furthermore, we considered a potential hardware malfunction and hence tested other LoRa equipment, but with no success. Further investigations are needed to fully evaluate and understand the performances obtained for IEEE 802.11b and LoRa overlapping transmissions in the 2.4 GHz ISM band.

These results answer the question "Does the Wi-Fi standard have an impact on the communication reliability of both technologies?" (**RQ4-6**). We emphasize that changing the IEEE 802.11 standard has less impact on LoRa performance than the physical parameters used to transmit LoRa frames. We also have the intuition that a small Wi-Fi ToA combined with a spread spectrum modulation schema ensures a friendly coexistence with LoRa in the 2.4 GHz ISM band. Our results indicate it is better to use an IEEE 802.11 standard using a modulation different from the spread spectrum technique used by LoRa to ensure an IEEE 802.11 FDR of about 80% irrespective of the LoRa channel center frequency.

4.6 Conclusions and engineering insights

In this chapter, we answer one of the main concerns about the deployment of LoRa in the 2.4 GHz ISM band: the coexistence with other wireless technologies. Through experiments, we study the mutual impact, on the FDR, of LoRa and Wi-Fi when they are overlapping transmissions. We have chosen to study Wi-Fi for this study of LoRa coexistence in the 2.4 GHz ISM band because Wi-Fi is the most popular technology in indoor environments. We evaluated several LoRa configurations, and varied physical parameters such as the center frequency of the LoRa channel, and also analyzed the impact of changing some of the implementation choices we made, e.g., the topology, and the IEEE 802.11 standard. The results allow us to provide an answer to the research questions **RQ4-2** to **RQ4-6** we raised at the beginning of this chapter (summarized at the end of this section). Gathering all the outcomes of our experiments provides an answer to the question "What is the impact when there are LoRa and Wi-Fi overlapping transmissions on both technologies' communication reliability?" (**RQ4-7**).

The various experimental results presented in Section 4.5 permit to highlight some technical principles to deploy a LoRa network in a Wi-Fi environment in the 2.4 GHz ISM band without implementing interference mitigation mechanisms [10] [133]. The following recommendations aim to highlight good practices to ensure a fair coexistence between LoRa and

Wi-Fi.

The first recommendation concerns the LoRa occupancy channel rate. As LoRa has no imposed duty-cycle in the 2.4 GHz ISM band, it can transmit as needed. We show in Subsection 4.5.1 that the higher the LoRa occupancy channel rate, the lower the Wi-Fi FDR (**RQ4-2**). So, one way to ensure a fair coexistence between LoRa and Wi-Fi is to limit the LoRa occupancy channel rate, by configuring the inter-frames arrival time and the maximum number of frames to send for a given period of time.

The second recommendation is to use high SF values (9 to 12) combined with bandwidths under 1 MHz (203 to 812 kHz). Indeed, Subsection 4.5.3 shows that the choice of the physical parameters of LoRa has an impact on Wi-Fi performance (**RQ4-4**).

The third recommendation is to design a deployment where LoRa gateways are as far away as possible from Wi-Fi APs, to have the lowest level of interference between LoRa and Wi-Fi (**RQ4-5**). We underline this need in Subsection 4.5.5.

Finally, the fourth recommendation is to choose the LoRa center frequency channel farthest away from the center frequency of the Wi-Fi channel. In Subsection 4.5.2 we show that a close frequency would decrease both FDR (**RQ4-3**). Thus, the Semtech proposal of a LoRa channel centered on 2403 MHz is a good option. The principle applies to the other LoRa channels (2425 and 2479 MHz) as they are neighbor to a BLE advertising channel and at the edge of a main Wi-Fi channel. The results obtained with another IEEE 802.11 standard (**RQ4-6**), in Subsection 4.5.6 are consistent with the proposed LoRa channels.

In our opinion, the best option to deploy a LoRa network in the presence of Wi-Fi without implementing interference mitigation mechanisms is to combine all of these recommendations.

In the next chapter, we focus on improving LoRa and Wi-Fi coexistence in the 2.4 GHz ISM band by proposing and implementing one interference mitigation mechanism.

RQ answered:

- **RQ4-1**: How to study the coexistence of two wireless technologies using the same frequency band? → Subsection 4.3.1
- **RQ4-2**: How does Wi-Fi performance vary as a function of the LoRa occupancy channel rate? → Subsection 4.5.1
- **RQ4-3**: How does the communication reliability of both technologies vary as a function of the frequency offset between LoRa and Wi-Fi center frequency channels? → Subsections 4.5.2 and 4.5.4
- **RQ4-4**: How does the Wi-Fi communication reliability vary as a function of the used LoRa bandwidth and therefore of the ToA? → Subsection 4.5.3 and 4.5.4
- **RQ4-5**: Does the topology of the experiment, e.g., the distance between equipment using different wireless technologies, have an impact on the communication performance of both technologies? → Subsection 4.5.5
- **RQ4-6**: Does the Wi-Fi standard have an impact on the communication reliability of both technologies? → Subsection 4.5.6
- **RQ4-7**: What is the impact when there are LoRa and Wi-Fi overlapping transmissions on both technologies' communication reliability? → Section 4.5

RQ raised:

- **RQ5-***: How to improve the coexistence of LoRa and Wi-Fi in the 2.4 GHz ISM band, in terms of frame delivery ratio, by implementing interference mitigation mechanisms? → Chapter 5

Chapter 5

Improving the coexistence of LoRa and Wi-Fi in the 2.4 GHz ISM band

5.1 Introduction

To increase the reliability of LoRa, as LoRa will compete with other wireless technologies in the 2.4 GHz ISM band, it is very useful to design strategies that help recover, and make LoRa signals more robust in the presence of simultaneous cross-technology transmissions, or design appropriate interference avoidance mechanisms.

In the previous chapter, we investigated the coexistence of LoRa and Wi-Fi, in a typical indoor environment, in the 2.4 GHz ISM band focusing on the physical layer. The results demonstrated that LoRa configurations can be leveraged to ensure a good frame delivery ratio for both LoRa and Wi-Fi, as well as the deployment of the end-devices compared to the location of the Wi-Fi access points.

To improve the coexistence between LoRa and Wi-Fi in the 2.4 GHz ISM band, we highlight several approaches to explore:

1. Choose the LoRa channels depending on the percentage of channel occupancy, obtained by a channel characterization,
2. Use specific PHY configurations for LoRa transmissions depending on the target application and, on the required trade-off between data rate and robustness,
3. Impose a duty-cycle to LoRa, and therefore improve Wi-Fi performance, but not LoRa performance,
4. Use cognitive radio approaches and more generally work on the implementation of MAC layer mechanisms,
5. Use an FH scheme to transmit LoRa frames depending on the percentage of channel occupancy, which relies on the Wi-Fi traffic model (i.e., chose the LoRa channels where Wi-Fi traffic is low).

In our opinion, approach number 2 is more about configuration than improving coexistence. Using specific parameters permits increasing the robustness of LoRa transmissions against

Wi-Fi overlapping transmissions. Such approaches are environment and network-specific of the LoRa network deployment contrary to a mitigation collision mechanism that dynamically adapts to the environment. Approach number 3 imposes a duty-cycle to LoRa which is in opposition with the appealing no duty-cycle constraints of the 2.4 GHz ISM band. Approach number 4 proposes to work on a MAC layer for LoRa. As no MAC layer is standardized yet for LoRa in the 2.4 GHz ISM band we find it would be complex and time-consuming to implement our MAC layer proposition on LoRa COTS equipment. Thus we propose to improve the coexistence of LoRa and Wi-Fi in the 2.4 GHz ISM band by combining the approaches number 1 and number 5 presented above as these approaches are implemented at the physical layer. The channels allowed in the FH scheme are selected according to their percentage of occupancy. We believe that using a frequency hopping strategy is a good trade-off between reliability improvement (i.e., FDR increase) and cost of implementation. Another motivation to evaluate FH in LoRa transmissions is because LoRa sub-GHz and the LR-FHSS modulation also use FH in their transmissions. We rely on our experimental results to design and develop a homemade simulator. We preferred simulations to real-world implementation, to enable the evaluation of more parameters than can be implemented on the COTS equipment. We validate our simulator by comparing the simulation results with the experimental results. Then, we evaluate three frequency hopping strategies and compare them. Note that the LoRa 2.4 GHz stack proposes an FH, similar to the one implemented in LoRa sub-GHz, that randomly chooses a channel to transmit among a list of available channels. Moreover, using a frequency hopping approach requires communicating the channels allowed for the frequency hopping between LoRa gateway and end-devices. Implementing and evaluating our frequency hopping strategy through simulations also permits us to eliminate the deployment cost of such gateway-to-end-device frequency hopping sequence communication on real hardware.

We formalize the proposal of using FH for LoRa transmission in the 2.4 GHz ISM band with the following research questions:

RQ5-1: How to design a simulator that can model real-world coexistence experiments?

RQ5-2: Is there a frequency hopping strategy that gives better results than the frequency hopping proposed in the actual LoRa 2.4 GHz stack?

RQ5-3: Is there a frequency hopping strategy that provides a Wi-Fi FDR, when interfered by LoRa transmissions, that is at least as good as when interfered by other wireless technologies (e.g., BT, IEEE 802.15.4)?

RQ5-4: Is frequency hopping a good option to improve LoRa and Wi-Fi coexistence in the 2.4 GHz ISM band?

The results described in this chapter help to answer each research question through the subsequent contributions:

- We propose a gateway protocol to scan the 2.4 GHz ISM band and select the less noisy channels that will be used by the end-devices to transmit.

- We design a homemade simulator based on the experimental results obtained in Chapter 4 to evaluate our proposed FH approach for LoRa 2.4 GHz.
- We extend our simulation scenario to a multi-non-overlapping Wi-Fi APs deployment to evaluate a more complex scenario than in our experiments.

5.2 Improving the coexistence: SLR process

Nowadays, Wi-Fi is the main wireless technology using the 2.4 GHz ISM band and is widely deployed in indoor environments, e.g., offices, universities, and residential buildings. Thus, the deployment of LoRa in the 2.4 GHz ISM band raises interest in the coexistence of this technology with the other wireless technologies already using the 2.4 GHz ISM band. The study of the mutual impact of LoRa and Wi-Fi overlapping transmissions demonstrates that several parameters (physical layer parameters, topology, modulation) could decrease the communication reliability of both technologies and thus prevent the deployment of LoRa in the 2.4 GHz ISM band (see Chapter 4).

In the literature, there are several propositions to improve the coexistence of different wireless technologies in the presence of overlapping transmissions [134] [135]. The two main approaches are cognitive radio and cross-technology. Cognitive radio proposes to share the spectrum between two technologies to avoid interference [11]. By sensing the channel, the secondary technology, i.e., the technology that is deployed in an environment where there is already a different technology using the same frequency band, is able to detect the transmission free periods of the primary technology to use these periods of time for its own transmissions. The coexistence of multiple technologies can also have some benefits. It is possible to modify the physical layer of a given technology to allow a transmitter to send frames that can be detected or decoded by the receiver of another technology. Going back to LoRa, several works propose techniques to allow cross-technology transmissions of LoRa, and Wi-Fi, BLE, or ZigBee [10] [133] [136] [137] [138] [139] [140].

However, in this chapter, we focus on FH applied to LoRa 2.4 GHz transmissions as this can be implemented on existing equipment without hardware modification. To evaluate the improvement of FH on LoRa and Wi-Fi communication reliability, we apply the SLR process presented in Appendix A.4 to select the articles of our state of the art. Our SLR process aims to collect papers in order to have an overview of the existing methodologies to improve the coexistence between two wireless technologies. We focus on studies that evaluate the benefits of FH transmissions when there are overlapping transmissions as this is the mechanism we propose to improve LoRa and Wi-Fi coexistence in the 2.4 GHz ISM band. We also analyze the papers that propose other interference mitigation mechanisms regardless of the performance metric to study if the targeted metric to improve defines the interference mitigation mechanism approach or not. In other words, we want to assess whether or not we can use the same mechanism to improve energy consumption, battery life, throughput, or communication reliability. We synthesized the selected articles in Table 5.1, based on the methodology used to investigate the coexistence (i.e., theoretical, network simulation, or

real experiments) and the approach used to improve the coexistence. The last line of the table highlights the novelty of our work compared to the existing literature.

We grouped the approaches into five categories. (1) Cooperative approaches are interference mitigation mechanisms based on the communication of information (such as channel quality) between the two technologies that have overlapping transmissions. Then, based on this information, the technologies choose either to transmit or not. (2) FH approaches group all the studies that proposed to implement an FH scheme to improve the performance of coexisting technologies. It can be a simple FH as implemented in BT, but it can also be an improvement of the usual FH implemented by a given technology. (3) Packet recovery approaches refer to studies where the interference mitigation mechanisms propose to detect and correct the corrupted transmissions. We also group in this category the studies that propose to embed frames from narrow technologies into frames from wider technologies. (4) The self-configuration category contains the studies that according to the information extracted from the channel, or the environment, the devices of the network decide what configuration to use or what interference mitigation mechanism to rely on. (5) Finally, we group all the other approaches, e.g., repeating, using a busy tone, in the category "Others".

Ref	Approach	Theoretical	Simulations	Experiments	Technology
[141]	Cooperative	X			Wi-Fi
[142] [143]	Cooperative		X		Wi-Fi
[144] [145] [146] [147]	Cooperative			X	Wi-Fi [144] [146] [147] Other [145]
[148] [149]	Cooperative	X		X	Other [148] Wi-Fi [149]
[150]	Cooperative	X	X	X	Wi-Fi
[151] [152] [153]	FH		X		Other [151] [152] [153]
[154] [155] [156]	FH			X	Other [154] [155] LoRa sub-GHz [156]
[157] [158]	FH	X	X		Other
[159]	FH	X		X	Other
[160] [161]	FH		X	X	Other
[162] [163]	Packet recovery			X	LoRa sub-GHz [162] Other [163]
[164] [165]	Packet recovery		X	X	Other
[166]	Packet recovery	X	X	X	Other
[167] [168] [169]	Self-configuration		X		Other [167] [169] LoRa sub-GHz [168]
[170] [171]	Self-configuration			X	Other
[172]	Self-configuration		X	X	LoRa sub-GHz
[173]	Others			X	Wi-Fi
[174]	Others	X	X		Other
[175]	Others		X	X	Wi-Fi
Our contribution	FH		X		Wi-Fi and LoRa 2.4 GHz

TABLE 5.1: Improving coexistence state of the art classification.

5.2.1 Improving the coexistence of wireless technologies

The different wireless technologies using the 2.4 GHz ISM band largely differ from each other, especially in terms of BW, transmission power, and modulation. Several works propose to reduce the impact of cross-technology interference between the main wireless technologies using this frequency band. However, all the studies do not focus on a specific

coexistence scenario but rather evaluate the destructive impact of overlapping transmissions [151] [169]. By sensing the channel and evaluating the quality of the channel, the device that performs the channel sensing decides whether or not the channel is usable. Then the stability of the channel is evaluated and the receiver informs the transmitter to add this channel in his FH sequence.

In an indoor environment, it is very common to have Wi-Fi and BT deploy next to each other, thus raising coexistence issues [142] [146] [152] [153] [158] [163] [165]. These technologies are also very often used jointly, especially in portable devices, e.g., laptops, and smartphones. BT and Wi-Fi both implement PHY and MAC mechanisms to avoid interference due to their proximity. However, the Wi-Fi CSMA/CA mechanism can result in false detection. Thus, the design of a cooperation mechanism between BT and Wi-Fi seems a good option to mitigate cross-technology interference [142]. In such a mechanism, BT updates the channels to use in its FH scheme according to the channel information received from the Wi-Fi AP. Some studies focus on allowing bi-directional and overlapping transmissions between Wi-Fi and BLE within the overlapped channel [146] [165]. This approach is different from dual-radio gateways. In the latter, the Wi-Fi and the BLE downlink packets have to be time and frequency separated. Experimental results show that the throughput for a communication distance up to 30 m, the throughput of Wi-Fi and BLE is more than 2 times higher than the throughput obtained with a dual-radio gateway. For instance, at a distance of 15 m, Wi-Fi has a throughput of 20 Mbps, and BLE has a throughput of 100 Kbps using a dual-radio gateway. The throughput increases to 40 Mbps and 250 Kbps for Wi-Fi and BLE respectively, using the bi-directional approach.

Similarly, in a home environment, it is likely to find both IEEE 802.15.4 and IEEE 802.11 networks. Thus, several works aim to mitigate the detrimental effect on the performance of cross-technology interference [97] [143] [149] [154] [159] [160] [163] [164] [166] [167] [170] [171] [173] [174] [175]. Improving the communication reliability of IEEE 802.15.4 and IEEE 802.11 is possible by implementing mechanisms that recover and correct the corrupted transmissions [164]. Interference are detected by sampling the RSSI, as interference introduces a temporary increase in the RSSI. Then the RSSI is compared to a threshold to mark the corrupted data bytes. Finally, the correctly decoded bytes are used in a recovery algorithm to reconstruct the original frame, i.e., correcting the corrupted bytes. The results show that for a Wi-Fi traffic saturating the channel, 17% of the correctly received bits within CRC-failed IEEE 802.15.4 frames are correctly decoded after applying the recovery algorithm. In comparison, for microwave oven and BT interference which are narrower interferer compared to Wi-Fi transmissions, on IEEE 802.15.4 transmissions, 40% of the correctly received bits within CRC-failed frames are correctly decoded after applying the recovery algorithm. Another approach to improve cross-technology interference between IEEE 802.15.4 and IEEE 802.11 is FH. Oppcast is a protocol that proposes to use only three channels for IEEE 802.15.4 transmissions [154]. The channel selection ensures the maximization of the frequency offset between the three selected channels. HOPSCOTCH proposes to classify the channels in two categories (1) clear, and (2) noisy [159]. The noisy channels are blacklisted for channel

hopping. This channel selection ensures that a clear channel offers a PDR over 50% thus mitigating cross-technology interference between IEEE 802.11g and IEEE 802.15.4. To improve the coexistence between IEEE 802.11 and IEEE 802.15.4 it is also possible to focus on one characteristic of one of the two overlapping technology [174]. In case a device does not receive a beacon frame over a defined time interval, the device scans the channel during an inactive period. The device defines the channel occupancy. According to this information, the coordinator determines the number of beacon frames to transmit that ensure a given targeted transmission probability. Simulation results show that for an IEEE 802.11 traffic load of 0.05 and 0.3 with 2 repetitions of the beacon frame, the beacon delivery ratio is 99% and 71% respectively. There are also several works dedicated to improving cross-technology interference in the context of IoT. RF-SIFTER is an additional layer, transparent for the PHY and the MAC layer of IoT system, that filters signals based on their BW. The filter allows IoT signals to pass through and reject signals with a wider BW than IoT signals as they are considered as interference [163]. Experiment results show that under heavy Wi-Fi interference with a channel utilization of 80%, RF-SIFTER provides a PDR above 60% while more conventional approaches used as baselines comparison provide a PDR below 15%.

As IEEE 802.11 networks usually coexist with IEEE 802.15.4 and BT/BLE networks, studies also focus on cross-technology interference between IEEE 802.15.4 and BT [145] [148] [154] [160] [161] [164] [170]. Some of the IEEE 802.15.4 channels overlap with BLE channels. One proposition to decrease the probability of cross-technology interference is to implement a mechanism that makes IEEE 802.15.4 and BLE cooperating by avoiding overlapping transmissions when they have overlapping channels [145] [148]. Experiments evaluate how such a time synchronization mechanism can improve the PDR when the IEEE 802.15.4 link is saturated and BLE is interfered with by the IEEE 802.15.4 traffic. The results show that on average the PDR is increased and there is no more burst of packet losses. For instance, for 1000 BLE packet transmissions when there are only two BLE channels used, without coexistence 120 packets are lost while only 15 packets are lost using the BLE adaptation mechanism described above. Another proposition is to enhance the actual FH mechanism implemented in IEEE 802.15.4 [161]. Experiment results show that when there is no interference the original FH mechanism (called TSCH) the average PDR is 100%. In case of interference, the PDR decreases to 82% using TSCH while using the enhanced FH mechanism the PDR is 92% on average.

More recently, licensed technologies like long term evolution (LTE) have started to be deployed in unlicensed frequency bands to meet the increasing traffic demand. As LTE can use a BW of 20 MHz, the coexistence with Wi-Fi transmissions is of interest [141] [144] [147] [150] [157]. The goal is to ensure a fair allocation between Wi-Fi and LTE to have the lower impact on throughput and delay in networks using these technologies. The IEEE 802.11 transmitters use the carrier sense to define slots to transmit. Experimental results show that using energy detection on the IEEE 802.11 is not sufficient. Indeed, the IEEE 802.11 transmitter considers the channel idle 90% of the time even when the LTE duty-cycle is 80% and the transmit power is -16 dBm. When the LTE transmit power is increased to 4 dBm, the

IEEE 802.11 transmitter correctly detects the LTE transmissions and increasingly marks the channel as busy as the LTE duty cycle is increased. Several works also propose a cooperative mechanism to improve the coexistence of Wi-Fi and LTE in the unlicensed frequency bands [141] [144]. The proposition is to dynamically select the channel and combine it with an adaptive radio duty cycle. LTE selects the least interfering channels according to the Wi-Fi APs deployment. For that LTE measures the power on different carrier channels and compares the energy sensed to a threshold to evaluate if the channel can be used. The objective for LTE is to be as transparent as possible for Wi-Fi by not interfering with Wi-Fi transmissions. Hence, LTE uses the unlicensed band only when there is a need for a higher downlink traffic load. Otherwise, LTE relies on its original operation mode on licensed frequency bands.

5.2.2 Improving LoRa coexistence

As LoRa uses unlicensed frequency bands, it has to coexist with several other wireless technologies. A few works propose to improve the performance of LoRa in the context of inter-technology overlapping transmissions [156] [162] [168] [172]. In the sub-GHz band, one proposition is to allocate a weight per channel based on the probability of usage of the channel [172]. For that, the network is divided into a set of areas. Then the PDR per channel and per area is computed periodically and used to estimate the level of interference. The end-devices use the channel according to the weights assigned to each channel instead of using all the channels uniformly. Simulation results highlight that the proposed approach increases the PDR by almost 50% in scenarios with very high interference levels. Regarding the 2.4 GHz ISM band, the need to ensure a fair coexistence, i.e., the less impact on performance, between LoRa and the other wireless technologies using this frequency band is of utmost importance [162]. A partial symbol recovery is proposed for LoRa interfered by Wi-Fi transmissions. The mechanism is implemented at the LoRa receiver where each LoRa symbol is processed. Frequency normalization is applied to trace the frequency changes over time. In case of interference, the frequency components will vary heavily while they will remain quite stable when there is no interference. The LoRa receiver uses the non-interfered chips for correlation detection to decode LoRa symbols. Experiment results analyze the PDR improvement of the symbol recovery mechanism under different Wi-Fi interference scenarios. For a low interference scenario, i.e., one Wi-Fi device and one Wi-Fi AP with an average of 350 packets per second, the standard LoRa SF10 PDR is 61.5% and increases to 91.7% by implementing the recovery symbol mechanism. The PDR improvement of the recovery symbol mechanism is extremely noticeable for high Wi-Fi interference, i.e., five Wi-Fi devices and one Wi-Fi AP with an average of 2600 packets per second. In this case, the standard LoRa SF10 PDR is only 12.2%. It increases to 67.1% with the recovery symbol mechanism which is 5.5 times the standard LoRa PDR.

We conclude that several approaches allow to improve the coexistence between two wireless technologies. Although a few studies propose to sense the frequency band to select the

channels on which to transmit, usually based on the channel quality, none of the cited studies propose to evaluate the benefits of FH for LoRa transmissions in the 2.4 GHz ISM band. Our work fills the gap by proposing a new frequency hopping strategy based on channel sensing to select the channel of the FH sequence for LoRa in the 2.4 GHz ISM band. We also compare our approach with two baseline FH strategies that are based on the FH mechanism implemented in LoRa sub-GHz and used the LoRa channels proposed by Semtech for the 2.4 GHz ISM band.

5.3 Frequency hopping strategies

In Section 2.3, we presented the operation of LoRa and more specifically the frequency hopping mechanism used to transmit data in the sub-GHz frequency band. The FH is performed at the frame layer, i.e., the frame is not fragmented to be sent. Recall that, in Europe, by default each packet is randomly sent on one of the three mandatory LoRa channels: 868.1 MHz, 868.3 MHz, and 868.5 MHz. The number of channels on which performing FH can be increased to eight.

We define three frequency hopping strategies to evaluate: (1) random FH, (2) round-robin FH and, (3) best channels FH. The first two are used as the baseline to compare with, and the third strategy is the implementation of the combination of two approaches we highlight in Section 5.1. As a reminder, the two approaches we combine propose to use an FH strategy for LoRa transmissions using the less noisy channels, which are also the channels with less wireless traffic. We summarize the available channels for the baseline strategies in Figure 5.1.

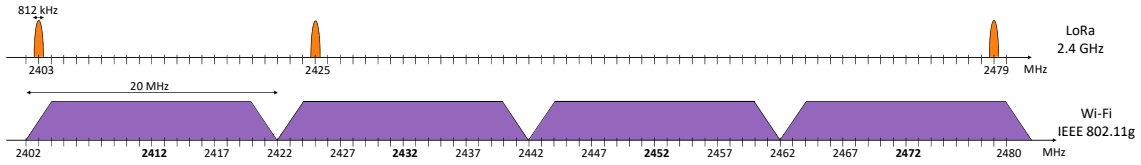

FIGURE 5.1: LoRa and Wi-Fi channels (center frequency, and bandwidth) used in our baseline frequency hopping strategies. The LoRa channels proposed by Semtech are in orange. The four independent Wi-Fi channels following the IEEE 802.11g standard in the 2.4 GHz ISM band are in purple. The center frequencies of Wi-Fi channels are highlighted in bold font.

The **random FH** strategy is a basic frequency hopping on the three LoRa channels proposed by Semtech. Each time a frame is transmitted, the end-device randomly chooses to send it on one of the three 812 kHz channels centered at 2403 MHz (channel 1), 2425 MHz (channel 2), or 2479 MHz (channel 3). The sequence of channels could be for example: 2-3-2-3-3-1. This frequency hopping strategy is referred to as baseline strategy as it implements a similar frequency hopping mechanism as in LoRa sub-GHz. The random FH strategy is already implemented in the LoRa 2.4 GHz stack.

The **round-robin FH** strategy is a variation of the random FH approach. Instead of randomly selecting one of the three Semtech LoRa channels, the end-device sends each frame

on the next LoRa channel in the list. The first frame is sent on the 2403 MHz LoRa channel. The second frame is sent on the 2425 MHz LoRa channel. The third frame is sent on the 2479 MHz LoRa channel. The fourth frame is sent on the 2403 MHz LoRa channel, and so on. We referred to the round-robin FH strategy as the second baseline strategy. We expect to obtain similar results with the round-robin FH than with the random FH strategy because on average sending randomly on three channels is equivalent to sending one-third of the frames on each of the three channels. However, we evaluate the round-robin FH strategy because depending on the center frequency of the Wi-Fi overlapping transmissions, using the round-robin FH strategy might achieve a higher FDR than using the random FH strategy.

The **best channels FH** strategy is our proposition to improve the coexistence of LoRa and Wi-Fi in the 2.4 GHz ISM band. We assume that the gateway senses, periodically, the entire 2.4 GHz ISM band, with a 1 MHz step, and assigns a noise level to each channel of the frequency band. Then, the gateway selects the three less noisy channels and transmits the list to the end-devices. After that, the LoRa channel used to transmit data is randomly picked by the end-devices, in the received list, for each frame.

5.4 Event-based simulator design

To answer the research question "How to design a simulator that can model real-world coexistence experiments?" (**RQ5-1**) we create a simulator. Our simulator consists of two parts: (1) generating the LoRa and Wi-Fi frames that will overlap, and (2) managing the collisions between frames of the different wireless technologies that have been generated.

The first step in the design of our simulator is to decide the layer at which we are going to implement our collision mitigation mechanism. Indeed, the robustness of a wireless transmission can be improved by applying mechanisms at the physical or at the MAC layer, but it can also be directly handled by the application. In our case, we want to provide an improvement of the coexistence of the wireless technologies of the 2.4 GHz ISM band irrespective of the application the LoRa network is targeting. The version of LoRa dedicated to the 2.4 GHz ISM band has no MAC layer standardized yet. Plus, we carried out our coexistence study (see Chapter 4) at the PHY layer. Finally, FH mechanisms are physical layer mechanisms. For all these reasons, we implement our collision mitigation mechanism at the PHY layer.

Usually, frequency hopping mechanisms are applied at the intra-frame level to ensure more robustness. Intra-frame FH signifies that the data frame is split into sub-frames, and each sub-frame is sent on a different channel following a given FH scheme. This is the case for the last technology released by Semtech: LR-FHSS. Instead, LoRa sub-GHz relies on frame level frequency hopping. Frame level FH refers to an FH mechanism where the entire frame is sent on a given channel, and each frame is sent over a different channel following a given FH scheme. We choose to implement a frame level frequency hopping as it allows us to stay close to the operation mode of LoRa sub-GHz. In addition, we have several arguments to validate our choice to implement a frame level frequency hopping:

- The experimental results showed that LoRa is robust to overlapping transmissions with Wi-Fi, so we expect that the potential gain of an intra-frame FH is not that significant and we estimate that it would be more beneficial to transmit LoRa frames free from interference,
- Implementing an intra-frame frequency hopping (and the resulting coding scheme) is complex as it requires to have data fragmentation and reconstitution mechanisms,
- The current LoRa 2.4 GHz gateways have only three reception paths, which limits the number of channels on which to perform the frequency hopping and the gain of implementing an intra-frame frequency hopping,
- The LoRa hardware dedicated to the 2.4 GHz ISM band (SX1280 [9]) does not allow fragmentation and so intra-frame frequency hopping.

The second step in the design of our simulator is the implementation of the simulator. Based on our coexistence experiments (see Chapter 4), we extract a theoretical model to implement. To this end, we analyze the RSSI values stored at the LoRa gateway to use them as an input in our simulator to generate our frames. As different repetitions of the same experiment give similar results (see Chapter 4), we have analyzed the RSSI values of two experiments to derive an average value per configuration and per technology. Remember that the LoRa gateway stores the channel RSSI and not the frame RSSI. Thus, depending on the SNR value, the stored RSSI by the LoRa gateway corresponds either to the LoRa signal or to the Wi-Fi signal. If the SNR value is positive, the LoRa signal is stronger than the Wi-Fi interfering signal and the RSSI stored corresponds to the LoRa signal. In contrast, a negative SNR value indicates that the LoRa signal is lower than the Wi-Fi interfering signal and the RSSI stored corresponds to the Wi-Fi signal. Analyzing the LoRa gateway logs, we can estimate the average LoRa RSSI free from interference to -55 dBm. We also estimate the average Wi-Fi RSSI free from interference to -45 dBm/-47 dBm. Note that the used RSSI values contain the residual noise of the channel. The average RSSI values we extracted from the results of our experiments are then implemented in our simulator.

Each frame, irrespective of the technology, is generated with the following parameters:

- A start time that is calculated from the previous frame (according to the previous start time and time on air), with an additional random variation that follows a Poisson distribution, where the λ parameter is the period, i.e., inter-frame time,
- An RSSI value according to the average RSSI value, extracted from the LoRa gateway logs of our coexistence experiments, with an additional random variation; the RSSI jitter varies between +/-5 dB from the average RSSI value,
- A frequency, which is the center frequency of the channel used to send frames,
- A name to allow to separate frames of the different technologies evaluated.

Frames are generated for a simulation time and stored in a vector corresponding to the technology they belong to. On the LoRa side, we evaluate several configurations and channels.

Thus, we have one vector per configuration and channel. We differentiate the frame from different technologies, and different configurations, according to their ToA and their name. For example, a Wi-Fi frame lasts approximately 1 ms for the IEEE 802.11g 12 Mbps standard, and a frame is transmitted every 100 ms, whereas an SF6, BW 1625 frame lasts 4 ms and is transmitted every 24 ms. After that, we implement two loops: one to compute the LoRa FDR under Wi-Fi interference, and one to compute the Wi-Fi FDR under LoRa interference. The frame processing is almost entirely the same for LoRa and Wi-Fi. Each LoRa frame (Wi-Fi respectively) is evaluated with each Wi-Fi frame (LoRa respectively).

We present the pseudo-code of our collision model implemented in our simulator in Algorithm 1.

Algorithm 1: Collision model simulator pseudo-code algorithm.

```
1  frame_vec: set of frames;
2  for frame in frame_vec do
3      if frequency overlap then
4          if time overlap then
5              if LoRa then
6                  if frequency_offset ≥ 6 MHz then
7                      change Wi-Fi RSSI to approximate signal attenuation due to frequency_offset;
8                  computeSIR;
9              if Wi-Fi then
10                 computeSIR;
11             if SIR < SIR_threshold then
12                 frame_lost += 1;
13 compute FDR;
```

In our simulator, a collision occurs only if a Wi-Fi frame and a LoRa frame overlap in frequency and in time.

We start by verifying that the frames overlap in frequency (line 3). If not, there is no interference between the technologies. Once the frequency overlap is proved, we verify that the frames overlap in time (line 4). If two frames have no time intersection, they do not interfere with each other. In case of time overlap, a collision occurs. The way we evaluate the loss or the reception of a frame differs for LoRa and Wi-Fi.

To ensure consistency between our simulator and our coexistence experiments, we implement the same IEEE 802.11 standard as in our experiments: the IEEE 802.11g standard. The IEEE 802.11g standard uses 20 MHz channel-wide and transmits data following an OFDM modulation. Due to the wider BW of the IEEE 802.11g standard, the signal strength decreases with distance from channel center frequency (see Figure 5.2). We observe that for a frequency offset of 11 MHz from the center frequency of the Wi-Fi channel, the signal is attenuated by 20 dB. It implies that a LoRa channel located 11 MHz away from the center frequency of the Wi-Fi interfering channel, the strength of the interfering signal received by the LoRa gateway is attenuated by 20 dB.

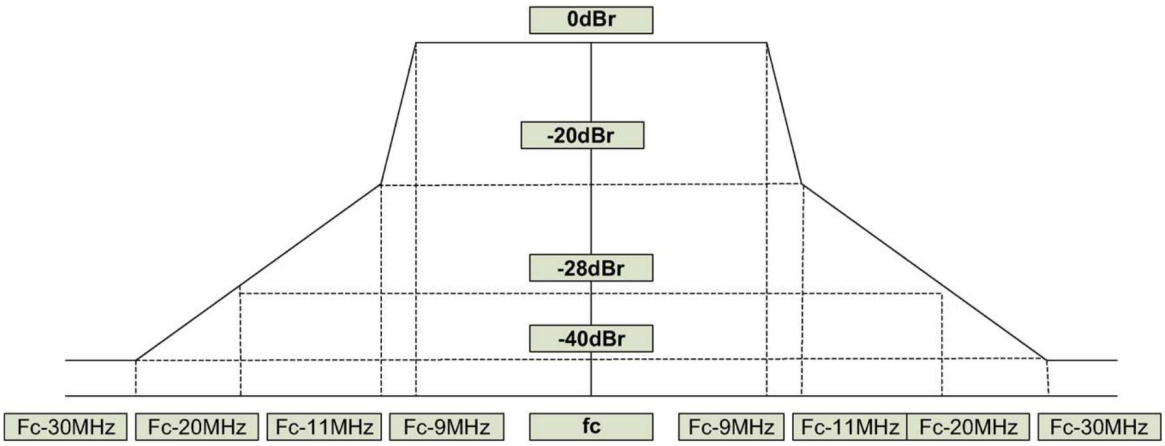

FIGURE 5.2: Wi-Fi signal strength attenuation over channel bandwidth [101]. dBr refers to decibel reference and compares the input power P to some reference power level P_0. fc refers to the center frequency channel in MHz.

Theoretically, an interfering signal is attenuated for a frequency offset of at least 9 MHz from the center frequency of the Wi-Fi channel. When validating our simulator, we obtain results in the same order of magnitude as our experiment results with a frequency offset of at least 6 MHz. Thus, if the LoRa channel is at least 6 MHz away from the Wi-Fi channel, we modify the RSSI of the Wi-Fi frame to approximate the attenuation due to the frequency offset between LoRa and Wi-Fi center frequencies (lines 5 to 7). Then, as LoRa and Wi-Fi frames interfere with each other, we compute the SIR (line 8). On the Wi-Fi side, we skip the attenuation step (lines 9 and 10). This is because a Wi-Fi channel overlapping in frequency with a LoRa channel always overlaps entirely the LoRa channel. As a consequence, we directly compute the SIR by extracting the RSSI values of the two collided frames. The last step before computing the FDR is to identify whether the collided frames are lost or not. Since we compute the SIR, we can compare this value to the smallest SIR value that allows frames to be correctly received and decoded (lines 11 and 12). For LoRa the SIR threshold depends on the configuration and it set according to Table B.2: -20 dB for SF12, -12.5 dB for SF9, and -5 dB for SF6. For Wi-Fi, we use a fix SIR threshold of 20 dB. We consider a frame received if the compute SIR is higher than the SIR threshold, otherwise, the frame is lost. Once each frame is categorized as received or lost, we compute the FDR (line 13).

The values used in the simulator as well as the implementation of the frequency hopping strategies are detailed in the next sections (see Sections 5.5 and 5.7).

5.5 Validating the simulator

As we develop our own simulator, we need to validate it before implementing the FH strategies we want to evaluate. In this section, we propose several simulations to validate the use of the simulator for estimating the performance improvement of using FH. We also provide a first insight into improving the coexistence between LoRa and Wi-Fi for a scenario close to the one used in our coexistence experiments.

5.5.1 Simulations using parameters from our coexistence experiments

To validate our simulator, i.e., the accuracy of the results obtained, we run a first set of simulations using the same LoRa parameters as in our coexistence experiments. We summarize the parameters in Table 5.2.

Technology	Configuration number	PHY Configuration	Center frequency (in MHz)	Time on Air (in ms)	Inter-frame time (in ms)
Wi-Fi	/	802.11g	2412 (channel 1)	2	12.5
LoRa	1	SF12, BW203, CR4/8	2402, 2404,	1054	9650
	2	SF9, BW812, CR4/8	2406, 2408,	38	327
	3	SF6, BW1625, CR4/5	2410, 2412	3	13

TABLE 5.2: Experiments parameters used to validate the simulator.

All of our simulations are run for 300 s (5 minutes) of simulated time. We repeat each scenario 50 times. Then we compute, and plot, the mean for both technologies using the frame delivery ratio as a performance metric.

In the simulator, a configuration is defined by a ToA and an inter-frame time in ms. The LoRa ToA is set according to the SX1280 calculator [94]. The inter-frame time has been found when designing the coexistence experiments. For instance, in our coexistence experiments, each configuration transmits for 5 minutes. We can approximate its value using Equation 5.1. Note that we evaluate three main configurations. Configurations 1 and 3 are the ones providing the highest communication range and the highest data rate respectively, whereas configuration 2 is an intermediate configuration.

$$\text{Period} = \frac{T_{exp}}{Nb_{Frames}} - \text{ToA} - Tx_{Delay}, \text{ where } Tx_{Delay} = 14 \text{ ms} \tag{5.1}$$

where:

$$\begin{aligned} T_{exp} &= \text{total duration of one configuration} \\ Nb_{Frames} &= \text{total number of frames sent for one configuration} \\ \text{ToA} &= \text{ToA of one frame} \\ Tx_{Delay} &= \text{additional delay coming from hardware operation} \end{aligned}$$

We compute Tx_{Delay} according to LoRa end-device logs. We extract the inter-frame time and compare it to the inter-frame time and the ToA we configure (see Equation 5.2). We approximate the LoRa hardware operation delay, Tx_{Delay}, to 14 ms.

$$Tx_{Delay} = \text{logged inter-frame} - (\text{configured inter-frame} + \text{ToA}) \approx 14 \text{ ms} \tag{5.2}$$

We compute the Wi-Fi ToA (see Equation 5.3) according to the payload size (1400 bytes) of the frame and the smallest data rate provided by the IEEE 802.11g standard (6 Mbps).

$$\frac{(1400 \times 8)}{6 \times 10^6 \text{ bps}} = 0.0019 \text{ s} \approx 2 \text{ ms}. \tag{5.3}$$

We set the inter-frame time to the usual Wi-Fi inter-beacon time: 100 ms. Recall that in our coexistence experiments, we stay at the PHY layer for both evaluated technologies. Thus, none of the Wi-Fi MAC mechanisms were used. The Wi-Fi `Wireshark` logs confirm that the MAC layer is disabled. By default, a Wi-Fi transmitter retransmits up to 7 times a frame that is not being acknowledged by the receiver. As the ACK mechanism is not present at the PHY layer, it explains why our receiver logs contain 8 frames for each transmitted frame. The first frame is the original one and the seven following frames are tagged with a 1-bit value indicating that this is a retry transmission. To compute the results of our coexistence experiments, we only kept the original frames. Therefore, to be in line with our experiments, we implement the same behavior in our simulator. The value of the inter-frame time is derived from this. An original Wi-Fi frame is transmitted each 100 ms, and in the meanwhile seven retry frames are transmitted. So, a frame is transmitted on average every $\frac{100 \text{ ms}}{8} = 12.5$ ms.

Figures 5.3 and 5.4 show LoRa and Wi-Fi FDR for three different LoRa configurations detailed in Table 5.2. The experiment results come from our coexistence experiments in an indoor environment (see Chapter 4), and are computed for only one experiment, as the trends observed are the same for every repetition we made. This allows us to have the same data visualization thus making it easier to compare results between experimentation and simulations. For each center frequency, bars are colored as follows: blue, orange, and green represent configuration 1 (highest communication range), 2 (intermediate), and 3 (highest data rate) respectively. For the simulation results, we plot the mean FDR computed over 50 simulations.

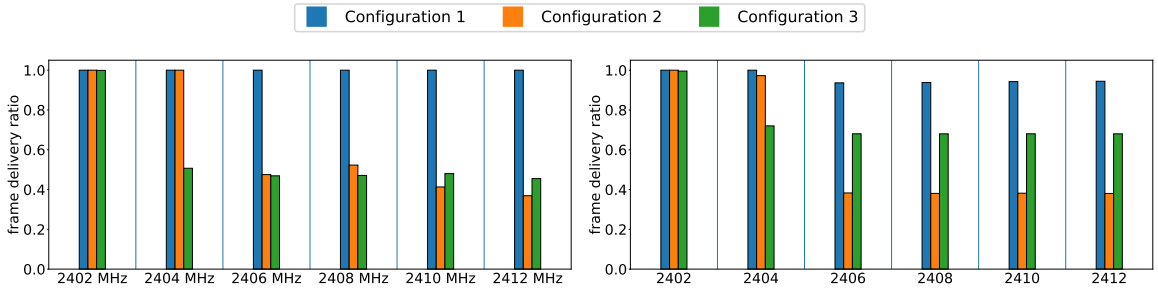

(a) LoRa FDR experiments results

(b) LoRa FDR simulations results

FIGURE 5.3: LoRa FDR experiment and simulation results comparison.

Experiment and simulation results are quite similar for center frequencies at 2402 MHz and 2404 MHz for all the three LoRa configurations. For example, in the order of the configurations tested, the LoRa FDR at 2402 MHz obtained through experiments is 100%, 100%, and 99.88%. Whereas in simulations we obtained 100%, 100%, and 99.55%. In the same way, at 2404 MHz we have an experimental FDR of 100%, 100%, and 50%, while in simulations we have a FDR of 100%, 97%, and 72%.

For configuration 1 (greatest communication range), the results obtained through experiment and simulation are similar. While experiment results always provide a LoRa FDR of

100%, the simulation results show some losses for center frequencies higher than 2404 MHz. Still, the FDR is on average never lower than 93%.

For configuration 2 (intermediate), for center frequencies from 2406 MHz to 2412 MHz, the LoRa FDR is around 40% and 38% for experiment and simulation respectively.

For configuration 3 (highest data rate), for center frequencies from 2406 MHz to 2412 MHz, we observe optimistic results with our simulator. In Figure 5.3a the LoRa FDR decreases to a minimum of 45% while in Figure 5.3b the minimum LoRa FDR is 68%. The difference between the experiment and simulation results for configuration 3 might come from the difference of environment. Configuration 3 relies on SF6, BW 1625 that provides the highest data rate but also the smallest communication range. During experiments, signals might be lost due to the propagation through walls and doors. In our simulations, the signal propagation is not implemented, so we only evaluate the losses due to frequency and time overlapping between LoRa and Wi-Fi frames. To summarize, our simulator considers that if LoRa and Wi-Fi frames do not overlap, the frame is received, which is not the case in the real world where obstacles can prevent from receiving an interference-free frame.

We highlight optimistic results for simulations using the highest data rate configuration which provides a higher FDR than the intermediate configuration. The expected results are the opposite: the higher the SF, and therefore the more robust the configuration is to interference, the higher the FDR. Indeed, the highest data rate configuration is more subject to destructive interference, thus preventing the reception of LoRa frames, than the intermediate configuration. This is probably due to the bandwidth used. The interference is spread on all the available bandwidth, so a large bandwidth is much more interfered than a narrow one.

On the Wi-Fi side (see Figure 5.4), irrespective of the center frequency of the LoRa channel, the results between experiment and simulation are equivalent. In Figure 5.4a, the Wi-Fi FDR is on average 88%, 85% and 50% for configurations 1 to 3 respectively. Looking at Figure 5.4b, we observe a Wi-Fi FDR of 89%, 88%, and 63% for the same order of configurations. Once again, we highlight the optimist behavior of our simulator when using configuration 3, i.e., the highest data rate configuration. We assume the same as for the LoRa results: in the simulator, a loss can happen only if two frames from overlapping technologies overlap in frequency and time, while in the real world some factors can lead to the loss of a frame, e.g., obstacles, other sources of interference.

After analyzing and comparing our experiment and simulation results, we consider our simulator valid. We keep in mind that the simulation results we could obtain are a best case scenario because, in our simulator, we do not implement losses due to signal propagation in the environment.

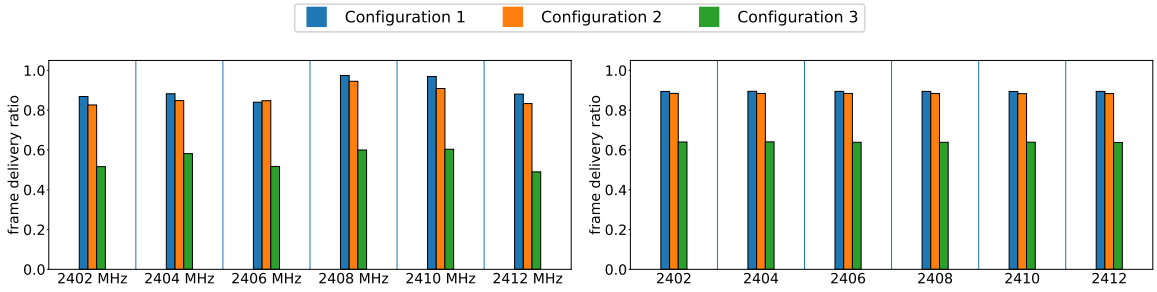

(a) Wi-Fi FDR experiments results

(b) Wi-Fi FDR simulations results

FIGURE 5.4: Wi-Fi FDR experiment and simulation results comparison.

5.5.2 Simulations extension using a fixed bandwidth

We decided to extend our simulator, based on our experimental parameters, to evaluate the same bandwidth for the three LoRa configurations: 812 kHz. Thus we only modify the greatest communication range configuration and the highest data rate configuration, as the intermediate configuration already uses a BW of 812 kHz. This bandwidth value is recommended by Semtech. A 812 kHz bandwidth ensures compliance with the FCC regulations in the 2.4 GHz ISM band. The FCC is in charge of implementing the laws and regulations for communications in the USA. The FCC 00-312 is an amendment of Part 15 for spread spectrum devices [176]. This amendment clarifies that for a bandwidth higher than 1 MHz the maximum output power is reduced proportionally to the increase in bandwidth over 1 MHz. For example, the output power is limited to 1 W and 320 mW for a 1 MHz signal and a 3 MHz signal respectively. In conclusion, using an 812 kHz bandwidth is a good trade-off between data rate and maximum output power. Note that the equivalent of FCC in Europe is ETSI. ETSI allows the same transmission power for every user of the 2.4 GHz ISM band: 100 mW.

Figure 5.5a shows that when the same BW is used the higher the SF, the higher the FDR. The major BW impact on LoRa FDR is for the configuration using SF6. In Figure 5.5b, an SF6 combined with a 1625 kHz bandwidth results in an average FDR of 68%. Dividing the bandwidth by two, i.e., 812 kHz, decreases the FDR to 30%. The results for the configuration using SF9 are the same in Figure 5.5a and Figure 5.5b because we do not change the configuration, i.e., we already used an 812 kHz bandwidth to validate our simulator. Finally, for the configuration using SF12, providing the highest communication range, the impact on the FDR by changing the BW from 203 kHz to 812 kHz is not significant. SF12 provides a good robustness against interference leading to a minimum FDR around 94% irrespective of the bandwidth.

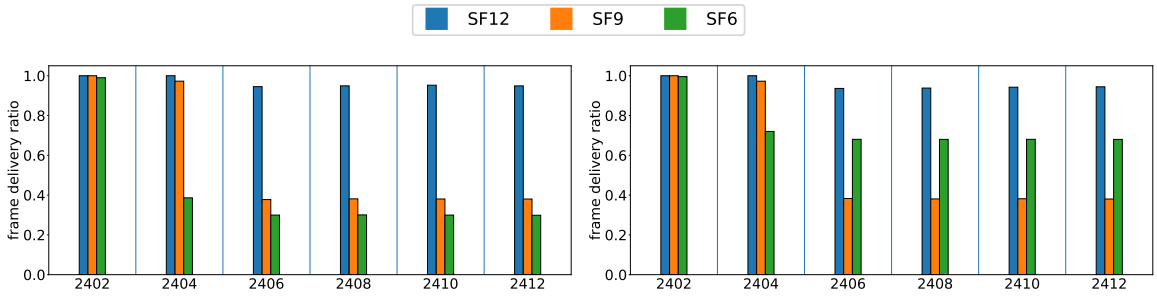

(a) LoRa FDR BW 812 kHz for all SFs

(b) LoRa FDR using experiments configurations

FIGURE 5.5: LoRa FDR simulations comparison for fixed and varied bandwidths. On the left BW is fixed to 812 kHz for all SFs. On the right BW changes depending on the SF: BW 203 kHz in blue, BW 812 kHz in orange, and BW 1625 kHz in green.

Using the same bandwidth allows to recover the performance decrease linked to the robustness of the SF observed in our coexistence experiments. High SF are more robust and thus have better resistance to interference. In Figure 5.5b we do not observe this feature: the LoRa FDR using an SF9 is lower than a LoRa end-device using an SF6. Remember that the combination of the SF and the BW gives a certain ToA and data rate. SF9 is more robust than SF6. But combining SF9 with an 812 kHz bandwidth results in a longer ToA and a lower data rate than using an SF6, BW 1625 configuration. Although the interference is spread over the entire available bandwidth, an SF6, BW 1625 configuration sends its frames at a high rate, resulting in a small number of losses due to interference. This is true only for a specific environment such as in our simulator where signal propagation is not taken into account.

The Wi-Fi FDR using LoRa configurations with a common bandwidth of 812 kHz is depicted in Figure 5.6a. As expected, the FDR for SF12 and SF9 are similar to the one obtained using the experimental parameters for all the LoRa channels tested. Using SF6 increases the Wi-Fi FDR from 63% to 83%. As the LoRa ToA increases using a bandwidth of 812 kHz instead of a bandwidth of 1625 kHz, LoRa frames interfere less frequently with Wi-Fi frames. A Wi-Fi frame lasts 2 ms and is transmitted every 100 ms. An SF6, BW 812 LoRa frame lasts 8 ms and is transmitted every 58 ms. An SF6, BW 1625 LoRa frame lasts 3 ms and is transmitted every 13 ms. Consequently, approximately one Wi-Fi frame over two coexists with one LoRa SF6, BW 812 frame, while a Wi-Fi frame coexists with a maximum of six LoRa SF6, BW 1625 frames.

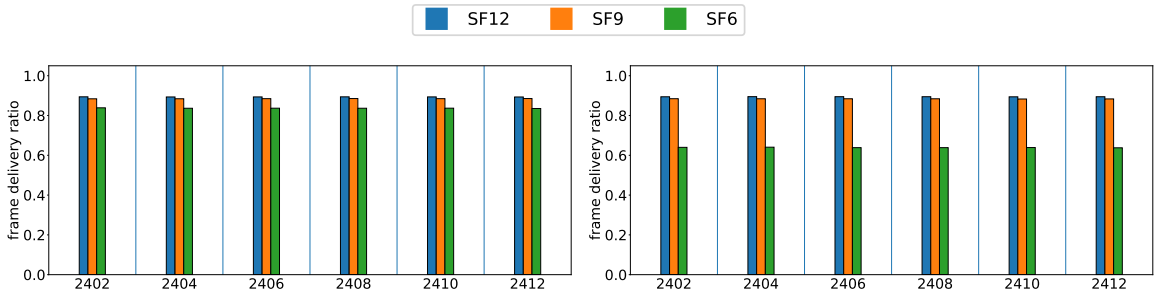

(a) Wi-Fi FDR for LoRa BW 812 kHz for all SFs **(b)** Wi-Fi FDR for LoRa experiments configurations

FIGURE 5.6: Wi-Fi FDR simulations comparison for LoRa fixed and varied bandwidths.

In Chapter 4, we highlighted that Wi-Fi is more sensitive to LoRa interference using wide bandwidth. Our simulations depicted the same conclusion. However, the increase of Wi-Fi FDR is at the expense of LoRa data rate. Recall that, the higher the SF and the narrow the BW, the lower the data rate. In other words, Wi-Fi is less impacted by LoRa transmissions using configurations that combine high SFs and narrow BWs, such as SF12, BW 203. Ensuring a fair coexistence implies improving both LoRa and Wi-Fi FDR while taking advantage of the characteristics of each technology.

5.6 Frequency hopping strategies using coexistence experiments context

We now explore the three frequency hopping strategies, detailed in Section 5.3, keeping the same context as in our coexistence experiments: one Wi-Fi AP centered at 2412 MHz, and several LoRa channels overlapping with Wi-Fi channel (see Figure 5.7).

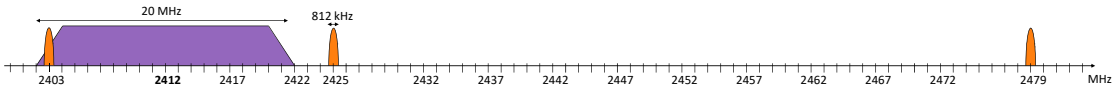

FIGURE 5.7: LoRa channels for FH strategies using Wi-Fi coexistence experiments context. The best channels FH strategy randomly chooses the first three channels located outside the Wi-Fi spectrum.

As we use simulations, we can free ourselves of the limitations coming from the implementation of the best channels FH strategy on real hardware. Thus, we exploit the three LoRa channels proposed by Semtech for the random and the round-robin FH strategies. We define the three less noisy channels for the best channels FH strategy through a simple evaluation of the channel: if the randomly selected LoRa channel is located inside the Wi-Fi spectrum, we do not validate the use of the channel. Once we have three valid LoRa channels, and thus generate the first three LoRa frames, we generate the rest of the LoRa frames by randomly selecting one of the three allowed channels. It implies that for each of the 50 runs of simulation, the selected LoRa channels can differ. For instance, with a Wi-Fi AP centered at

2412 MHz, the first simulation run can allow the use of LoRa channels centered at 2424 MHz, 2438 MHz, and 2470 MHz. The second simulation run will not necessarily allow the same LoRa channels, as they are randomly chosen at the condition to be located outside of the Wi-Fi spectrum. Thus, we can have LoRa channels centered at 2446 MHz, 2447 MHz, and 2448 MHz. For that reason, we labeled the results with "Channel" followed by numbers 1 to 3.

We summarize the parameters used to evaluate the frequency hopping strategies in Table 5.3.

Technology	Configuration number	PHY Configuration	Center frequency (in MHz)	Time on Air (in ms)	Inter-frame time (in ms)
Wi-Fi	/	802.11g	2412 (channel 1)	2	12.5
LoRa	1	SF12, BW812, CR4/8	2403, 2425, 2479	263	2360
	2	SF9, BW812, CR4/8	or	38	327
	3	SF6, BW812, CR4/8	3 best channels	8	58

TABLE 5.3: Simulations parameters used to evaluate the FH strategies.

The LoRa results are compiled in Figure 5.8. The results of using the random FH and the round-robin FH strategies are very similar. As the LoRa channels are fixed beforehand, the only channel overlapping with the Wi-Fi AP is the one centered at 2403 MHz. Thus for the channels outside of the Wi-Fi spectrum, the LoRa FDR is 100%. The 2403 MHz channel is located at the edge of the Wi-Fi channel, so the power of the Wi-Fi interference is lower as it decreases with the increase of the frequency offset. We see that only the less robust configuration (configuration 3) suffers from frame losses. The LoRa FDR is 75.25% and 75.43% for the random FH and the round-robin FH strategies respectively. These results are expected because on average, randomly selecting one of three possible channels is the same as using them one after the other. We also expected the results of the best channels FH strategy: the LoRa channels are located outside of the Wi-Fi spectrum, i.e., the channels used by each technology are not overlapping, so no interference occurs providing a LoRa FDR of 100% for all the configurations tested.

Figure 5.9 presents the Wi-Fi FDR depending on the LoRa configurations and the FH strategies.

As for LoRa, the Wi-Fi FDR is 100%, except for the overlapping channel. Contrary to LoRa, the impact of the overlapping channel has less impact on the Wi-Fi FDR.

We summarize all the results of this section in Table 5.4 considering one Wi-Fi AP. Note that the results provided for the LoRa channels centered at 2402 MHz and 2404 MHz, through experiments and simulations, correspond to a scenario in which no interference mitigation mechanisms are implemented. As we base our simulator on our experiments, in which we do not analyze the LoRa channels proposed by Semtech, we study the two channels located on each side of the 2403 MHz Semtech LoRa channel proposition.

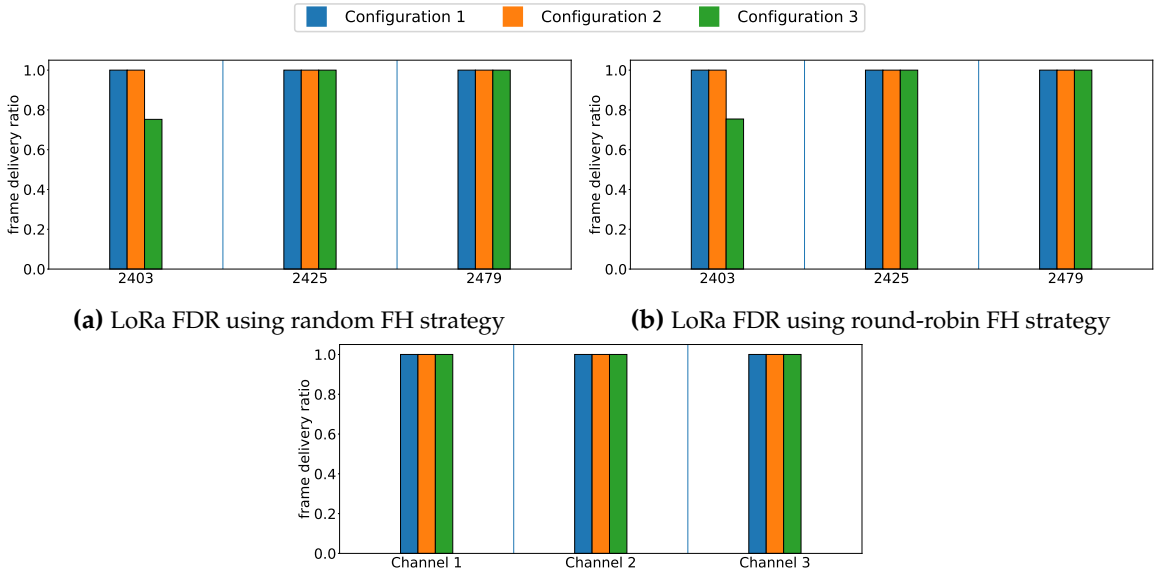

(a) LoRa FDR using random FH strategy

(b) LoRa FDR using round-robin FH strategy

(c) LoRa FDR using best channels FH strategy

FIGURE 5.8: LoRa FDR depending on the FH strategy.

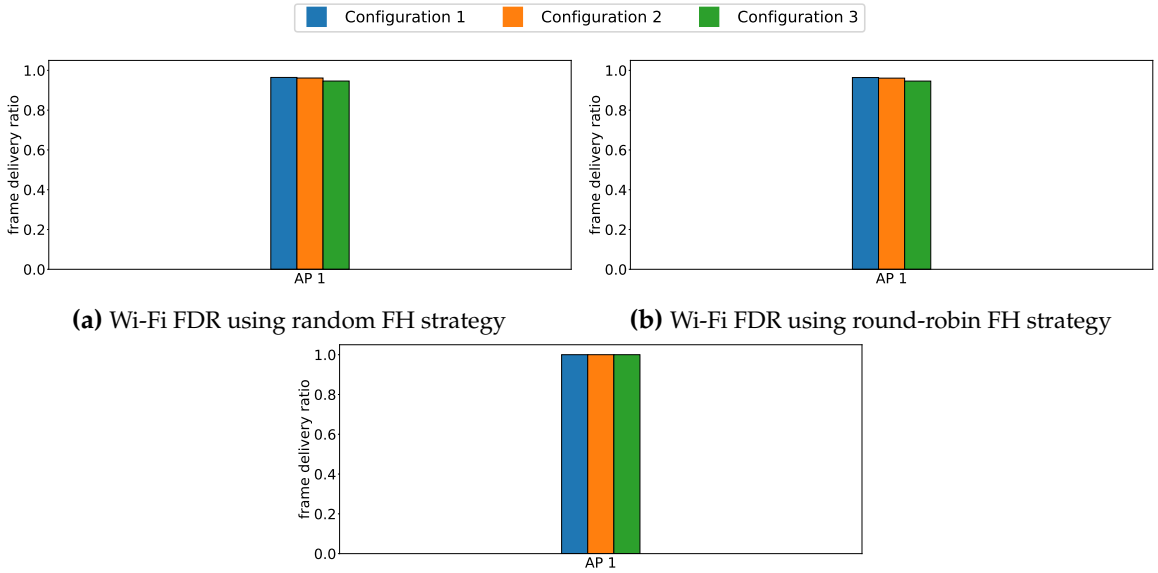

(a) Wi-Fi FDR using random FH strategy

(b) Wi-Fi FDR using round-robin FH strategy

(c) Wi-Fi FDR using best channels FH strategy

FIGURE 5.9: Wi-Fi FDR depending on the FH strategy.

1 Wi-Fi AP (2412 MHz)									
	LoRa channels 2402 and 2404 MHz						Semtech LoRa channels (2403, 2425 and 2479 MHz)		Less noisy channels of the 2.4 GHz ISM band
	Experiments		Simulations		Simulations Extension 812 kHz		Random FH	Round-robin FH	Best channels FH
	2402 MHz	2404 MHz	2402 MHz	2404 MHz	2402 MHz	2404 MHz			
LoRa Conf 1	98.83%	100%	100%	100%	100%	100%	100%	100%	100%
LoRa Conf 2	99.45%	83.04%	100%	97.25%	100%	97.26%	100%	100%	100%
LoRa Conf 3	97.61%	49.80%	99.56%	72.00%	98.99%	38.62%	75.25%	75.43%	100%
Wi-Fi for LoRa Conf 1	89.30%	89.78%	89.42%	89.48%	89.40%	89.33%	96.44%	96.39%	100%
Wi-Fi for LoRa Conf 2	86.43%	85.26%	88.45%	88.42%	88.40%	88.42%	96.15%	96.09%	100%
Wi-Fi for LoRa Conf 3	54.33%	53.85%	64.00%	64.08%	83.87%	83.65%	94.63%	94.61%	100%

TABLE 5.4: Simulated FDR synthesis using the coexistence experiments context.

We conclude that using a basic frequency hopping strategy, i.e., using the LoRa channels proposed by Semtech, which is simple to implement, allows to significantly improve the LoRa FDR. This conclusion is more visible for the less robust configuration. In fact, in our coexistence experiments, the LoRa configuration 3, under Wi-Fi interference, gives a FDR of nearly 50%. Using the random (or the round-robin) FH strategy, the FDR increases to 75%. The Wi-Fi FDR is also improved for all configurations but more significantly for the LoRa configuration 3: we increase the FDR from 54% to 94% by implementing a frequency hopping strategy.
These results validate Semtech's choice to implement random frequency hopping on the proposed channels in the LoRa 2.4 GHz stack. We also respond to the research question "Is there a frequency hopping strategy that gives better results than the frequency hopping proposed in the actual LoRa 2.4 GHz stack?" (**RQ5-2**). Indeed, running simulations using the same context as in our coexistence experiments demonstrate that the best channels FH strategy always provide a FDR of 100% for both LoRa and Wi-Fi, and thus is better than the random FH strategy proposed in the actual LoRa 2.4 GHz stack.

5.7 Frequency hopping strategies comparison

In this section, we evaluate the same three FH strategies, as in the previous section, for a variable Wi-Fi environment. In the following series of simulations, we use the LoRa configurations presented in Table 5.3. Figure 5.10 introduces the four Wi-Fi cases we evaluate in this section.

Usually, when we talk about Wi-Fi independent channels, we think of channels 1, 6, and 11 which are centered at 2412 MHz, 2437 MHz, and 2462 MHz. Indeed, most of the Wi-Fi APs are deployed by default on one of these three channels. However, recall that in Subsection 2.2.2 we presented the difference between the different standards of the IEEE

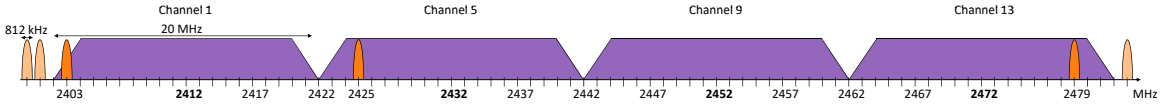

FIGURE 5.10: LoRa and Wi-Fi channels for FH strategies study. Dark orange ellipse arcs are the LoRa channels proposed by Semtech. Light orange ellipse arcs are the LoRa channels located outside the four independent Wi-Fi channels. Purple rectangles represent the four independent channels in IEEE 802.11g.

802.11 family. The IEEE 802.11b standard transmits over 22 MHz bandwidth channels and uses a DSSS modulation. The three independent channels are channels 1, 6, and 11. A fourth independent channel is channel 14 centered at 2484 MHz but is only available in Japan. In comparison, the IEEE 802.11g (and n) standards transmit over 20 MHz channels and use an OFDM modulation. Note that in the USA, channels 12 and 13 are not used, i.e., they are not part of the FCC list of authorized channels. In our case, we base our simulation on the ETSI regulations. Hence, instead of three independent channels as in the USA, we have four independent channels: 1, 5, 9, and 13 centered respectively at 2412 MHz, 2432 MHz, 2452 MHz, and 2472 MHz.

To evaluate the gain of the three considered FH strategies, we define the following evaluation scenarios. The LoRa channels are fixed at 2403 MHz, 2425 MHz, and 2479 MHz for the random and the round-robin FH strategies. In the best channels FH strategy, the LoRa channels randomly take any frequency as long as they do not overlap with Wi-Fi access points. This implies that the more Wi-Fi APs the less choice for LoRa channels. Contrary to Subsection 5.5.1, evaluating the case of a single Wi-Fi AP, the centered frequency is no longer fixed to 2412 MHz. The Wi-Fi AP randomly peaks a center frequency in the list of the four independent channels of the IEEE 802.11g standard. With a single Wi-Fi AP there is a possibility that none of the LoRa channels of the random (and the round-robin) FH strategies are overlapped. Indeed, LoRa channel 1 overlaps with Wi-Fi channel 1, LoRa channel 2 overlaps with Wi-Fi channel 2, and LoRa channel 3 overlaps with Wi-Fi channel 4. Note that the LoRa channels are located at the edge of one Wi-Fi channel. In the same way, using the four independent Wi-Fi channels, let only three possible LoRa non-overlapped channels: 2400 MHz, 2401 MHz, and 2483 MHz, colored in light orange in Figure 5.10.

For each frequency hopping strategy, we evaluate a number of Wi-Fi AP from 1 to 4. In each run of 50 simulations, the Wi-Fi AP can take a different center frequency. In the case of several APs, the center frequency follows a random selection without replacement, i.e., each AP has a different center frequency. We make this choice because, although we know that in a real environment, it is unlikely to have only 4 APs, which are independent of each other, implementing the possibility of having several APs on the same frequency makes it harder to assess the impact of interference on the FDR. More, our simulator is based on our coexistence experiments, in which we only evaluated the case of one independent access point interfering (and interfered) with LoRa transmissions.

Extending the number of Wi-Fi APs from 1 to a maximum of 4, implies to modify the LoRa

channel selection algorithm of the best channels FH strategy. We take a closer look at the pseudo-code of this selection mechanism in Algorithm 2.

Algorithm 2: LoRa channel selection simulator pseudo-code algorithm.

```
1  L_channel: list of LoRa channels; if LoRa then
2      if L_channel.size() < 3 then
3          while L_channel.size() < 3 do
4              flag = OK;
5              freq = random(ISM);
6              for y in range(Nb_AP) do
7                  if freq not in range(W_channel[y] − 10, W_channel[y] + 10) then
8                      flag = OK;
9                  else
10                     flag = KO;
11                     break;
12             if flag = OK then
13                 if freq not in L_channel then
14                     L_channel.append(freq)
15     else
16         freq = random(L_channel)
```

The first LoRa frame generated is assigned to a random frequency in the range of the 2.4 GHz ISM band (2400 MHz to 2483.5 MHz). The LoRa channel is evaluated to decide if it is valid or not regarding the spectrum of the first Wi-Fi AP, i.e., we verify that both channels are not overlapping. If the LoRa channel overlaps with the Wi-Fi channel, LoRa tries another channel. If the channel is valid for the first Wi-Fi AP, we test it for the second Wi-Fi AP. We loop until we find three LoRa channels valid for all the Wi-Fi APs. Once the condition has been met, we generate the rest of the LoRa frames using one of the three previously validated frequencies. The rest of the processing is the same as the one presented in Algorithm 1. On the LoRa side, we measure the FDR per configuration and per channel. We also compute the overall FDR for a configuration, regardless of the channel used. Wi-Fi FDR is quite similar. Instead of evaluating the FDR per LoRa configuration and per channel, we calculate the Wi-Fi FDR depending on the LoRa interfering configuration and per AP. We also compute the global Wi-Fi FDR for a LoRa configuration, regardless of which AP is interfered.

We present the results of the random FH, round-robin FH, and best channels FH strategies depending on the number of Wi-Fi access points in the following subsections.

5.7.1 Evaluation of random frequency hopping

We start by analyzing the random FH strategy. The channel allocation of this FH strategy means that depending on the IEEE 802.11 standard used, the LoRa channels are either at the edge of the most common used Wi-Fi channels, or outside the Wi-Fi spectrum.

Figure 5.11 shows that increasing the number of Wi-Fi APs decreases the LoRa FDR except for the most robust configuration.

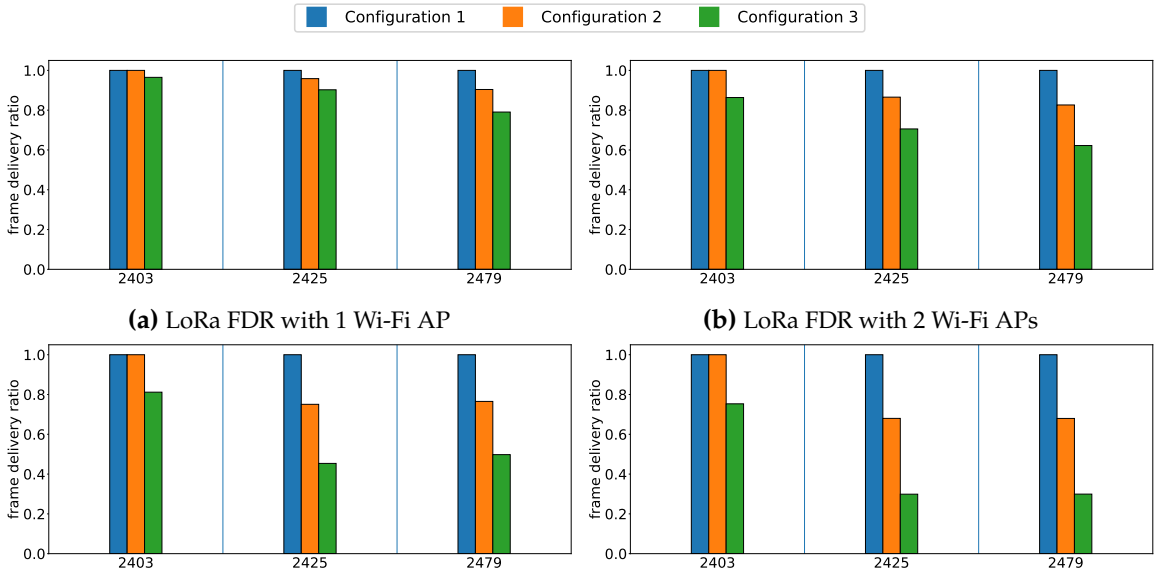

(a) LoRa FDR with 1 Wi-Fi AP

(b) LoRa FDR with 2 Wi-Fi APs

(c) LoRa FDR with 3 Wi-Fi APs

(d) LoRa FDR with 4 Wi-Fi APs

FIGURE 5.11: LoRa random FH strategy FDR depending on the number of Wi-Fi APs.

If we analyze the configurations one by one, we highlight a common trend by adding Wi-Fi APs. Configuration 1 is the one providing the highest communication range and is also the most robust against interference. We observe that irrespective of the LoRa channel or the number of Wi-Fi APs, the FDR is always 100%.

This is not the case for the two other configurations that suffer from losses. For example, the intermediate configuration, when one Wi-Fi AP is interfering (see Figure 5.11a) provides a FDR of nearly 96% and 90% for the LoRa channels centered at 2425 MHz and 2479 MHz respectively. The FDR decreases to nearly 68% for both channels but with four Wi-Fi APs interfering (see Figure 5.11d). The same FDR decrease is observed, when the number of Wi-Fi APs increases, with the LoRa configuration providing the highest data rate and thus the less robust to interference. For the 2403 MHz LoRa channel, the FDR decreases from 96% to 75% when the number of Wi-Fi APs is increased from 1 to 4. For the 2425 MHz LoRa channel, the FDR decreases from 90% to 30% when the number of Wi-Fi APs is increased from 1 to 4. For the 2479 MHz LoRa channel, the FDR decreases from 79% to 30% when the number of Wi-Fi APs is increased from 1 to 4.

We observe that irrespective of the number of Wi-Fi AP, configuration 2 using the LoRa channel centered at 2403 MHz always received 100% of the frames sent (orange bars in Figure 5.11d). We can explain the difference of FDR between the three LoRa channels by their frequency offset with the corresponding overlapping Wi-Fi AP. As mentioned before, LoRa channel 1 overlaps with Wi-Fi channel 1. The frequency offset between their center frequencies is 9 MHz. LoRa channel 2 overlaps with Wi-Fi channel 2, and LoRa channel 3 overlaps with Wi-Fi channel 4. Both LoRa channels have a frequency offset of 7 MHz with their respective overlapping Wi-Fi channel. As the LoRa configuration 2 is an intermediate configuration, i.e., uses the median spreading factor, an additional frequency offset of

2 MHz, compared to the other LoRa channels, seems to be sufficient to ensure a FDR of 100%. Recall that, the higher the frequency offset between LoRa and Wi-Fi center frequencies, the higher the Wi-Fi signal is attenuated at the LoRa receiver, and thus the higher the LoRa FDR.

From these results, we highlight that the relation between SF and robustness to interference is satisfied. This indicates that our simulator provides consistent results compared to a real LoRa transmission under interference. Plus, the LoRa FDR decreases as the number of access points increases. For example, the configuration 2 on the 2479 MHz channel, suffers from a progressive decrease in its FDR, with values of 90%, 82%, 76%, and 68% respectively for a number of APs increasing from 1 to 4.

We analyze the results of the Wi-Fi FDR depending on the LoRa configurations interfering and the AP interfered in Figure 5.12.

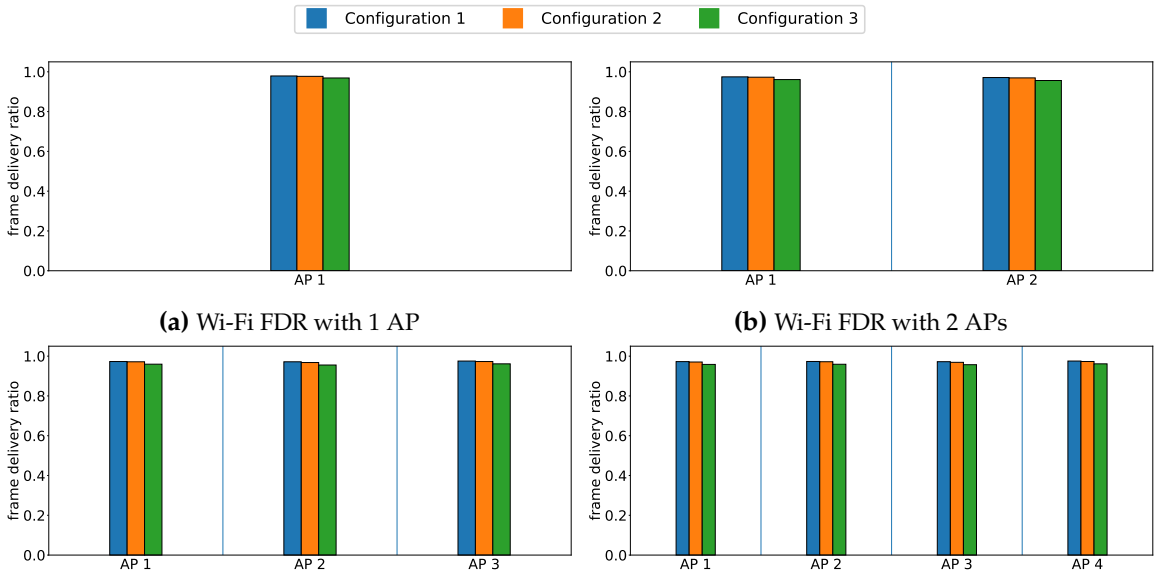

(a) Wi-Fi FDR with 1 AP

(b) Wi-Fi FDR with 2 APs

(c) Wi-Fi FDR with 3 APs

(d) Wi-Fi FDR with 4 APs

FIGURE 5.12: Wi-Fi FDR under LoRa random FH strategy and several APs.

The results show that the Wi-Fi FDR is independent of the number of APs we use. For example, using one AP interfered by the most robust LoRa configurations, i.e., SF12, BW 812, the Wi-Fi FDR is 97.91%. When we increase the number of APs from 1 to 4, the resulting Wi-Fi FDRs under the same LoRa interference are in the same order of magnitude, about 97%. We observe the same trend for the other LoRa configurations with a slightly higher impact using the highest data rate LoRa configuration as it interferes more often with the Wi-Fi transmissions.

We conclude that the number of APs using a random FH strategy for LoRa transmissions has no impact on the Wi-Fi FDR. We see that irrespective of the number of APs and the LoRa configurations, the lower Wi-Fi FDR is 95% (configuration 3 AP number 2 in Figure 5.12c). These results are explained by the fact that the LoRa channels are located far away from the center frequency of the Wi-Fi APs leading to a weak power of interference. Plus, we only consider independent access points meaning that there is no intra-technology interference. In other words, we assume that there is no interference between the different Wi-Fi APs. Note that in a real deployment, intra-technology interference has to be taken into account.

5.7.2 Evaluation of round-robin frequency hopping

We now evaluate the second baseline FH strategy: the round-robin FH. Instead of randomly choosing one of the three LoRa channels, each frame is sent on the next available channel starting at 2403 MHz. This means that exactly one frame over three is sent on the 2403 MHz, 2425 MHz and 2479 MHz LoRa channel respectively.

Figures 5.13 and 5.14 show the LoRa and Wi-Fi FDR depending on the LoRa channels, the LoRa configurations, and the number of Wi-Fi APs.

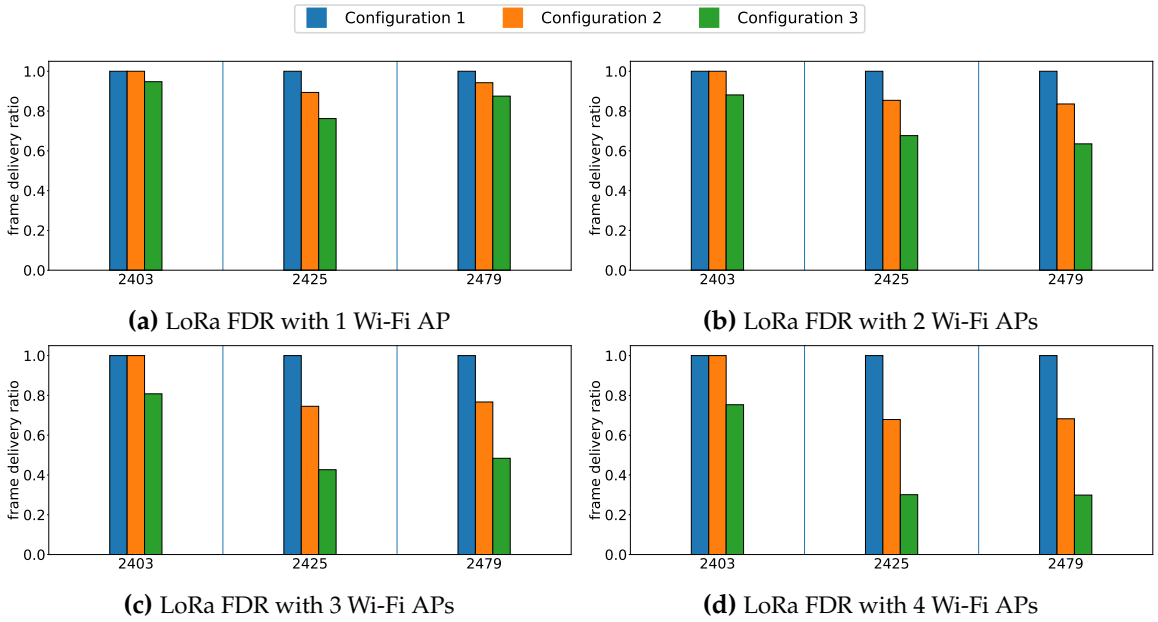

(a) LoRa FDR with 1 Wi-Fi AP

(b) LoRa FDR with 2 Wi-Fi APs

(c) LoRa FDR with 3 Wi-Fi APs

(d) LoRa FDR with 4 Wi-Fi APs

FIGURE 5.13: LoRa round-robin FH strategy FDR depending on the number of Wi-Fi APs.

In Figure 5.13, we observe the same trend as using the random FH strategy for the configuration 1: irrespective of the LoRa channel used to transmit, and the number of Wi-Fi APs, the LoRa FDR is always 100% as it is the most robust to interference LoRa configuration.

Here also, configuration 2 using the 2403 MHz channel gives a FDR of 100% whatever the number of Wi-Fi APs interfering. This conclusion has been explained in the previous section:

due to a sufficient distance between LoRa and Wi-Fi center frequencies, the Wi-Fi interfering signal arrives at the LoRa receiver with a weak power thus allowing the good reception and demodulation of the LoRa signal. For the other channels, the FDR decreases with the increase of the number of Wi-Fi APs. For example for channel 2479 MHz, the LoRa FDR is respectively 94%, 83%, 76%, and 68% for a number of Wi-Fi APs increasing from 1 to 4.

Configuration 3, which is the less robust to interference, depicts the same trends. For the LoRa channel centered at 2479 MHz, the FDR gradually decreases from 87% to 30% by increasing the Wi-Fi APs from 1 to 4.

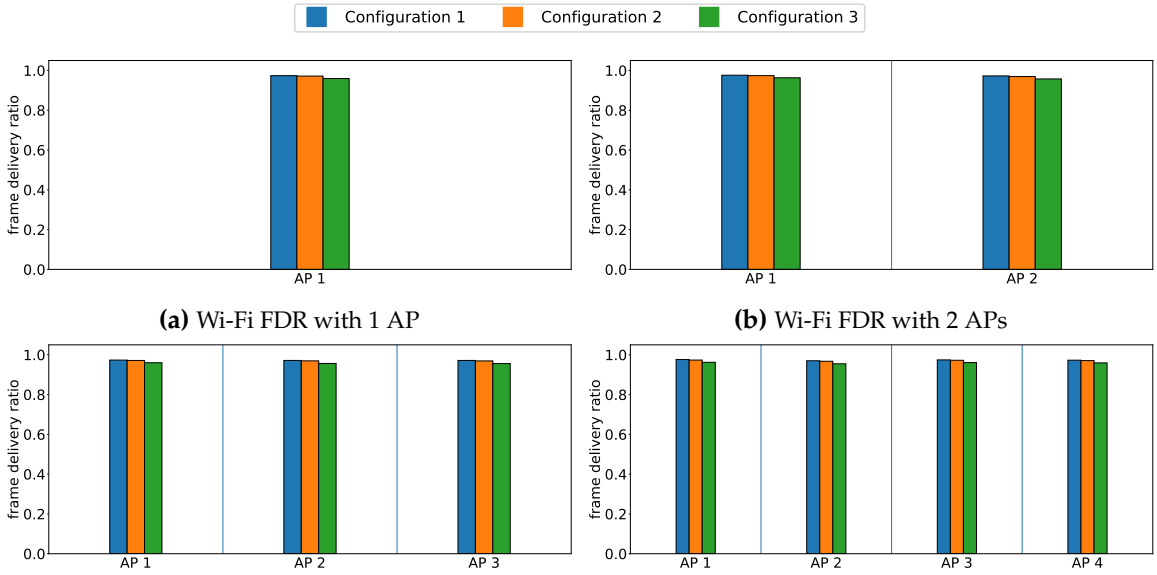

(a) Wi-Fi FDR with 1 AP

(b) Wi-Fi FDR with 2 APs

(c) Wi-Fi FDR with 3 APs

(d) Wi-Fi FDR with 4 APs

FIGURE 5.14: Wi-Fi FDR under LoRa round-robin FH strategy and several APs.

The Wi-Fi results exhibit the same conclusions as using a random FH strategy for LoRa transmissions. Configuration 3 impacts a bit more the Wi-Fi FDR due to the occurrence of its transmissions: a LoRa SF6, BW 812 interferes with one over two Wi-Fi frames. In comparison, a LoRa SF9, BW 812 frame is interfered by a maximum of three Wi-Fi frames. The higher number of periods where LoRa transmissions, using configuration 3, overlap with Wi-Fi transmissions result in a Wi-Fi FDR average of 96%.

Generally speaking, regardless of the LoRa configuration used and the number of access points, the Wi-Fi FDR is between 97.60% (configuration 1, AP number 1 in Figure 5.14b) and 95.47% (configuration 3, AP number 2 in Figure 5.14d).

On average using a round-robin FH strategy or a random FH strategy gives the same results. Thus we conclude the same as in Subsection 5.7.1: (1) LoRa FDR decreases by increasing the number of Wi-Fi access points, and (2) the Wi-Fi FDR is on average the same irrespective of the LoRa configurations interfering and the number of APs used.

5.7.3 Evaluation of best channels frequency hopping

The last FH strategy we evaluate is the best channels FH. The proposition of this frequency hopping strategy is to sense the entire 2.4 GHz ISM band and select the less noisy channels. In our simulator, this is implemented by selecting the first three LoRa channels which are located outside of the spectrum of all the Wi-Fi APs.

As it can be seen in Figure 5.10, even with four non-overlapping Wi-Fi APs, there are still three LoRa channels outside the Wi-Fi APs spectrum. For that reason, and because the results are obvious, we jointly analyze the LoRa and Wi-Fi results represented in Figures 5.15 and 5.16. Note that as the LoRa channels are randomly selected at the beginning of each run of simulation, we labelled the results with Channel [1 to 3] instead of giving the center frequency as in the random and round-robin FH results.

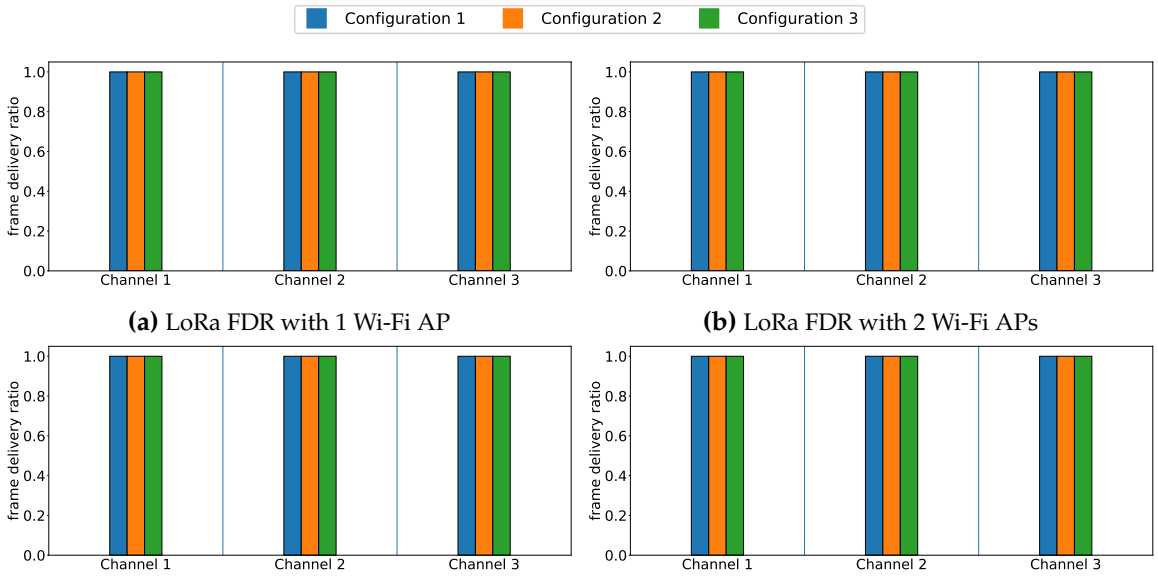

(a) LoRa FDR with 1 Wi-Fi AP

(b) LoRa FDR with 2 Wi-Fi APs

(c) LoRa FDR with 3 Wi-Fi APs

(d) LoRa FDR with 4 Wi-Fi APs

FIGURE 5.15: LoRa best channels FH strategy FDR depending on the number of Wi-Fi APs.

As expected, both LoRa and Wi-Fi FDR are 100% irrespective of the LoRa configuration, the LoRa channel, and the number of Wi-Fi APs.

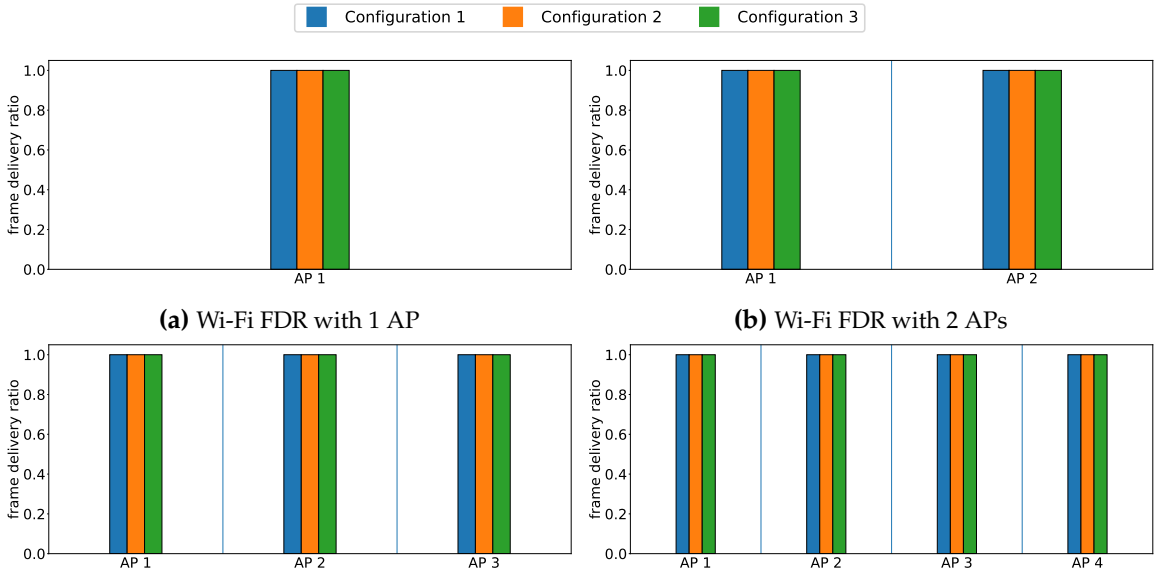

(a) Wi-Fi FDR with 1 AP

(b) Wi-Fi FDR with 2 APs

(c) Wi-Fi FDR with 3 APs

(d) Wi-Fi FDR with 4 APs

FIGURE 5.16: Wi-Fi FDR under LoRa best channels FH strategy and several APs.

Note that in the case where three LoRa channels are not available outside the Wi-Fi spectrum, the best channels, keeping the four independent Wi-Fi access points, seem to be located at the beginning of Wi-Fi channel 1 and at the end of Wi-Fi channel 4, as well as at the intersections of Wi-Fi channels 1 and 2, and 2 and 3. In other words, the less noisy channels, when overlapped by Wi-Fi APs are 2402 MHz, 2422 MHz, 2442 MHz, and 2482 MHz. This implies that in the case of IEEE 802.11b traffic, which is 22 MHz wide, further investigations are necessary to evaluate the improvement of the best channels FH strategy. This is true especially for the Wi-Fi channels intersections where although the interfering signal arrives with low power, the interfered signal will be interfered by two different channels. Thus, additive interference must be taken into account, and studied, when evaluating the gain of using frequency hopping for LoRa transmissions.

We summarize the results of the entire section in Table 5.5. The difference with the results analyzed in the previous subsections is that the we compute a global FDR per technology. Global LoRa FDR represents the FDR per configuration regardless of the channel used, which means that the configuration variations are smoothed. Global Wi-Fi FDR represents the FDR for a given LoRa configuration whatever the AP interfered by the LoRa transmission.

These global results emphasize that for both random and round-robin FH strategies, the LoRa FDR decreases as the number of Wi-Fi APs increases. For example, using the random FH strategy, the less robust configuration, i.e., configuration 3, results in a LoRa FDR of 88% when one Wi-Fi AP is interfering. The LoRa FDR decreases up to 45% when the number of

	Random FH				Round-robin FH				Best channels FH			
	1 AP	2 AP	3 AP	4 AP	1 AP	2 AP	3 AP	4 AP	1 AP	2 AP	3 AP	4 AP
LoRa Conf 1	100.00%	100.00%	100.00%	100.00%	100.00%	100.00%	100.00%	100.00%	100.00%	100.00%	100.00%	100.00%
LoRa Conf 2	95.48%	89.78%	83.74%	78.73%	94.53%	89.65%	83.74%	78.71%	100.00%	100.00%	100.00%	100.00%
LoRa Conf 3	88.67%	73.16%	58.77%	44.99%	86.16%	73.08%	57.27%	45.09%	100.00%	100.00%	100.00%	100.00%
Wi-Fi per LoRa confs	97.91% 97.72% 96.90%	97.29% 97.11% 95.86%	97.33% 97.08% 95.87%	97.33% 97.11% 95.90%	97.38% 97.17% 95.95%	97.42% 97.16% 96.02%	97.22% 97.00% 95.74%	97.33% 97.11% 95.93%	100.00% 100.00% 100.00%	100.00% 100.00% 100.00%	100.00% 100.00% 100.00%	100.00% 100.00% 100.00%

TABLE 5.5: LoRa and Wi-Fi FDR depending on the FH strategy and the number of APs.

Wi-Fi APs increases up to 4. By analyzing the LoRa FDR depending on the channel used (see Figure 5.11) we find that the global FDR is improved thanks to a better reception on LoRa channel 2403 MHz. Here also, we clearly see the equivalence of using a random or a round-robin FH strategies as the computed FDR are in the same order of magnitude.

On the Wi-Fi side, the results are quite similar for all the LoRa configurations and whatever the number of APs there are, using the random or the round-robin FH strategies for LoRa transmissions. We insist on the fact that the Wi-Fi FDR obtained under LoRa interference using FH strategies is as good as in an interference-free scenario, according to our experimental results. More, in our coexistence experiments, we underlined that the addition of LoRa and BT interference, coming from the transmission of the BT beacon, results in a Wi-Fi FDR of 80% for a LoRa channel centered at 2402 MHz which is also the center frequency of one of the BT advertising channel. Notice that in our coexistence experiments, LoRa frames were transmitted on a fixed channel. This indicates that implementing an FH strategy in LoRa 2.4 GHz ensures a coexistence with Wi-Fi as good as before the LoRa deployment in the 2.4 GHz ISM band.

Finally, we point out that using the best channels FH strategy ensures a FDR of 100% for both technologies even when there are four Wi-Fi access points covering almost the entire spectrum of the 2.4 GHz ISM band.

The study of the best channels FH strategy provides an answer to the question "Is there a frequency hopping strategy that guarantees a Wi-Fi FDR, when interfered by LoRa transmissions, that is at least as good as when interfered by other wireless technologies (e.g., BT, IEEE 802.15.4)?" (**RQ5-3**). It also underpins the answer to the question "Is there a frequency hopping strategy that gives better results than the one proposed in the actual LoRa 2.4 GHz stack?" (**RQ5-2**) given in Subsection 5.5.1.
These results show that the gain of using a more costly frequency hopping protocol is a good option when the number of Wi-Fi access points is high. Indeed, even for the less robust configuration and using the random FH strategy, the LoRa FDR is 88.67% when there is one Wi-Fi AP, and a FDR of 96.90% is guaranteed for Wi-Fi transmissions. The FDR improvement by implementing the best channels FH strategy is very significant, compared to the random and the round-robin FH strategies, for a number of Wi-Fi APs of at least three. In this case, the LoRa FDR, depending on the baseline FH strategy applied, for the less robust configuration increases from 58.77%, and 57.27% respectively to 100%.

5.8 Implementation proposal for our solution

The results presented in this chapter are obtained through simulations. However, we design a proposition to implement our solution on COTS hardware. We propose an original methodology to select the channels used in the best channels FH strategy [1]. We also propose to implement our methodology into a LoRa gateway.

5.8.1 Methodology for wireless technology detection

As LoRa takes place in a congested frequency band, our methodology for wireless technology detection aims to indicate what is happening on a channel at a given time. Indeed, we want to (1) evaluate if the future LoRa deployment will be impacted, and (2) if the technologies already using the 2.4 GHz ISM band will be impacted by the future LoRa deployment.

The existing literature encompasses several works on measurements and analysis of spectrum occupancy. For example, Höyhtyä et al. make measurements in the 2.4 GHz ISM band to estimate the idle time of the channels to potentially use those inactivity periods for cognitive radios, especially LTE [102] [178]. In both papers, the authors highlight the difficulty of differentiating a radio signal from a noise. Thus, they introduce a threshold to evaluate if the data collected is noise or signal. The authors obtain an amount of time when the spectrum is occupied, and they make assumptions of what applications it could correspond to, e.g., cameras or amateur radio services.

Contrary to existing works, we do not estimate the idle time of channels. Instead, we propose an original methodology to characterize the use of a frequency band. Characterizing

[1] This section extends the study published in a short paper [177] and presented at [2].

the use of a frequency band means being able to analyze the spectrum and associate potential signals to known technologies using this frequency band. To demonstrate the validity of our method, we also apply the proposed methodology to two recorded signals and verify that we are able to associate the signals to the right technology (Wi-Fi and Bluetooth).

Our methodology for wireless technology detection resulting from the characterization of the radio environment of the 2.4 GHz ISM band consists of the following steps:

1. We sense the radio environment, for approximately one minute, and we capture the wireless signals that are present using a software-defined radio (the USRP B200 mini [179] in our case) connected to a laptop. We used the GNURadio software [180], which allows us to visualize the I/Q signals and save them into binary files.

2. We perform a Fast Fourier Transform (FFT) on the obtained signal, to convert it into individual spectral components. We apply Parseval's theorem to compute the energy hence we can output a heatmap of energy distribution. Parseval's theorem demonstrated that the energy of a function in the time (or space) domain is equal to the energy of its representation in the frequency domain.

3. We compute a threshold to define if the observed energy is either a noise or a radio signal from a wireless technology. We compare each energy sample to this threshold, and we store the result in a gradient matrix: 0 if the energy sample is below the threshold, otherwise 1, 2, or 3 depending on how many times the energy sample is above the threshold value. For example, if the energy e is such that $2 \times threshold \leq e \leq 3 \times threshold$, the corresponding stored value is 2.

4. We convert the matrix into a figure to visualize the energy levels. According to the bandwidth containing the signal, we associate the result to a wireless technology.

For all the post-processing of data (steps 2 to 4), we use Python programming combined with the JupyterLab software [181].

One question that arises is how much of the recorded bandwidth should we analyze. Remember that, from Figure 2.1, we note that LoRa uses a narrow bandwidth in comparison with the other technologies in this frequency band. To be able to identify a LoRa signal (bandwidths from 203 kHz to 1625 kHz), a Bluetooth signal (bandwidth equal to 1 MHz), a Bluetooth Low Energy signal (bandwidth equal to 2 MHz), and a Wi-Fi signal (bandwidth equal to 20 MHz for the IEEE 802.11g standard), we claim that a 4 MHz recorded bandwidth is sufficient. Indeed with a 4 MHz recorded bandwidth, we can detect and map a signal to the right wireless technologies if we split the recorded bandwidth into sub-channels of 200 kHz. The sub-channels bandwidth allow detecting the narrowest LoRa signal, i.e., a LoRa signal using a 203 kHz bandwidth. Plus, the LoRa bandwidth values are multiples of 200 kHz which motivates our choice of using 200 kHz bandwidth sub-channels. We summarize in Table 5.6 the number of 200 kHz channels, over the 4 MHz recorded bandwidth, corresponding to each wireless technology that can be detected with our methodology. Note

that we cannot differentiate the IEEE 802.11 standard use by a Wi-Fi signal with our methodology.

Technology detected	Number of 200 kHz channels
Wi-Fi	20
BLE	10
BT	5
LoRa	1 / 2 / 4 / 8

TABLE 5.6: Technology identification according to the number of occupied channels.

According to Equation 5.5, one sample of energy is measured every 0.25 μs. We choose to compute the FFT on 1000 samples, which results in a time granularity of 250 μs. This is an arbitrary value, chosen after several tests, we estimate to be sufficient to have a fine time granularity to correctly see the variations of the observed BW.

$$\text{Period (in s)} = \frac{1}{\text{bandwidth (in Hz)}} \tag{5.4}$$

$$= \frac{1}{4 \times 10^6} = 0.25\ \mu\text{s} \tag{5.5}$$

One of the main challenges of the proposed methodology is to compute the threshold value. To this end, we worked on two captures: one with no signal in it, and one with only the BT beacon. The choice of the capture containing the signal is arbitrary meaning that we could have used a capture with Wi-Fi signal. After applying the FFT on the recorded channel, we plot its energy distribution. We observed two lobes in the energy distribution whether or not there is a signal in the capture analyzed. The difference between a capture with no signal and one with a signal is the amplitude of the lobes. For example, in a capture of a Wi-Fi signal, we observe a higher amplitude for the second lobe, while in a capture with no signal the two lobes have approximately the same amplitude. We make the assumption that the first lobe could be a Gaussian noise. Thus, we decide to compute the threshold with a higher value than the first lobe. In the capture with no signal, we notice that between the 10% of the smallest energy values and the 99.5% of the smallest energy values, there is a factor of 2. We estimate that this is a reasonable assumption to consider that 10% of the smallest energy values are noise. So, we compute the threshold as the 10% of the smallest energy values multiplied by two.

Next, we apply the proposed methodology to two different captured files of one minute each.

5.8.2 Validation of signal identification

We present here two results: the detection of a Bluetooth signal (see Figure 5.17) and the detection of a Wi-Fi signal (see Figure 5.18). These figures represent the output of our methodology (the heatmap which is the gradient matrix with energy levels), where each line represents 250 μs and each rectangle represents 200 kHz. The line number represents the x-th

interval of time of 250 μs since the beginning of the capture. For instance, the line **50000** is the interval of time between 12.5 s and 12.5 s + 250 μs after the beginning of the capture.

In Figure 5.17, we observe that lines **50888** and **50889** have a sample energy at least three times above the threshold value. Six consecutive rectangles are detected as a signal. This means a signal of about 1200 kHz bandwidth was detected. Since Bluetooth uses 1 MHz of bandwidth, we can associate this signal to the Bluetooth technology. Note that our methodology does not give exact results: for the BT signal the bandwidth colored, and highlighted with a blue ellipse, in the figure is slightly wider than the real signal. Also, we almost always have the two center channels colored in brown. This comes from the USRP: a constant energy is present at the listening frequency which is not a permanent signal but rather an electromagnetic noise generated by the USRP itself.

FIGURE 5.17: Heatmap of a Bluetooth signal centered at 2402 MHz.

Figure 5.17 corresponds to the record of a Bluetooth advertisement on channel 37 centered at 2402 MHz. Bluetooth periodically advertises on three channels (37, 38, and 39). The interval between two consecutive advertisements varies from 20 ms to 10 s. After each advertisement, a random delay (between 0 and 10 ms) is added to avoid collision on the medium. Thus, thanks to our methodology, we are able to detect a Bluetooth signal and its periodicity.

In our second example, we apply our characterization methodology to the recording of a Wi-Fi signal using channel 11 centered at 2462 MHz. Usually, a Wi-Fi access point sends a beacon every 100 ms. The duration of a beacon depends on the IEEE 802.11 standard used to transmit.

In Figure 5.18, we observe that lines **54297**, **54303**, **54321** and **54324** have all the rectangles colored. This means that there is a signal using at least 4 MHz of bandwidth. As the other main wireless technologies using the 2.4 GHz ISM band have narrower bandwidths, we can associate these four wide signals to Wi-Fi. We make the assumption that lines, where most rectangles are filled with color, are also Wi-Fi signals, e.g., line **54318**. The observed empty rectangles are probably a result of how we compute the threshold value. We also recall that a Wi-Fi spectrum is not uniform on a given bandwidth. This can explain some of the empty rectangles as well.

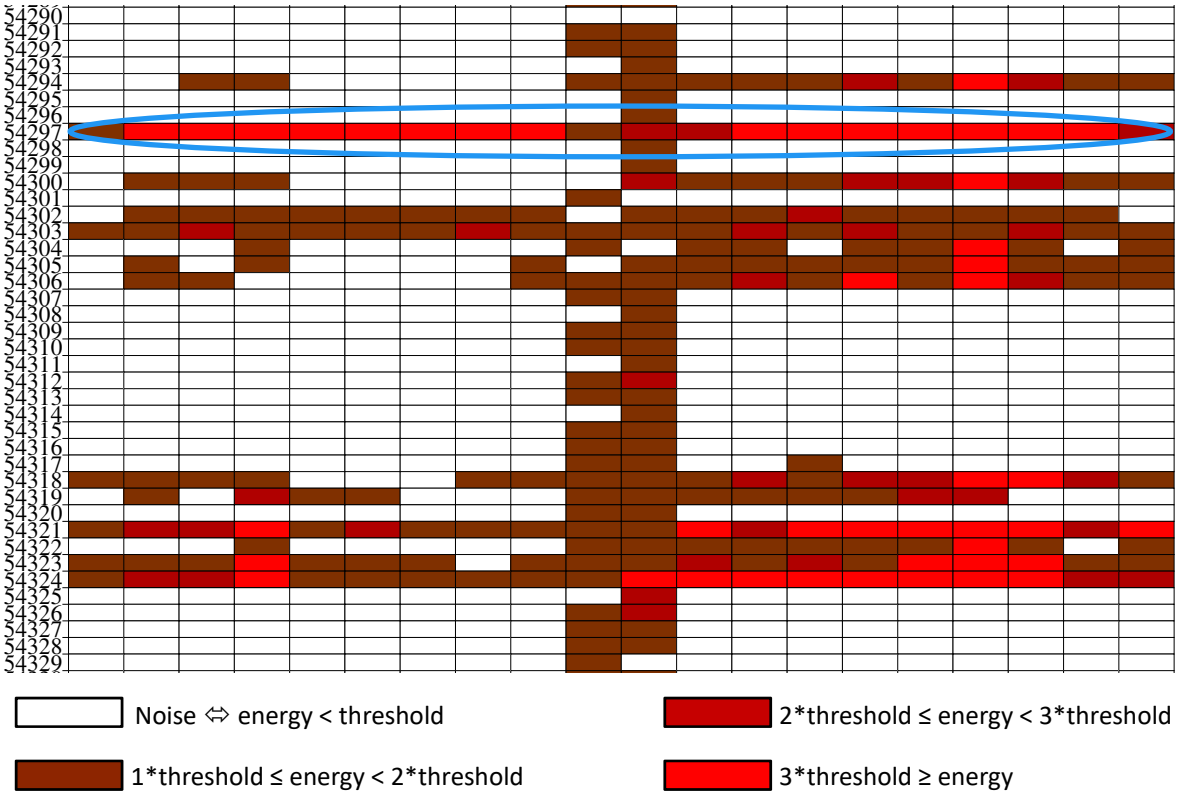

FIGURE 5.18: Heatmap of a Wi-Fi signal centered at 2462 MHz.

The main challenge in this type of work, i.e., identifying a wireless technology only based on its signal footprint, is to distinguish between the noise and the signal. We considered a threshold to differentiate between them, but it impacts the resulting energy heatmap after applying the FFT on each recorded sample. Plus, the energy of a signal is not constant over time, so it might happen that in some cases, we have an energy higher than the threshold on one sub-channel and not on the adjacent sub-channel, making the signal mapping impossible because of insufficient information. Also, since the LoRa signal can be decoded under the noise level, more work is needed to have a good signal identification in this case.

However, going back to our motivation for this work (the study of the use of the 2.4 GHz ISM band), the proposed methodology gives us a fundamental building block to investigate the coexistence between LoRa and the other wireless technologies. We can now gather important information for studying interference detection and propose mitigation schemes.

5.8.3 Gateway channel selection protocol

We highlighted in Section 5.3 that to implement our frequency hopping strategies on real hardware, we needed to design a protocol to choose the channels on which to perform the frequency hopping and to communicate them to all the users of the network. In LoRa networks end-devices cannot directly communicate with each other. As each LoRa end-device is directly connected to a gateway, downlink communication, i.e., from the gateway to the end-device can be broadcast to the entire network. For instance, a firmware update will be

broadcast to all the end-devices of the network, while an ACK will be sent only to the end-device requiring confirmed traffic. Hence, the selection protocol has to be implemented at the gateway side. Figure 5.19 summarizes our proposition of channel selection by the LoRa gateway and communication to the end-devices.

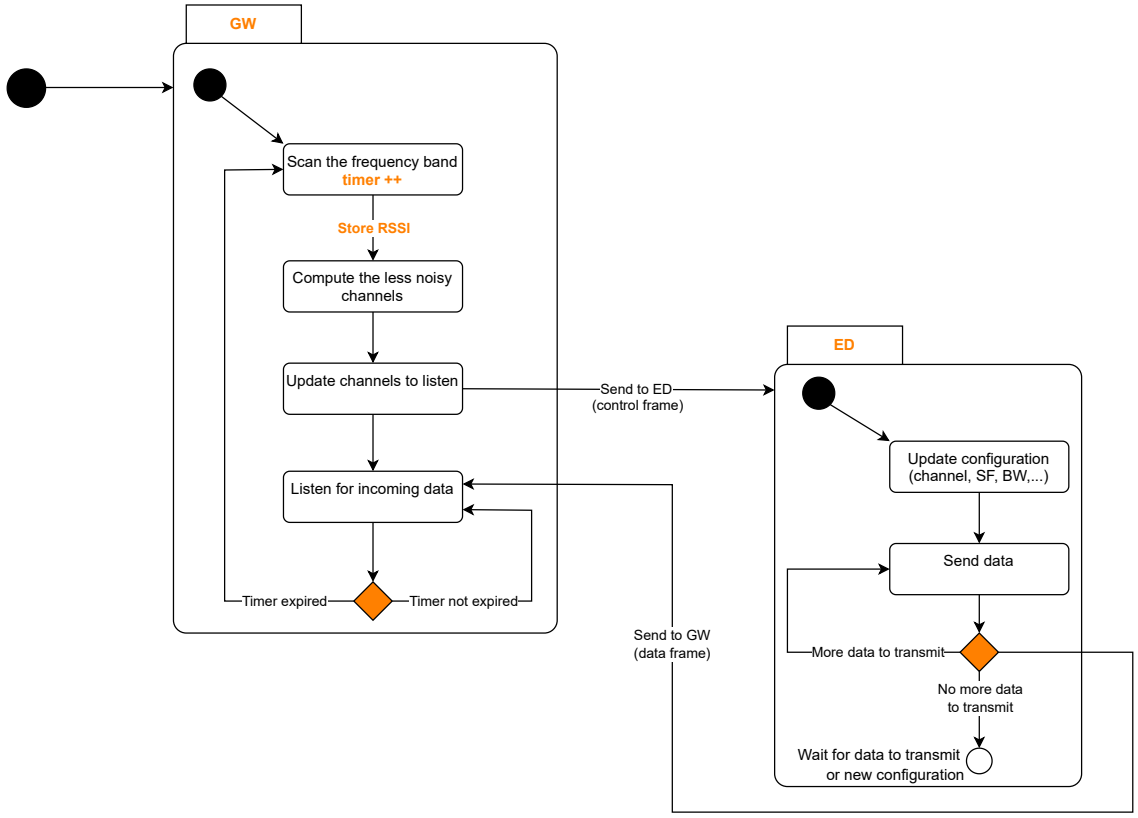

FIGURE 5.19: LoRa gateway channel selection protocol, and communication to end-device.

The application of frequency hopping strategy on LoRa hardware is divided into two parts: (1) the gateway part, which is in charge of the selection of the channels to use for the frequency hopping, and to communicate them to the end-devices, and (2) the end-device part, which is in charge of updating the channels allowed to send frames.

The gateway starts by scanning the 2.4 GHz ISM band. As the gateway is plugged into the electrical network, the energy consumption of such an operation is not an issue. The scan of the frequency band is a periodical operation, thus at the beginning of each scanning procedure a timer is triggered. For each sensed channel, the RSSI is stored in a file, i.e., one RSSI value per frequency scanned. According to the RSSI values, the gateway can extract the less noisy channels. The permitted channels are stored in a list and sent to the end-devices of the network. Note that even if the allowed channels list does not change between two scanning procedures, the list is still sent to the network. It allows for to prevent from potential failures, e.g., end-devices dead battery, non-reception of the channels list.

Remember that current gateways can only receive three parallel configurations. With the

proposed protocol, and to guarantee communication with all network end-devices, a common channel has to be set for all nodes joining a network. In this way, frequency hopping will be possible on two channels rather than three. The remaining channel will be used by the gateway to scan the frequency band and to send the allowed channel list to the end-devices. It is expected that in the future LoRa 2.4 GHz gateways will have more reception paths thus permitting the implementation of our proposition of FH on three channels. In LoRaWAN sub-GHz (EU868 regions specific constraints) a common join channel is used for all the join requests and responses. It is likely that our channel selection protocol will be implemented in the future LoRaWAN protocol dedicated to the 2.4 GHz ISM band. Hence, likewise LoRaWAN for the sub-GHz bands, the information on the channels to be used for frequency hopping could be transmitted jointly with the ACK or ADR commands either in a Data Downlink message or a Join Accept message.

We design the gateway channel selection protocol according to our coexistence experiments operation. Indeed, in our experiments, the gateway sends a message to the end-device which allows the end-device to start sending frames. The downlink message contains the configuration, i.e., channel, SF, BW, on which the gateway is listening. This allows the end-device to adapt its own configuration to be able to communicate with the gateway. Our gateway selection protocol adds in the downlink message the list of the allowed channels on which the end-devices can transmit.

After receiving the update from the gateway, the end-device refreshes its configuration. Then the end-device starts sending frames following the frequency hopping strategy implemented. Each end-device has a number of frames to send per configuration evaluated. Once the end-device has sent all the frames in the queue, it sends a message to the gateway to inform that it has no more frames to transmit. When the timer triggered at the beginning of the scanning procedure expires, the gateway starts over the operation. Otherwise, the network is on standby waiting for the timer to expire or for end-devices to transmit data. Note that the end-device process described here is specific to our coexistence experiments implementation where each end-device has an amount of frames to transmit before switching to another configuration and/or channel. We can adapt the end-device operation to more common LoRa applications, where traffic is generally sporadic. In this case, the end-device part of the protocol will change. The end-device will still update the list of channels allowed to transmit according to the gateway downlink message. It will also update its SF depending on the ADR command. Then, each frame sent from the end-device to the gateway contains information on whether or not the end-device still has data to transmit.

The refreshment of the channels to use for the frequency hopping depends on the application. For instance, an application such as the temperature of a building does not need a high quality of service (QoS) and neither frequent updates. So, the timer could have a value such that the channel selection happens twice a day.

In the same manner, the time during which each channel is sensed must be correctly dimensioned. The value has to be large enough to be able to detect if a channel is busy or

not. A channel is considered busy if the average RSSI over the channel sense period is poor. We assume that a poor RSSI corresponds to the presence of a signal in the channel. On the contrary, a channel is considered idle if the average RSSI over the channel sense period is good. The threshold to define whether a channel is idle or busy can be set according to our methodology for signal association (see Subsection 5.8.1). Additionally, the sensing period has to be set to avoid as much as possible false negatives (false positives respectively). A false negative corresponds to a channel labeled "busy" when it is not. A false positive is an opposite situation: a channel is labeled "idle" when it is not. These two mistakes may happen when the amount of time for the scan is not sufficient. For example, if the sensing procedure is not long enough, the gateway may detect a signal on a given channel and thus store a poor RSSI value. Thus, the channel will not be used for frequency hopping. But in reality, the signal detected may be the end of a transmission, and so with a longer listening time the channel would have been classified as "idle". Similarly, the gateway may listen too briefly to each channel and miss the start of a transmission, thus considering a channel "idle" instead of "busy". This can lead to the use of noisy channels for LoRa frequency hopping and result in losses rather than FDR improvement.

5.9 Conclusions

In this chapter, we designed a simulator to evaluate several frequency hopping approaches in an effort to improve the coexistence of LoRa and Wi-Fi in the 2.4 GHz ISM band. Gathering all the conclusions from our results analysis provides an answer to the remaining research question "Is frequency hopping a good option to improve LoRa and Wi-Fi coexistence in the 2.4 GHz ISM band?" (**RQ5-4**). We summarized at the end of this section, the research questions we raised around the improvement of using FH in a coexistence scenario, which we have answered throughout this chapter.

Our main contribution in this chapter is the design of an algorithm to improve the coexistence of LoRa 2.4 GHz and Wi-Fi (**RQ5-1**). We propose an original methodology and an implementation on the LoRa gateway to select the less noisy channels to use for frequency hopping. Our motivation was two-fold: (1) confirming that the LoRa channels proposed by Semtech were a viable solution for a fair coexistence between LoRa and Wi-Fi in the 2.4 GHz ISM band, and (2) quantifying the gain of using a frequency hopping strategy more complex than the one proposed in the LoRa 2.4 GHz stack.

We demonstrate that depending on the targeted application, implementing the best channels FH strategy is not recommended (**RQ5-2**). In fact, for a temperature measurement application in a building, a reception rate of 75% seems to be sufficient. On the other hand, for an application requiring a higher QoS, the best channels FH strategy will be preferred. Note that in our simulator, the protocol overhead and the energy consumption of such frequency hopping strategies are not represented. It should also be noted that in a real-world implementation, Wi-Fi APs would use CSMA/CA and MCS mechanisms to deliver the best data rate depending on the environment (interference, noise). Using the best channels FH

strategy could therefore have a greater impact on Wi-Fi link quality. Indeed, to ensure a good link quality, Wi-Fi APs would decrease their data rates under heavy LoRa interference resulting in a degraded user experience. Generally speaking, the best channels FH strategy is highly recommended for LoRa, since in an indoor environment there is rarely only one Wi-Fi AP, and in the case of multiple Wi-Fi APs, there are several APs per channel.

We conclude that despite using a frequency hopping strategy for LoRa transmissions allows to improve the coexistence in terms of FDR when there are Wi-Fi overlapping transmissions, the number of Wi-Fi APs can drastically decrease the LoRa FDR. Indeed, the LoRa FDR can be as low as in our coexistence experiments where frequency hopping techniques are not used (**RQ5-3**).

This chapter concludes our scientific contributions. In the next chapter, we emphasize some general outcomes and present future work perspectives that close this manuscript.

RQ answered:

- **RQ5-1**: How to design a simulator that can model real-world coexistence experiments? → Section 5.4
- **RQ5-2**: Is there a frequency hopping strategy that gives better results than the frequency hopping proposed in the actual LoRa 2.4 GHz stack? → Ssection 5.6 and Subsection 5.7.3
- **RQ5-3**: Is there a frequency hopping strategy that provides a Wi-Fi FDR, when interfered by LoRa transmissions, that is at least as good as when interfered by other wireless technologies (e.g., BT, IEEE 802.15.4)? → Subsection 5.7.3
- **RQ5-4**: Is frequency hopping a good option to improve LoRa and Wi-Fi coexistence in the 2.4 GHz ISM band? → Sections 5.6 and 5.7

Chapter 6

Conclusion

In this chapter, we conclude this manuscript by summarising our contributions and providing future work perspectives.

6.1 Conclusions

The main research goal of this work was to study the feasibility of a LoRa network in the 2.4 GHz ISM band. More precisely, to analyze the performance in terms of connectivity and communication range as well as identify the opportunities and the challenges brought by this new version of the LoRa technology.

In Chapter 2 we made a detailed presentation of LoRa and Wi-Fi that would set up the technical background for the rest of the manuscript. We emphasized the worldwide available set of frequencies and the common regional parameters of the 2.4 GHz ISM band. We also underlined that this frequency band is overcrowded and we proposed a comparison of the main wireless technologies using the 2.4 GHz ISM band in terms of number of channels, bandwidth, and power transmission. Finally, we presented the general characteristics of the LoRa technology and a LoRaWAN network, before introducing the new version of LoRa dedicated to the 2.4 GHz ISM band.

The next three chapters constitute the scientific contributions of this thesis. In Chapter 3, we did several experiments to investigate the performance of LoRa in the 2.4 GHz ISM band. We focused on the connectivity and the communication range achieved by LoRa in indoor and outdoor environments. We exhaustively evaluate the impact of each possible LoRa configuration by varying three parameters: the spreading factor, the bandwidth, and the coding rate. We did a comparison of the LoRa frame delivery ratio depending on the frequency band used to transmit (868 MHz and 2.4 GHz in our case). We ended our experiments by analyzing the impact of daily life activities, i.e., presence of people in the building and the wireless usage, on LoRa 2.4 GHz FDR. We demonstrated that despite a shorter communication range in the 2.4 GHz ISM band, LoRa is able to cover a two-floor building with one gateway and also reach a distance up to 2 km, using the greatest communication range configuration, in an outdoor environment under line-of-sight conditions. Moreover,

our results show that activities inside a building (people mobility and wireless communications) degrade the LoRa connectivity and thus have to be taken into account in future LoRa deployments.

In Chapter 4 we focused on the coexistence of LoRa in the 2.4 GHz ISM band. We proposed a methodology to experimentally study the mutual impact of two wireless technologies in an indoor scenario using the same frequency band. We then applied it on LoRa and Wi-Fi in the 2.4 GHz ISM band. This permitted us to provide some guidelines for future LoRa 2.4 GHz indoor deployment without implementing any interference mitigation mechanisms. Among others, we highlighted that: (1) the LoRa configuration has to be chosen depending on the targeted applications (data rate versus reliability), (2) the Wi-Fi FDR can suffer from enormous losses depending on the modulation of the IEEE 802.11 standard used, and (3) the deployment of LoRa end-devices need to take into account the location of Wi-Fi APs to have the lowest level of interference between LoRa and Wi-Fi overlapping transmissions.

Finally, in Chapter 5, we presented an approach to improve the coexistence between LoRa and Wi-Fi. We extracted a theoretical model of interference from our experiment results and implemented it in a homemade Python simulator. We then evaluated three frequency hopping strategies: two baseline strategies using the three LoRa channels proposed by Semtech, and a novel proposition to select the three best channels of the 2.4 GHz ISM band which corresponds to the less noisy channels. We also proposed an original methodology to sense a frequency band on a representative bandwidth and then associate a signal to a known wireless technology. We validated our approach by applying it to two recorded signals: BT and Wi-Fi. Our methodology could be used for channel characterization to select the channels of our best channels FH strategy. We also designed the corresponding protocol of sensing and selecting channels that would be executed by the LoRa gateway. Our results emphasize that the FH strategy to implement depends on the targeted application and the number of Wi-Fi APs overlapping with LoRa channels.

For the most part, we followed the principles of openness and reproducibility in our contributions. We also applied these principles to the SoA of this manuscript. We gave a general description of our methodology in the introduction of this manuscript (see Subsection 1.3.2) and we detailed the entire systematic literature review process we applied in Appendix A. Since our work is mostly based on experiments, we faced several difficulties, which are enumerated in Appendix D. The results of our experiment are extremely dependent on the location where we run them. Consequently, providing the LoRa official gateway and end-device public code along with a detailed methodology (equipment references, modus operandi, etc.) and experiment data allows the industrial and scientific community to reuse our work to evaluate other types of environments, metrics, or parameters. This way, a fair comparison between results is possible and forms a common basis of observations for future LoRa deployment in the 2.4 GHz ISM band.

6.2 Perspectives

The work presented in this manuscript constitutes a first milestone in understanding LoRa operation in the 2.4 GHz ISM band. In Subsection 1.1.3 we identify some challenges that need to be investigated before deploying LoRa networks in the 2.4 GHz ISM band. In the following, we discuss future research directions that arise from the contributions of this manuscript.

6.2.1 Around channel characterization

In Subsection 5.8.1, we proposed a methodology to identify a wireless technology only based on its signal footprint. We highlighted the difficulty of choosing a good threshold value to distinguish between the noise and the signal, particularly because the energy of a signal is not constant over time. Mapping a signal to LoRa could be even more complicated as LoRa can decode signals under the noise level.

Future work will include fine-tuning of the threshold value, the automation of the technology identification process, and an improvement to our methodology to allow the detection of concurrent transmissions with signals from different wireless technologies. We also consider using our methodology as a tool that we can combine with interference mitigation mechanisms.

6.2.2 Around LoRa 2.4 GHz indoor connectivity and applications

We dedicated Chapter 3 to the study of the LoRa connectivity and communication range in indoor and outdoor scenarios. As the communication range is decreased when LoRa uses the 2.4 GHz ISM band instead of sub-GHz bands, and the main wireless technologies of the 2.4 GHz ISM band are designed for short-range indoor applications, we propose some leads to explore in an indoor environment.

Short-term future work includes enhancing our indoor experiments by changing more parameters:

- **Environment change:** One application of LoRa in the sub-GHz bands is smart metering, we thus need to evaluate deep indoor environments for LoRa in the 2.4 GHz ISM band. We can also evaluate industrial environments where steel structures are present and will probably affect LoRa transmissions.
- **Gateway coverage:** We demonstrate that in our scenario one LoRa gateway covers a two-floor building with a high frame delivery ratio for the greatest communication range configuration, which is also the more robust LoRa configuration. To allow higher data rate, or a trade-off between data rate and robustness depending on the targeted application, it would be useful to evaluate a multi-gateways deployment.

In addition, we underline another possible research direction around LoRa in the 2.4 GHz ISM band: hardware improvement, especially the gateway evolution. At the time of this

manuscript writing, LoRa 2.4 GHz gateways can receive only three different configurations in parallel. The sub-GHz LoRa gateways allow to receive either 8, 16 (and even 64) configurations at the same time. Thus, we can reasonably assume that a new version of LoRa 2.4 GHz gateways will authorize at least the reception of 8 different configurations simultaneously as there are 8 different SF in LoRa 2.4 GHz (from 5 to 12).

6.2.3 Around LoRa coexistence in the 2.4 GHz ISM band

In this manuscript, we particularly focused on the main challenge raised by the deployment of LoRa in the 2.4 GHz ISM band: the coexistence with other wireless technologies using the same frequency band.

In Chapter 4, we presented the results of a worst case topology coexistence between LoRa and Wi-Fi in the 2.4 GHz ISM band. Nevertheless, there are several extensions that would be interesting to investigate to have more insights on the coexistence of LoRa in this frequency band.

First of all, we evaluated two IEEE 802.11 standards along with one data rate and one modulation per standard. It could be interesting to study the latest widely distributed IEEE 802.11 standard: IEEE 802.11ax. The modulation in IEEE 802.11ax is similar as in IEEE 802.11g but the IEEE 802.11ax standard allows higher data rates and various bandwidths. A coexistence study between LoRa and IEEE 802.11ax would give useful insights on a potential LoRa network deployment as the IEEE 802.11ax standard is currently deployed. This study implies having a library similar to `Scapy` allowing to choose the IEEE 802.11 standard to generate the IEEE 802.11ax traffic. The objective of repeating our coexistence experiments and testing other IEEE 802.11 standards is to study the impact that different traffic loads have on the performance of LoRa in the 2.4 GHz ISM band. Also, we highlighted an unexpected behavior in the study of LoRa and IEEE 802.11b concurrent transmissions. More investigations are needed to understand what happens when the two technologies interfering with each other use the same modulation, spread spectrum in this case. We plan to start preliminary work on this point by generating a Dirac with a signal generator to check if the results of the study between LoRa and IEEE 802.11b could come from spectrum aliasing.

Another interesting study to conduct would be to repeat the same coexistence performance evaluation, this time implementing the Wi-Fi MAC layer. Indeed, Wi-Fi implements mechanisms such as the MCS, backoff timer, and acknowledgements, to increase the robustness against interference. In our study, we decided to implement only the PHY layer of Wi-Fi because LoRa has no standardized MAC layer in the 2.4 GHz ISM band yet, allowing a coexistence study in the same conditions for both technologies. We expect the Wi-Fi results to be better by implementing the MAC layer mechanisms as the MCS will decrease the data rate, if necessary, to ensure the connectivity of the transmission link. The acknowledgement mechanism also certifies that the transmitted frames are well received, by retransmitting the frames if necessary.

Finally, the methodology presented to study the coexistence of two wireless technologies in the same frequency band could be applied to evaluate the coexistence of LoRa with other wireless technologies operating in the 2.4 GHz ISM band, such as Bluetooth and BLE. Indeed, BT is the second most used technology in the 2.4 GHz ISM band. We use it to connect headphones, computer mouse, wireless keyboard, etc. We carried out a quick performance evaluation of LoRa and BT by supervising three Erasmus interns [182]. Preliminary results tend to confirm our intuition: as long as LoRa is not transmitting on the advertising channels of BT, there is no impact on the frame delivery ratio when there are concurrent transmissions. We make the assumption that the FH scheme implemented by BT makes the technology robust to interference. In addition, BT changes its frequency channel every 625 μs which results in a very short period for potential concurrent transmissions with LoRa 2.4 GHz. Still, we need to further investigate the coexistence of LoRa and BT in the 2.4 GHz ISM band to validate our first observations. We also want to apply our coexistence methodology to explore the coexistence of LoRa 2.4 GHz and IEEE 802.15.4 as the latter is a widely used standard, especially for industrial actuators networks.

6.2.4 Around frequency hopping in LoRa 2.4 GHz

In Chapter 5 we proposed several approaches to improve the coexistence of LoRa and Wi-Fi in the 2.4 GHz ISM band. We decided to evaluate through simulations the gain of implementing frequency hopping strategies for LoRa transmissions.

We based our simulations on our experiment results. Remember that in our coexistence study, we were in an apartment surrounded by Wi-Fi APs that we could not control. Additionally, we consider that Wi-Fi APs do not interfere with each other. Finally, we evaluated only one Wi-Fi AP on a fixed channel. For all these reasons, future work is to repeat the coexistence experiment in a controlled environment and then add several Wi-Fi APs to investigate the interference impact on LoRa performance. Furthermore, in our simulations, we consider only Wi-Fi APs deployed on non-overlapping channels. It is important to assess the impact on LoRa performance when the LoRa channel is located at the intersection of two independent Wi-Fi channels. In the same way, evaluating how LoRa reacts to interference from several Wi-Fi APs located on the same channel, e.g., three APs using the Wi-Fi channel 1, is crucial to better modeled real-world Wi-Fi deployment. The experiment results could then be implemented in our simulator to study the scalability of our approach. We believe that our simulator will scale easily for this new scenario with several APs using overlapping channels.

During the validation of our simulator we saw that for some LoRa configurations, the simulator gives optimistic results compared to experimentation. We assume that this comes from the fact that in our simulator we do not implement signal propagation degradation due to walls, doors, and external interference. Thus, an improvement of our simulator is to implement signal propagation models. Another interesting change in the simulator is to vary the LoRa and Wi-Fi configurations to study different data rates, periods of concurrent transmissions, and IEEE 802.11 standards.

Finally, improving the coexistence of LoRa with other wireless technologies in the 2.4 GHz ISM band raises multiple research opportunities, such as using cognitive radios and developing a new MAC protocol. In the future, a focus on energy efficiency will be needed to comply with the IoT requirements.

Appendix A

SLR process

In this appendix, we provide the general SLR process used in the different SoA of this manuscript. We also detail the varying criteria we applied depending on the chapter of contributions it refers to.

A.1 General step of our SLR process

First, we searched within five online databases (namely, IEEE Xplore [1], ACM Digital Library [2], Springer Link [3], Wiley Online Library [4], and ScienceDirect [5]) articles corresponding to the combination of the words that summarize the best our focus of interest, e.g., "LoRa" and "interference". We also added papers manually that correspond to Google Scholar [6] alerts containing the words "LoRaWAN", "LoRaWAN sub-GHz", "IoT LoRaWAN", "LoRa 2.4" or "interference 2.4". These alerts were defined to keep abreast of recent papers published on these subjects. We define two mandatory inclusion criteria to select the potential papers of our state of the art:

- Studies in the English language,
- Studies that are peer-reviewed (i.e., no application notes, white papers, or papers from arXiv).

This gives us a certain number of papers but with a possibility of having duplicated papers. Indeed, the different databases that we interrogated to retrieve papers can reference the same papers depending on the journals or the conferences where articles are published. We evaluated only one occurrence of each paper by removing the duplicates.

After that, we manually evaluated each article based on the title and the abstract. The exclusion step aims to remove papers that are not exactly in the scope of our topic. The mandatory exclusion criterion was to eliminate all the studies published before 2012. This corresponds

[1] https://ieeexplore.ieee.org/Xplore/home.jsp
[2] https://dl.acm.org/
[3] https://link.springer.com/
[4] https://onlinelibrary.wiley.com/
[5] https://www.sciencedirect.com/
[6] https://scholar.google.com/

to the year in which Cycleo (creator of LoRa technology) was acquired by Semtech (current owner of the technology).

Then, we classified the articles depending on the rank of the conference or the journal where the study was published according to CORE [183] and Scimago [184]. We kept the works published in A+, A, and B conferences, as well as Q1 and Q2 journals. Finally, we synthesized each SLR process in a table to highlight the methodology used to investigate the focus of our contributions. The resulting tables of our different SoA are presented in the corresponding chapter.

To summarize, we apply the same SLR process for the different SoA of this manuscript. We start with common inclusion and exclusion criteria for all our topics of interest. We then add criteria depending on the focus of the contribution studied. We only modify the keywords used to search papers in the online databases mentioned earlier.

A.2 LoRa performance: SLR process criteria

- **Searched keywords:** "LoRa", "LoRaWAN" or "LoRa 2.4 GHz" with "performance" or "coverage",
- **Additional inclusion criteria:**
  - Studies that propose techniques to evaluate performance, e.g., delivery ratio, coverage,
  - Studies that focus on indoor or outdoor applications,
  - Studies that make the comparison of LoRa with, at least, another IoT technology,
  - Studies that focus on the performance of LoRa in terms of connectivity or communication range.
- **Number of papers including the duplicated entries:** 239 papers,
- **Number of papers after removing the duplicated entries:** 208 papers,
- **Additional exclusion criteria:**
  - Studies that target small/specific networks such as wireless body area networks (WBANs), as the main characteristic of LoRa is long-range communications and so aims to cover at least a home (WPANs), and more often a bigger area (WLANs),
  - Studies that propose to improve performance by combining LoRa with another technology such as cellular networks, as we aim to evaluate the connectivity and the communication range of LoRa to assess the possibility of deploying LoRa in the 2.4 GHz ISM band,
  - Studies that evaluate critical environments, e.g., snow, ice,

  - Studies that were not about LoRa; the keywords searched in databases may return articles containing only one of the requested keywords.

- **Number of paper after the exclusion step:** 88 papers,
- **Number of paper after rank classification:** 44 papers.

A.3 Wireless technologies coexistence: SLR process criteria

- **Searched keywords:** "LoRa" or "2.4 GHz" with "interference" or "coexistence",
- **Additional inclusion criteria:**
  - Studies that propose techniques to characterize the coexistence/interference between at least two technologies,
  - Studies that focus on LoRa coexistence/interference regardless of the frequency band,
  - Studies that focus on the coexistence/interference of wireless technologies regardless of the frequency band.
- **Number of papers including the duplicated entries:** 274 papers,
- **Number of papers after removing the duplicated entries:** 221 papers,
- **Additional exclusion criteria:**
  - Studies about improving the coexistence or mitigating interference, as we focus on the link quality in terms of frame delivery ratio with overlapping transmissions,
  - Studies that compared a licensed technology with an unlicensed technology, e.g., LTE and Wi-Fi, because regulations are not the same and so the methodology to conjointly evaluate this type of coexistence differs from when both technologies are using the same frequency band,
  - Studies targeting small/specific networks (e.g., WBANs), as we focus on WPANs and WLANs indoor applications that are already supported by Wi-Fi,
  - Studies focusing on designing hardware,
  - Studies that were not about coexistence or interference; the keywords searched in databases may return articles containing only one of the requested keywords.
- **Number of paper after the exclusion step:** 93 papers,
- **Number of paper after rank classification:** 33 papers.

A.4 Improving coexistence: SLR process criteria

- **Searched keywords:** "interference mitigation" with "channel hopping", "LoRa" or "2.4 GHz",
- **Additional inclusion criteria:**
  - Studies that propose techniques to improve the coexistence of LoRa with other wireless technologies in the same frequency band regardless of the interference mitigation mechanism implemented,
  - Studies that evaluate the gain of implementing frequency hopping regardless of the performance metric evaluated,
  - Studies that propose techniques to improve the coexistence between two wireless technologies regardless of the performance metric evaluated.
- **Number of papers including the duplicated entries:** 218 papers,
- **Number of papers after removing the duplicated entries:** 203 papers,
- **Additional exclusion criteria:**
  - Studies that propose techniques to detect interference or evaluate the impact of interference on performance, as this was the focus of our work in Chapter 4,
  - Studies that propose to improve coexistence but without implementing any mechanisms, e.g., modifying the hardware to increase receiver sensitivity, or adapting the transmission parameters to add robustness to interference,
  - Studies that target specific networks (e.g., WBANs), as we focus on WPANs and WLANs indoor applications that are already supported by Wi-Fi,
  - Studies that target licensed networks (e.g., cellular networks), as the resource allocation is not the same in licensed and unlicensed frequency bands,
  - Studies that focus on cognitive radio approaches, as our study aims to improve the performance of LoRa and Wi-Fi when there are overlapping transmissions, which is not the mode of operation of cognitive radios,
  - Studies that propose to improve LoRa performance but not in a coexistence scenario, e.g., intra-technology interference.
- **Number of paper after the exclusion step:** 59 papers,
- **Number of paper after rank classification:** 35 papers.

Appendix B

Estimation of the maximum communication range of LoRa

In this appendix, we provide some reminders on signal propagation, and detail the computation of the theoretical LoRa maximum communication range, based on preliminary outdoor experimental results. We used this estimation to chose the location of our outdoor experiments in Chapter 3.

B.1 Reminder

During a transmission, the signal is submitted to the environment. Phenomenons like people between the transmitter and the receiver, walls, doors, or other transmissions from the same technology or from another wireless technology can interfere with our transmission. Thus the SNR gives insight on the noise level, i.e., the power of all the interference. Also, as we transmit in a real-world environment, the signal suffers from losses due to the distance to cover.

B.1.1 Power signal formulas

SNR conversion

$$\text{SNR}_W = \frac{P_s}{P_n}$$

$$\begin{aligned}\text{SNR}_{dB} &= 10 * log_{10}(\frac{P_s}{P_n}) \\ &= 10 * log_{10}(P_s) - 10 * log_{10}(P_n)\end{aligned}$$

where:

SNR_W = SNR in Watt

P_s = signal power in Watt

P_n = noise power in Watt

SNR_{dB} = SNR in dB

Noise Power

$P_{n(dB)} = -174 + 10 * log(BW) + NF$

where:

$P_{n(dB)}$ = noise power in dB

BW = bandwidth in Hz

NF = noise figure in dB

The noise figure for LoRa devices is usually between 5 and 7 dB.

The noise power is proportional to the bandwidth.
Multiplying by a factor of 2 in the logarithm scale is equal to adding 3 in the dB scale.
Dividing by a factor of 2 in the logarithm scale is equal to subtracting 3 in the dB scale.

B.1.2 Receiver sensitivity

The receiver sensitivity for a couple SF/BW is given by the datasheet of LoRa end-devices [9]. With the receiver sensitivity, it is possible to compute the SNR. We summarize the value of SF12 for different BW in Table B.1.

$SNR = sensitivity - P_{n(dB)}$ where $NF = 5$ dB in $P_{n(dB)}$

SF	BW (in kHz)	Sensitivity (in dBm)	SNR (in dB)
12	203	-130	-14
	406	-128	-15
	812	-126	-16
	1625	-120	-13

TABLE B.1: Sensitivity and SNR for SF12 and various BWs.

When the BW increases, the noise becomes stronger. To guarantee the same SNR, the receiver sensitivity is decreased.

LoRa has the particularity to be able to correctly demodulate a signal received under the noise floor. This means that even for a negative SNR value, depending on the configuration used to transmit, the connectivity can be maintained.

For SF12, the SNR limit value to demodulate a signal is -20 dB [33]. For other SF, the SNR limit value is decreased by 2.5 dB per SF (see Table B.2) .

SF	LoRa demodulator SNR (in dB)
12	-20
11	-17.5
10	-15
9	-12.5
8	-10
7	-7.5
6	-5
5	-2.5

TABLE B.2: SNR limit value to correctly demodulate a LoRa signal depending on the SF.

B.1.3 Impact of the distance on the signal power

In free space:
When the radio signal travels by a distance d, the signal power is P dB.
When the radio signal travels by a distance $d * \sqrt{2}$, the signal power is $(P - 3)$ dB.
When the radio signal travels by a distance $d * 2$, the signal power is $(P - 6)$ dB.

What is the signal power for a distance of 2 km?

At 1.4 km, the signal power is P dB. Compute the signal power at $d = 2$ km.
$ratio = \frac{\text{signal power to compute}}{\text{signal power of a known distance}} = \frac{2}{1.4} = 1.4$
A distance of 2 km is equals to $1.4 * \sqrt{2}$.
At 2 km, from the free space statements, the signal power is $P - 3$ dB.

B.2 Applying on our experimental performance evaluation scenario

In our case, and to choose the location to perform our outdoor experiment, we need to evaluate the maximum communication range of the most robust LoRa configuration we want to use.

B.2.1 Compute SF12 maximum operating distance

From our preliminary outdoor experiment, we observe a SNR above -5 dB at 700 m, using SF12, and BW = 203 kHz to transmit. According to the free space statements:

- At $d = 2 * 700 = 1.4$ km, $SNR = -11$ dB.
- At $d = 2 * 2 * 700 = 2.8$ km, $SNR = -17$ dB which is higher than the SF12 SNR limit value for demodulating a signal.
- At $d = \sqrt{2} * 2 * 2 * 700 = 3.9$ km, $SNR = -20$ dB which is equal to the SF12 SNR limit value for demodulating a signal.

The theoretical reachable distance with SF12, BW 203 kHz is 3.9 km.

B.2.2 SF allocation to guarantee the connectivity depending on the distance

Which SF has a communication range of 1.4 km with a BW of 203 kHz?

At 1.4 km for SF12 and BW 203 kHz, $SNR = -11$ dB.
This is higher than the SF9 SNR limit value for demodulating a signal(-12.5 dB) and lower than the SF8 SNR limit value for demodulating a signal (-10 dB).

At 1.4 km, using a 203 kHz bandwidth, the lower SF value to guarantee the connectivity is SF9.

Which SF has a communication range of 700 m with a BW of 406 kHz?

At 700 m for SF12 and BW 203 kHz, $SNR = -5$ dB. So, the lower SF value to be used is SF6.
Here, the bandwidth is doubled in comparison with the previous example. Therefore $SNR = P - (N + 3) = -5 - 3 = -8$ dB.
This is lower than the SF7 SNR limit value for demodulating a signal (-7.5 dB).

At 700 m, using a 406 kHz bandwidth, the lower SF value to guarantee the connectivity is SF8.

Which SF has a communication range of 2 km with a BW of 406 kHz?

At 1.4 km for SF12 and BW 203 kHz, $SNR = -11$ dB.
By applying $P - 10 * log_{10}(ratio^2)$, with $ratio = \frac{2}{1.4}$, we obtain $P - 3 = -11 - 3 = -14$ dB.
The bandwidth is doubled. Therefore $SNR = -14 - 3 = -17$ dB.
This is higher than the SF11 SNR limit value for demodulating a signal (-17.5 dB).

At 2 km, using a 406 kHz bandwidth, the lower SF value to guarantee the connectivity is SF11.

Appendix C

Theoretical Wi-Fi FDR computation

In this appendix, we provide the assumption, define the variables, and detail the computation of the theoretical Wi-Fi FDR we used in the simulations of Chapter 4.

Assumption

When LoRa and Wi-Fi frames have overlapping ToA, the Wi-Fi frame is lost.

Variables definition

$WiFi_{ToA}$ = Wi-Fi time on air

$WiFi_{sleep}$ = Wi-Fi sleep time, i.e., inter-frame time

$WiFi_p$ = Wi-Fi period = $WiFi_{ToA} + WiFi_{sleep}$

$LoRa_{ToA}$ = LoRa time on air

$LoRa_{sleep}$ = LoRa sleep time, i.e., inter-frame time

$LoRa_p$ = LoRa period = $LoRa_{ToA} + LoRa_{sleep}$

$LoRa_{OR}$ = LoRa occupancy channel rate

P_{inter} = probability of interference

During a $WiFi_p$, the number of LoRa frames is:
$x = \frac{\frac{1}{LoRa_p}}{\frac{1}{WiFi_p}} = \frac{WiFi_p}{LoRa_p}$

The time during which LoRa and Wi-Fi frames overlap is:
$y = x \times (WiFi_{ToA} + LoRa_{ToA})$

What is the probability that a Wi-Fi frame is interfered by a LoRa frame during a Wi-Fi period?

$$
\begin{aligned}
P_{inter} &= \frac{y}{WiFi_p} \\
&= \frac{x \times (WiFi_{ToA} + LoRa_{ToA})}{WiFi_p} \\
&= \frac{WiFi_p}{LoRa_p} \times \frac{WiFi_{ToA} + LoRa_{ToA}}{WiFi_p} \\
&= \frac{WiFi_{ToA} + LoRa_{ToA}}{\frac{LoRa_{ToA}}{LoRa_{OR}}} \\
&= (\frac{WiFi_{ToA}}{LoRa_{ToA}} + 1) \times LoRa_{OR}
\end{aligned}
$$

$$\text{FDR} = 1 - P_{inter}$$
$$\text{FDR} = 1 - (\frac{WiFi_{ToA}}{LoRa_{ToA}} + 1) \times LoRa_{OR}$$

Appendix D

Experiment issues

In this appendix, we enumerate the main difficulties we faced when running the different experiments of this manuscript. We consider that providing our experiment issues and how we fix them participate in making our work reproducible. Additionally, this contributes to the will of the scientific community to share experiments experiences, as in the FAILSAFE [1] workshop collocated with the ACM SenSys conference. Note that the experiment issues listed in this appendix are not exhaustive.

D.1 Environment-related issues

The first category of experiment issues comes from the environment of our experiments.

1. **Weather.** When we setup our outdoor experiments we ran a series of test to verify that our experiments were running. Through the repetitions of our tests, we observe a significant variability in our results. Our analysis showed that the results variability was a consequence of the weather. Indeed, our LoRa end-devices are highly sensitive to humidity and temperature. To fix this issue, we postponed our outdoor experiments to a period of the year when the weather is more stable, i.e., we postponed our experiments from January to March. In the meantime, we ran the indoor experiments.
2. **Laptop batteries.** For all our outdoor experiments we had to take into account the laptop battery autonomy as we could not charge it during the experiments. To fix this potential issue, we decided to use two laptops thus allowing battery autonomy for at least half a day.
3. **Influx of people.** At first, for our indoor experiments that are run in the faculty building, we started our experiments irrespective of the time of the day. This lead to have running experiments during the inter-course or at the lunch break. In such cases, we observed a high concentration of people in the corridors and the hall of the building resulting in a decrease of our performance as our transmissions had to pass through a higher number of obstacles. We fixed this issue by scheduling our experiments when the number of people in the corridors was as low as possible, i.e., when students were in class. Note that this experiment issue is not a problem in our office building indoor

[1] FAILSAFE 2017 (first edition) and FAILSAFE 2020 (second edition)

experiments as one series is run during the week-end and the second one is a long-run experiment that aims to observe the performance variations due to the presence, and the mobility, of people inside the building.

4. **External interference.** During our coexistence experiments we observe a performance decreases for the 2402 MHz LoRa center channel frequency compared to the other channels evaluated. We observed this decrease in performance for period where LoRa and Wi-Fi transmissions overlap but also when Wi-Fi is transmitting alone. We analyzed our environment using an USRP and observed a high peak of energy centered at 2402 MHz corresponding to a BT beacon. An in-depth analysis showed that when our cell phone is not in standby mode, the BT beacon is sent with the maximum power, resulting in external interference for our experiments and therefore a decrease in performance. We fixed this issue by turning off the BT of the surroundings devices during our experiments.

5. **Change in the environment.** During our coexistence experiment campaign, we evaluate two IEEE 802.11 standard. As the results obtained for the IEEE 802.11b standard were confusing, we repeated our experiments in another indoor environment: a single-family home environment. Recently, in the context of a future work, we wanted to repeat our experiment to increase the distance between transmitters an receivers. For that, we decided to run our experiment in the same single-family home environment as before. Unfortunately, we were not able to repeat our experiments. Every time we ran our experiments, they failed at 2406 and 2408 MHz. Note that, between the first series of experiment and the recent one more than a year has passed. We analyzed the logs and concluded that something has changed in the environment. We assume that a device is interfering on these two frequencies. We also assume that the device is not located inside the home where we run our experiments. Indeed, we try to turn off all the wireless networks inside the house, i.e., Wi-Fi APs, BT transmitters, and surveillance cameras, and observed the same experiments failure. Further investigation are needed, probably using a spectrum analyzer, to find what device and what technology are causing the destructive interference we observed.

D.2 Hardware and software-related issues

The second category of experiment issues comes from the equipment, and the corresponding tools, we used to setup our experiments.

1. **USB port number.** Remember that in the experiments where we compare the performance of LoRa sub-GHz and LoRa 2.4 GHz, we use three LoRa sub-GHz gateways and three LoRa sub-GHz end-devices, as well as one LoRa 2.4 GHz gateway and three LoRa 2.4 GHz end-devices. All the gateways were powered via USB by our laptop thus requiring four USB ports. Our laptops have only three USB ports. To fix this issue, we use a port multiplier to have sufficient USB ports for each device.

2. **End-devices batteries.** All our LoRa sub-GHz experiments use Arduino UNOs with SX1276 radio chip powered by batteries. In this series of experiment, we evaluate several distances which depend on the evaluated scenario, i.e., outdoor or indoor. When repeating our experiments, we observed a performance decrease even for the highest communication range configurations and at distance where we previously obtained a good connectivity with a FDR around 100%. We assume that comes from how AA batteries discharge. We fixed this issue by replacing the batteries with fully charged batteries regularly and thus ensuring the same level of battery for each experiment.

3. `screen` **is terminating.** When we setup our first experiments we needed to know when the end-devices have finished to send their frames. The easiest way for that was to read the USB port on which we plug the gateways. This is possible using the Linux `screen` utility. Unfortunately, during our test to verify that our experiments were running, we randomly had a message `screen is terminating`. Even if it was not an issue for these experiments as we know exactly the number of frames sent and thus only needed the gateways logs to compute the FDR, we had to find a solution for our future experiments. We fixed this issue by using `cat` and redirecting the information read on the USB port into a text file.

4. **Gateway deadlock.** In our coexistence experiments, we configured the number of frames and the inter-frame time to ensure the same period per LoRa configuration. Our initial experiments highlighted a hardware limitation: by continuously sending LoRa frames using a SF5, BW 1625 configuration results in the gateway shut down. We assume that the small inter-frame times led to gateway failure. Further analysis showed the gateway had no time to demodulate incoming frames before switching to listening for new ones and eventually became blocked in a deadlock. We fixed this issue by finding the smallest SF providing a stable operation that is SF6.

5. `Scapy` **parameters.** When we designed our coexistence experiments, we wanted to evaluate different Wi-Fi MCS to quantify the impact of the MCS on LoRa transmissions. Even if the MCS is a MAC mechanism, we wanted to implement it but without using the adaptive part of the mechanism. Instead, we wanted to fix the MCS value and to vary it over repetitions of our experiments. However, we were not able to find how to easily change the MCS value and thus decide not to use it. As far as we know, there might be the possibility to change the MCS value by modifying the Radiotap header used by `Scapy`. Additionally, we recently found that the wireless interface traffic rate can be modified directly in the hardware parameters but not through `Scapy`. Varying the traffic rate can be seen as a kind of MCS mechanism where the modulation is fixed and only the traffic rate changes.

6. **Transmission synchronization.** The design of our coexistence experiments requires to have periods of time where Wi-Fi and LoRa transmissions overlap and other periods of time where only one technology is transmitting. We thus need to synchronize the different technologies. As we generate our Wi-Fi traffic using `Scapy`, we had to

put our computers in monitor mode to send the Wi-Fi traffic but also to be able to visualize the IEEE 802.11 frames in `Tcpdump/Wireshark`. Therefore, we had to design a synchronization process to respect our coexistence experiments timeline. We fixed this issue by modifying the LoRa gateway to end-devices communication protocol used in previous experiments, and Python and Bash scripts with timers for Wi-Fi.

7. **Reconfiguration frames.** The design of our gateway to end-devices communication protocol requires the LoRa gateway to send downlink activation frames to allow the end-device to star transmitting. Thus, these downlink frames have to be robust to interference and signal propagation. We ran some tests to evaluate which configuration to use to send the activation frames. As in our coexistence experiments we started by evaluating a LoRa channel centered at 2402 MHz, and we observed a repetitive loss of the downlink frames using a SF9, BW 203 configuration for example. We solved part of the issue by turning off the BT of the surrounding devices as they were beaconing on their three advertising channels, 2402 MHz being the center frequency of one of them. We completely solved the issue by concluding that in order to always receive at least one downlink frame we have to send the activation frame using the most robust configuration, i.e., SF12, BW 203. As a consequence to this issue and our solution to fix it, in our Bandwidth experiment we could only test two different BW during an experiment as the actual LoRa 2.4 GHz gateways can receive only three different configurations in parallel.

Bibliography

[1] Usman Raza, Parag Kulkarni, and Mahesh Sooriyabandara. "Low Power Wide Area Networks: An Overview". In: *IEEE Communications Surveys & Tutorials* 19.2 (Jan. 2017), pp. 855–873.

[2] Semtech. *LoRa Technology*. https://www.semtech.com/lora. Accessed on: 2021-10-13.

[3] ETSI. *3GPP TS 36.141 version 13.6.0 Release 13*. Standard. Accessed on: 2024-06-13. ETSI, Apr. 2021.

[4] Ingenu. *How RPMA works?* https://www.ingenu.com/technology/rpma/how-rpma-works/. Accessed on: 2024-06-13.

[5] LoRa Alliance Technical Committee. *LoRaWAN 1.1 Specification*. Standard. Final release. Accessed on 2024-08-26. LoRa Alliance, Oct. 2017.

[6] Dave Kjendal. "LoRa-Alliance Regional Parameters Overview". In: *Journal of ICT Standardization* (Apr. 2021), pp. 35–46.

[7] Ladislav Polak and Jiri Milos. "Performance analysis of LoRa in the 2.4 GHz ISM band: coexistence issues with Wi-Fi". In: *Telecommunication Systems* 74.3 (July 2020), pp. 299–309.

[8] Danalto. *Location Tracking: Out With the Old and In With LoRa® 2.4 GHz*. https://www.danalto.com/location-tracking-new-vs-old/. Accessed 2022-07-08.

[9] Semtech. *SX1280 Documentation*. https://www.semtech.fr/products/wireless-rf/lora-connect/sx1280. Accessed 2024-03-21.

[10] Zhijun Li and Yongrui Chen. "BLE2LoRa: Cross-Technology Communication from Bluetooth to LoRa via Chirp Emulation". In: *IEEE SECON*. Italy, 2020.

[11] Beibei Wang and K.J. Ray Liu. "Advances in cognitive radio networks: A survey". In: *IEEE Journal of Selected Topics in Signal Processing* 1.2 (Feb. 2011), pp. 5–23.

[12] Semtech. *SX1302 Documentation*. https://www.semtech.com/products/wireless-rf/lora-core/sx1302. Accessed 2024-06-14.

[13] Marco Centenaro, Lorenzo Vangelista, and Ryuji Kohno. "On the impact of downlink feedback on LoRa performance". In: *IEEE PIMRC*. Canada, 2017.

[14] Semtech. *LR1120 Datasheet*. https://www.semtech.fr/products/wireless-rf/lora-edge/lr1120. Accessed 2024-05-16.

[15] Edouard Lumet, Antonin Le Floch, Rahim Kacimi, Mathieu Lihoreau, and André-Luc Beylot. "LoRaWAN Relaying: Push the Cell Boundaries". In: *ACM MSWiM*. Spain, 2021.

[16] Semtech. *Physical Layer Proposal 2.4GHz*. https://www.semtech.com/uploads/technology/LoRa/phy-layer-2g4.pdf. Accessed on: 2024-06-13.

[17] GDR RSD. *GT Reproductibilité*. https://gdr-rsd.fr/gt-reproductibilite/. Accessed 2024-08-26.

[18] Loic Desquilbet, Sabrina Granger, Boris Hejblum, Arnaud Legrand, Pascal Pernot, Nicolas P. Rougier, Elisa de Castro Guerra, Martine Courbin-Coulaud, Ludovic Duvaux, Pierre Gravier, Grégoire Le Campion, Solenne Roux, and Frédéric Santos. *Vers une recherche reproductible*. Ed. by Unité régionale de formation à l'information scientifique et technique de Bordeaux. Unité régionale de formation à l'information scientifique et technique de Bordeaux, May 2019.

[19] Renzo E. Navas, Frederic Cuppens, Nora Boulahia Cuppens, Laurent Toutain, and Georgios Z. Papadopoulos. "MTD, Where Art Thou? A Systematic Review of Moving Target Defense Techniques for IoT". In: *IEEE Internet of Things Journal* 8.10 (May 2021), pp. 7818–7832.

[20] International Telecommunication Union (ITU). *Radio Regulations*. Standard. Accessed on: 2024-02-09. International Telecommunication Union (ITU), 2020.

[21] Z-Wave Alliance. *Application Work Group Z-Wave Specifications*. https://z-wavealliance.org/development-resources-overview/specification-for-developers/. Accessed on: 2024-06-13.

[22] IEEE 802.11 Working Group. "IEEE Standard for Information Technology - Telecommunications and information exchange between systems - Local and Metropolitan networks - Specific requirements - Part 11: Wireless LAN Medium Access Control (MAC) and Physical Layer (PHY) Specifications: Higher Speed Physical Layer (PHY) Extension in the 2.4 GHz band". In: *IEEE Std 802.11b-1999* (Jan. 2000).

[23] IEEE 802.11 Working Group. "IEEE Standard for Information Technology – Local and metropolitan area networks – Specific requirements – Part 11: Wireless LAN Medium Access Control (MAC) and Physical Layer (PHY) Specifications: Further Higher Data Rate Extension in the 2.4 GHz Band". In: *IEEE Std 802.11g-2003* (June 2003).

[24] Core Specification Working Group. *Bluetooth Core Specification v5.3*. Standard. Accessed on 2024-05-14. Core Specification Working Group, July 2021.

[25] IEEE P802.15 Working Group. *IEEE Std 802.15.4-2020, IEEE Standard for Low-Rate Wireless Networks*. Standard. Accessed on 2024-05-15. IEEE P802.15 Working Group, July 2020.

[26] ZigBee Alliance. *ZigBee Specification*. Standard. Accessed on 2024-05-15. ZigBee Alliance, Aug. 2015.

[27] FieldComm Group. *HART Protocol Specifications*. Standard. Accessed on 2024-05-15. FieldComm Group, Jan. 2023.

[28] Network Working Group. *Transmission of IPv6 Packets over IEEE 802.15.4 Networks*. RFC 4944. Accessed on 2024-05-15. Network Working Group, Sept. 2007.

[29] IEEE 802.11 Working Group. "IEEE Standard for Information Technology – Local and metropolitan area networks – Specific requirements – Part 11: Wireless LAN Medium

Access Control (MAC) and Physical Layer (PHY) Specifications: Amendment 5: Enhancements for Higher Throughput". In: *IEEE Std 802.11n-2009* (Oct. 2009).

[30] IEEE 802.11 Working Group. "IEEE Standard for Information Technology - Telecommunications and information exchange between systems - Local and Metropolitan area Networks - Specific requirements - Part 11: Wireless LAN Medium Access Control (MAC) and Physical Layer (PHY) Specifications Amendment 1: Enhancements for High-Efficiency WLAN". In: *IEEE Std 802.11ax-2021* (May 2021).

[31] IEEE 802.11 Working Group. "IEEE Draft Standard for Information Technology - Telecommunications and information exchange between systems - Local and Metropolitan area networks - Specific requirements - Part 11: Wireless LAN Medium Access Control (MAC) and Physical Layer (PHY) Specifications Amendment: Enhancements for Extremely High Throughput (EHT)". In: *IEEE P802.11be/D3.0* (Jan. 2023).

[32] Lorenzo Vangelista. "Frequency Shift Chirp Modulation: The LoRa Modulation". In: *IEEE Signal Processing Letters* 24.12 (Dec. 2017), pp. 1818–1821.

[33] Semtech. *SX1272 Documentation*. https://www.semtech.fr/products/wireless-rf/lora-connect/sx1272. Accessed 2024-03-21.

[34] Semtech. *SX1276 Documentation*. https://www.semtech.fr/products/wireless-rf/lora-connect/sx1276. Accessed 2024-05-15.

[35] Daniele Croce, Michele Gucciardo, Stefano Mangione, Giuseppe Santaromita, and Ilenia Tinnirello. "Impact of LoRa Imperfect Orthogonality: Analysis of Link-Level Performance". In: *IEEE Communications Letters* 22.4 (Apr. 2018), pp. 796–799.

[36] Olivier Seller. "LoRaWAN Link Layer". In: *Journal of ICT Standardization* (Apr. 2021), pp. 1–12.

[37] LoRa Alliance Technical Committee Regional Parameters Workgroup. *RP002-1.0.2 LoRaWAN® Regional Parameters*. Tech. rep. Accessed on 2024-08-26. LoRa Alliance, Oct. 2020.

[38] Davide Magrin, Marco Centenaro, and Lorenzo Vangelista. "Performance evaluation of LoRa networks in a smart city scenario". In: *IEEE ICC*. France, 2017.

[39] Antonino Pagano, Daniele Croce, Ilenia Tinnirello, and Gianpaolo Vitale. "A Survey on LoRa for Smart Agriculture: Current Trends and Future Perspectives". In: *IEEE Internet of Things Journal* 10.4 (Feb. 2023), pp. 3664–3679.

[40] Nadège Varsier and Jean Schwoerer. "Capacity limits of LoRaWAN technology for smart metering applications". In: *IEEE ICC*. France, 2017.

[41] Gwendoline Hochet Derévianckine, Alexandre Guitton, Oana Iova, Baozhu Ning, and Fabrice Valois. "Opportunities and Challenges of LoRa 2.4 GHz". In: *IEEE Communications Magazine* 61.10 (Oct. 2023), pp. 164–170.

[42] Carlos Fernández Hernández, Gwendoline Hochet Derévianckine, Alexandre Guitton, Oana Iova, and Fabrice Valois. "Indoor Performance Evaluation of LoRa® 2.4 GHz". In: *IEEE WCNC*. United Kingdom, 2023.

[43] Carlos Fernández Hernández, Gwendoline Hochet Derévianckine, Alexandre Guitton, Oana Iova, and Fabrice Valois. "On a testé pour vous : LoRa 2.4 GHz à

l'intérieur". In: *CoRes 2023 - 8èmes Rencontres Francophones sur la Conception de protocoles, l'évaluation de performances et l'expérimentation de Réseaux de communication*. In French. France, 2023.

[44] Hongxu Zhu, Kim Fung Tsang, Yucheng Liu, Yang Wei, Hao Wang, Chung Kit Wu, and Wai Hin Wan. "Index of Low-Power Wide Area Networks: A Ranking Solution toward Best Practice". In: *IEEE Communications Magazine* 59.4 (Apr. 2021), pp. 139–144.

[45] Jules Courjault, Baptiste Vrigneau, and Olivier Berder. "Fast performance evaluation of LoRa communications over Rayleigh fading channels". In: *IEEE WCNCW*. Morocco, 2019.

[46] Davide Magrin, Martina Capuzzo, and Andrea Zanella. "A Thorough Study of LoRaWAN Performance Under Different Parameter Settings". In: *IEEE Internet of Things Journal* 7.1 (Jan. 2020), pp. 116–127.

[47] José Luis Gallardo, Mohamed A. Ahmed, and Nicolás Jara. "LoRa IoT-Based Architecture for Advanced Metering Infrastructure in Residential Smart Grid". In: *IEEE Access* 9 (2021), pp. 124295–124312.

[48] João Luís Verdegay de Barros, Marcos Eduardo Pivaro Monteiro, Guilherme de Santi Peron, Guilherme Luiz Moritz, Ohara Kerusauskas Rayel, and Richard Demo Souza. "LoRaWAN vs. 6TiSCH: Which one scales better?" In: *Computer Communications* 184 (Feb. 2022), pp. 1–11.

[49] Richard Verhoeven, Stash Kempinski, and Nirvana Meratnia. "Performance Evaluation of Wi-Fi HaLow, NB-IoT and LoRa for Smart City Applications". In: *ACM PE-WASUN*. Canada, 2022.

[50] Oana Iova, Amy Murphy, Gian Pietro Picco, Lorenzo Ghiro, Davide Molteni, Federico Ossi, and Francesca Cagnacci. "LoRa from the City to the Mountains: Exploration of Hardware and Environmental Factors". In: *ACM EWSN*. Sweden, 2017.

[51] Aloÿs Augustin, Jiazi Yi, Thomas Clausen, and William Mark Townsley. "A Study of LoRa: Long Range & Low Power Networks for the Internet of Things". In: *Sensors* 16.9 (Sept. 2016).

[52] Keith E. Nolan, Wael Guibene, and Mark Y. Kelly. "An evaluation of low power wide area network technologies for the Internet of Things". In: *IEEE IWCMC*. Cyprus, 2016.

[53] Tara Petrić, Mathieu Goessens, Loutfi Nuaymi, Laurent Toutain, and Alexander Pelov. "Measurements, performance and analysis of LoRa FABIAN, a real-world implementation of LPWAN". In: *IEEE PIMRC*. Spain, 2016.

[54] Andrew J Wixted, Peter Kinnaird, Hadi Larijani, Alan Tait, Ali Ahmadinia, and Niall Strachan. "Evaluation of LoRa and LoRaWAN for wireless sensor networks". In: *IEEE SENSORS*. USA, 2016.

[55] Martin Bor and Utz Roedig. "LoRa Transmission Parameter Selection". In: *IEEE DCOSS*. Canada, 2017.

[56] P. J. Radcliffe, Karina Gomez Chavez, Paul Beckett, Justin Spangaro, and Conrad Jakob. "Usability of LoRaWAN Technology in a Central Business District". In: *IEEE VTC Spring*. Australia, 2017.

[57] Giannis Kazdaridis, Stratos Keranidis, Polychronis Symeonidis, Panagiotis Tzimotoudis, Ioannis Zographopoulos, Panagiotis Skrimponis, and Thanasis Korakis. "Evaluation of LoRa Performance in a City-wide Testbed: Experimentation Insights and Findings". In: *ACM WiNTECH*. Mexico, 2019.

[58] Philip Branch. "Propagation Measurements and Models of 915 MHz LoRa Radio in a Block Cave Gold Mine". In: *IEEE ICOIN*. Korea (South), 2021.

[59] Pei Tian, Fengxu Yang, Xiaoyuan Ma, Carlo Alberto Boano, Xin Tian, Ye Liu, and Jianming Wei. "Dataset: Environmental Impact on the Long-Term Connectivity and Link Quality of an Outdoor LoRa Network". In: *ACM SenSys*. Portugal, 2021.

[60] Laure Moiroux-Arvis, Christophe Cariou, and Jean-Pierre Chanet. "Evaluation of LoRa technology in 433-MHz and 868-MHz for underground to aboveground data transmission". In: *Computers and Electronics in Agriculture* 194 (Mar. 2022), p. 106770.

[61] Manuel Perez, Fabian Eduardo Sierra-Sanchez, Fabian Chaparro, Diego Mendez Chaves, Carlos-Ivan Paez-Rueda, Gabriel Perilla Galindo, and Arturo Fajardo. "Coverage and Energy-Efficiency Experimental Test Performance for a Comparative Evaluation of Unlicensed LPWAN: LoRaWAN and SigFox". In: *IEEE Access* 10 (Sept. 2022), pp. 97183–97196.

[62] Juan Ramón Santana, Pablo Sotres, Jesús Pérez, Luis Sánchez, Jorge Lanza, and Luis Muñoz. "LoRaWAN-based Smart Parking Service: Deployment and Performance Evaluation". In: *ACM PE-WASUN*. Canada, 2022.

[63] Jules Courjault, Baptiste Vrigneau, Olivier Berder, and Manav R. Bhatnagar. "A Computable Form for LoRa Performance Estimation: Application to Ricean and Nakagami Fading". In: *IEEE Access* 9 (Apr. 2021), pp. 81601–81611.

[64] Veronica Toro-Betancur, Gopika Premsankar, Mariusz Slabicki, and Mario Di Francesco. "Modeling Communication Reliability in LoRa Networks with Device-level Accuracy". In: *IEEE INFOCOM*. Canada, 2021.

[65] Houssem Eddin Elbsir, Mohamed Kassab, Sami Bhiri, and Mohamed Hedi Bedoui. "Evaluation of LoRaWAN class B performances and its optimization for better support of actuators". In: *Computer Communications* 198 (Jan. 2023), pp. 128–139.

[66] Alonso Llap and Moises Nunez. "Evaluating Energy Consumption and Maximum Communication Distance for SX1280 LoRa Transceiver at 2.4 GHz towards Adaptive Networks". In: *IEEE WiMob*. Canada, 2023.

[67] Pablo Avila-Campos, Fabian Astudillo-Salinas, Andres Vazquez-Rodas, and Alcides Araujo. "Evaluation of LoRaWAN Transmission Range for Wireless Sensor Networks in Riparian Forests". In: *International ACM MSWIM*. USA, 2019.

[68] Silvia Demetri, Marco Zúñiga, Gian Pietro Picco, Fernando Kuipers, Lorenzo Bruzzone, and Thomas Telkamp. "Automated Estimation of Link Quality for LoRa: A Remote Sensing Approach". In: *ACM IPSN*. Canada, 2019.

[69] Guillermo Del Campo, Igor Gomez, Silvia Calatrava Sierra, Rocio Martinez, and Asuncion Santamaria. "Power Distribution Monitoring Using LoRa: Coverage Analysis in Suburban Areas". In: *ACM EWSN*. Spain, 2018.

[70] Luca Feltrin, Chiara Buratti, Enrico Vinciarelli, Roberto De Bonis, and Roberto Verdone. "LoRaWAN: Evaluation of Link- and System-Level Performance". In: *IEEE Internet of Things Journal* 5.3 (June 2018), pp. 2249–2258.

[71] Fernando M. Ortiz, Thales T. De Almeida, Ana E. Ferreira, and Luís Henrique M.K. Costa. "Experimental vs. simulation analysis of LoRa for vehicular communications". In: *Computer Communications* 160 (July 2020), pp. 299–310.

[72] Davide Magrin, Martina Capuzzo, Andrea Zanella, Lorenzo Vangelista, and Michele Zorzi. "Performance Analysis of LoRaWAN in Industrial Scenarios". In: *IEEE Transactions on Industrial Informatics* 17.9 (Sept. 2021), pp. 6241–6250.

[73] Pierre Neumann, Julien Montavont, and Thomas Noël. "Indoor deployment of low-power wide area networks (LPWAN): A LoRaWAN case study". In: *IEEE WiMob*. USA, 2016.

[74] Bashima Islam, Md Tamzeed Islam, Jasleen Kaur, and Shahriar Nirjon. "LoRaIn: Making a Case for LoRa in Indoor Localization". In: *IEEE PerCom Workshops*. Japan, 2019.

[75] Giovanni Stanco, Alessio Botta, Flavio Frattini, Ugo Giordano, and Giorgio Ventre. "On the performance of IoT LPWAN technologies: the case of Sigfox, LoRaWAN and NB-IoT". In: *IEEE ICC*. Korea, Republic of, 2022.

[76] Takoua Mahjoub, Maymouna Ben Said, and Hatem Boujemaa. "On the Performances of Packet Error Rate for LoRa Networks". In: *IEEE IWCMC*. Croatia, 2022.

[77] Thomas Janssen, Noori BniLam, Michiel Aernouts, Rafael Berkvens, and Maarten Weyn. "LoRa 2.4 GHz Communication Link and Range". In: *Sensors* 20.16 (Aug. 2020), p. 4366.

[78] Mads Lauridsen, Huan Nguyen, Benny Vejlgaard, Istvan Z. Kovacs, Preben Mogensen, and Mads Sorensen. "Coverage Comparison of GPRS, NB-IoT, LoRa, and SigFox in a 7800 km^2 Area". In: *IEEE VTC Spring*. Australia, 2017.

[79] Marco Centenaro, Lorenzo Vangelista, Andrea Zanella, and Michele Zorzi. "Long-range communications in unlicensed bands: the rising stars in the IoT and smart city scenarios". In: *IEEE Wireless Communications* 23.5 (Oct. 2016), pp. 60–67.

[80] Dhaval Patel and Myounggyu Won. "Experimental Study on Low Power Wide Area Networks (LPWAN) for Mobile Internet of Things". In: *IEEE VTC Spring*. Australia, 2017.

[81] Nishant Poddar, Sikandar Zulqarnain Khan, Jakob Mass, and Satish Narayana Srirama. "Coverage Analysis of NB-IoT and Sigfox: Two Estonian University Campuses as a Case Study". In: *IEEE IWCMC*. Cyprus, 2020.

[82] Weitao Xu, Jun Young Kim, Walter Huang, Salil S. Kanhere, Sanjay K. Jha, and Wen Hu. "Measurement, Characterization, and Modeling of LoRa Technology in Multi-floor Buildings". In: *IEEE Internet of Things Journal* 7.1 (Jan. 2020), pp. 298–310.

[83] Harish V. Mekali, Anurag Agarwal, Manvendra Singh, Jobish John, Gaurav S. Kasbekar, and Maryam Shojaei Baghini. "Experimental Analysis of LoRa Transmission Parameters". In: *ACM Q2SWinet*. Canada, 2022.

[84] Rida El Chall, Samer Lahoud, and Melhem El Helou. "LoRaWAN Network: Radio Propagation Models and Performance Evaluation in Various Environments in Lebanon". In: *IEEE Internet of Things Journal* 6.2 (Apr. 2019), pp. 2366–2378.

[85] Asif M. Yousuf, Edward M. Rochester, Behnam Ousat, and Majid Ghaderi. "Throughput, Coverage and Scalability of LoRa LPWAN for Internet of Things". In: *IEEE/ACM IWQoS*. Canada, 2018.

[86] Jansen C. Liando, Amalinda Gamage, Agustinus W. Tengourtius, and Mo Li. "Known and Unknown Facts of LoRa: Experiences from a Large-scale Measurement Study". In: *ACM Transactions on Sensor Networks* 15.2 (May 2019), pp. 1–35.

[87] Zehua Sun, Huanqi Yang, Kai Liu, Zhimeng Yin, Zhenjiang Li, and Weitao Xu. "Recent Advances in LoRa: A Comprehensive Survey". In: *ACM Transactions on Sensor Networks* 18.4 (Nov. 2022), pp. 1–44.

[88] Melchizedek Alipio and Miroslav Bures. "Current testing and performance evaluation methodologies of LoRa and LoRaWAN in IoT applications: Classification, issues, and future directives". In: *Internet of Things* 25 (Apr. 2024), p. 101053.

[89] Mads Lauridsen, Benny Vejlgaard, Istvan Z. Kovacs, Huan Nguyen, and Preben Mogensen. "Interference Measurements in the European 868 MHz ISM Band with Focus on LoRa and SigFox". In: *IEEE WCNC*. USA, 2017.

[90] Google. *Google Maps*. https://www.google.com/maps/. Accessed 2024-31-05.

[91] GNU Project. *Screen User's Manual*. https://www.gnu.org/software/screen/manual/. Accessed 2024-31-05.

[92] Semtech. *LoRa 2.4 GHz Gateway*. https://github.com/Lora-net/gateway_2g4_hal. Accessed 2024-03-20.

[93] Semtech. *LoRa Basic Modem*. https://github.com/Lora-net/SWL2001/tree/master. Accessed 2024-03-20.

[94] Semtech. *SX1280 LoRa Calculator: fast evaluation of link budget and time on air*. https://os.mbed.com/components/SX1280RF1ZHP/. Accessed 2021-06-07.

[95] NetSpot Pro. *Netspot Wi-Fi planning*. https://www.netspotapp.com/. Accessed 2024-06-18.

[96] Gwendoline Hochet Derévianckine, Alexandre Guitton, Oana Iova, Baozhu Ning, and Fabrice Valois. "Hate or Love in the 2.4 GHz ISM band: The Story of LoRa and IEEE 802.11g". under review. Nov. 2023.

[97] Mohd Adib Sarijari, Anthony Lo, Mohd Sharil Abdullah, Sonia Heemstra De Groot, Ignas G.M.M. Niemegeers, and Rozeha A. Rashid. "Coexistence of Heterogeneous and Homogeneous Wireless Technologies in Smart Grid-Home Area Network". In: *IEEE ICPADS*. Korea (South), 2013.

[98] Fadillah Purnama Rezha and Soo Young Shin. "Performance Analysis of ISA100.11a Under Interference From an IEEE 802.11b Wireless Network". In: *IEEE Transactions on Industrial Informatics* 10.2 (May 2014), pp. 919–927.

[99] Domenico Garlisi, Antonino Pagano, Fabrizio Giuliano, Daniele Croce, and Ilenia Tinnirello. "A Coexistence Study of Low-Power Wide-Area Networks based on LoRaWAN and Sigfox". In: *IEEE WCNC*. United Kingdom, 2023.

[100] Angesom Ataklity Tesfay, Eric Pierre Simon, Sofiane Kharbech, and Laurent Clavier. "Deep Learning-based receiver for Uplink in LoRa Networks with Sigfox Interference". In: *IEEE WiMob*. Greece, 2022.

[101] Wenqi Guo, William M. Healy, and MengChu Zhou. "Impacts of 2.4-GHz ISM Band Interference on IEEE 802.15.4 Wireless Sensor Network Reliability in Buildings". In: *IEEE Transactions on Instrumentation and Measurement* 61.9 (Sept. 2012), pp. 2533–2544.

[102] Marko Höyhtyä, Janne Lehtomäki, Joonas Kokkoniemi, Marja Matinmikko, and Aarne Mämmelä. "Measurements and analysis of spectrum occupancy with several bandwidths". In: *IEEE ICC*. Hungary, 2013.

[103] Woonghee Lee, Albert Yongjoon Chung, and Hwangnam Kim. "Channel quality estimation using Bluetooth for other standards in the 2.4 GHz ISM band". In: *IEEE ICC*. Malaysia, 2016.

[104] Charalampos Orfanidis, Laura Marie Feeney, Martin Jacobsson, and Per Gunningberg. "Investigating interference between LoRa and IEEE 802.15.4g networks". In: *IEEE WiMob*. Italy, 2017.

[105] Nika Mostahinic and Hazem Refai. "Spectrum Occupancy for 802.11a/n/ac Homogeneous and Heterogeneous Networks". In: *IEEE IWCMC*. Morocco, 2019.

[106] Orion Afisiadis, Matthieu Cotting, Andreas Burg, and Alexios Balatsoukas-Stimming. "On the Error Rate of the LoRa Modulation With Interference". In: *IEEE Transactions on Wireless Communications* 19.2 (Feb. 2020), pp. 1292–1304.

[107] Orion Afisiadis, Sitian Li, Joachim Tapparel, Andreas Burg, and Alexios Balatsoukas-Stimming. "On the Advantage of Coherent LoRa Detection in the Presence of Interference". In: *IEEE Internet of Things Journal* 8.14 (July 2021), pp. 11581–11593.

[108] Sneihil Gopal, Sanjit K. Kaul, Rakesh Chaturvedi, and Sumit Roy. "Coexistence of Age and Throughput Optimizing Networks: A Spectrum Sharing Game". In: *IEEE/ACM Transactions on Networking* 29.4 (Aug. 2021), pp. 1494–1508.

[109] Clement Demeslay, Philippe Rostaing, and Roland Gautier. "Theoretical Performance of LoRa System in Multipath and Interference Channels". In: *IEEE Internet of Things Journal* 9.9 (May 2022), pp. 6830–6843.

[110] Jiaojiao Liu, Yuanmei Yan, Hua Yu, and Biyun Ma. "Approximate BER Performance of LoRa Modulation With Heavy Multipath Interference". In: *IEEE Wireless Communications Letters* 12.5 (May 2023), pp. 853–857.

[111] Tallal Elshabrawy and Joerg Robert. "Analysis of BER and Coverage Performance of LoRa Modulation under Same Spreading Factor Interference". In: *IEEE PIMRC*. Italy, 2018.

[112] Amin Azari, Meysam Masoudi, Čedomir Stefanović, and Cicek Cavdar. "Reliable and Energy-Efficient IoT Systems: Design Considerations in Coexistence Deployments". In: *IEEE Transactions on Network and Service Management* 20.3 (Sept. 2023), pp. 2412–2427.

[113] Till Wollenberg, Sebastian Bader, and Andreas Ahrens. "Measuring channel occupancy for 802.11 wireless LAN in the 2.4 GHz ISM band". In: *ACM MSWiM*. Cyprus, 2012.

[114] Benny Vejlgaard, Mads Lauridsen, Huan Nguyen, Istvan Z. Kovacs, Preben Mogensen, and Mads Sorensen. "Interference Impact on Coverage and Capacity for Low Power Wide Area IoT Networks". In: *IEEE WCNC*. USA, 2017.

[115] Felix Wunsch, Max Ströer, Marcus Müller, Holger Jäkel, and Friedrich K. Jondral. "LPWAN Applications in the 2.4 GHz Band: A Viable Choice?" In: *IEEE VTC-Fall*. USA, 2018.

[116] Laura Marie Feeney, Charalampos Orfanidis, Martin Jacobsson, and Per Gunningberg. "Preliminary results on LoRaWAN and IEEE 802.15.4-SUN Interference". In: *ACM SenSys*. China, 2018.

[117] Michael Baddeley, Carlo Alberto Boano, Antonio Escobar-Molero, Ye Liu, Xiaoyuan Ma, Victor Marot, Usman Raza, Kay Römer, Markus Schuss, and Aleksandar Stanoev. "Understanding Concurrent Transmissions: The Impact of Carrier Frequency Offset and RF Interference on Physical Layer Performance". In: *ACM Transactions on Sensor Networks* 20.1 (Jan. 2024), pp. 1–39.

[118] Sven Zacharias, Thomas Newe, Sinead O'Keeffe, and Elfed Lewis. "2.4 GHz IEEE 802.15.4 channel interference classification algorithm running live on a sensor node". In: *2012 IEEE SENSORS*. Taiwan, 2012.

[119] Tallal Elshabrawy, Phoebe Edward, Mohamed Ashour, and Joerg Robert. "Practical Evaluation of LoRa under Co-Technology Interference". In: *IEEE VTC2020-Fall*. Canada, 2020.

[120] Muhammad Khurram Ehsan, Asghar Ali Shah, Muhammad Rizwan Amirzada, Neelma Naz, Kostromitin Konstantin, Muhammad Sajid, and Asad Raza Gardezi. "Characterization of sparse WLAN data traffic in opportunistic indoor environments as a prior for coexistence scenarios of modern wireless technologies". In: *Alexandria Engineering Journal* 60.1 (Feb. 2021), pp. 347–355.

[121] Liljana Gavrilovska, Pero Latkoski, Vladimir Atanasovski, Ramjee Prasad, Albena Mihovska, Octavian Fratu, and Pavlos Lazaridis. "Radio Spectrum: Evaluation approaches, coexistence issues and monitoring". In: *Computer Networks* 121 (July 2017), pp. 1–12.

[122] Minar El-Aasser, Phoebe Edward, Mohamed Mandour, Mohamed Ashour, and Tallal Elshabrawy. "A comprehensive hybrid bit-level and packet-level LoRa-LPWAN simulation model". In: *Internet of Things* 14 (June 2021).

[123] Beibei Wang and K J R Liu. "Advances in cognitive radio networks: A survey". In: *IEEE Journal of Selected Topics in Signal Processing* 5.1 (Feb. 2011), pp. 5–23.

[124] Angesom Ataklity Tesfay, Eric Pierre Simon, Sofiane Kharbech, and Laurent Clavier. "Deep Learning-based Signal Detection for Uplink in LoRa-like Networks". In: *IEEE PIMRC*. Finland, 2021.

[125] Martin C. Bor, Utz Roedig, Thiemo Voigt, and Juan M. Alonso. "Do LoRa Low-Power Wide-Area Networks Scale?" In: *ACM MSWiM*. Malta, 2016.

[126] Philippe Biondi and the Scapy community. *Scapy documentation*. https://scapy.readthedocs.io/en/latest/. Accessed 2023-08-17.

[127] The Tcpdump Group. *Tcpdump documentation*. https://www.tcpdump.org/. Accessed 2023-08-17.

[128] Wireshark Foundation. *Wireshark*. https://www.wireshark.org/. Accessed 2024-06-26.

[129] Intel. *Intel Dual Band Wireless-AC 8265*. https://www.intel.com/content/www/us/en/products/sku/94150/intel-dual-band-wirelessac-8265/specifications.html. Accessed 2024-07-23.

[130] Broadcom. *BCM43013*. https://www.broadcom.com/products/wireless/wireless-lan-bluetooth/bcm4313. Accessed 2024-07-23.

[131] Mikhail Afanasyev, Tsuwei Chen, Geoffrey M. Voelker, and Alex C. Snoeren. "Analysis of a Mixed-Use Urban Wifi Network: When Metropolitan Becomes Neapolitan". In: *ACM IMC*. Greece, 2008.

[132] Vladimir Brik, Shravan Rayanchu, Sharad Saha, Sayandeep Sen, Vivek Shrivastava, and Suman Banerjee. "A Measurement Study of a Commercial-Grade Urban Wifi Mesh". In: *ACM IMC*. Greece, 2008.

[133] Gonglong Chen, Wei Dong, and Jiamei Lv. "LoFi: Enabling 2.4GHz LoRa and WiFi Coexistence by Detecting Extremely Weak Signals". In: *IEEE INFOCOM*. Canada, 2021.

[134] Dong Chen, Yuan Zhuang, Jianzhu Huai, Xiao Sun, Xiansheng Yang, Muhammad Awais Javed, Jason Brown, Zhengguo Sheng, and John Thompson. "Coexistence and Interference Mitigation for WPANs and WLANs From Traditional Approaches to Deep Learning: A Review". In: *IEEE Sensors Journal* 21.22 (Nov. 2021), pp. 25561–25589.

[135] Yuan He, Xiuzhen Guo, Xiaolong Zheng, Zihao Yu, Jia Zhang, Haotian Jiang, Xin Na, and Jiacheng Zhang. "Cross-Technology Communication for the Internet of Things: A Survey". In: *ACM Computing Surveys* 55.5 (May 2023), pp. 1–29.

[136] Junyang Shi, Xingjian Chen, and Mo Sha. "Enabling Cross-technology Communication from LoRa to ZigBee in the 2.4 GHz Band". In: *ACM Transactions on Sensor Networks* 18.2 (May 2022), pp. 1–23.

[137] Junyang Shi, Di Mu, and Mo Sha. "Enabling Cross-technology Communication from LoRa to ZigBee via Payload Encoding in Sub-1 GHz Bands". In: *ACM Transactions on Sensor Networks* 18.1 (Feb. 2022), pp. 1–26.

[138] Shuai Tong, Yangliang He, Yunhao Liu, and Jiliang Wang. "De-spreading over the air: long-range CTC for diverse receivers with LoRa". In: *ACM MobiCom*. Australia, 2022.

[139] Piotr Gawłowicz, Anatolij Zubow, and Falko Dressler. "Wi-Lo: Emulation of LoRa using Commodity 802.11b WiFi Devices". In: *IEEE ICC*. Korea, Republic of, 2022.

[140] Xiaolong Zheng, Dan Xia, Fu Yu, Liang Liu, and Huadong Ma. "Enabling Cross-Technology Communication From WiFi to LoRa With IEEE 802.11ax". In: *IEEE/ACM Transactions on Networking* 32.3 (June 2024), pp. 1936–1950.

[141] Shweta S. Sagari. "Coexistence of LTE and WiFi heterogeneous networks via inter network coordination". In: *ACM MOBISYS PhD forum*. USA, 2014.

[142] Yukimasa Nagai, Toshinori Hori, Yosuke Yokoyama, Naoki Shimizu, Akira Otsuka, and Tetsuya Yokotani. "Advanced wireless cooperation mechanisms for interference mitigation in the 2.4 GHz ISM band". In: *IEEE CCNC*. USA, 2012.

[143] Dong Chen, Jamil Khan, Muhammad Awais Javed, and Jason Brown. "Interference mitigation techniques for a dense heterogeneous area network in machine-to-machine communications". In: *Transactions on Emerging Telecommunications Technologies* 30.12 (Dec. 2019).

[144] Junaid Ansari. "Coexistence features of LTE-U for spectrum sharing with collocated Wi-Fi: demo". In: *ACM MobiHoc*. Germany, 2016.

[145] Onur Carhacioglu, Pouria Zand, and Majid Nabi. "Cooperative Coexistence of BLE and Time Slotted Channel Hopping Networks". In: *IEEE PIMRC*. Italy, 2018.

[146] Zicheng Chi, Yan Li, Xin Liu, Yao Yao, Yanchao Zhang, and Ting Zhu. "Parallel inclusive communication for connecting heterogeneous IoT devices at the edge". In: *ACM SenSys*. USA, 2019.

[147] Swetank Kumar Saha, Christina Vlachou, Dimitrios Koutsonikolas, and Kyu-Han Kim. "DeMiLTE: Detecting and Mitigating LTE Interference for Enterprise Wi-Fi in 5 GHz". In: *ACM Mobihoc*. Italy, 2019.

[148] Onur Carhacioglu, Pouria Zand, and Majid Nabi. "Time-domain cooperative coexistence of BLE and IEEE 802.15.4 networks". In: *IEEE PIMRC*. Canada, 2017.

[149] Hannah Brunner, Michael Stocker, Maximilian Schuh, Markus Schuß, Carlo Alberto Boano, and Kay Römer. "Understanding and Mitigating the Impact of Wi-Fi 6E Interference on Ultra-Wideband Communications and Ranging". In: *ACM/IEEE IPSN*. Italy, 2022.

[150] Cristina Cano, Douglas J. Leith, Andres Garcia-Saavedra, and Pablo Serrano. "Fair Coexistence of Scheduled and Random Access Wireless Networks: Unlicensed LTE/WiFi". In: *IEEE/ACM Transactions on Networking* 25.6 (Dec. 2017), pp. 3267–3281.

[151] Mohammad J. Abdel Rahman, Marwan Krunz, and Richard Erwin. "Interference mitigation using spectrum sensing and dynamic frequency hopping". In: *IEEE ICC*. Canada, 2012.

[152] Muhammad Farrukh Yaqub, Ammar Haider, Iqbal Gondal, and Joarder Kamruzzaman. "Self and static interference mitigation scheme for coexisting wireless networks". In: *Computers & Electrical Engineering* 40.2 (Feb. 2014), pp. 307–318.

[153] J. So and Y. Kim. "Interference-aware frequency hopping for Bluetooth in crowded Wi-Fi networks". In: *Electronics Letters* 52.17 (Aug. 2016), pp. 1503–1505.

[154] Mobashir Mohammad, Xiang-Fa Guo, and Mun Choon Chan. "Competition: Tackling Cross-technology Interference using Spatial and Channel Diversity for Robust Data Collection." In: *ACM EWSN*. Sweden, 2017.

[155] Mohd Adib Sarijari, Mohd Sharil Abdullah, Anthony Lo, and Rozeha A. Rashid. "Experimental studies of the ZigBee frequency agility mechanism in home area networks". In: *IEEE LCNW*. Canada, 2014.

[156] Christophe Moy and Lilian Besson. "Decentralized Spectrum Learning for IoT Wireless Networks Collision Mitigation". In: *IEEE DCOSS*. Greece, 2019.

[157] Cheng-Shang Chang, Wanjiun Liao, and Tsung-Ying Wu. "Tight Lower Bounds for Channel Hopping Schemes in Cognitive Radio Networks". In: *IEEE/ACM Transactions on Networking* 24.4 (Aug. 2016), pp. 2343–2356.

[158] Yunbo Song and Dan Ye. "Multi-channel transmission scheduling with hopping scheme under uncertain channel states". In: *Journal of the Franklin Institute* 360.5 (Mar. 2023), pp. 3800–3824.

[159] Dingwen Yuan, Michael Riecker, and Matthias Hollick. "HOPSCOTCH: An adaptive and distributed channel hopping technique for interference avoidance in Wireless Sensor Networks". In: *IEEE LCN*. USA, 2012.

[160] Hong Liu and Jesper L. Nielsen. "An efficient interference mitigation method for wireless hearing instruments network". In: *IEEE PIMRC*. Australia, 2012.

[161] Rasool Tavakoli, Majid Nabi, Twan Basten, and Kees Goossens. "Dependable Interference-Aware Time-Slotted Channel Hopping for Wireless Sensor Networks". In: *ACM Transactions on Sensor Networks* 14.1 (Feb. 2018), pp. 1–35.

[162] Kai Sun, Zhimeng Yin, Weiwei Chen, Shuai Wang, Zeyu Zhang, and Tian He. "Partial Symbol Recovery for Interference Resilience in Low-Power Wide Area Networks". In: *IEEE ICNP*. USA, 2021.

[163] Xiong Wang, Jun Huang, Bizhao Shi, Zhe Ou, Guojie Luo, Linghe Kong, Daqing Zhang, and Chenren Xu. "RF-SIFTER: Sifting Signals at Layer-0.5 to Mitigate Wideband Cross-Technology Interference for IoT". In: *ACM MobiCom*. Spain, 2023.

[164] Anwar Hithnawi. "Exploiting physical layer information to mitigate cross-technology interference effects on low-power wireless networks". In: *ACM SenSys*. Italy, 2013.

[165] Zicheng Chi, Yan Li, Hongyu Sun, Yao Yao, and Ting Zhu. "Concurrent Cross-Technology Communication Among Heterogeneous IoT Devices". In: *IEEE/ACM Transactions on Networking* 27.3 (June 2019), pp. 932–947.

[166] Anwar Hithnawi, Su Li, Hossein Shafagh, James Gross, and Simon Duquennoy. "CrossZig: Combating Cross-Technology Interference in Low-Power Wireless Networks". In: *ACM/IEEE IPSN*. Austria, 2016.

[167] Hiba Dakdouk, Erika Tarazona, Reda Alami, Raphaël Féraud, Georgios Z. Papadopoulos, and Patrick Maillé. "Reinforcement Learning Techniques for Optimized Channel Hopping in IEEE 802.15.4-TSCH Networks". In: *ACM MSWIM*. Canada, 2018.

[168] Brecht Reynders, Qing Wang, Pere Tuset-Peiro, Xavier Vilajosana, and Sofie Pollin. "Improving Reliability and Scalability of LoRaWANs Through Lightweight Scheduling". In: *IEEE Internet of Things Journal* 5.3 (June 2018), pp. 1830–1842.

[169] J. Logeshwaran, R. N. Shanmugasundaram, and Jaime Lloret. "Load based dynamic channel allocation model to enhance the performance of device-to-device communication in WPAN". In: *Wireless Networks* 30.4 (May 2024), pp. 2477–2509.

[170] Frederik Hermans, Olof Rensfelt, Thiemo Voigt, Edith Ngai, Lars-Åke Norden, and Per Gunningberg. "SoNIC: classifying interference in 802.15.4 sensor networks". In: *ACM IPSN*. USA, 2013.

[171] Anwar Hithnawi, Hossein Shafagh, and Simon Duquennoy. "TIIM: technology-independent interference mitigation for low-power wireless networks". In: *ACM IPSN*. USA, 2015.

[172] Rafał Marjasz, Konrad Połys, Anna Strzoda, and Krzysztof Grochla. "Improving Delivery Ratio in LoRa Network". In: *ACM MobiWac*. Spain, 2021.

[173] Jongyeop Kim, Wonhong Jeon, Kyung-Joon Park, and Jihwan P. Choi. "Coexistence of Full-Duplex-Based IEEE 802.15.4 and IEEE 802.11". In: *IEEE Transactions on Industrial Informatics* 14.12 (Dec. 2018), pp. 5389–5399.

[174] Jin-Seok Han, Tae-Hoon Kim, and Yong-Hwan Lee. "Robust transmission of the IEEE 802.15.4 signal in the presence of co-channel interference". In: *IEEE WCNC*. China, 2013.

[175] Jianlin Guo, Yukimasa Nagai, Benjamin A. Rolfe, Takenori Sumi, Philip Orlik, Joerg Robert, Kazuto Yano, Steve Shellhammer, Shoichi Kitazawa, Yasuhiko Inoue, and Tuncer Baykas. "IEEE 802.19.3 Coexistence Recommendations for IEEE 802.11 and IEEE 802.15.4 Based Systems Operating in SUB-1 GHz Frequency Bands". In: *IEEE Communications Standards Magazine* 7.2 (June 2023), pp. 72–82.

[176] Federal Communications Commission (FCC). *Amendment of Part 15 of the Commission's Rules Regarding Spread Spectrum Devices*. https://www.fcc.gov/document/amendment-part-15-commissions-rules-regarding-spread-spectrum. Accessed 2024-04-24.

[177] Gwendoline Hochet Derévianckine, Alexandre Guitton, Oana Iova, Baozhu Ning, and Fabrice Valois. "Mais qui se cache ici?" In: *CoRes 2024 - 9èmes Rencontres Francophones sur la Conception de Protocoles, l'Évaluation de Performance et l'Expérimentation des Réseaux de Communication*. In French. France, 2024.

[178] Marko Höyhtyä, Marja Matinmikko, Xianfu Chen, Juhani Hallio, Jani Auranen, Reijo Ekman, Juha Röning, Jan Engelberg, Juha Kalliovaara, Tanim Taher, Ali Riaz, and Dennis Roberson. "Measurements and analysis of spectrum occupancy in the 2.3–2.4 GHz band in Finland and Chicago". In: *2014 9th International Conference on Cognitive Radio Oriented Wireless Networks and Communications (CROWNCOM)*. Finland, 2014.

[179] Ettus Research. *Ettus USRP B200 mini*. https://www.ettus.com/all-products/usrp-b200mini-i-2/. Accessed 2024-08-30.

[180] GnuRadio. *GnuRadio software radio ecosystem*. https://www.gnuradio.org/. Accessed on 2024-02-21.

[181] Jupyter. *Jupyter Lab*. https://jupyter.org/. Accessed on 2024-02-21.

[182] Szymon Grabarek, Konrad Rodak, and Sikorska Kinga. "Coexistence experiments on LoRa and BLE in the 2.4 GHz ISM band"". Intern research project. June 2023.

[183] Computing Research & Education. *CORE*. http://portal.core.edu.au/conf-ranks/. Accessed 2024-03-01.

[184] Scimago Lab. *Scimago*. https://www.scimagojr.com/. Accessed 2024-03-01.

FOLIO ADMINISTRATIF

THESE DE L'INSA LYON, MEMBRE DE L'UNIVERSITE DE LYON

NOM : **HOCHET DERÉVIANCKINE** DATE de SOUTENANCE : **17/12/2024**

Prénoms : **Gwendoline, Sylvie, Isabelle**

TITRE : **Feasibility and Performance of a LoRa 2.4 GHz Network**
(Faisabilité et performances d'un réseau LoRa 2.4 GHz)

NATURE : **Doctorat** Numéro d'ordre : **2024ISAL0127**

École Doctorale : **Informatique et Mathématiques de Lyon**

Spécialité : **Informatique**

RÉSUMÉ :
The long-range (LoRa) technology and the LoRaWAN protocol, which mainly uses the sub-GHz frequency bands, subject to regional laws, have become widely used as a result of the rise of the Internet of Things (IoT). To overcome these limitations, Semtech has released a version of LoRa dedicated to the 2.4 GHz industrial, scientific, and medical (ISM) band, which, among others, is worldwide available and has no duty-cycle limitations. However, this frequency band is already used by many wireless technologies, such as Wi-Fi and Bluetooth (BT), as well as by common devices like microwaves and surveillance cameras. It is essential to evaluate the feasibility and the possible performance of this frequency band shift before deploying LoRa on a large scale in the 2.4 GHz ISM band.

This thesis proposes a comprehensive experimental evaluation of LoRa technology in the 2.4 GHz ISM band, including a comparison of its communication range and reliability with the European sub-GHz band (868 MHz). We also study the co-existence of LoRa and Wi-Fi when they are overlapping transmissions. To improve the coexistence, we propose and compare several frequency hopping (FH) strategies for LoRa. Although the latter proposal is based on simulation, we also propose an original methodology for evaluating a frequency band and selecting the less noisy channels, which could facilitate the implementation of FH strategies in future LoRa 2.4 GHz gateways. Our work provides important recommendations for the deployment and expansion of LoRa in the 2.4 GHz ISM band.

MOTS-CLÉS : **Internet of Things, LoRa, 2.4 GHz ISM band, performance evaluation, coexistence**

Laboratoire(s) de recherche : **CITI**

Directeur de thèse : **Fabrice VALOIS**

Président du Jury : **Thomas NOËL**

Composition du Jury :

PALATTELLA Maria Rita	Directrice de Recherche	LIST	Rapporteure
PHAM Congduc	Professeur des Universités	UPPA	Rapporteur
CAILLOUET Christelle	Maître de Conférences HDR	Université Côte d'Azur	Examinatrice
DONSEZ Didier	Professeur des Universités	UGA	Examinateur
NOËL Thomas	Professeur des Universités	Université de Strasbourg	Examinateur
ORIFIAMMA Davide	Director R&D	Semtech	Invité
GUITTON Alexandre	Professeur des Universités	UCA	Co-encadrant de thèse
IOVA Oana	Maître de Conférences	INSA-LYON	Co-encadrante de thèse
VALOIS Fabrice	Professeur des Universités	INSA-LYON	Directeur de thèse